REPORT DOCUMENTATION PAGE

Form Approved
OMB No. 0704-0188

1. AGENCY USE ONLY *(Leave blank)*	2. REPORT DATE	3. REPORT TYPE AND DATES COVERED
	Dec 3, 1998	Final Technical Report June 1995–Aug 98

4. TITLE AND SUBTITLE
Identification of Proteins that Participate in Bacterial Adhesion

5. FUNDING NUMBERS
G N0014-95-11086

6. AUTHOR(S)
G.G. Geesey

7. PERFORMING ORGANIZATION NAMES(S) AND ADDRESS(ES)
Montana State University
Bozeman, MT 59717

8. PERFORMING ORGANIZATION REPORT NUMBER

9. SPONSORING / MONITORING AGENCY NAMES(S) AND ADDRESS(ES)
Office of Naval Research
800 N Quincy St.
Arlington, VA 22217

10. SPONSORING / MONITORING AGENCY REPORT NUMBER
Not applicable

11. SUPPLEMENTARY NOTES

19990127 033

a. DISTRIBUTION / AVAILABILITY STATEMENT
Distribution Unlimited

12. DISTRIBUTION CODE

13. ABSTRACT ***(Maximum 200 words)***

Bacteria from diverse habitats in the marine environment adhere to inert surfaces through extracellular polysaccharides following initial contact with the substratum. Although proteins may also participate in the initial adhesion process, polysaccharides are the most obvious structures anchoring bacterial cells to surfaces after the initial contact event. A biofilm-forming marine bacterium, *Hyphomonas* strain VP-6, produces two separate adhesive surface polysaccharides; a temporally synthesized, polar, neutral or positively-charged holdfast molecule, and a negatively-charged, capsular molecule which surrounds the cell. Another biofilm-forming marine bacterium, *Hyphomonas* strain MHS-3, produces a single adhesive polysaccharide, which surrounds the main body of the prosthecate cell, and is synthesized only at cell reproduction stages. Capsular polysaccharides produced by these bacteria also serve as the matrix for biofilm development. MHS-3 also produces proteinaceous polar fimbriae, which may tether the cell to the substratum during initial contact, but is not used as a holdfast during later stages of cell adhesion after excretion of adhesive polysaccharide. VP-6 also produces polar fimbriae, which may participate in adhesion. In addition, VP-6 produces a polysaccharide-associated 64-kDa protein, the function of which remains unclear. A molecular level approach to biological adhesion to solid surfaces in seawater medium offers a level of understanding of biofouling not previously achieved through cellular or population level studies.

14. SUBJECT TERMS	15. NUMBER OF PAGES
adhesive biopolymers, bacterial adhesins, Hyphomonas, protein conditioning films, mussel adhesive protein, extracellular polysaccharides, bacteial adhesion	4
	16. PRICE CODE

17. SECURITY CLASSIFICATION OF REPORT	18. SECURITY CLASSIFICATION OF THIS PAGE	19. SECURITY CLASSIFICATION OF ABSTRACT	20. LIMITATION OF ABSTRACT
unclassified	unclassified	unclassified	SAR

FINAL REPORT

Grant#: N0014-95-11086

PRINCIPAL INVESTIGATOR: Gill Geesey

INSTITUTION: Montana State University, Bozeman

GRANT TITLE: Identification of Proteins that Participate in Bacterial Adhesion

AWARD PERIOD: June 1, 1995 - August 31, 1998

OBJECTIVE: The research was undertaken to achieve a better understanding of the molecular mechanisms of bacterial adhesion to solid surfaces submerged in seawater.

APPROACH: Biofouling of surfaces was evaluated *in situ* at deep-sea hydrothermal vents and under highly controlled laboratory conditions. Reduced adhesion mutants of model, primary film-forming, marine bacteria were isolated and their cell surface properties compared with those of wild-type adhesive strains using High Performance Size Exclusion Chromatography (HPSEC) followed by conventional biochemical assays, transmission electron microscopy of thin section and negatively-stained bacterial preparations, Time-of-Flight-Secondary Ion Mass Spectroscopy (ToF-SIMS), attenuated total reflectance Fourier transform infrared specroscopy (ATR/FT-IR) and X-ray photoelectron spectroscopy (XPS).

ACCOMPLISHMENTS: Geesey participated in a French Government-sponsored oceanographic research cruise to the Mid-Atlantic Ridge to study microbiological colonization and fouling of surfaces in the vicinity of deep-sea hydrothermal vents during November-December 1995. All surfaces, ranging in composition from synthetic organic polymers to metals and metal alloys such as copper, titanium, aluminum and stainless steels, when deployed at the "Snake Pit" site in water ranging in temperature from 5-20°C, became rapidly colonized over a 12-day period by hydrothermal vent microbial populations. Succession of microbial populations over the 12-day period was determined by surface phospholipid fatty acid (PLFA) extraction and analysis. Filamentous, *Thiothrix*-like bacteria containing C18:1•7 PLFA were found to dominate the community of both early and late colonizers, regardless of surface type. The cell proximal to the surface excreted a holdfast of fibrous material that anchored the entire filament to the substratum. This holdfast material resembled that excreted from the polar region of cells of a *Hyphomonas* strain (VP-6) isolated from the Guaymas hydrothermal vent region.

The holdfasts of two bacteria known to be primary colonizers of surfaces submerged in seawater were identified and characterized. *Hyphomonas* strain VP-6 adheres to solid surfaces as a first step in biofilm formation. Fine-structure microscopy and the use of specific stains and lectins revealed that it synthesizes two different extracellular polymeric substances (EPS). One is a temporally synthesized, polar holdfast and the other is a capsular structure that surrounds the entire cell, including the prosthecum, and is present during the complete life cycle of the organism. The timing and location of EPS elaboration correlate with adhesion to surfaces, suggesting that the EPS serves not only as the biofilm matrix but also as a primary adhesin. The temporality and polarity of VP-6 EPS expression differ substantially from those properties of EPS expression in another *Hyphomonas* strain, MHS-3.

Hyphomonas strain MHS-3, another primary colonizer of surfaces immersed in seawater, synthesizes two structures that mediate adhesion to solid substrata; capsular polysaccharide and proteinaceous fimbriae. Specific stains, gold-labeled lectins, and monoclonal antibodies, along

with transmission electron microscopy of synchronized populations, revealed that both structures are polarly and temporally expressed. The timed synthesis and placement of the fimbriae and capsule correlated with the timing and locus of MHS-3 cell adhesion. A mutant of MHS-3, displaying reduced adhesion to solid surfaces also lacked the capsular polysaccharide present on wild-type adhesive cells.

Aqueous suspensions of MHS-3 wild-type and mutant cells with reduced adhesion were evaluated by ToF-SIMS with the intention of gaining a better understanding of the chemical differences in of their cell surface properties. The spectra of both preparations were indistinguishable, suggesting whatever differences influenced cell adhesion were not present on cells in suspension. Comparisons with attached cells have not yet been made.

A molecular level approach to bacterial cell adhesion to solid surfaces in seawater was used to gain a better understanding of the interaction of protein and polysaccharide adhesive components of bacterial EPS at solid surfaces. Surface adsorption behavior of EPS components from MHS-3 was investigated using ATR/FT-IR spectroscopy. The protein fraction of the crude EPS (EPS_c)(propanol recipitated/extracted with EDTA) dominated the adsorption onto a Ge substratum. Removal of the Protease K accessible portion of the EPS_c protein, and treatment with RNase and DNase yielded a polysaccharide enriched, hygroscopic substance (EPS_p) which contained at least one adhesive polysaccharide component which adsorbed relatively strongly from dilute solutions indicating a strong affinity for the surface.

Conditioning the substratum with EPS_c diminished adsorption of the polysaccharide fractions in EPS_p and EPS_c protein was not displaced. EPS_c adsorption on substrata conditioned with EPS_p was impeded. However, the projected surface coverage of protein after long times, based on an empirical data fit, was the same as that for a clean substratum. The EPS_c proteins did not displace the pre-adsorbed adhesive polysaccharide fraction. SDS-PAGE of indicated that EPS_c proteins were a selectively enriched subset of total cell protein. The results indicate that adhesive components of EPS, with respect to a hydrophilic Ge surface, can be either protein or polysaccharide and that they may compete for interfacial binding sites.

EPS_p was separated into four fractions using HPSEC. Comparison of chromatograms of EPS_p from MHS-3 and a reduced adhesion strain (MHS-3 rad) suggested that one EPS fraction (fr2ps), which consisted of carbohydrate, served as an adhesin. Adsorption of this fraction to germanium (Ge) was investigated using ATR/FT-IR spectroscopy. Binding curves indicated that the isolated fraction had relatively high affinity for Ge when ranked against an adhesive protein from *Mytilis edulis*, Mussel Adhesive Protein (MAP) and an acidic polysaccharide (alginate from *Macrocystis pyrifera*). Spectral features were used to identify the fraction as a polysaccharide previously reported to adsorb preferentially out of the EPS_p mixture. Conditioning the Ge substratum with either Bovine Serum Albumin (BSA) or MAP decreased the adsorption of the adhesive polysaccharide significantly. Conditioning Ge with these proteins also reduced adhesion of whole cells.

That a protein conditioning film could alter the adhesive binding of purified adhesive polysaccharide as well as whole cells to surfaces prompted a molecular level examination of the interactions between proteins and surfaces. X-ray photoelectron spectroscopy (XPS), ATR/FT-IR and atomic force microscopy (AFM) were used to evaluate MAP film structure on polystyrene (PS) and poly(octadecyl methacrylate) (POMA) surfaces. The chemistry of the synthetic polymer surface was found to have a significant effect on protein-surface and protein-protein interactions. The protein layer on PS is stabilized through interactions that prevent the protein layer from being disrupted upon dehydration. The adsorbed MAP on the POMA surface is representative of a loosely bound protein layer that becomes highly perturbed upon dehydration. These results suggest that the substratum exerts some degree of control over the structure of the protein conditioning film and that this, in

turn, may influence interactions between the protein film and adhesive polymers of surface colonizing bacteria.

That fr2ps adheres strongly to Ge suggests that its molecular properties evolved to render it adhesive towards mineral oxides. In order to characterize these molecular interactions, the effect of divalent cations and pH on the adsorption of fr2ps to Ge was determined using ATR/FT-IR spectroscopy and XPS. The results indicated that divalent cations participate in binding of fr2ps to Ge oxide and that atomic size of the cation is important. There was no evidence for significant participation of hydrogen bonding to the oxide surface. The value of such a molecular level approach to understanding bacterial adhesion to surfaces was emphasized in recent reviews.

CONCLUSIONS: Bacteria have evolved various multiple holdfast structures that enable them to adhere tenaceously to solid surfaces and form fouling biofilms in seawater. Whereas, proteinaceous fimbriae appear to serve as holdfasts during initial contact with the surface, negatively-charged polysaccharides appear to mediate subsequent association with and biofilm formation on the surface. An organic conditioning film present on all surfaces submerged in seawater as well as seawater cations influence the interactions between the holdfast molecules elaborated by the bacteria and the solid substratum. A molecular level approach is useful in elucidating the molecular basis of biofouling of surfaces in seawater.

SIGNIFICANCE: Few bacteria produce polar adhesive EPS. Previously, published reports indicate that *Caulobacter* spp., *Asticcacaulis biprosthecum*, *Thiothrix* spp., *Seliberia stellata*, and *Bradyrhizobium japonicum* produce these molecules. The MHS-3 capsular EPS is not just unusual; it is unique among the examples cited above because it is an extensive, integral EPS capsule, whereas the others are not.

This research is the first to demonstrate fimbril production in *Hyphomonas*, one of several genera to produce polar fimbriae. Polar fimbriae of *Pseudomonas aeruginosa* have been implicated in adhesion to mammalian tissues during pathogenesis and to solid surfaces such as stainless steel and polystyrene. Interestingly, *Thiothrix* spp., *Caulobacter* spp., and *A. biprosthecum* also produce polar tuffs of fimbriae at the same locus as the holdfast.

The temporal and spatial regulation of the adhesive structures of MHS-3 and VP-6 can be correlated with putative function. MHS-3 appears to synthesize capsular EPS and fimbriae simultaneously. The value of these events as an attachment strategy could be that two chemically distinct adhesive molecules are presented, which should allow interactions with a wide array of surfaces. The fimbriae are 1-2 μm long and the EPS capsule is 200-300 nm thick. Alternatively, fimbriae could mediate long-range, primary binding of a cell to a surface, since they extend beyond the EPS capsule and can tether the cell to the surface and then retract to bring the EPS adhesive capsule in contact with the surface to initiate more binding interactions and a more stable association with the surface. A similar adhesion process could also be invoked for VP-6, with its 2 types of polysaccharide adhesives and polar fimbriae. Thus, protein and polysaccharide molecules are likely to participate in bacterial cell adhesion to surface submerged in seawater.

AWARD INFORMATION: Ace Baty received his M.S. in Chemical Engineering from Montana State University in August,1996. Steve Langille received his Ph.D. in Microbiology from the University of Maryland, College Park, MD, in December,1997. Gill Geesey was elected as a Fellow of the American Academy of Microbiology in July, 1995. Geesey also received an award for exemplary service in fostering excellence in research from the National Water Research Institute in October, 1996.

PUBLICATIONS:

Langille, S.E. and R.M. Weiner (1998) Spatial and temporal deposition of *Hyphomonas* strain VP-6 capsules involved in biofilm formation. Appl. Environ. Microbiol. 64:2906-2913.

Guezennec, J., O.Ortega-Morales and G. Geesey (1998) Bacterial colonization of artificial substrata in the vicinity of deep-sea hydrothermal vents. FEMS Microb. Ecol. 26:89-99.

Bhosle, N., P.A. Suci, A.M. Baty, R.M. Weiner, and G.G. Geesey (1998) Influence of divalent cations and pH on adsorption of a bacterial polysaccharide adhesin. J. Colloid Interface Sci. 205:89-96.

Suci, P.A. and G.G. Geesey (1998) Molecular level approach to microbial adhesion to inert surfaces. Recent Res. Devel. Microbiol. 2:107-113.

Quintero, E.J., K. Busch, and R.M. Weiner (1998) Spatial and temporal deposition of adhesive extracellular polysaccharide capsule and fimbriae by *Hyphomonas* strain MHS-3. Appl. Environ. Microbiol. 64:1246-1255.

Baty, A.M., P.K. Leavitt, C.A. Siedlecki, B.J. Tyler, P.A. Suci, R.E. Marchant and G.G. Geesey (1997) Adsorption of adhesive proteins from the marine mussel, *Mytilus edulis*, on polymer films in the hydrated state using angle dependent XPS and AFM. Langmuir 13:5702-5710.

Weiner, R., S Langille, G. Geesey and E. Quintero (1997) Function of bacterial (Hyphomonas spp.) capsular exopolysaccharide in biofouling. pp., 373-386, *In* J. Saxema (ed), Recent Advances in Marine Science and Technology, 96, PACON International, Honolulu, HA.

Baty, A.M., B. Frolund, G.G. Geesey, S. Langille, E.J. Quintero, P.A. Suci and R.M. Weiner (1996) Adhesion of biofilms to inert surfaces: A molecular level approach directed at the marine environment. Biofouling 10:111-121.

Frolund, B., P.A. Suci, S. Langille, R.M. Weiner and G.G. Geesey (1996) Isolation and partial characterization of a non-specific bacterial polysaccharide adhesin from *Hyphomonas* MHS-3. Biofouling 10:17-30.

Schamberger, P.C., F., Caccavo, Jr., F. van Ommen Kloeke, G.G. Geesey, (1996) Microbial Cell Fingerprinting--Development of TOF-SIMS for the Study of Microbial Cell Surfaces. pp. 91-95, *In* Surfaces in Biomaterials Symposium Notebook.

Weiner, R.M., S. Langille, and E. Quintero (1995) Structure, function and immunochemistry of bacterial exopolysaccharides. J. Ind. Microbiol. 15:339-346.

Quintero, E.J. and R.M. Weiner (1995) Physical and chemical characterization of the polysaccharide capsule of the marine bacterium, *Hyphomonas* strain MHS-3. J. Ind. Microbiol. 15:347-351.

Suci, P.A., B. Frolund, E.J. Quintero, R.M. Weiner and G.G. Geesey (1995) Adhesive extracellular polymers of *Hyphomonas* MHS-3: interaction of polysaccharides and proteins. Biofouling 9:95-114.

Schamberger, P.C., A.M. Baty III, B. Frolund, B.J.,Tyler, G.G. Geesey, P.J. McKeown, L.E. Davis, (1995) Application of TOF-SIMS to the Study of Biological Adhesives. pp.147-152, *In* Surfaces in Biomaterials Symposium Notebook.

Journal of Industrial Microbiology (1995) 15, 347–351

Physical and chemical characterization of the polysaccharide capsule of the marine bacterium, *Hyphomonas* strain MHS-3

EJ Quintero and RM Weiner

Department of Microbiology, University of Maryland, College Park, MD 20742, USA

***Hyphomonas* MHS-3 is a biphasic, marine bacterium that synthesizes an exopolysaccharide (EPS) capsule, which has a role in attaching the adherent, prosthecate developmental stages to solid substrata. To correlate structure with function, we characterized this integral EPS. It has a relatively homogeneous molecular weight of approximately 60 000 daltons, is acidic, and putatively contains large concentrations of *N*-acetylgalactosamine (GalNAc). The theoretical identity of the anionic component of the polymer, and the similarities between *Hyphomonas* MHS-3 EPS and other adhesive marine/aquatic bacterial EPS are discussed.**

Keywords: polysaccharides; bacterial capsule; adhesion; biofilm

Introduction

The mechanism of bacterial adhesion to marine surfaces has not yet been fully elucidated. Previously, we reported evidence that a marine bacterium, *Hyphomonas* MHS-3 (MHS-3), adheres via an exopolysaccharide (EPS) capsule, which is produced in copious amounts. This paper reports on its structure and discusses how it may contribute to adhesiveness.

Hyphomonads have a biphasic life cycle, one phase being sessile, and the other flagellated and free-swimming (swarmers) [22]. *Hyphomonas* was chosen for this study, in part, because it is a primary colonizer of marine surfaces [3]. Only the sessile phase synthesizes the adhesive EPS capsule which also forms a large part of the biofilm matrix (Quintero and Weiner, submitted for publication). Multiple layers of cells become imbedded in this hydrated matrix [8]. In fact, more than 80% of the marine bacteria associated with deep sea aggregates possess EPS capsules, which are thought to be responsible for attachment to and formation of particular aggregates in the water column [11].

In addition to their putative role in adhesion, EPS biofilm matrices serve several different functions which enhance survival and influence the surrounding environment. They retain extracellular enzymes near the cell [32], protect against desiccation [5,7], and enhance virulence of pathogenic bacteria [10,23,25]. Some biofilms also cue marine invertebrate larval settlement and metamorphosis, which helps to establish a thriving community [16,31,37,38]. EPS are instrumental in metal binding [6], and generally protect cells from toxic compounds [9]. Finally, it has been demonstrated that EPS is critical in the second step of bacterial adhesion, that is, the irreversible attachment or cementation of the cells to surfaces [9,18].

Correspondence: Dr EJ Quintero, Department of Microbiology, University of Maryland, College Park, MD 20742, USA
Received 16 November 1994; accepted 11 May 1995

Materials and methods

Bacterial strains, media and chemicals

Wild-type *Hyphomonas* strain MHS-3 (MHS-3) was isolated from shallow water sediments in Puget Sound, WA, USA by J Smit, and kindly given to R Weiner. Reduced adhesion (MHS-3 rad) phase variants were isolated by their different colony morphology on agar plates (named for their low adhesion to surfaces and less biofilm formation in broth cultures). These strains were cultured in Marine Broth 2216 (MB; [41]) (37.4 g L^{-1}; Difco Laboratories, Detroit, MI, USA). Except where noted, *Hyphomonas* MHS-3 was always grown at 25° C. Marine agar (MA) was prepared by adding agar to Marine broth, to a final concentration of 2% w/v. Except when indicated otherwise, all chemicals were purchased from Sigma Chemical Co (St Louis, MO, USA) or Fisher Scientific (Pittsburgh, PA, USA).

EPS purification

Teflon mesh was introduced into the culture vessels to provide more surface for biofilm formation (mesh opening 1.8 mm, thread diameter 0.5 mm; Tetko Inc, Briarcliff, NY, USA). Briefly, EPS was purified as follows: cultures were grown to early stationary phase, the spent medium was discarded, and the flocs and the biofilm (mechanically removed from culture vessel walls and from teflon mesh) were centrifuged at 16 000 × *g* for 20 min. The supernatant fluid was precipitated with four volumes of ice-cold 2-propanol, and the cell pellet blended in a Waring blender with 10 mM EDTA, 3% NaCl for 1 min at 4° C to shear off the capsular EPS. The suspension was again centrifuged, the cell pellet discarded and the sheared EPS in the supernatant phase was precipitated with 2-propanol as described above. The precipitate was resuspended in minimum volume of dH_2O and dialyzed exhaustively against dH_2O, and lyophilized. The following steps are a modification of the purification procedure of Read and Costerton [29]. The crude EPS was dissolved in a minimum volume of 0.1 M $MgCl_2$. DNase and RNase were added to a final concentration of 0.1 mg ml^{-1} each, and incubated at 37° C for 4 h. Protease K was added to a final concentration of 0.1 mg ml^{-1} and

the mixture was incubated at 37° C overnight. The residual protein was removed by hot phenol extraction, followed by a chloroform extraction. This was repeated as necessary until no protein was detected by the BCA assay (see colorimetric and enzymatic assays). The EPS solution was dialyzed exhaustively against dH_2O and lyophilized. This partially purified EPS was redissolved in dH_2O, and further purified by gel permeation chromatography to separate the capsular EPS from contaminating lipopolysaccharide.

Column chromatography

Solutions (1 mg ml^{-1}) of EPS were chromatographed on a column (45 × 1.5 cm) of Sephacryl S-400-HR gel permeation resin (Pharmacia, Piscataway, NJ, USA) using 50 mM ammonium acetate, pH 7.0 (containing 0.02% NaN_3) as the elution buffer, at a flow rate of 0.5 ml min^{-1}. Fractions of 3 ml were collected and analyzed for total carbohydrate by the colorimetric assay of Dubois *et al* [12]. Solutions (1 mg ml^{-1}) of dextran molecular weight standards of 5 000 000, 2 000 000, 500 000, 70 000, 40 000, and 10 000 daltons (Pharmacia; Sigma Chemical Co) were used to standardize the column. Ion-exchange chromatography was performed using a Mono Q anion exchange column (quaternary amine column) (Pharmacia) in a Pharmacia LKB (Piscataway, NJ, USA) FPLC system, comprised of a LCC-500 plus controller module, two P-500 pumps and a FRAC-200 fraction collector. EPS solutions (500 μl of 2 mg ml^{-1} solutions) in 20 mM Tris buffer, pH 8.0, were loaded into the column. Samples were first eluted with 5 ml of Tris buffer, then with a linear gradient of NaCl from 0.05 to 1.0 M (in buffer) at a flow rate of 1 ml min^{-1}. Fractions of 1 ml were collected and analyzed for total carbohydrate.

Colorimetric and enzymatic assays

All chemicals utilized to prepare reagents for these tests were high purity or reagent grade, and all glassware was acid-washed prior to use. The carbohydrate (CHO) assay of Dubois *et al* [12] was used to measure the neutral hexose content of samples. Glucose standards (10–100 μg ml^{-1}) were used to prepare the standard curve. Total protein was measured using the Pierce BCA (bicinchoninic acid) protein reagent (Pierce, Rockford, IL, USA), using reagents and protocols supplied by the manufacturer. Standards (10–100 μg ml^{-1}) were prepared with bovine serum albumin (BSA). Uronic acids were quantified following the procedure of Blumenkrantz and Asboe-Hansen [4]. The metaphenylphenol reagent was purchased from Eastman Kodak Co (Rochester, NY, USA).

The presence of acetyl groups on the EPS was assayed using a modified colorimetric procedure [14,20]. Just prior to the test, a working reagent was prepared by mixing equal volumes of 8.0 M hydroxylamine hydrochloride and glycine reagent (1.0 M glycine in 8.5 M NaOH); 200 μl of test sample were mixed with 400 μl of this reagent in a large glass test tube and incubated at room temperature for 3 h. Then, 2.5 ml of 1.0 M HCl and 6 ml of ferric chloride reagent (0.1 M $FeCl_3$ in 0.01 M HCl) were added, and the absorbance was measured immediately at 540 nm (A_{540}) before precipitate formed.

Pyruvylation of the EPS was tested using an enzymatic assay developed by Duckworth and Yaphe [13]. Briefly, 1.5 ml of 0.08 N oxalic acid was added to 5 mg of EPS (in 1.5 ml dH_2O) and refluxed for 5 h at 100° C to hydrolyse pyruvate from EPS backbone. After cooling, 230 mg of calcium carbonate were added to each tube to neutralize the solution, and the amount of free pyruvate present was assayed using lactate dehydrogenase (Sigma Chemical Co), following the manufacturer's specifications. The presence of lipopolysaccharide (LPS) was determined using the *Limulus* Amebocyte Lysate (LAL) assay (Associates of Cape Cod, Inc, Woods Hole, MA, USA) according to manufacturer's instructions. LPS was also identified using polyacrylamide gel electrophoresis with sodium dodecyl sulfate (SDS-PAGE), and the silver staining procedure of Tsai and Frasch [33], as modified by Hitchcock and Brown [15] to visualize it.

Monosaccharide analysis of EPS

High performance anion exchange chromatography (HPAE) was used to identify the major monosaccharide components of the EPS, following a protocol described by Reddy *et al* [30]. Briefly, 200 μg of purified EPS were hydrolysed in 200 μl of 2 N HCl at 100° C for 2 h. Samples were dried under a stream of nitrogen and resuspended in 200 μl of dH_20; the injection volume was 20 μl. The system used for HPAE consisted of a Dionex BioLC gradient pump (Dionex Corp, Sunnyvale, CA, USA) with a pulsed amperometric detector (PAD). A Carbopac PA1 (4 × 250 mm) pellicular anion exchange column (Dionex Corp) with a Carbopac guard column was used at a flow rate of 1 ml min^{-1} at room temperature. Two different eluants (degassed with helium) were used: eluant 1, 15 mM NaOH, useful for the analysis of neutral and amino sugars, and eluant 2, 100 mM NaOH, 150 mM sodium acetate, effective in the analysis of acidic monosaccharides. A monosaccharide standard solution (85 μg ml^{-1} of each sugar, 20 μl injected) was run after each hydrolysed EPS sample to identify the monomers.

Infrared spectroscopy (IR)

IR analysis was carried out to test for the presence of sulfate groups in the EPS [19]. One milligram of EPS was mixed with 100 mg of potassium bromide (IR grade), and ground with mortar and pestle. About half the fine powder was placed into a die and compressed into a translucent pellet. The pellet was placed into a Perkin Elmer 1600 Series FTIR (Perkin-Elmer Co, Norwalk, CT, USA), and a spectrum was obtained. Chondroitin sulfate was used as a standard.

Results

Chemical characterization of MHS-3 EPS

The partially purified capsular EPS (treated with nucleases, protease, hot phenol and chloroform extraction) was contaminated with small amounts (<2%) of LPS; however, as noted in the materials and methods section, no protein was detected (lower limit, 5 μg mg^{-1} EPS). Anion exchange chromatography revealed that both the LPS and the EPS were negatively charged (Figure 1). The capsular EPS sharply eluted at 0.25 M NaCl; the LPS broadly eluted from

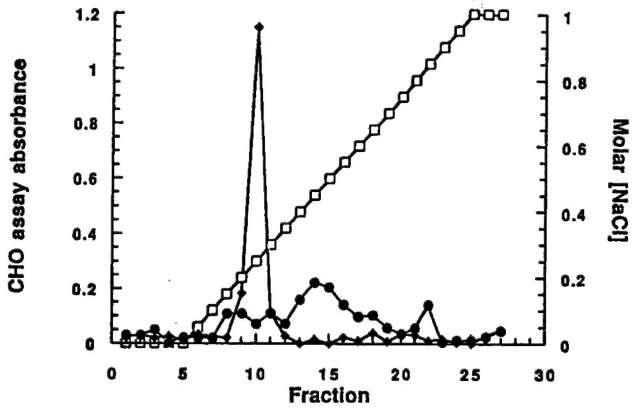

Figure 1 Anion exchange chromatography of partially purified *Hyphomonas* MHS-3 LPS and capsular EPS. The samples were chromatographed in a Mono Q quaternary amine column. The capsular EPS eluted with 0.25 M NaCl. LPS eluted broadly, between 0.15 M and 0.8 M NaCl, with a major fraction which eluted at 0.4 M NaCl. —◆— Capsular EPS; —●— LPS; —□— molar (NaCl)

0.15 M to about 0.8 M NaCl. However, this procedure was not useful for purification, since both species coeluted.

In contrast, gel permeation chromatography did separate EPS and LPS (Figure 2). The separation was facilitated because the LPS aggregated into micelles and bilayer vesicles [42]. LPS aggregates eluted with an average molecular weight of approximately 2 000 000 daltons, and the EPS was calculated to have an average molecular weight of approximately 60 000 daltons (Figure 2). LPS was identified in silver-stained SDS-PAGE gels and by the results of the LAL assay (data not shown).

The purified capsular EPS was characterized using colorimetric and enzymatic assays. No LPS was detected (LAL assay, lower limit 6 pg LPS per mg EPS) after final gel permeation chromatography; nor was it detected in LPS-silver-stained gels (negative data not shown). The polymer

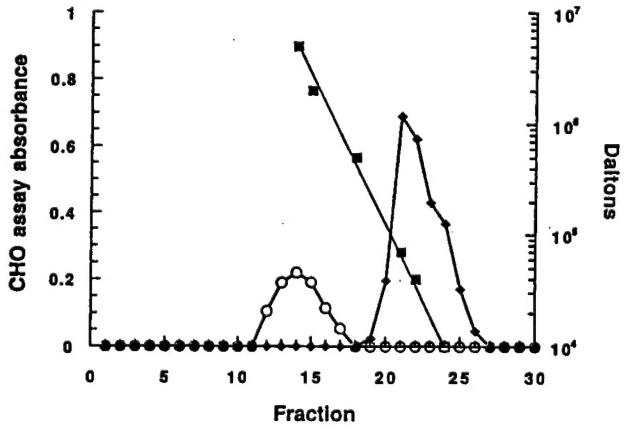

Figure 2 Gel permeation chromatography of partially purified *Hyphomonas* MHS-3 LPS and capsular EPS. The medium was Sephacryl S-400-HR resin. The elution profile of the dextran molecular weight standards is indicated, and the average molecular weights can be read on the *y*-axis. The peak of capsular EPS elution centered around fraction #21, indicating that the average molecular weight of the EPS is 60 000 daltons. LPS usually aggregates into micelles in aqueous solution. This is reflected in its elution pattern at 2 000 000 daltons MW. Its true molecular weight is much lower, as indicated by SDS-PAGE. —○— LPS; —◆— capsular EPS; —■— molecular weight

Table 1 Chemical characterization of *Hyphomonas* MHS-3 capsular EPS

Group	Quantity (μg mg^{-1} EPS)[a]	Assay reference
Neutral hexose	710	[12]
Uronic acid	ND[b]	[4]
Acetyl groups	75	[14,22]
Pyruvate	ND	[13]
Sulfate	ND	[21]

[a]Amount detected per mg dry weight of purified EPS
[b]Not detected (<5 μg mg^{-1})

was acetylated, but neither uronic acids nor pyruvate were detected (Table 1). However, the absence of uronic acid and pyruvate groups could not be confirmed by IR due to 'water noise' between the 1400–1900 cm^{-1} frequencies. The absence of an absorbance peak at 1250 cm^{-1} (Figure 3) suggested that the EPS does not have sulfate groups. On the other hand, an absorbance peak at 1654 cm^{-1} confirmed the presence of acetyl groups. This absorbance frequency is in the area where the carbonyl stretching band of amides is found, characteristic of acetamido groups in *N*-acetylated sugars. In fact, most amino sugars found in microbial EPS are usually *N*-acetylated [8].

The High Performance Anion Exchange Chromatography analysis of the hydrolysed EPS revealed that the major monosaccharide component of the polymer is galactosamine (Figure 4a). Again, no uronic acids were detected (Figure 4b). Several minor unknown peaks (considered degradation products of acid-labile sugars) and a glucose peak were found in the neutral sugar chromatogram (Figure 4a), but the areas under these peaks were so small as to suggest they were contaminants.

Discussion

Chemical characterization of the capsular EPS, synthesized by MHS-3, indicates that it contains *N*-acetyl-galactosamine. HPAE data confirms galactosamine as a major component, and the colorimetric assay for acetyl groups is posi-

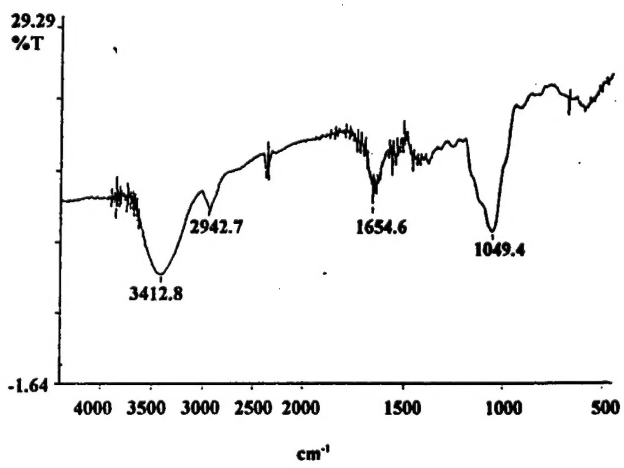

Figure 3 IR spectrum of *Hyphomonas* MHS-3 capsular EPS. The absorbance peak at a frequency of 3413 cm^{-1} is attributed to OH groups, at 1049 cm^{-1} to C—O, and at 1654 cm^{-1} to C=O in acetamido groups

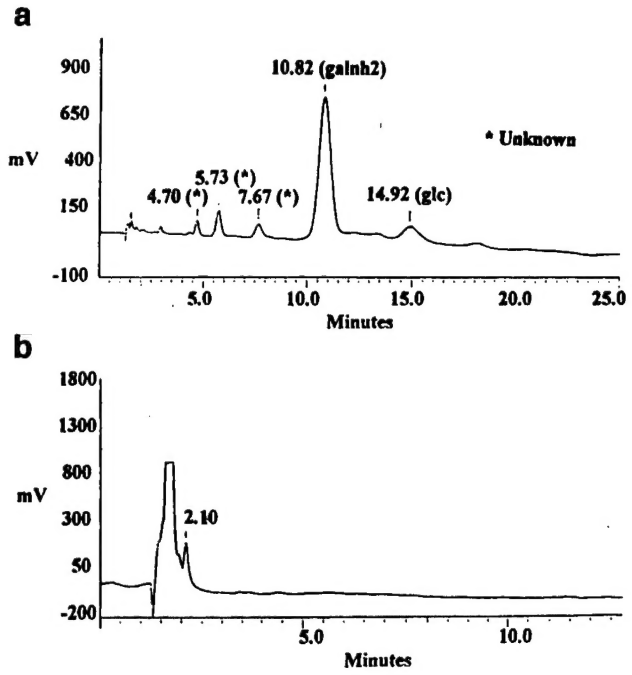

Figure 4 HPAE chromatograms of hydrolysed purified *Hyphomonas* MHS-3 capsular EPS. Two eluants were used: eluant 1 (a), 15 mM NaOH, was used for the analysis of neutral and amino sugars. Galactosamine (galnh2) was the only major monosaccharide component detected. Unknown peaks and glucose (glc) were found in trace amounts and deemed to be contaminants. Eluant 2 (b) (100 mM NaOH, 150 mM sodium acetate) was used in the analysis of acidic monosaccharides; none was detected

tive. Finally, IR analysis reveals the presence of amide groups in the MHS-3 EPS, which implies the presence of acetamido groups (*N*-acetyl linkage).

Hyphomonas MHS-3 EPS is acidic, since it was retained in anion exchange columns, and because it binds polycationic ferritin (data not shown). Nonetheless, the identity of the negative charge still remains to be elucidated. Sulfate and pyruvate groups were not detected. Less commonly appearing acidic groups such as succinate (found in succinoglucans, [17]) and phosphate [24] were not screened. However, though uronic acids were not detected by colorimetric assay nor HPAE analysis, their presence cannot be ruled out. This is because aminuronic acids (amino sugars that are also uronic acids) are not detected by the existent colorimetric assays for uronic acids ([27]; E Rosenberg, personal communication). Also, since these sugars are acid-labile [27], they would have been destroyed during the acid hydrolysis of the EPS, and thus, they would not have been detected by HPAE either.

Therefore, the *Hyphomonas* MHS-3 EPS could conceivably contain *N*-acetylgalactosaminuronic acid. So far, only two bacterial polysaccharides have been reported to contain this sugar, the *O*-antigen polysaccharide of *Pseudomonas aeruginosa* LPS [40], and the major acidic EPS of *Pseudomonas solanacearum* [27]. *P. solanacearum* EPS and *Hyphomonas* MHS-3 EPS may share some features. *P. solanacearum* EPS is a heteropolymer composed of equimolar amounts of *N*-acetylgalactosamine (GalNAc), 2-*N*-acetyl-2-deoxy-L-galacturonic acid (*N*-acetyl-galactosaminuronic acid) (GalANAc), and the bacillosamine derivative 2-*N*-acetyl-4-*N*-(3-hydroxybutanoyl)-2,4,6-tri-deoxy-D-glucose (Bac2NAc4N(30HBut)) [27]. Interestingly, early characterization of *P. solanacearum* EPS revealed *N*-acetyl-galactosamine as the only component [1]. An acid-resistant glycosidic linkage between two acid-labile sugars could explain the fact that neither GalANAc nor Bac2NAc4N(30HBut) had initially been detected [27]. *Hyphomonas* MHS-3 capsular EPS could well have a similar structure, which would pose the same analytical problems.

The average molecular weight of *Hyphomonas* MHS-3 EPS is approximately 60 000 daltons. *P. aeruginosa* has been reported to produce a low molecular weight EPS (chemically distinct from the high molecular weight alginate also synthesized) only when growing in a biofilm [2]. The low molecular weight EPS is around 10 000 daltons, and contains mannose, galactose and an unidentified amino sugar. It has been proposed to be involved in the attachment of *P. aeruginosa* to surfaces [2]. *Staphylococcus aureus* also synthesizes a low molecular weight EPS (30 000 daltons) [26].

In the prosthecate genera *Caulobacter* and *Asticcacaulis*, attachment to surfaces appears to be mediated by a polar, acidic EPS organelle termed holdfast [28,36]. It is interesting that the *Hyphomonas* MHS-3 capsular EPS also shares certain commonalities with these adhesive EPS. The *Hyphomonas* MHS-3 EPS and those of *Caulobacter* spp [28] and *Asticcacaulis biprosthecum* [36] are all acidic exopolysaccharides. Furthermore, as we suggest above, *Hyphomonas* MHS-3 EPS contains the amino sugar, *N*-acetylgalactosamine. During lectin analysis of the adhesive holdfast of 26 different species of *Caulobacter*, 15 out of 16 marine species and 6 out of 10 freshwater species contained the amino sugar *N*-acetylglucosamine [21]. Additionally, the acidic, polar slime EPS synthesized by *Rhizobium japonicum* is bound by *Glycine max* lectin (SBA) [34,35]. This lectin binds polymers containing *N*-acetylgalactosamine. It is conceivable that the presence of acidic groups and amino sugars may be characteristic of a class of adhesive EPS.

The *Hyphomonas* MHS-3 capsular EPS appears to be an integral EPS, since it is not released into the culture medium. This is consistent with several general characteristics of adhesive EPS [8], since enhanced solubility should work against adhesion. Furthermore, adhesive properties are probably dependent on the conformational state of the polymer, since the arrangement of functional groups may change at different conformations. *Pseudomonas* sp strain S9 synthesizes two forms of EPS, one integral and the other peripheral [39]. The integral EPS was associated with cell adhesion to surfaces, and the peripheral EPS with cell desorption from the surface during starvation.

Thus, it is possible that in *Hyphomonas* MHS-3, structure follows function, and that the EPS capsule may be a primary adhesive, in addition to its role in the formation of biofilm.

Acknowledgements

This work was supported by grants from the Maryland Industrial Partnerships (MIPS), the Office of Naval

Research (ONR) N00014-93-1-0168, and Oceanix Biosciences Corp, Hanover, MD, USA.

References

1 Akiyama Y, S Eda, S Nishikawaji, H Tanaka, T Fujimori, K Kato and A Ohnishi. 1986. Extracellular polysaccharide produced by a virulent strain (U-7) of *Pseudomonas solanacearum*. Agric Biol Chem 50: 747–751.

2 Allison DG. 1992. Polysaccharide interactions in bacterial biofilms. In: Biofilms—Science and Technology (Melo LF, TR Bott, M Fletcher and B Capdeville, eds), pp 371–376, NATO Series E: Applied Sciences, vol 223, Kluwer Academic Publishers, Boston.

3 Baier R, A Meyer, V DePalma, R King and M Fornalik. 1983. Surface microfouling during the induction period. J Heat Trans 105: 618–624.

4 Blumenkrantz N and G Asboe-Hansen. 1973. A new method for quantitative determination of uronic acids. Anal Chem 54: 484–489.

5 Boyle CD and AE Reade. 1983. Characterization of two extracellular polysaccharides from marine bacteria. Appl Environ Microbiol 46: 392–399.

6 Brierly CL. 1990. Bioremediation of metal-contaminated surface and groundwaters. Geomicrobiol J 8: 201–223.

7 Bushby HVA and KC Marshall. 1977. Water status of rhizobia in relation to their susceptibility to desiccation and to their protection by momtmorillonite. J Gen Microbiol 99: 19–27.

8 Christensen BE. 1989. The role of extracellular polysaccharides in biofilms. J Biotechnol 10: 181–202.

9 Costerton JW. 1984. Mechanisms of microbial adhesion to surfaces. Direct ultrastructural examination of adherent bacterial populations in natural and pathogenic ecosystems. In: Current Perspectives in Microbial Ecology (Klug MJ and CA Reddy, eds), pp 115–123, Proc 3rd Int Symp Microbial Ecol, Michigan State University.

10 Costerton JW, TJ Marrie and KJ Cheng. 1985. Phenomena of bacterial adhesion. In: Bacterial Adhesion (Savage DC and M Fletcher, eds), pp 3–43, Plenum Press, New York.

11 Cowen JP. 1992. Morphological study of marine bacterial capsules: implications for marine aggregates. Mar Biol 114: 85–95.

12 Dubois M, KA Gilles, JK Hamilton, PA Rebers and F Smith. 1956. Colorimetric method for determination of sugars and related substances. Anal Chem 28: 350–356.

13 Duckworth M and W Yaphe. 1970. Definitive assay for pyruvic acid in agar and algal polysaccharides. Chem Ind 23: 47–48.

14 Hestrin S. 1949. The reaction of acetylcholine and other carboxylic acid derivatives with hydroxylamine, and its analytical application. J Biol Chem 180: 249–261.

15 Hitchcock P and T Brown. 1983. Morphological heterogeneity among *Salmonella* lipopolysaccharide chemotypes in silver-stained polyacrylamide gels. J Bacteriol 154: 269–277.

16 Kirchman D, S Graham, D Reish and R Mitchell. 1982. Bacteria induce settlement and metamorphosis of *Jauna (Dexiospira) brasiliensis* Grube (Polychaeta: Spirorbidae). J Exp Mar Biol Ecol 56: 153–163.

17 Linton JD, M Evans, DS Jones and DN Gouldney. 1987. Exocellular succinoglucan production by *Agrobacterium radiobacter* NCIB 11883. J Gen Microbiol 133: 2961–2969.

18 Marshall KC. 1992. Biofilms: an overview of bacterial adhesion, activity, and control at surfaces. Am Soc Microbiol News 58: 202–207.

19 Matsuda M, W Worawattanamateekul and K Okutani. 1992. Simultaneous production of muco- and sulfated polysaccharides by marine *Pseudomonas*. Nippon Susian Gakkaishi 58: 1735–1741.

20 McComb EA and RM McCready. 1957. Determination of acetyl in pectin and in acetylated carbohydrate polymers. Anal Chem 29: 819–821.

21 Merker RI and J Smit. 1988. Characterization of the adhesive holdfast of marine and freshwater Caulobacters. Appl Environ Microbiol 54: 2078–2085.

22 Moore RL, RM Weiner and R Gebers. 1984. Genus *Hyphomonas* Pongratz 1957 nom rev emend, *Hyphomonas polymorpha* Pongratz 1957 nom rev emend, and *Hyphomonas neptunium* (Leifson 1964) comb nov emend (*Hyphomicrobium neptunium*). Int J Syst Bacteriol 34: 71–73.

23 Moxon ER and JS Kroll. 1990. The role of bacterial polysaccharide capsules as virulence factors. In: Current Topics in Microbiology and Immunology, vol 150 (Jann K and B Jann, eds), pp. 65–85, Springer-Verlag, New York.

24 Nasu M, J Ogaki, T Nishihara, T Ishikawa and M Kondo. 1984. Occurrence of galactosamine-6-phosphate as a constituent of *Bacillus megaterium* spore coat. Microbiol Immunol 28: 181–188.

25 Nichols WW, MJ Evans, MPE Slack and HL Walmsley. 1989. The penetration of antibiotics into aggregates of mucoid and non-mucoid *Pseudomonas aeruginosa*. J Gen Microbiol 135: 1291–1303.

26 Ohtomo T, Y Ohshima, Y Usui and K Yoshida. 1985. Partial purification and characterization of compact colony-forming active substance from an unencapsulated strain of *Staphylococcus aureus*. In: The Staphylococci (Jeljaszewicz J, ed), pp 277–285, Zbl Bakt Suppl 14, Gustav Fischer Verlag, New York.

27 Orgambide G, H Montrozier, P Servin, J Roussel, D Trigalet-Demery and A Trigalet. 1991. High heterogeneity of the exopolysaccharides of *Pseudomonas solanacearum* strain GMI 1000 and the complete structure of the major polysaccharide. J Biol Chem 266: 8312–8321.

28 Poindexter JS. 1981. The Caulobacters: ubiquitous unusual bacteria. Microbiol Rev 45: 123–179.

29 Read RR and JW Costerton. 1987. Purification and characterization of adhesive exopolysaccharides from *Pseudomonas putida* and *Pseudomonas fluorescens*. Can J Microbiol 33: 1080–1090.

30 Reddy GP, U Hayat, C Abeygunawardana, C Fox, AC Wright, DR Maneval Jr, CA Bush and JG Morris Jr. 1992. Purification and determination of the structure of capsular polysaccharide of *Vibrio vulnificus* M06-24. J Bacteriol 174: 2620–2630.

31 Szewzyk U, C Holmström, M Wrangstadh, MO Samuelsson, JS Maki and S Kjelleberg. 1991. Relevance of the exopolysaccharide of marine *Pseudomonas* sp strain S9 for the attachment of *Ciona intestinalis* larvae. Mar Ecol Prog Ser 75: 259–265.

32 Tonn SJ and JE Gander. 1979. Biosynthesis of polysaccharides by prokaryotes. Annu Rev Microbiol 33: 169–199.

33 Tsai CM and CE Frasch. 1982. A sensitive silver stain for detecting lipopolysaccharides in polyacrylamide gels. Anal Biochem 119: 115–119.

34 Tsien HC and EL Schmidt. 1977. Polarity in the exponential-phase *Rhizobium japonicum* cell. Can J Microbiol 23: 1274–1284.

35 Tsien HC and EL Schmidt. 1981. Localization and partial characterization of soybean lectin-binding polysaccharide of *Rhizobium japonicum*. J Bacteriol 145: 1063–1074.

36 Umbreit TH and JL Pate. 1978. Characterization of the holdfast region of wild-type cells and holdfast mutants of *Asticcacaulis biprosthecum*. Arch Microbiol 118: 157–168.

37 Weiner RM, M Walch, MP Labare, DB Bonar and RR Colwell. 1989. Effect of biofilms of the marine bacterium *Alteromonas colwelliana* (LST) on set of the oysters *Crassostrea gigas* (Thunberg, 1793) and *C. virginica* (Gmelin, 1791). J Shellfish Res 8: 117–123.

38 Weiner RM, D Sledjeski, E Quintero, S Coon and M Walch. 1992. Periphytic bacteria cue oyster larvae to set on fertile benthic biofilms. Abstracts of the 6th International Symposium on Microbial Ecology, Barcelona, Spain.

39 Wrangstahd M, U Szewzyk, J Ostling and S Kjelleberg. 1990. Starvation-specific formation of a peripheral exopolysaccharide by a marine *Pseudomonas* sp, strain S9. Appl Environ Microbiol 56: 2065–2072.

40 Yokota S, H Ochi, I Uezumi, H Ohtsuka, K Irie and H Noguchi. 1990. *N*-Acetyl-L-galactosaminuronic acid as an epitope common to the *O*-polysaccharide of *Pseudomonas aeruginosa* serotype A and H (Homma) recognized by a protective human monoclonal antibody. Eur J Biochem 192: 109–113.

41 Zobell C. 1941. Studies on marine bacteria. 1. The cultural requirements of heterotrophic aerobes. J Mar Res 4: 42–75.

42 Zubay GL. 1984. Biochemistry, p 1268, Addison-Wesley Publishing Co, Reading, MA.

Journal of Industrial Microbiology (1995) 15, 339–346

Structure, function and immunochemistry of bacterial exopolysaccharides

R Weiner, S Langille and E Quintero

Department of Microbiology, University of Maryland, College Park, MD 20742, USA

There has been much written on bacterial exopolysaccharides (EPS) and their role in virulence. Less has been published regarding EPS in free living species. This review focuses on that subject, emphasizing their functions in the environment and the use of antibody probes to study them.

Keywords: polysaccharides; bacterial capsule; biofilm

Composition and structure of bacterial polysaccharides

Bacterial surface polysaccharides come in two general forms, those bound to the cell surface by attachment to lipid A lipopolysaccharide (LPS), and those associated with the cell surface as a capsule, exopolysaccharide (EPS). EPS are very hydrated polymers with 99% of their wet weight comprised of water [111]. They have considerable heterogeneity, from the simple α, 1-4 linked, unbranched glucose polymers called dextrans, to the highly complex, branched, and substituted heteropolysaccharides made up of oligosaccharide repeating subunits such as xanthan and colanic acid [17,112]. EPS can also be substituted, normally ester or *N*-linked, with pyruvate, acetate, formate, sulfate, phosphate and other side groups [49].

Part of the structural diversity of EPS is due to the fact that two identical sugars can bond to form 11 different disaccharides. In contrast two identical amino acids can form only one dipeptide. Additionally, EPS contain a wide variety of sugars as for example glucose, mannose, glucuronic acid, and rhamnose in xanthan gum [32], galactose and glucose (*Rhizobium meliloti* [50]), xylose (*Cryptococcus neoformans* [9]), hexosamines, aminouronic acids, aldoses, diaminohexoses [56], 2,3-diamino-2,3-dideoxyuronic acid, and 5,7-diamino-3,5,7,9-tetradeoxynonulosonic acid [137]. Furthermore, the noncarbohydrate side groups that are found in bacterial EPS add to their heterogeneity that, as a consequence of all of these considerations, far exceeds that of proteins and is reflected in the hundreds of *O*-antigen serotypes of enterobacteria [49]. Functions for this heterogenicity have been ascribed to pathogens [24] but not environmental strains [106].

The molecular weights of LPS [15,39,43,78,92] and EPS [17,65,99,117] are also extraordinarily heterogeneous. With incomplete stringent control over the number of subunits added to a chain [6], long and short polymers are synthesized, although one molecular weight species predominates. EPS forms higher order structures [49]. Xanthan gum is thought to from double-strand antiparellel helices [84], while the EPS from various *Klebsiella* spp form left-handed helices [48]. The EPS component of many bacterial films forms thick fibers when examined with electron microscopy [3,8,94]. It has been suggested that these fibers are attached to discrete areas on the outer surface of the cell [8,94]. While EPS and LPS have partial synthetic pathway commonality in some species [58], the remainder of this review shall primarily be concerned with EPS.

Transport attachment and localization of bacterial EPS

A major unanswered question is how the hydrophilic EPS is transported across the hydrophobic interior of the outer membrane to the outer surface of the outer membrane of Gram-negative bacteria. It has been suggested [8], but not documented [12,88], that adhesion sites (Bayer junctions) between the inner and outer membrane are sites of both LPS and EPS transport. Lipid A and *O*-antigen are synthesized separately on the inner face of the inner membrane and are joined on the periplasmic face of the inner membrane [82]. For *E. coli* EPS, a 60-kilodalton periplasmic protein is required for translocation to the outer surface of the outer membrane, whereas a protein is not required for LPS translocation [98,103]. Immunochemical analysis of *Pseudomonas* sp strain S9, suggests that EPS polymerization (or crosslinking) can occur on the outer surface of the outer membrane [135].

The fine structure of the fibrillar structures [3,8,94] radiating out from the cell surface suggests that EPS is bound at a limited number of discrete sites. Once these sites are filled, excess EPS may become the source of slime ([133]; EPS found free in the media). Alternatively, only EPS molecules of the correct length may bind to attachment sites, with larger and smaller molecules forming the slime [112]. Immunoelectron microscopy of a marine pseudomonad suggests that shorter EPS molecules are integrally bound to the outer membrane (integral capsule) while the longer polymers are loosely (peripherally) associated [34]. Without knowledge of export mechanisms it is difficult to theorize just how EPS may be site-specifically deposited. Along with caulobacters, hyphomicrobia are good models to study

Correspondence: Dr R Weiner, Dept of Microbiology, University of Maryland, College Park, MD 20742, USA
Received 7 November 1994; accepted 20 April 1995

mechanisms of EPS deposition. Since export is both polar and temporal, a rare occurrence in procaryotes [93,119,120,122,130], the machinery can be readily correlated with zones of production.

Regulation of bacterial EPS production

Many environmental factors can affect the rate of EPS synthesis in bacteria. They include increased oxygen [7], limitation of nitrogen [51,79] and cations (eg magnesium, sulfate, phosphate and calcium [27,51,112]), desiccation [87,112,129], low temperature [117], growth on minimal media [117] and growth phase [17,121,129,134]. In most of these cases, enhanced EPS synthesis is a response to environmental stress (eg nutrient limitation).

The question of regulation of EPS production has been approached using molecular techniques to analyze the genetic regulation of EPS synthesis in *E. coli* and *Alteromonas atlantica*. The regulatory circuit controlling colanic acid capsule synthesis in *E. coli* includes at least four proteins. RcsA and RcsB are positive *trans*-acting regulators of capsule synthesis and RcsC is a negative regulator [13,42,89]. RcsA is unstable due to its sensitivity to the Lon protease [116]. RcsC and RcsB are similar to many two-component (sensor-effector) regulatory systems [110]. Even though it is still not clear under what environmental stimulus RcsC (the sensor) activates RcsB (the effector), this is the first genetic evidence linking an environmental stimulus to increased EPS production.

The genetic mechanism for regulation of *A. atlantica* EPS synthesis differs markedly from that of colanic acid [5] and more closely resembles the antigenic phase variation described for *Salmonella, E. coli* and *Neisseria* [1,104,114]. These variable systems involve complex reversible genomic rearrangements which can turn EPS synthesis (or antigenic variation) off or on. Under conditions favorable for EPS production, those bacteria which are 'on' will predominate. If the conditions change so that EPS production is no longer favored, those bacteria which were already 'off' will out-compete the 'on' bacteria and predominate [5]. In caulobacters and hyphomonads, EPS regulation is temporal and less influenced by environmental factors [85,124]. In *Pseudomonas aeruginosa*, the intricate regulatory cascade of alginate expression is being worked out [30,35,97,131].

Functions of EPS

EPS is produced by the majority of Gram-negative bacteria, some of which invest more than 70% of their energy in its production [45]. Consequently many species grow faster on laboratory media after they mutate and stop producing EPS. This suggests that some environmental factor selects for continuous EPS production. The existence of a genetic switch in the marine bacterium *A. atlantica* [5] to insure the concurrent existence of both EPS-producing and non-producing forms of the organism emphasizes both the importance of EPS and its demand on cellular resources. Polar EPS synthesis, if EPS is an adhesin, may be another resource-saving mechanism.

As discussed in excellent earlier reviews by Decho [29] and Dudman [31a], many functions have been proposed for bacterial EPS (Table 1). They can be divided into four groups, functioning: a) as a physical protective barrier; b) as a response to environmental stress; c) in cell/cell recognition and interaction; or d) in biofilm formation/adhesion. The ability of EPS to act as a physical barrier has been demonstrated with pathogenic bacteria. Encapsulation of *E. coli, Klebsiella* sp, and pneumococci renders them resistant to phagocytosis, complement fixation, and antibody [37,102]. In fact, the pathogenicity of bacteria can be artificially increased by coating them with hog gastric mucin, a charged mucopolysaccharide [49]. Even though bacteria may be subjected to phagocytosis-like predation in the natural environment, they are not exposed to antibody or complement. There, EPS may protect against bacteriophage [118], hydrophobic toxins [127] and desiccation [81, 87].

In response to stress, when essential cations are required, anionic EPS would sequester them, increasing the gradient across the cell membranes [45]; or, excretion of the charged polymer may provide the driving force for importation of other charged ions [128]. Polymerization of EPS would also produce excess reducing power, used to drive high affinity or high energy uptake systems [45,115]. In symbiotic relationships, the EPS and LPS of some nitrogen-fixing bacteria, most notably *R. meliloti*, but also others [10,68,95], function in the host-specific, bacterial invasion of developing root nodules on leguminous plants [33,64]. The EPS is involved in the initial recognition and attachment of the bacteria, leading directly to morphogenic changes in the plant [10,33,64,95]. Kirchman *et al* [60] showed that *Pseudomonas marina* EPS is an inductive cue for the metamorphosis of the marine polychaete, *Janua brasiliensis*. The metamorphic trigger might involve the binding of a larval lectin to the EPS [59]. Other marine invertebrates however do not specifically bind with bacterial films prior to larval settlement and metamorphosis [125,126].

Nevertheless, it has long been recognized that there is an ordered sequence of periphytic succession for colonization of clean surfaces immersed in seawater. In the initial phase, after possible coating by organic matter [70], bacteria attach to a surface and begin to grow, forming microcolonies within several hours [19,25,31,36,77]. Subsequently, diatoms, fungi, protozoans, micro-algae and other microorganisms attach to the surface, adding to the primary slime layer [25,31,36,77,105]. This primary microbial colonization often appears to be a prerequisite for the final stage of succession in which large organisms, viz, invertebrates, attach and grow on the surface [23,26,139].

The biofilm/adhesion functions of EPS are extremely important medically and commercially. The importance of biofilm formation on bacterial growth in dilute nutrient environments has been recognized since Zobell and Anderson's [140] early work on the relationship between bacterial growth and solid surfaces. The involvement of EPS in initial adhesion of the cells [3,20,44], as the structural matrix of the biofilm and as an active metabolic component of the biofilm, has received much attention [eg 21,22,75,101,113]. Briefly, some EPS may function as an initial adhesion [3], more as a permanent adhesion [44] and many as the biofilm matrix [125].

Table 1 Exopolysaccharide and cell survival

Function	Survival advantage	References
Physical/protective barrier	Protection from desiccation, predation and the immune system. Resistance to toxins, antibiotics and poisons	[49,81,118,127]
Cell–cell recognition and interaction	Plant symbiosis, formation of nodules and microcolonies, invertebrate larvae settlement	[10,33,59,64,95]
Response to environmental stress	Sequestering and import of charged ions, production of excess reducing power	[45,115,128]
Adhesion and biofilm formation	Immobilization onto nutrient-rich surfaces, dissociation from nutrient-depleted surfaces	[3,44,125]

There are two major theories to explain the probability of bacterial attachment to a substratum in aqueous environments [76]. Each states that the adhesion of microorganisms to surfaces is influenced by long-range, short-range, and hydrodynamic forces. The DLVO (letters after first initials of surnames of its proposers) theory assumes that interaction between two objects is comprised of an attractive component, governed by Van der Waals forces, and a potential repulsive component due to overlap of electrical double layers associated with charged groups [70]. These yield two distances at which a particle may be attracted to the substratum. At a primary minimum (*ca* 1 nm), attractive forces are strong; at the secondary minimum (*ca* 15 nm), forces are weaker. These distances are divided by an intermediate repulsion barrier. Microorganisms may accumulate at the secondary minimum and much of the strategy in surface colonization is concerned with remaining at the secondary minimum and overcoming the repulsive barrier to reach the primary minimum [84]. Microorganisms synthesize a variety of tethers for this purpose. All have narrow diameter and sufficient length to minimize and 'break through' the repulsive layer [20]. Such structures have been reported [20] to include capsular exopolysaccharides, pili and flagella, eg long fibular EPS could form an adhesive bridge minimizing electrostatic repulsion [44].

A second, Stern, theory predicts that there will be a net charge distribution at any solid surface and that as a consequence, counter ions are held closely at the surface forming a Stern layer while the rest of the ions are less restricted forming a diffuse ionic atmosphere [70]. This model, probably less applicable in a marine habitat, also predicts a double layer of attractive domains sandwiching a repulsive barrier and would require similar structures to function as tethers as would the DLVO model.

Once bacteria are attached to the surface, multiple events can transpire to carry it to the primary minimum at which multiple bonds of a more permanent nature may be formed between the organism and substratum. This attachment is generally considered to involve hydrophobic bonds of outer membrane components of Gram-negative bacteria or more likely capsular EPS, cement-like biofilm. The roles of EPS in this process have been discussed with the conclusion that 'much more information is required' [16,74].

Christensen [16] points out though, that even with an explosion of new data, structure–function relationships remain largely untested. In a few species it was observed that EPS was not involved in, or inhibited, attachment [14,28,61,62,109,132,133]. An uncharged high molecular weight EPS synthesized by bacteria isolated from fish scales was not adhesive but instead served to decrease drag [100]. Whether an EPS functions as an adhesive or not may be dictated by its chemistry and that of the substratum. EPS is clearly important in the structural matrix of the biofilm. It can bind ions [67] and other nutrients and, thus, functions as more than a relatively inert 'cement'.

Immunochemistry of polysaccharides

Since capsules were recognized as an important virulence factor, the immunochemistry of polysaccharides has been intensively studied [11,47,55,57,73,86,108]. The unique immunological attributes of polysaccharide antigens are summarized in Table 2. Polysaccharides are unusual in that their immunogenicity varies with each animal, eg pneumococcal EPS is non-immunogenic in rabbits but an excellent immunogen in mice [72]. Polysaccharides are also unique in being T-independent antigens, ie they can directly stimulate B-cell antibody production and division without the help of T-cells [41] because their long repetitive structures can directly interact with and activate B-cells [41,52]. As a consequence, there may be little memory and subsequent challenge may not evoke an anamnestic response. It also means that anti-polysaccharide antibodies will be mostly IgM [41].

One of the major factors influencing the antigenicity of a polysaccharide is molecular weight [49]. Dextrans with an average molecular weight >90 000 are good immunogens while dextrans of an average molecular weight <50 000 are non-immunogenic [54]. The size of molecular aggregates [71,116] may be at least as important as polysaccharide chain length [55]. Kabat [53] working with anti-dextran antibodies was able to elucidate the size (six glucose residues) of the antigen-binding site on the antibody. In addition he showed that the nonreducing terminal glucose (designated the immunodominant sugar) contributed most to the antigenicity of the dextran, with each succeeding glucose contributing a smaller increment. Terminal nonreducing sugars on the side chains of the branched mannan antigens of yeast are also usually immunodominant [4,96]. Charge is another important factor in the antigenicity of polysaccharides, with the negatively charged moieties being immunodominant [49]. These include uronic acids, sulfate and phosphate groups [41]. Although phosphate and uronic acids, along with pyruvate and *O*-acetyl groups, can be part of the antigenic determinant, the specificity of the antibody is not always directed against the ionic portion of the polysaccharide [49]. Depyruvylation of xanthan abolishes the binding of anti-xanthan monoclonal anti-

Table 2 Special immunological characteristics of polysaccharide antigens

Characteristic	Postulated mechanism	References
T-independent immune response	Lack of MHC class II presentation of carbohydrate moities due to the inability of mammalian cells to degrade polysaccharides	[2]
Very poor memory	Due to lack of T-cell involvement; even very poor B-cell memory may be masked by antigen tolerance	[80]
IgM antibody isotype	T-independent immune responses generally don't induce the cytokines necessary for a class switch to IgA or IgG	[46]
Larger molecules are more immunogenic	Larger molecules may be more efficient at crosslinking receptors on the surface of B-cells which induces antibody production	[91]
Immunogenicity of polysaccharides varies between animals	Possibly due to the mimicking of host carbohydrate moities to which the host immune system is tolerant	[24]
Immunological paralysis (also caused by other types of antigens)	Caused by the persistence of polysaccharide in the animal (due to the failure of the host to degrade these molecules); also caused by the flooding of B-cell receptors during high zone tolerance preventing the membrane alterations necessary for B-cell stimulation	[49]

bodies [43], however it is not necessarily true that pyruvate directly interacts with the antibody. Pyruvate substitution of hexoses frequently imposes conformational rigidity and depyruvylation could abolish antibody recognition by changing the overall conformation of the polysaccharide. In fact, it may well be that conformational determinants, vs structural determinants, are important [53] and that antibodies recognize the overall three-dimensional shape of the antigenic determinant rather than a specific chemical property such as charge [41].

One of the simplest ways to examine the contribution of any specific portion of the EPS to its antigenicity is by selectively removing or degrading each substituent. The chemically modified EPS can then be tested for its ability to bind antibodies raised against the native molecule [49]. Methods which specifically alter polysaccharide substituents [66] include treatment with NaOH (breakage of ester bonds including *O*-acetyl, pyruvate, phosphate, sulphate), $NaBH_4$ (reduction of uronic acids), oxalic acid (depyruvylation) and periodic acid (oxidation of terminal non-reducing sugars and uronic acids) [66,107].

Although much work has been done on the immunochemistry of pathogenic bacterial EPS, to date many of these powerful approaches have not been applied to environmental bacterial EPS. This is especially the case with monoclonal antibody (hybridoma) technology [38]. Monoclonal antibodies have been produced against xanthan and algal alginate [123], but none has been reported against any marine bacterial EPS until D Sledjeski [106] in our laboratory made them against *Shewanella colwelliana*.

Recently, however, polyclonal antiserum was used as a probe for the microscopic investigation of EPS production by a marine pseudomonad during starvation [134], which synthesized both an integral and a peripheral EPS [34] of unknown functions. Integral EPS was constitutively produced while the peripheral EPS was synthesized as a response to starvation. It was speculated that the integral EPS was involved in adhesion while the peripheral EPS aided in detachment from the surface. Because polyclonal antisera were used, it was unclear whether these were the same EPS of different lengths or two structurally different EPS. Polyclonal antibodies have also been used to show that bacteria adhere differently to different surfaces (titanium or aluminum) based upon differences in the EPS structure [138]. In fact, although it is widely reported that different benthic species have different affinities for different surfaces, only rarely [63] has it been demonstrated that different EPS bind to different surfaces with varying affinities. In this scenario, EPS heterogeneity would be driven by the survival value of adhering a little better than others to specific surface habitats.

Lectins

Lectins are sugar-binding proteins of non-immune origin (from a wide variety of plants and animals) which agglutinate cells and/or precipitate glycoconjugates [40]. They are usually classified into categories according to their carbohydrate specificity: mannose, galactose, *N*-acetylglucosamine, *N*-acetylgalactosamine, L-fucose, *N*-acetylneuraminic acid, to name the most common [136]. These specificities are usually determined by assessing which monosaccharide(s) are the most effective inhibitors of agglutination of erythrocytes, or precipitation of carbohydrate-containing polymers by the lectin [69].

Lectins usually form dimers, with one sugar-binding site per subunit, although there are a few exceptions. The dissociation kinetics of lectin-carbohydrate complexes are very slow [69]. There is evidence for the importance of molecular shape in lectin-carbohydrate interactions; some lectins react poorly with monosaccharides, but combine readily with oligosaccharides. Some recognize only terminal nonreducing saccharides, while others also recognize internal sugar sequences [69]. At the present time, there are numerous applications for lectins, a number of which differ from those of antibodies. They are used without modifications as agglutinins; radiolabelled or conjugated with enzymes, biotin, fluorescent dyes, or colloidal gold as label and indicators for glycoproteins, or specific tissues or cell strains [69]. Lectins immobilized on chromatography resins or solid substrates are used to isolate or purify oligosaccharides, glycoproteins, and bacterial cells [90].

Directions

Important theoretical questions, intricately involving EPS, have been posed and briefly discussed in an earlier review [29]. Bacterial EPS have also been widely commercialized, having multiple uses [18] including burgeoning applications in metal bioremediation [12a]. Yet the extraordinary diversity of these polymers coupled with the fact that only a small percentage of environmental bacteria have yet been isolated, promises the discovery of new and unique EPS with different properties and applications. Antibodies and other molecular probes will be used to learn of their function and regulation, and for their purification.

Acknowledgements

We thank D Sledjeski for critical reading of the manuscript. R Weiner and S Langille were supported by a grant from Oceanix Biosciences Corporation and Ernesto Quintero by a grant from the Office of Naval Research (ONR) N 00014-93-1-01-68.

References

1 Abraham JM, CS Freitag, JR Clements and BI Eisenstein. 1985. An invertible element of DNA controls phase variation of type 1 fimbriae of *Escherichia coli*. Proc Natl Acad Sci USA 82: 5724–5727.
2 Ada GL. 1987. How does the immune system handle antigen proteins versus carbohydrate? In: Towards Better Carbohydrate Vaccines (Bell R and G Torrigiani, eds), pp 335–345, John Wiley and Sons, London.
3 Allison DG and IW Sutherland. 1987. The role of exopolysaccharides in adhesion of freshwater bacteria. J Gen Microbiol 133: 1319–1327.
4 Ballou CE. 1982. A study of the immunochemistry of three yeast mannans. J Biol Chem 245: 1197–1203.
5 Bartlett DH, ME Wright and M Silverman. 1988. Variable expression of extracellular polysaccharide in the marine bacterium *Pseudomonas atlantica* is controlled by genome rearrangement. Proc Natl Acad Sci USA 85: 3923–3927.
6 Batchelor RA, GE Araguchi, RA Hull and S Hull. 1991. Regulation by a novel protein of the bimodal distribution of lipopolysaccharide in the outer membrane of *E. coli*. J Bacteriol 173: 5699–5704.
7 Bayer AS, F Eftekhar, J Tu, CJ Nost and DP Speert. 1990. Oxygen dependent up-regulation of mucoid exopolysaccharide (alginate) production in *Pseudomonas aeruginosa*. Infect Immun 58: 1344–1349.
8 Bayer M and H Thurow. 1977. Polysaccharide capsule of *Escherichia coli*: microscope study of its size, structure, and sites of synthesis. J Bacteriol 130: 911–936.
9 Bhattacharjee AK, JE Bennett and CPJ Glaudemans. 1984. Capsular polysaccharides of *Cryptococcus neoformans*. Rev Infect Dis 6: 619–624.
10 Binns AN and MF Thomashow. 1988. Cell biology of *Agrobacterium* infection and transformation of plants. Ann Rev Microbiol 42: 575–606.
11 Bortolussi R, P Ferrieri, B Bjorksten and PG Quie. 1978. Capsular K1 polysaccharide of *Escherichia coli*: relationship to virulence in newborn rats and resistance to phagocytosis. Infect Immun 25: 293–298.
12 Boulnois GJ and K Jann. 1989. Bacterial polysaccharide capsule synthesis, export and evolution of structural diversity. Mol Microbiol 3: 1819–1823.
12a Brierley CL. 1991. Bioremediation of metal-contaminated surface and groundwaters. Geomicrobiol J 8: 201–223.
13 Brill JA, C Quinlan-Walshe and S Gottesman. 1988. Fine-structure mapping and identification of two regulators of capsule synthesis in *Escherichia coli* K12. J Bacteriol 170: 2599–2611.
14 Brown CM, DC Ellwood and JR Hunter. 1977. Growth of bacteria at surfaces: influence of nutrient limitation. FEMS Microbiol Lett 1: 163–166.
15 Carlson RW. 1984. Heterogeneity of *Rhizobium* lipopolysaccharides. J Bacteriol 158: 1012–1017.
16 Christensen BE. 1989. The role of extracellular polysaccharides in biofilms. J Biotechnol 10: 181–202.
17 Christensen B, J Kjosbakken and O Smidsrod. 1985. Partial chemical and physical characterization of two extracellular polysaccharides produced by marine periphytic *Pseudomonas* sp strain NCMB 2021. Appl Environ 50: 837–845.
18 Colwell R, E Pariser and A Sinsheep (eds). 1985. Biotechnology of Marine Polysaccharides. Hemisphere Pub, Washington, 559 pp.
19 Corpe WA. 1973. Microfouling: the role of primary film forming bacteria. In: Proceedings of the Third International Congress on Marine Corrosion Fouling (Ackjer RF, BF Brown, JR DePalma and WP Iverson, eds), pp 598–609, Northwestern University Press, Evanston, IL.
20 Costerton JW, T Marrie and K-J Cheng. 1985. Phenomena of bacterial adhesion. In: Bacterial Adhesion (Savage D and M Fletcher, eds), pp 3–43, Plenum Press, NY.
21 Costerton JW, K-J Cheng, GG Geesey, TI Ladd, JCNM Dasgupta and TJ Marrie. 1987. Bacterial biofilms in nature and disease. Ann Rev Microbiol 41: 435–464.
22 Costerton JW, TJ Marrie and K-J Cheng. 1981. The bacterial glycocalyx in nature and disease. Annu Rev Microbiol 35: 299–324.
23 Crisp DJ and JS Ryland. 1960. Influence of filming and of surface texture on the settlement of marine organisms. Nature 185: 119.
24 Cross A. 1990. The biologic significance of bacterial encapsulation. Curr Top Microbiol Immunol 150: 87–95.
25 Cundell AM and R Mitchell. 1977. Microbial succession on a wooden surface exposed to the sea. Int Biodeterior Bull 13: 67–73.
26 Daniel A. 1995. The primary film as a factor in settlement of marine foulers. J Madras Univ 25B: 89–200.
27 Davidson DW. 1978. Production of polysaccharide by *Xanthomonas campestris* in continuous culture. FEMS Lett 3: 347–349.
28 Dawson MP, BA Humphrey and KC Marshall. 1981. Adhesion: a tactic in the survival strategy of a marine vibrio during starvation. Curr Microbiol 6: 196–199.
29 Decho AW. 1990. Microbial exopolymer secretions in ocean environments: their role(s) in food webs and marine processes. Oceanogr Mar Biol Ann Rev 28: 73–153.
30 Deretic V, MJ Schurr, JC Boucher and DW Martin. 1994. Conversion of *Pseudomonas aeruginosa* to mucoidy in cystic fibrosis: environmental stress and regulation of bacterial virulence b, alternative sigma factors. J Bacteriol 176: 2773–2780.
31 DiSalvo LH and GW Daniels. 1975. Observations on estuarine microfouling using the scanning electron microscope. Microbial Ecol 2: 234–240.
31a Dudman WF. 1977. The role of surface polysaccharides in natural environments. In: Surface Carbohydrates of the Prokaryotic Cell (Sutherland IW, ed), pp 357–414, Academic Press, London.
32 Evans CTG, RG Yeo and DC Ellwood. 1979. Continuous culture studies on the production of extracellular polysaccharides. In: Microbial Polysaccharides and Polysaccharases (Berkely RCW, GW Gooday and DC Ellwood, eds), Academic Press, London, New York, and San Francisco.
33 Finan TM, AM Hirsch, JA Leigh, E Johansen, GA Kuldau, S Deegan, GC Walker and ER Singer. 1985. Symbiotic mutants of *Rhizobium meliloti* that uncouple plant from bacterial differentiation. Cell 40: 869–877.
34 Fletcher M and GD Floodgate. 1973. An electron-microscopic demonstration of an acidic polysaccharide involved in the adhesion of a marine bacterium to solid surfaces. J Gen Microbiol 74: 325–334.
35 Franklin MJ and DE Ohman. 1993. Identification of *alg* F in the alginate biosynthetic cluster of *Pseudomonas aeruginara* which is required for alginate acetylation. J Bacteriol 175: 5057–5065.
36 Gerchakov SM, DS Mardzalek, FJ Roth and LR Udey. 1976. Succession of periphytic microorganisms on metal and glass surfaces in natural seawater. In: Proceedings of the Fourth International Congress of Marine Corrosion Fouling, Gaithersberg, MD, USA.
37 Glynn AA. 1972. Microbial Pathogenicity in Man and Animals. p 75. Cambridge Univ Press, London and New York.
38 Goding JW. 1987. Monoclonal Antibodies: Principles and Practice. p 9. Academic Press, London, UK.
39 Goldman RC and L Leive. 1980. Heterogeneity of antigenic-side

chain length in lipopolysaccharide from *Escherichia coli* 0111 and *Salmonella typhimurium* LT2. Eur J Biochem 107: 145–153.

40 Goldstein IJ, RC Hughes, M Monsigny, T Osawa and N Sharon. 1980. What should be called a lectin? Nature 285: 66.

41 Goodman JW. 1984. Immunogenicity and antigenic specificity. In: Basic and Clinical Immunology (Stites DP, JD Stobo, HH Fudenberg and JV Wells, eds), 5th edn, Lange Medical Publications, Los Altos, CA.

42 Gottesman S, P Trisler and A Torres-Cabassa. 1985. Regulation of capsular polysaccharide synthesis in *Escherichia coli* K-12: characterization of three regulatory genes. J Bacteriol 162: 1111–1119.

43 Haaheim LR, G Kleppe and IW Sutherland. 1989. Monoclonal antibodies reacting with exopolysaccharide xanthan from *Xanthomonas campestris*. J Gen Microbiol 135: 605–612.

44 Hammond SM, PA Lambert and AN Rycroft. 1984. The Bacterial Cell Surface. Croon Helm Ltd, Kent, UK.

45 Harder W and L Dijkhuizen. 1983. Physiological responses to nutrient limitation. Ann Rev Microbiol 3: 1–23.

46 Howard JG. 1987. T-independent responses to polysaccharides: their nature and delayed ontogeny. In: Towards Better Carbohydrate Vaccines (Bell R and G Torrigiani, eds), pp 221–231, John Wiley and Sons, London.

47 Hungerer D, K Jann, F Orskov and I Orskov. 1967. Immunochemistry of K antigens of *Escherichia coli* 4. The K antigens of *E. coli* O 9:K 30H:12. Eur J Biochem 2: 115–126.

48 Issac DH. 1985. Bacterial polysaccharides. In: Polysaccharides Topics in Structure and Morphology (Atkins EDT, ed), pp 141–184, The Macmillan Press, London.

49 Jann K and O Westphal. 1975. Microbial polysaccharides. In: The Antigens (Sela M, ed), pp 1–110, vol 3, Academic Press, New York, San Francisco and London.

50 Jannsson PE, L Kenne, B Lindberg, H Ljunnggren, U Ruden and S Svennsson. 1977. Demonstration of an octasaccharide repeating unit in the extracellular polysaccharide of *Rhizobium meliloti* by sequential degradation. J Am Chem Soc 99: 3812–3815.

51 Jarman TR, L Deavin, S Slocombe and RC Righelato. 1978. Investigation of the effect of environmental conditions on the rate of exopolysaccharide synthesis in *Azotobacter vinelandii*. J Gen Microbiol 107: 59–64.

52 Kabat EA. 1976. Structural Concepts in Immunology and Immunohistochemistry. Holt, Rhinehart and Winston, New York.

53 Kabat EA. 1966. The nature of an antigenic determinant. J Immunol 97: 1–11.

54 Kabat EA and AE Bezer. 1958. The effect of variation in molecular weight on the antigenicity of dextran in man. Arch Biochem Biophys 78: 306–318.

55 Kayhty H. 1985. Antibody response to bacterial surface components. In: Enterobacterial Surface Antigens: Methods for Molecular Characterization (Korhonen TK, EA Dawes and PH Makela, eds), pp 91–108, Elsevier Sci Pub Co, NY.

56 Kenne L and B Lindberg. 1983. Bacterial polysaccharides. In: The Polysaccharides, vol 2 (Aspinall GO, ed), Academic Press, New York.

57 Kerby GPA. 1950. A comparison of the removal of mucoid and nonmucoid variants of *Klebsiella pneumonia* type B from the splanchnic circulating blood of the intact animal. J Immunol 64: 131–137.

58 Kingsley M, D Gabriel, G Marlow and P Roberts. 1993. The opsX locus of *Xanthomonas campestris* affects host range and biosynthesis of lipopolysaccharide and extracellular polysaccharide. J Bacteriol 175: 5839–5850.

59 Kirchman DL, DS Graham, D Reis and R Mitchell. 1983. Lectins may mediate in the settlement and metamorphosis of *Janua (Dexiospira) brasiliensis* (grube). Mar Biol Lett 3: 1–12.

60 Kirchman DL, DS Graham, D Reis and R Mitchell. 1982. Bacteria induce settlement and metamorphosis of *Janua (Dexiospira) brasiliensis* (grube). J Exp Mar Biol Ecol 56: 153–163.

61 Kjelleberg S, BA Humphrey and KC Marshall. 1982. Effect of interfaces on small, starved marine bacteria. Appl Environ Microbiol 43: 1166–1172.

62 Kjelleberg S and M Hermansson. 1984. Starvation-induced effects on bacterial surface characteristics. Appl Environ Microbiol 48: 497–503.

63 Labare M, K Guthrie and R Weiner. 1989. Polysaccharide exopolymer from periphytic marine bacteria. J Adhesion Sci Technol 3: 213–223.

64 Leigh JA, ER Signer and GC Walker. 1985. Exopolysaccharide-deficient mutants of *Rhizobium meliloti* that form inefficient nodules. Proc Natl Acad Sci USA 82: 6231–6234.

65 Lifely RM, U Norwicka and C Moreno. 1986. Analysis of the chain length of oligomers and polymers of sialic acid isolated from *Neiseria meningitidis* group B and C and *Escherichia coli* K1 and K92. Carbohydr Res 156: 123–135.

66 Lindberg B, J Lonngren and S Svensson. 1975. Specific degradation of polysaccharides. In: Advances in Carbohydrate Chemistry and Biochemistry, vol 31 (Tipson S and D Horton, eds), pp 185–240, Academic Press, New York.

67 Lion LW, KM Schuler, KM Hsieh and WC Ghiorse. 1988. Trace metal interactions with microbial biofilms in natural and engineered systems. CRC Crit Rev Environ Control 17: 273–306.

68 Lippincott JA, BB Lippincott and JJ Scott. 1984. Adherence and host recognition in *Agrobacterium* infection. In: Current Perspectives in Microbial Ecology (Klug MJ and CN Reddy, eds), Am Soc Microbiol, Washington, DC.

69 Lis H and N Sharon. 1986. Lectins as molecules and as tools. Ann Rev Biochem 55: 35–67.

70 Loeb GI. 1985. Properties of non-biological surfaces and their characterization. In: Bacterial Adhesion (Savage D and M Fletcher, eds), pp 111–129, Plenum Press, NY.

71 Lui T-Y, EC Gotschlich, W Egan and JB Robbins. 1977. Sialic acid-containing polysaccharides of *Neisseria meningitidus* and *Escherichia coli* strain BOS-12: structure and immunology. J Infect Dis 136: S71–S77.

72 Macleod CM, RG Hodges, M Heidelberger and B Robinson. 1946. Antibody formation in volunteers following injection of pneumococci or their type-specific polysaccharides. J Exp Med 83: 303–320.

73 Macleod CM and MR Krauss. 1950. Relation of virulence of pneumococcal strains for mice to the quantity of capsular polysaccharide formed in vitro. J Exp Med 92: 1–9.

74 Marshall KC. 1985. Mechanisms of bacterial adhesion at solid-water interfaces. In: Bacterial Adhesion (Savage D and M Fletcher, eds), pp 133–160, Plenum Press, NY.

75 Marshall KC (ed). 1984. Microbial Adhesion and Aggregation. Springer-Verlag, Berlin, Heidelberg, New York, and Tokyo.

76 Marshall KC. 1988. Adhesion and growth of bacteria at surfaces in oligotrophic habitats. Can J Microbiol 34: 503–506.

77 Marshall KD, R Stout and R Mitchell. 1971. Selective sorption of bacteria from seawater. Can J Microbiol 17: 1413–1416.

78 Meissener J, N Pfennig, JH Krauss, H Mayer and J Weckesser. 1988. Lipopolysaccharides of *Thiocystis violacea*, *Thiocapsa pfennig* and *Chromatium tepidum*, species of the family *Chromatiaceae*. J Bacteriol 170: 3217–3222.

79 Mian FA, TR Jarman and RC Righelato. 1978. Biosynthesis of exopolysaccharide by *Pseudomonas aeruginosa*. J Bacteriol 134: 418–422.

80 Moreno C. 1987. Carbohydrates as immunogens and tolerogens, antibody vs cell mediate immune responses. In: Towards Better Carbohydrate Vaccines (Bell R and G Torrigiani, eds), pp 262–277, John Wiley and Sons, London.

81 Morgan P and CS Dow. 1986. Bacterial adaptations for growth in low nutrient environments. In: Microbes in Extreme Environments (Herbert RA and GA Codd, eds), pp 187–214, Society for General Microbiology Publication #17, Academic Press, London, Orlando.

82 Mulford CA and MJ Osborn. 1983. An intermediate step in translocation of lipopolysaccharide to the outer membrane of *Salmonella typhimurium*. Proc Natl Acad Sci USA 80: 1159–1163.

83 Okuyawa K, S Arnott, RM Moorhouse, MD Walkinshaw, EDT Atkins and C Wolf-Ullish. 1980. Am Chem Soc Symp Ser 141: 411–419.

84 Oliveira D. 1992. Physico-chemical aspects of adhesion. In: Biofilms—Science and Technology (Melo R *et al*, eds), pp 45–58, Kluver Academic Publishers, Boston.

85 Ong C, M Wong and J Smit. 1990. Attachment of the adhesive holdfast organelle to the cellular stalk of *Caulobacter crescentus*. J Bacteriol 172: 1448–1456.

86 Opal S, A Cross and P Gemski. 1982. K antigen and serum sensitivity of rough *Escherichia coli*. Infect Immun 37: 956–960.

87 Ophir T and DL Gutnick. 1994. A role of exopolysaccharide in the

protection of microorganisms from dessication. Appl Environ Microbiol 60: 740–745.
88 Osborn MJ. 1984. Biogenesis of the bacterial outer membrane of *Salmonella*. Harvey Lect Ser 78: 87–103.
89 Parker CT, AW Kloser, CA Schnaitman, MA Stein, S Gottesman and BW Gibson. 1992. Role of *rfo* G and rfa P genes in determining the lipopolysaccharide core structure and cell surface properties of *Escherichia coli* K-12. J Bacteriol 174: 2525–2538.
90 Patchett RA, AF Kelly and RG Kroll. 1991. The adsorption of bacteria to immobilized lectins. J Appl Bacteriol 71: 277–284.
91 Peeters CCAM, D Everberg, P Hoogerhout, H Kayhty, L Soarinen, CAA van Boeckel, GA van der Marel, JH van Boom and JT Poolman. 1992. Synthetic trimer and tetramer of 3-β-D-ribose-(1-1)-D-ribitol-*S*-phosphate conjugated to protein induce monkeys. Infect Immun 60: 1826–1833.
92 Perez GI, JA Hopkins and MJ Blaser. 1985. Antigenic heterogeneity of lipopolysaccharides from *Campylobacter jejuni* and *Campylobacter fetus*. Infect Immun 48: 528–533.
93 Poindexter J. 1981. The caulobacters: ubiquitous, unusual bacteria. Microbiol Rev 45: 155–170.
94 Politis DJ and RN Goodman. 1980. Fine sructure of the extracellular polysaccharide of *Erwinia amylovora*. Appl Environ Microbiol 40: 596–604.
95 Pueppke SG. 1984. Adsorption of bacteria to plant surfaces. In: Microbe Interactions: Molecular Genetic Perspectives (Kosuge T and EW Nester, eds), Macmillan Press, New York.
96 Raschke WC and CE Ballou. 1972. Characterization of a yeast mannan containing *N*-acetyl-D-glucosamine as an immunochemical determinant. Biochemistry 11: 3807–3816.
97 Rehm BHA, G Boheim, J Tommassen and UK Winkler. 1994. Overexpression of *alg* E in *Escherichia coli*: subcellular localization, purification, and ion channel properties. J Bacteriol 176: 5639–5647.
98 Roberts I, R Mountford, N High, D Bitter-Suermann, K Jann, K Timmis and G Boulnois. 1986. Molecular cloning and analysis of genes for production of K5, K7, K12, and K92 capsular polysaccharides in *Escherichia coli*. J Bacteriol 168: 1228–1233.
99 Rohr TA and FA Troy. 1980. Structure and biosynthesis of surface polymers containing polysialic acid in *Escherichia coli*. J Biol Chem 255: 2332–2342.
100 Sar N and E Rosenberg. 1988. Fish skin bacteria: production of friction-reducing polymers. Microbial Ecol 17: 27–38.
101 Savage DC and MH Fletcher (eds). 1985. Bacterial Adhesion: Mechanisms and Physiological Significance. Plenum Press, New York.
102 Schwarzmann S and JR Boring III. 1971. Antiphagocytic effect of slime from a mucoid strain of *Pseudomonas aeruginosa*. Infect Immun 3: 762–767.
103 Silver RP, W Aaronson and WF Vann. 1987. Translocation of capsular polysaccharides in pathogenic strains of *Escherichia coli* requires a 60-kilodalton periplasmic protein. J Bacteriol 169: 5489–5495.
104 Silverman M and M Simon. 1983. Phase variation and related systems. In: Mobile Genetic Elements (Shapiro JA, ed), pp 537–557, Academic Press, New York.
105 Skerman TM. 1956. The nature and development of primary films on submerged surfaces in the sea. N Zealand J Sci Technol B 38: 44–57.
106 Sledjeski D. 1990. Investigation of *Shewanella colwelliana* exopolysaccharide using monclonal antibody probes. Doctoral Dissertation, 205 pp, U MD library Col Pk, MD.
107 Sledjeski D and R Weiner. 1993. Production and characterization of monoclonal antibodies specific for *Shewanella colwelliana* exopolysaccharides. Appl Environ Microbiol 59: 1565–1572.
108 Smith HW and MB Huggins. 1980. The association of the O18, K1 and H7 antigens and the ColV plasmid of a strain of *Escherichia coli* with its virulence and immunogenicity. J Gen Microbiol 121: 387–400.
109 Stenstrom TA. 1989. Bacterial hydrophobicity, an overall parameter for the measurement of adhesion potential to soil particles. Appl Environ Microbiol 55: 142–147.
110 Stout V and S Gottesman. 1990. RcsB and RcsC: a two-component regulator of capsule synthesis in *Escherichia coli*. J Bacteriol 172: 659–669.
111 Sutherland IW. 1972. Bacterial exopolysaccharides. Adv Microb Physiol 8: 143–213.
112 Sutherland IW. 1982. Biosynthesis of microbial exopolysaccharides. In: Advances in Microbial Physiology, vol 23 (Rose AH and JG Morris, eds), Academic Press, New York.
113 Sutherland IW. 1983. Microbial exopolysaccharides—their role in microbial adhesion in aqueous systems. CRC Crit Rev Microbiol 10: 173–219.
114 Swanson J, S Bergstrom, K Robbins, O Barrera, D Corwin and JM Koomey. 1985. Gene conversion involving the pilin structural gene correlates with pilus$^+$–pilus$^-$ changes in *Neisseria gonorrhoea*. Cell 47: 267–276.
115 Tempest DW and OM Neijssel. 1981. Metabolic compromises involved in the growth of microorganisms in nutrient-limited (chemostat) environments. In: Basic Life Sciences, vol 18. Trends in the Biotechnology of Fermentations for Fuels and Chemicals (Hollaender A, ed), pp 335–356, Plenum Press, New York and London.
116 Torres-Cabassa AS and S Gottesman. 1987. Capsule synthesis in *Escherichia coli* K-12 is regulated by proteolysis. J Bacteriol 169: 981–989.
117 Troy FA II. 1979. The chemistry and biosynthesis of selected bacterial capsular polymers. Ann Rev Microbiol 33: 519–560.
118 Troy FA, FE Frerman and EC Heath. 1971. The biosynthesis of capsular polysaccharide in *Aerobacter aerogenes*. J Biol Chem 246: 118–133.
119 Tsien HC and EL Schmidt. 1977. Polarity in the exponential-phase *Rhizobium japonicum* cell. Can J Microbiol 23: 1274–1284.
120 Tsien HC and EL Schmidt. 1981. Localization and partial characterization of soybean lectin-binding polysaccharide of *Rhizobium japonicum*. J Bacteriol 145: 1063–1074.
121 Tsunashima Y, K Moro and B Chu. 1978. Characterization of group C meningococcal polysaccharide by light-scattering spectroscopy. III. Determinant of molecular weight. Biopolymers 17: 251–265.
122 Umbreit T and J Pate. 1978. Characterization of the holdfast region of wild-type cells and holdfast mutants of *Asticcacaulis biprosthecum*. Arch Microbiol 118: 157–168.
123 Vreeland V, E Zablackis and WM Laetsch. 1988. Monoclonal antibodies to carrageenan. In: Algal Biotechnology (Stadler T, ed), Elsevier Applied Science, London and New York.
124 Wali RM, GR Hudson, DA Danald and RM Weiner. 1980. Timing of swarmer cell cycle morphogenesis and macromolecular synthesis by *Hyphomicrobium neptunium* in synchronous culture. J Bacteriol 144: 406–412.
125 Wardell JN, CM Brown and B Flannigan. 1983. Microbes and surfaces. In: Microbes in Their Natural Environments (Slater JH, R Whittenbury and JWT Wimpenny, eds), Cambridge Univ Press, London, New York, and Sydney.
126 Weiner RM, RA Devine, DM Powell, L Dagasan and RL Moore. 1985. *Hyphomonas oceanitis* sp nov, *Hyphomonas hirschiana* sp nov, and *Hyphomonas jannaschiana* sp nov. Int J Syst Bacteriol 35: 237–243.
127 Weller PE, AL Smith, P Anderson and DH Smith. 1977. The role of encapsulation and host age in the clearance of *Haemophilus influenzae* bacteremia. J Infect Dis 135: 34–41.
128 Wilkinson JF. 1958. The exocellular polysaccharides of bacteria. Bacteriol Rev 22: 46–73.
129 Williams AG and JWT Wimpenny. 1977. Exopolysaccharide production by *Pseudomonas* NCIB11264 grown in batch culture. J Gen Microbiol 102: 13–21.
130 Williams TM, RF Unz and JT Doman. 1987. Ultrastructure of *Thiothrix* spp and 'type 021N' bacteria. Appl Environ Microbiol 53: 1560–1570.
131 Wozniak DJ and DE Ohman. 1994. Transcriptional analysis of the *Pseudomonas aeruginosa* genes *alg* R, *alg* D reveals a hierarchy of alginate gene expression which is modulated by *alg* T. J Bacteriol 176: 6007–6014.
132 Wrangstadh M, PL Conway and S Kjelleberg. 1988. The role of an extracellular polysaccharide produced by the marine *Pseudomonas* sp S9 in cellular detachment during starvation. Can J Microbiol 35: 309–312.
133 Wrangstadh M, PL Conway and S Kjelleberg. 1986. The production and release of an extracellular polysaccharide during starvation of a marine *Pseudomonas* sp and the effect thereof on adhesion. Arch Microbiol 145: 220–227.
134 Wrangstadh M, U Szewzyk, J Ostling and S Kjelleberg. 1990. Starvation-specific formation of a peripheral exopolysaccharide by a mar-

ine *Pseudomonas* sp, strain S9. Appl Environ Microbiol 56: 2065–2072.

135 Wright A, M Dankert and PW Robbins. 1965. Evidence for an intermediate stage in the biosynthesis of the salmonella *O*-antigen. Proc Natl Acad Sci USA 54: 235–241.

136 Wu AM and S Sugii. 1991. Coding and classification of D-galactose, *N*-acetyl-D-galactosamine, and β-D-Gal*p*-[1→3(4)]-β-D-Glc*p*NAc, specificities of applied lectins. Carbohydrate Res 213: 127–143.

137 Yu, AK and NK Kochetkov. 1987. 2,3-diamino-2, 3, -dideoxyuronic and 5,7-diamino, 3, 5, 7, 9-tetradeoxynonulosonic acids: new components of bacterial polysaccharides. FEMS Microbiol Lett 46: 381–385.

138 Zambon JJ, PS Huber, AE Mayer, J Slots, MS Fornalk and RE Baier. 1984. *In situ* identification of bacterial species in marine microfouling films by usinng an immunofluorescence technique. Appl Environ Microbiol 48: 1214–1220.

139 Zobell CE and EC Allen. 1935. The significance of marine bacteria in the fouling of submerged surfaces. J Bacteriol 29: 230–251.

140 Zobell CE and DQ Anderson. 1936. Observations on the multiplication of bacteria in different volumes of stored sea water and the influence of oxygen tension and solid surfaces. Biolog Bull 71: 324–342.

Application of TOF-SIMS to the Study of Biological Adhesives

Patrick C. Schamberger, Ace M. Baty, Bo Frølund, Bonnie J. Tyler, Gill G. Geesey
Center for Biofilm Engineering
409 Cobleigh Hall
Montana State University
Bozeman, MT 59715

and

Patrick J. McKeown, Larry E. Davis
Physical Electronics
6509 Flying Cloud Drive
Eden Prairie, MN 55344

Introduction

Using the molecular information provided by Time-of-Flight Secondary Ion Mass Spectrometry (TOF-SIMS) to study synthetic polymer surfaces is well established(1). It has been demonstrated that prior to cell attachment and fouling of submerged surfaces, a conditioning film of macromolecules which are naturally occurring polymers (proteins, polysaccharides) forms on the exposed material surface (2). Understanding the interactions between material surfaces and conditioning film molecules is critical to preventing or promoting biofilm adhesion and growth. The focus of this presentation is to demonstrate the applicability of TOF-SIMS to studying naturally occurring polymers and understanding the adhesion of biological macromolecules to surfaces. Specifically, two adhesive systems were studied, the mussel adhesive protein (MAP) expressed by the marine mussel *Mytilus edulis* and polysaccharides expressed by two bacterial strains of a marine *Hyphomonas*.

Mussel Adhesive Proteins (MAP)

There are many natural organisms whose survival depends on the ability to adhere to a surface in an aqueous environment. The mussel adhesive proteins (MAP) are the bioadhesive used by the marine mussel *Mytilus edulis* to anchor itself to a variety of surfaces in a seawater environment (3). Despite the tenacity with which the adhesion of the mussel to surfaces occurs naturally, this function has yet to be duplicated with purified proteins out of the natural environment. An understanding of the binding mechanism of MAP is necessary to develop MAP as an aqueous environment adhesand in biomaterial applications and to prevent the adhesion of mussels to marine vessels.

MAP and an individual MAP fraction (*Mytilus edulis* fractioned protein 1, MeFP-1) have been exposed to polystyrene (PS), and poly(octadecylmethacrylate) (POMA) substrata for analysis by TOF-SIMS. Representative positive ion spectra for the MeFP-1 exposed surfaces are shown in Figures 1 and 2 respectively. Freeze dried MAP powder was analyzed by pressing the protein onto indium foil. The positive ion spectra for this sample is shown in Figure 3. Differences observed between the three spectra suggest a surface mediated effect. Upon cursory inspection, the POMA spectra contains many more peaks in the region of 100 to 150 m/z and apparently related peaks from 490 to 560 m/z. In contrast, the PS surface lacks these peaks, however, contains peaks in the region of 400 to 470 m/z. The freeze dried protein has observable mass fragment peaks out to 850 m/z suggesting that a denaturing effect on a material surface or differences due to the fractions present may be responsible for the observed differences between the powder and the MeFP-1 on the polymer surfaces. Analysis of isolated MAP fractions will be presented to determine if a particular fraction of the mixture of MAP proteins contributes to the adhesion of these proteins to each of these surfaces.

Polysaccharides and the adhesion of *Hyphomonas* bacterial strains

Bacteria colonizing a surface are typically embedded in a matrix consisting of extracellular polymeric substances (EPS) (4,5). The possible roles of the EPS matrix are numerous; however, the fact that EPS serves to anchor cells to each other and to the substratum points out their role in biofilm formation. To address the possible roles of EPS in biofilm formation the marine strain of *Hyphomonas* serves as a good model organism. One advantage of *Hyphomonas* is that it participates in both the early colonization of submerged surfaces and in the subsequent biofilm formation (6). Another advantage is that a variant strain, Reduced Adhesive (RAD), has been isolated, which seems to be less able to form biofilms as compared to the the *Hyphomonas* Wild Type (WT) strain. By comparing the EPS obtained from the RAD and WT strains one may be able to correlate differences in EPS composition to differences in biofilm formation, therefore understanding the adhesion process.

TOF-SIMS spectra from these two strains colonized on agar and polystyrene surfaces will be presented along with spectra of purified polysaccharide fractions. Figures 4 and 5 show positive ion TOF-SIMS spectra of the WT and RAD strains growing on an agar plate. Note that differences can be observed between the two strains. The WT strain has less even numbered mass peaks (indicative of nitrogen in the mass fragment suggesting protein) in the region from 100 to 150 m/z as compared to the RAD strain. Additionally, the peak a 299 and 581 m/z present on the WT strain is absent from the RAD strain spectrum. These differences and the relationship of TOF-SIMS spectra of the purified fractions of the polysaccharides will be discussed.

References

(1) Hercules, D.M., *J. of Mol. Structure*, **292** (1993) 49-64.
(2) Gristina, A.G., *Science*, **237** (1984) 1588.
(3) Waite, J.H., *Int. J. Adhesion Adhesives*, **7** (1987) 9.
(4) Cooksey, K.E. In "*Biofilms: Science and Technology.*" Melo, L. et. al. Kluwer: The Netherlands, (1992) pp. 137-147.
(5) Costerton, J.W., Cheng, K.J., Ladd, G.G., Nickel, J.C. Dasgupta, M., Marrie, T.J., *Ann. Rev. Microbiol.* **41** (1987) 435-464.
(6) Quintero, E.J., Weiner, R.M. submitted to *J.I.M.*, (1995).

Acknowledgements

The authors wish to acknowledge Professor Herbert Waite of the College of Marine Studies at the University of Deleware, Lewis, DE for graciously suppling the MAP and isolated MAP protein fractions.

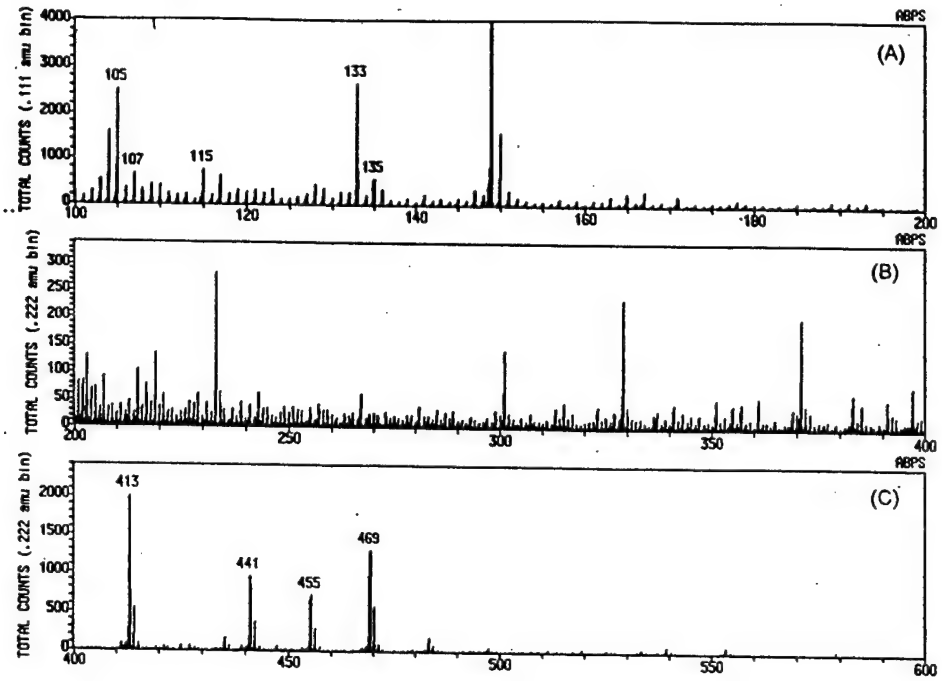

Figure 1: TOF-SIMS positive ion spectra of mussel adhesive fraction MeFP-1 on polystyrene
(A) 100 to 200 m/z
(B) 200 to 400 m/z
(C) 400 to 600 m/z

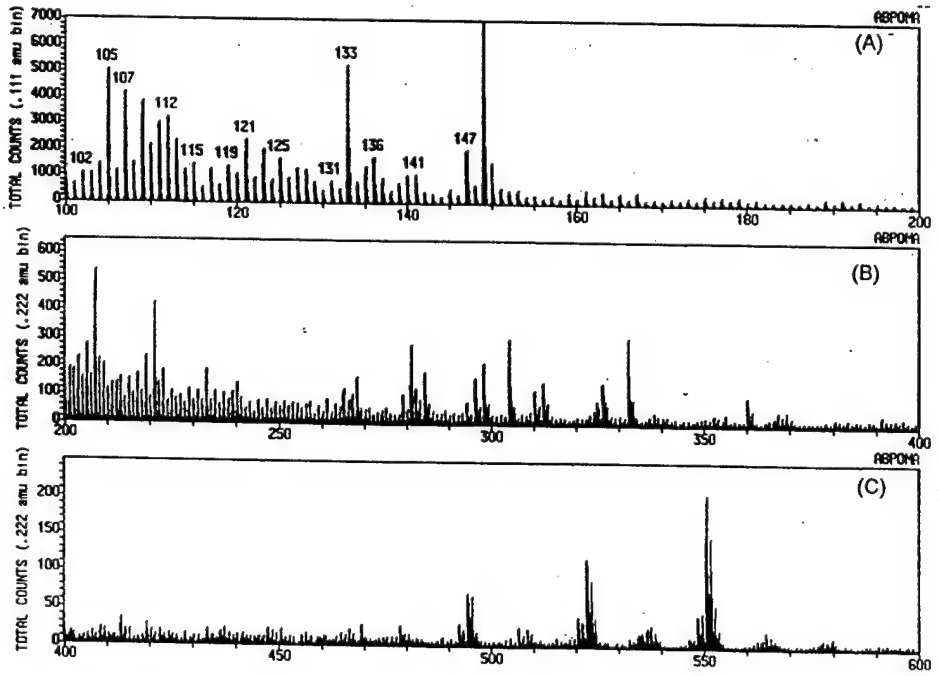

Figure 2: TOF-SIMS positive ion spectra of mussel adhesive fraction MeFP-1 on poly(octadecylmethacrylate
(A) 100 to 200 m/z
(B) 200 to 400 m/z
(C) 400 to 600 m/z

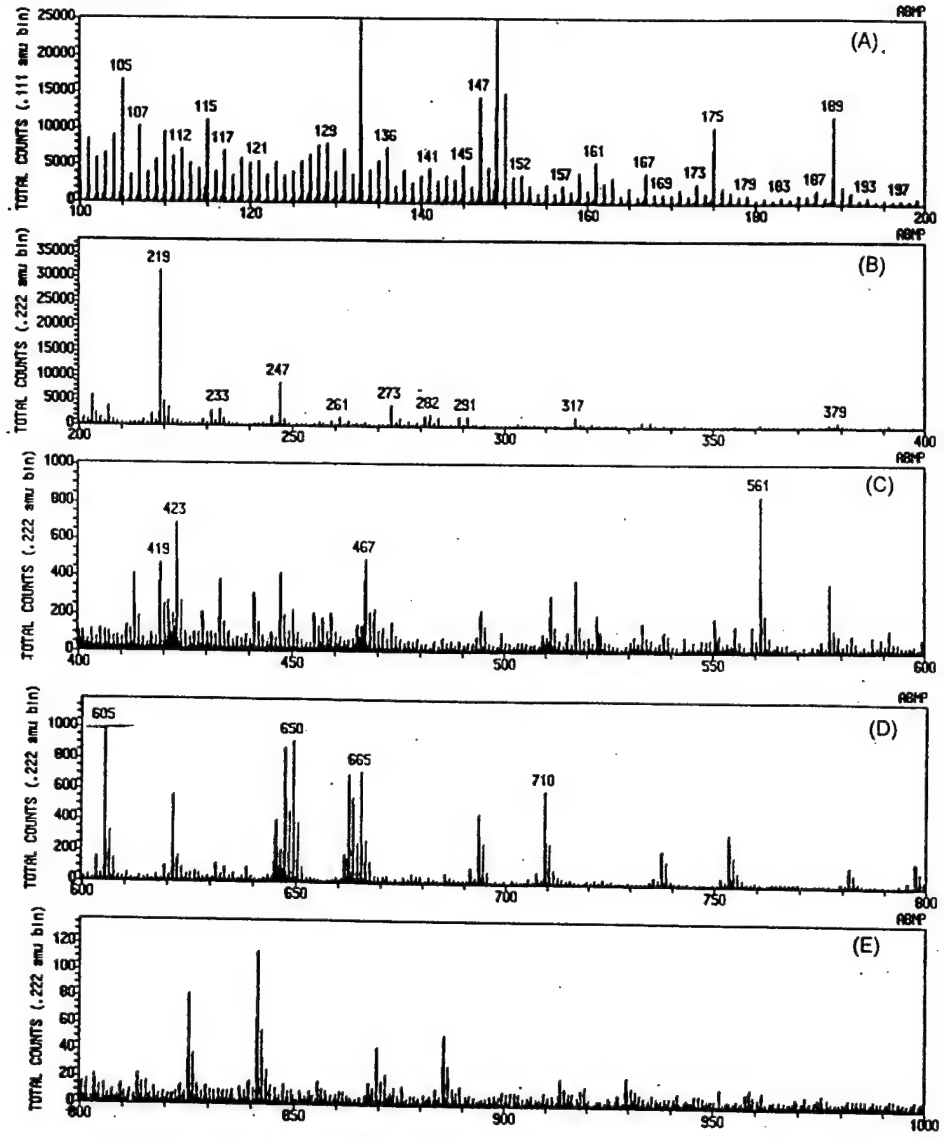

Figure 3: TOF-SIMS positive ion spectra of mussel adhesive protein freeze dried powder pressed onto indium foil

(A) 100 to 200 m/z
(B) 200 to 400 m/z
(C) 400 to 600 m/z
(D) 600 to 800 m/z
(E) 800 to 1000 m/z

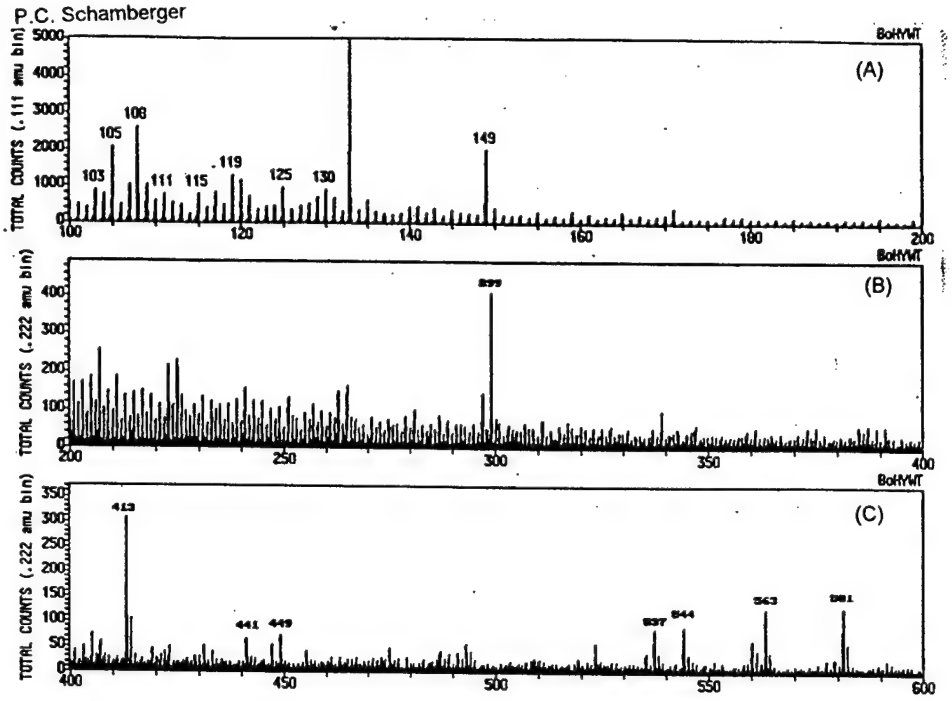

Figure 4: TOF-SIMS positive ion spectra of Wild Type strain of *Hyphomonas* bacteria on an agar plate
(A) 100 to 200 m/z
(B) 200 to 400 m/z
(C) 400 to 600 m/z

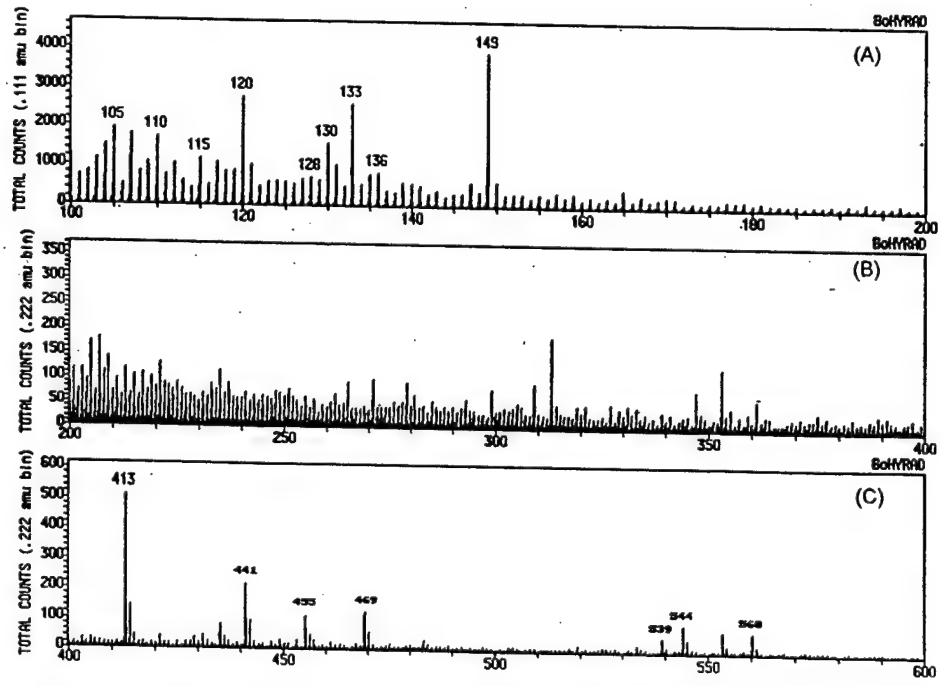

Figure 5: TOF-SIMS positive ion spectra of REduced Adhesive strain of *Hyphomonas* bacteria on an agar plate
(A) 100 to 200 m/z
(B) 200 to 400 m/z
(C) 400 to 600 m/z

Biofouling, 1995, Vol. 9 (2), pp. 95–114
Reprints available directly from the publisher
Photocopying permitted by license only

ADHESIVE EXTRACELLULAR POLYMERS OF *HYPHOMONAS* MHS-3: INTERACTION OF POLYSACCHARIDES AND PROTEINS

P A SUCI*[1], B FRØLUND[2], E J QUINTERO[3], R M WEINER[3] and G G GEESEY[1]

[1]*Center for Biofilm Engineering, Montana State University, MT 59717, USA*
[2]*Environmental Engineering Laboratory, Aalborg University, Sohngaardsholmsvej 57, 9000 Aalborg, Denmark.*
[3]*Department of Microbiology, University of Maryland, College Park, MD 20742, USA*

(Received 10 April 1995; in final form 5 June 1995)

The adsorption behavior of extracellular polymeric substances (EPS) from the marine bacterium *Hyphomonas* MHS-3 was investigated using attenuated total reflection Fourier transform infrared (ATR/FT-IR) spectrometry. The protein fraction of the crude EPS (EPS_c) (propanol precipitated/extracted with EDTA) dominated the adsorption onto the germanium substratum. Removal of the Protease K accessible portion of the EPS_c protein, and treatment with RNase and DNase, yielded a hygroscopic substance (EPS_p) which contained at least one adhesive polysaccharide component. Conditioning the substratum with EPS_c diminished adsorption of the polysaccharide fractions in EPS_p; pre-adsorbed EPS_c protein was not displaced. The rate of EPS_c adsorption on substrata conditioned with EPS_p was slower than to clean germanium; however, the projected surface coverage of protein after long times, based on an empirical datafit, was the same as that for a clean substratum; the EPS_c proteins did not displace the pre-adsorbed adhesive polysaccharide fraction. SDS-PAGE (Coomassie blue stain) revealed an extensive homology between proteins from cell lysates and EPS_c proteins. However, distinct differences in the banding pattern suggested that proteins did not originate primarily from cell lysis during the extraction procedure. The results indicate that adhesive components of EPS, with respect to a hydrophilic surface (germanium), can be either protein or polysaccharide and that they may compete for interfacial binding sites.

KEYWORDS: extracellular polymeric substances, adhesion, marine bacterium, ATR/FT-IR, adsorption

INTRODUCTION

Bacteria which have colonized a surface are typically enveloped in a matrix of extracellular polymeric substances (EPS) (Costerton *et al.*, 1987; Cooksey, 1992). Many of the functions of the EPS matrix are probably related to maintainance of a favorable local environment for cell subsistence (Geesey, 1992). The intercellular polymer network may serve to store nutrients (Lange, 1976), shield cells from antagonists (Hoyle *et al.*, 1990) or optimize biofilm architecture (de Beer *et al.*, 1993; Tetz *et al.*, 1993; Korber *et al.*, 1994). In addition, the composition of the EPS matrix can influence subsequent fouling by invertebrate larvae, presumably by providing chemical cues for settlement (Holmström & Kjelleberg, 1994). Scanning electron micrographs of biofilms typically reveal strands of EPS anchoring the cells to each other and to the substratum (Fletcher & Floodgate, 1973; Allison & Sutherland, 1987). These results suggest that the EPS plays an adhesive role.

*Corresponding author

The cell adhesion process has been described in terms of a reversible adsorption step followed by processes which secure the cells to the substratum irreversibly (Allison & Sutherland, 1987; Croes *et al.*, 1993). Formation of this more tenacious anchor has been associated with extracellular polysaccharide production (Croes *et al.*, 1993). Presence of a polysaccharide rich capsule can either enhance (Shea *et al.*, 1994) or reduce (Pringle *et al.*, 1983; Rosenberg & Kjelleberg, 1986; Wrangstadh *et al.*, 1986) initial attachment to surfaces. In general, the results suggest that particular extracellular polysaccharides have an inherently adhesive character, especially with respect to hydrophilic surfaces. Although the primary research focus has been on the polysaccharide portion of the EPS, the EPS typically contains a protein component (Humphrey *et al.*, 1979; Abu *et al.*, 1991; Vincent *et al.*, 1994). Most proteins which have been examined adsorb strongly to a variety of substrata (Brash & Horbett, 1987). As a class, this implicates them as potential adhesive elements of the EPS matrix.

Much progress has been made in characterizing proteinaceous adhesins employed by pathogenic bacteria for initial attachment to specific host tissues (Jann & Jann, 1990). However, the adhesins and molecular interactions involved in securing other biofilm forming bacteria to substrata, including marine bacteria, have not been clearly identified. Many studies have attempted to delineate general attributes of substrata or cells which enhance or inhibit cell attachment *e.g.* wettability or hydrophobicity (Dexter *et al.*, 1975; Fletcher & Loeb, 1979; Rosenberg & Kjelleberg, 1986; Busscher *et al.*, 1990). There is a growing consensus that hydrophobic interactions play a dominant role (Doyle & Rosenberg, 1990). In one case EPS strands connecting cells to the substratum were identified as an acidic polysaccharide (Fletcher & Floodgate, 1973). However, in general, the primary adhesive biomolecules which lie immediately proximal to the surface have not been characterized. Identification of these primary adhesive biomolecules and the molecular interactions involved in binding to various substrata may be a prerequisite for further advances in control of microfouling.

Adsorption behavior has been used to determine whether EPS components mediate initial attachment by correlation with whole cell behavior (Pringle & Fletcher, 1986). Adsorption studies can also be used to identify EPS components which have inherently sticky properties and thus are candidates for primary adhesive EPS components. The present study investigates adsorption behavior of components of *Hyphomonas* MHS-3 (MHS-3) EPS on germanium using attenuated total reflection Fourier transform (ATR/FT-IR) spectrometry. MHS-3 is a prosthecate, biofilm-forming marine bacterium which can thrive under both oligotrophic and copiotrophic conditions and has been implicated as a primary colonizer in the microfouling process (Shen *et al.*, 1989; Quintero & Weiner, 1995a,b). Recent studies indicate that the MHS-3 polysaccharide-rich extracellular capsule serves as an adhesin (Quintero & Weiner, 1995b).

MATERIALS AND METHODS

Materials

Synthetic seawater consisted of the following (w/v): 2.3% NaCl, 0.24% Na_2CO_3, 0.033% KCl, 0.4% $MgCl.6H_2O$, 0.066% $CaCl_2.2H_2O$, pH adjusted to 8.0 with HCl. Electrophoresis reagents were from Bio-Rad Laboratories (Richmond, CA); cleaning reagents were from Aldrich Chemical Company; chemicals for colorometric assays were analytical grade. Trypsin (Bovine Pancreas Type I), RNase, DNase and Protease K were from the Sigma Chemical Company (St. Louis, MO).

Culturing of bacteria

Hyphomonas strain MHS-3 (MHS-3) was isolated from shallow water sediments in Puget Sound, WA and cultured in Marine Broth 2216 (37.4 $g \cdot l^{-1}$) (Difco Laboratories, Detroit, MI) at 25°C on a rotating shaker at 100 $rev \cdot min^{-1}$. Teflon™ mesh was introduced into culture vessels to provide greater surface for attached growth (mesh opening, 1.8 mm, thread diameter, 0.5 mm, Tetko, Incorporated, Briarcliff, NY).

Isolation and Purification of EPS

Cells were harvested from an early stationary phase culture (defined conventionally in terms of planktonic growth). The spent medium was discarded and the flocs and the biofilm were mechanically removed from the culture vessel walls and the teflon mesh and resuspended in synthetic seawater. The cell suspension was centrifuged at 16,000 xg for 20 min. The EPS in the supernatant was precipitated with 4 volumes of ice-cold 2-propanol and the cell pellet blended in a Waring blender with 10 mM EDTA, 3% NaCl for 1 min at 4°C. The cell suspension was again centrifuged for 15 min at 16,000 xg. The cell pellet was discarded and the supernatant was precipitated with 2-propanol as above. The precipitated EPS fractions were pooled and resuspended in a minimum volume of dH_2O and dialyzed exhaustively against dH_2O. This crude EPS (EPS_c) was lyophilized.

Polysaccharide-enriched EPS (EPS_p) was prepared by a modified protocol (Read & Costerton, 1987). EPS_c was dissolved in a minimum volume of 0.1 M $MgCl_2$. DNase and RNase were added to a final concentration of 0.1 $mg \cdot ml^{-1}$, and incubated at 37°C for 4 h. Protease K was added to 0.1 $mg \cdot ml^{-1}$ and incubated at 37°C overnight. The residual protein was removed with a hot phenol extraction, followed by a chloroform extraction. This preparation was dialyzed exhaustively against dH_2O and lyophilized. All EPS fractions were stored desiccated, at room temperature.

Electrophoresis (SDS/PAGE)

Tris/glycine-based gels (Shapiro *et al.*, 1967) were cast and run in a Model 220 Vertical Slab Electrophoresis Cell (Bio-Rad Laboratories, Richmond, CA). The composition (w/v) of the stacking gel was 3% acrylamide/0.08% bisacrylamide; separating gels were 9% acrylamide/0.24% bisacrylamide. The running buffer was (w/v) 0.1% SDS, 2.88% glycine, 0.6% Tris base. The sample buffer was 15% glycerol, 0.2% dithiothreitol. Molecular masses were estimated using Sigma SDS protein standards (M-2789).

MHS-3 lysate was prepared from log phase planktonic cultures. 1 ml aliquots were centrifuged (10,000 xg) for 10 min and the supernatant discarded.

Appropriate amounts of EPS_c and pelleted bacteria were suspended in 50 μl sample buffer, sonicated for 10 min and boiled for 10 min before being introduced to the sample wells.

Colorometric Assays

Neutral hexoses were determined using the phenol sulfuric assay with glucose as the standard (Dubois *et al.*, 1956). Proteins were estimated using the Lowry procedure (bovine serum albumin standard) (Lowry *et al.*, 1951). Uronic acid content was determined using the meta-hydroxy diphenyl method of Blumenkrantz and Asboe-Hansen (1973) modified by Kintner and Van Burren (1982) with glucuronic acid as the standard.

Surface Preparation

Single crystal, cylindrical germanium (Ge) internal reflection elements (IRE) (Spectra Tech, Stamford, CT) were cleaned by ultrasonication in a base bath (saturated KOH in isopropyl alcohol) for 10 min followed by a series of rinses which all consisted of ultrasonication in various liquids for 10 min. Following the base bath were two rinses in ultrapure water followed by a gentle scrubbing with undiluted Micro™ cleaning solution using cotton swabs. The cleaning solution was flushed off in a hard stream of ultrapure water. The IRE was then subjected to the following rinses: ultrapure water (2×), ethyl alcohol, chloroform and dichloromethane. Auger electron spectroscopy (Phi 595 scanning Auger microprobe) indicated that the elemental percent composition of the first few monolayers of Ge coupons (Exotic Materials Incorporated, Costa Mesa, CA) cleaned by this protocol, was 9.11 ± 1.38% carbon, 6.51 ± 2.01% oxygen, and 83.92 ± 2.24% Ge. This is approximately the same level of hydrocarbon contamination obtained after exposing a carbon-free (Argon etched) Ge coupon to air for 1 min.

Adsorption Protocol

For adsorption experiments the cylindrical IRE was positioned within a stainless steel flow chamber (Circle Cell™, Spectra Tech). The interior cavity of the flow chamber is cylindrical with a diameter of 0.476 cm and a length of 2.7 cm. The volume contained in the annular region between the surface of the IRE and chamber wall is 0.289 cm^3. Fluid was introduced and displaced through entrance and exit ports at each end of the cavity. The IRE was held in place in the chamber by two teflon O-rings.

A simple flow through system was used to deliver solutions into the flow chamber. Teflon valves (Cole-Parmer, Niles, IL) served to shuttle the appropriate solution into tubing leading to the flow chamber. All tubing leading into the flow chamber as well as the fittings were teflon (0.08 cm ID). Tubing was cleaned after each experiment by sonicating in base bath. The section of tubing connecting the reservoir containing protein to the flow chamber was made as short as possible (~20 cm). Effluent tubing was teflon and viton™ (Cole-Parmer, Niles, IL). Fluid was pumped by threading the viton through a peristaltic pump (Sage Instruments, Cambridge, MA) at 0.5 $ml \cdot min^{-1}$. All glassware was acid cleaned (No Chromix™ in concentrated H_2SO_4).

Before each adsorption experiment the surface was exposed to flowing seawater for 20 min. A vial containing approximately 1 ml of the desired concentration of EPS was inserted into the flow system and the contents immediately pumped through a short section of leader tubing and through the flow chamber for 105 s. Flow was then stopped to allow adsorption for 100 min. Adsorption was performed under these static conditions to conserve EPS. Flow was then resumed and the surface was rinsed with synthetic seawater for 120 min.

FT-IR Spectrometry

During the course of each experiment infrared (IR) spectra were acquired periodically using a Perkin Elmer Model 1800 Fourier transform infrared (FT-IR) spectrophotometer. Experimental details are described elsewhere (Suci & Geesey, 1995). FT-IR measurements were made in a temperature controlled room (25 ± 1°C). For experiments in which the substratum was conditioned with either EPS_c or EPS_p the spectrum acquired immediately before the second adsorption reaction was initiated was used as the background.

Transmission spectra were measured in a 15 μm pathlength demountable cell with calciumfluoride windows (Spectra-Tech).

Estimation of Surface Coverage

Surface coverage of the protein portion of the EPS_c was estimated using a published correlation based on the area of the amide II band (Pitt & Cooper, 1988). This correlation can be converted for application to the present experimental ATR configuration by utilizing the water absorbance at 1640 cm^{-1} (Pitt, 1987) as a normalization factor. The normalized conversion factor is 0.746 ± 0.104 $\mu g \cdot cm^{-2}$ area amide II band. Surface coverage of putative polysaccharide fractions was estimated by comparing absorbances obtained in transmission mode with those obtained in the ATR mode. The estimates are approximate and are predicated on the assumption that the extinction coefficient for IR absorbance is the same for solution phase and adsorbed molecules. This assumption is supported by data on ATR/FT-IR of adsorbed protein (Pitt & Cooper, 1988), but has not been tested for polysaccharides. With this assumption the following relation can be derived:

$$\Gamma = \ln 10[A_{w,t}/A_{a,t}][1/(1-T_{w,e})][c_{a,t}][d_p/2]A_{a,e} \qquad \text{Eqn 1}$$

where Γ is the surface coverage of adsorbed substance (a) in $mg \cdot cm^{-2}$, ln10 is the natural log of 10, $A_{w,t}$ is the absorbance of water at 1640 cm^{-1} in the transmission cell (baseline subtracted: 1740 to 1540 cm^{-1}), $A_{a,t}$ is the absorbance of the substance in the transmission cell, $T_{w,e}$ is the transmittance of water in the ATR mode at 1640 cm^{-1}, $c_{a,t}$ is the concentration of the substance in the transmission cell ($mg \cdot ml^{-1}$), d_p is the penetration depth of the evanescent field, and $A_{a,e}$ is the absorbance of the adsorbed substance in the ATR mode. The penetration depth, d_p, can be calculated from the incident angle of the internal reflections and the relative refractive index at the interface for a particular wavenumber (Knutzen & Lyman, 1985). Equation 1 employs the absorbance of water in the transmission and ATR modes as a normalization factor. The expression yields a conversion factor of 0.97 $\mu g \cdot cm^{-2}$·area amide II band for a bovine serum albumin standard which is close to that of Pitt and Cooper (1988) for human serum albumin. In order to use Equation 1 to determine the surface coverage of putative polysaccharides in EPS_p, $c_{a,t}$ was assumed to be equivalent to the carbohydrate content of EPS_p.

Langmuir and Exponential Fits

The binding curves were fit to a Langmuir model. The equation describing Langmuir adsorption is:

$$A = A_s[((1/Kc_b)+1)^{-1}] \qquad \text{Eqn 2}$$

where K is the binding (association) constant, c_b is the concentration of the substance in bulk solution, A is the absorbance (or area in $abs \cdot cm^{-1}$) and A_s is the (estimated) saturation value of the absorbance (projected plateau for large bulk concentrations). Best fits for the parameters K and A_s were obtained by nonlinear regression using the software provided with the SigmaPlot™ application (Jandell Scientific, Corte Madera, CA). A_s can be converted to projected surface coverage (Γ) using Equation 1.

Theoretical justification for application of the Langmuir model relies on demonstration of reversible adsorption. In the present case the adsorbed components analyzed are

essentially irreversibly bound. There is no rigorous theoretical model which applies to the case of irreversible adsorption (Andrade, 1985). The use of the Langmuir model in the present context is intended to be empirical; it serves to quantify the data in terms of affinity of the adsorbate for the surface for comparison purposes.

In order to quantify the hindered adsorbance of protein on pre-adsorbed putative polysaccharide another empirical fit was employed:

$$A = p_1(1-\exp[(t-p_2)/\tau]) \qquad \text{Eqn 3}$$

where A is the absorbance at time t and a best fit for parameters p_1, p_2 and τ (the time constant) is found using nonlinear regression as described above. The static adsorption conditions preclude discrimination of adsorption kinetics from diffusion limited mass transfer to the interface. However, the above empirical (essentially first order) fit allows a semi-quantitative comparison of data sets to be made.

RESULTS

Biochemical Assays

Composition of the major components of *Hyphomonas* crude EPS (EPS_c) and partially purified EPS (EPS_p) are shown in Table 1. Extraction of protein and nucleic acids from EPS_c had a profound effect on the solubility characteristics. Whereas EPS_c must be sonicated for an extended period (> 1 h) in order to solubilize 1 $mg \cdot ml^{-1}$ in seawater, EPS_p is completely dispersed instantly in seawater at > 30 $mg \cdot ml^{-1}$. This difference in solubility is probably a reflection of a difference in the colloidal structure and also suggests that EPS_p is relatively hydrophilic compared to EPS_c.

Coomassie blue stained SDS-PAGE (Fig. 1) of cell lysates from planktonic cultures and EPS_c indicated an extensive homology between the two sets of proteins. At least one distinct high molecular weight band ((approximately 154kD) and two faint lower molecular weight bands (approximately 44 and 49kD) were present in the cell lysate which were absent, or at least much less prominent, in the EPS_c proteins implying that EPS_c proteins did not originate primarily from bacteria lysed during the extraction procedure. However, many of the EPS_c proteins could well have originated from cells lysed during biofilm development. Slight differences in the banding pattern between 11kD and 13kD suggest that some proteins are present in EPS_c which are absent in the cell lysate. These are candidates for specialized EPS proteins.

IR Spectra and Time Course of Binding

Three IR spectra of EPS_c are shown in Figure 2. The spectrum of the bulk EPS_c taken in transmission mode (Fig. 2a) contains bands at 1645 cm^{-1} and 1550 cm^{-1} which are typical

Table 1 Major components of *Hyphomonas* MHS-3 EPS ($\mu g \cdot mg^{-1}$)

Component	*EPS_c*	*EPS_p*
Neutral hexose	277	635
Protein	409	135
Uronic acids	5	30

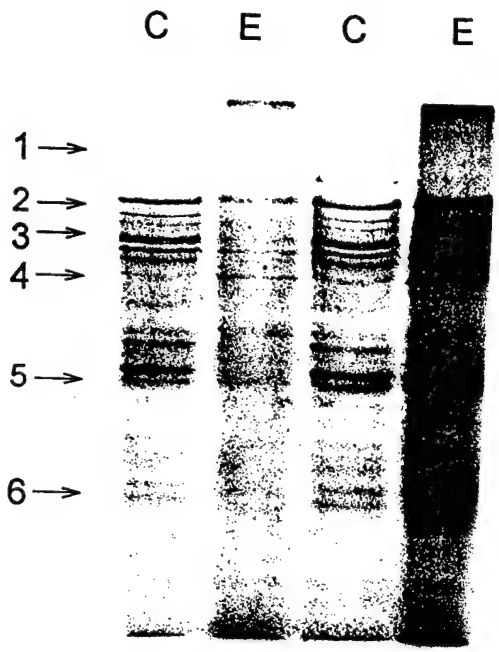

Fig. 1 Coomassie blue stained SDS-PAGE. C = cell lysate; E = EPS_c. Molecular weight calibration is indicated as follows (kD): 1 = 205, 2 = 116, 3 = 97.4, 4 = 66, 5 = 29, 6 = 14.2.

of the protein amide I and II bands, respectively (Miyazawa & Blout, 1961; Bandekar & Krimm, 1980). The broad band centered at approximately 1086 cm^{-1} is in a region where carbohydrates (including polysaccharides) have characteristic vibrations (Cael *et al.*, 1975). RNA and DNA also contain overlapping bands in this region which have a prominent maximum between 1085 cm^{-1} and 1090 cm^{-1} (Taillandeir *et al.*, 1985). Figures 2b and c are spectra of EPS_c, taken in ATR mode, during adsorption and after a 120 min rinse period, respectively. The amide I and II bands contribute a larger proportion of the spectral absorbance for these two latter spectra than the broad spectral feature contained within the carbohydrate/RNA/DNA region (1120 cm^{-1} to 900 cm^{-1}). Although a small amount of absorbance is present in this region of the spectrum after the rinse period (Fig. 2c), the amide bands dominate the spectrum.

Figure 3 shows the time course of adsorption and desorption of the EPS_c based on the area of the amide II band. Although there is a small amount of material lost from the interface when the rinse#1 is initiated, the adsorption is essentially irreversible. After an hour exposure to trypsin (1 $mg \cdot ml^{-1}$, under static conditions) the adsorbed material can be easily removed by flowing seawater (rinse#2).

Three spectra of EPS_p are shown in Figure 4. The spectra are displayed in the same order as in Figure 2, *i.e.* Figure 4a is a transmission spectrum of bulk EPS_p and Figures 4b and c are spectra taken in ATR mode during adsorption (Fig. 4b) and at the end of the rinse period (Fig. 4c). In contrast to EPS_c the broad spectral feature in the region of the spectrum associated with carbohydrate resonance frequencies (1120 cm^{-1} to 900 cm^{-1}) is prominent for both the bulk (Fig. 4a) and adsorbed (Fig. 4b,c) material. This broad feature contains no apparent band or shoulder at 1085 cm^{-1} to 1090 cm^{-1} which would suggest the presence of nucleic acids. Although the bands centered at 1646 cm^{-1} and

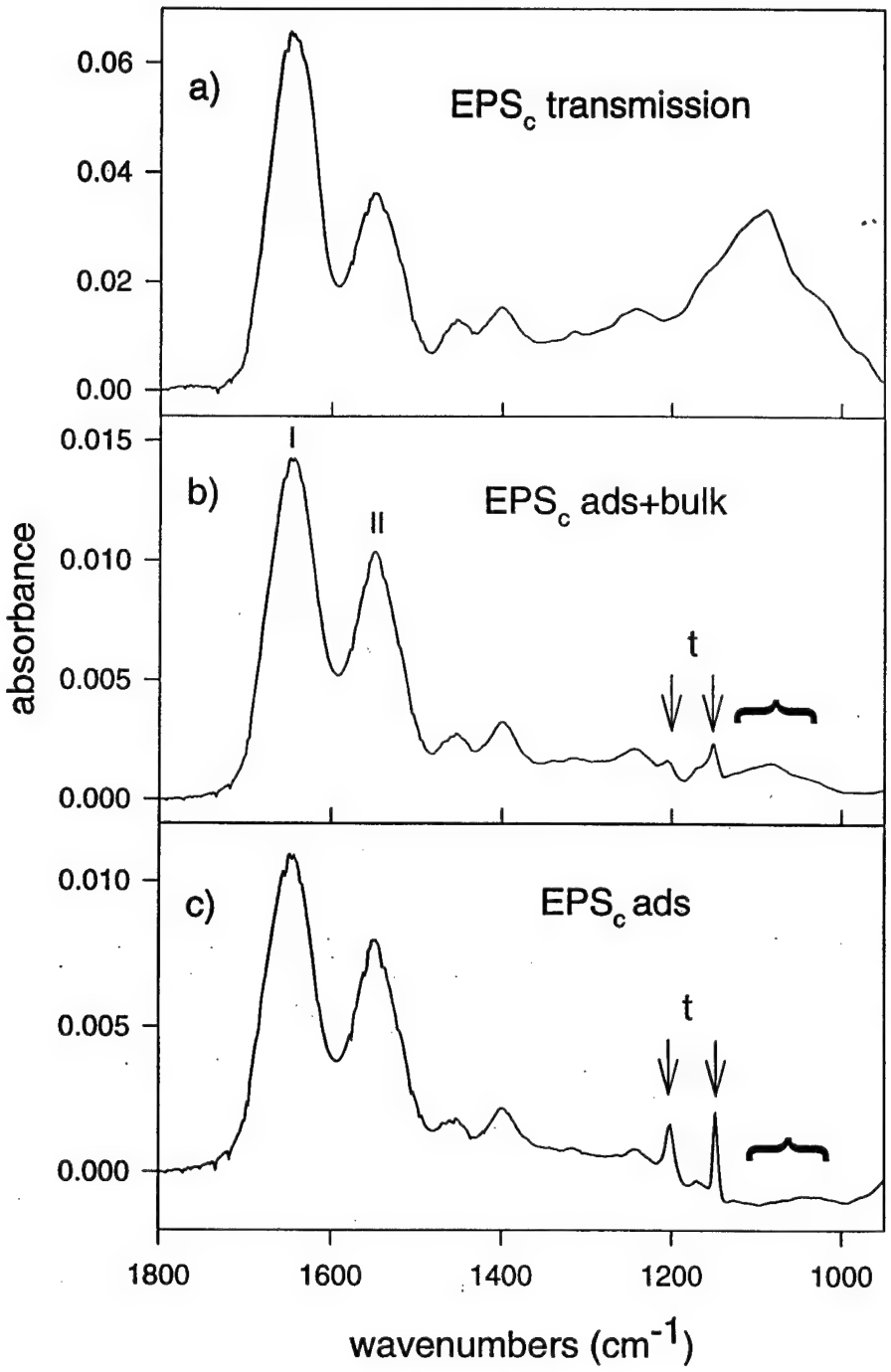

Fig. 2 a = IR transmission spectrum of EPS_c (approximately 20 mg·ml^{-1}); b = ATR spectrum of 1 mg·ml^{-1} EPS_c in the flow chamber; amide I and II bands are indicated; bracketed portion contains bands emanating potentially from carbohyrates, RNA and DNA; c = ATR spectrum of adsorbed EPS_c at the end of the rinse period. Arrows in b and c indicate positions of bands emanating from Teflon O-rings.

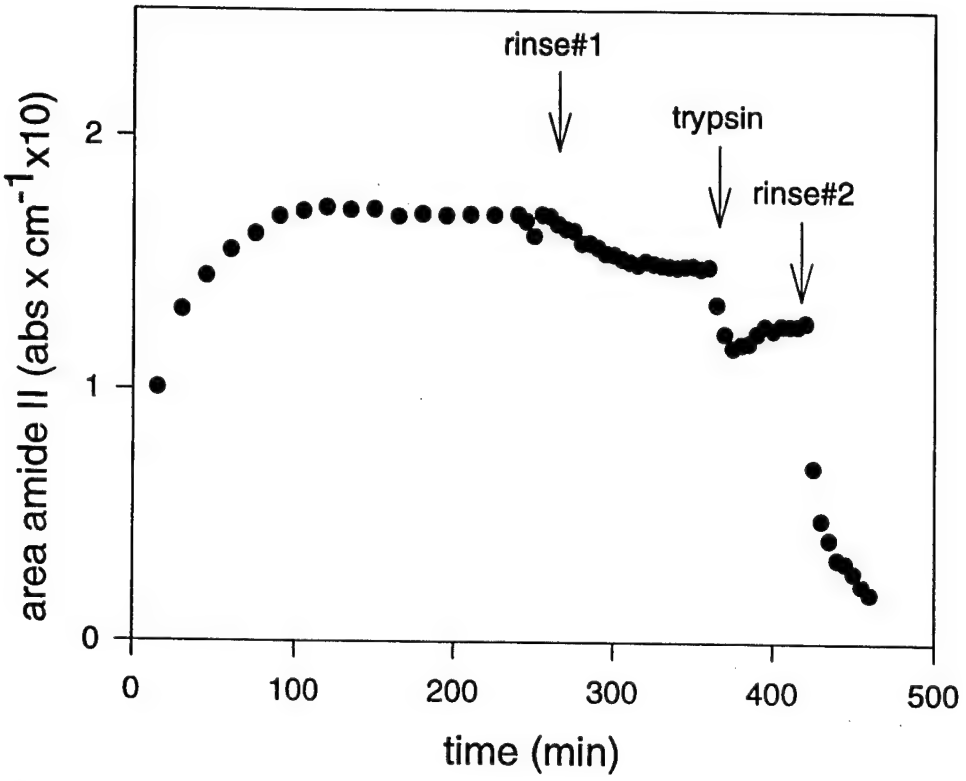

Fig. 3 Time course of adsorption and desorption of EPS_c protein based on areas of the amide II band. Times of rinses with seawater (rinse#1 and #2) are indicated, as well as time of introduction of trypsin into the flow chamber.

1561 cm^{-1} in the spectrum of the bulk EPS_p (Fig. 4a) may be protein amide bands, they are somewhat atypical in this respect. It is rare to find a protein amide II absorbance above 1560 cm^{-1} (Krimm, 1962; Nevskaya & Chirgadze, 1976; Moore & Krimm, 1976). Furthermore, the amide I and II bands of proteins are typically of more equal half-widths (Fink *et. al.*, 1987; Ishida & Griffiths, 1993a). The wide band at 1561 cm^{-1} may be composed of overlapping bands from protein peptide linkages and N-acetyl groups of a polysaccharide (Quintero & Weiner, 1995a). Amide vibrations of N-acetyl groups of hyaluronic acid are close to 1565 cm^{-1} (Parker, 1983) and that of N-methylacetamide is at 1567 cm^{-1} (Miyazawa *et al.*, 1958). In contrast to the EPS_c, the putative amide I and II bands contribute proportionately less to the spectra of the adsorbed material (both during adsorption and after the rinse) than to the spectrum of the bulk material. This is especially evident for the band centered at 1561 cm^{-1} which is undetectable for adsorption experiments with bulk EPS_p less than 0.2 $mg \cdot ml^{-1}$ (spectra not shown). In summary, the carbohydrate fraction of EPS_p (rather than any residual protein) appears to dominate the adsorption process.

In Figure 4c bands used to follow the adsorption reaction involving components of EPS_p are indicated (EPS_p I and II). These bands were chosen for the technical reason that they are less obscured by the water background absorbance centered at 1640 cm^{-1} and the

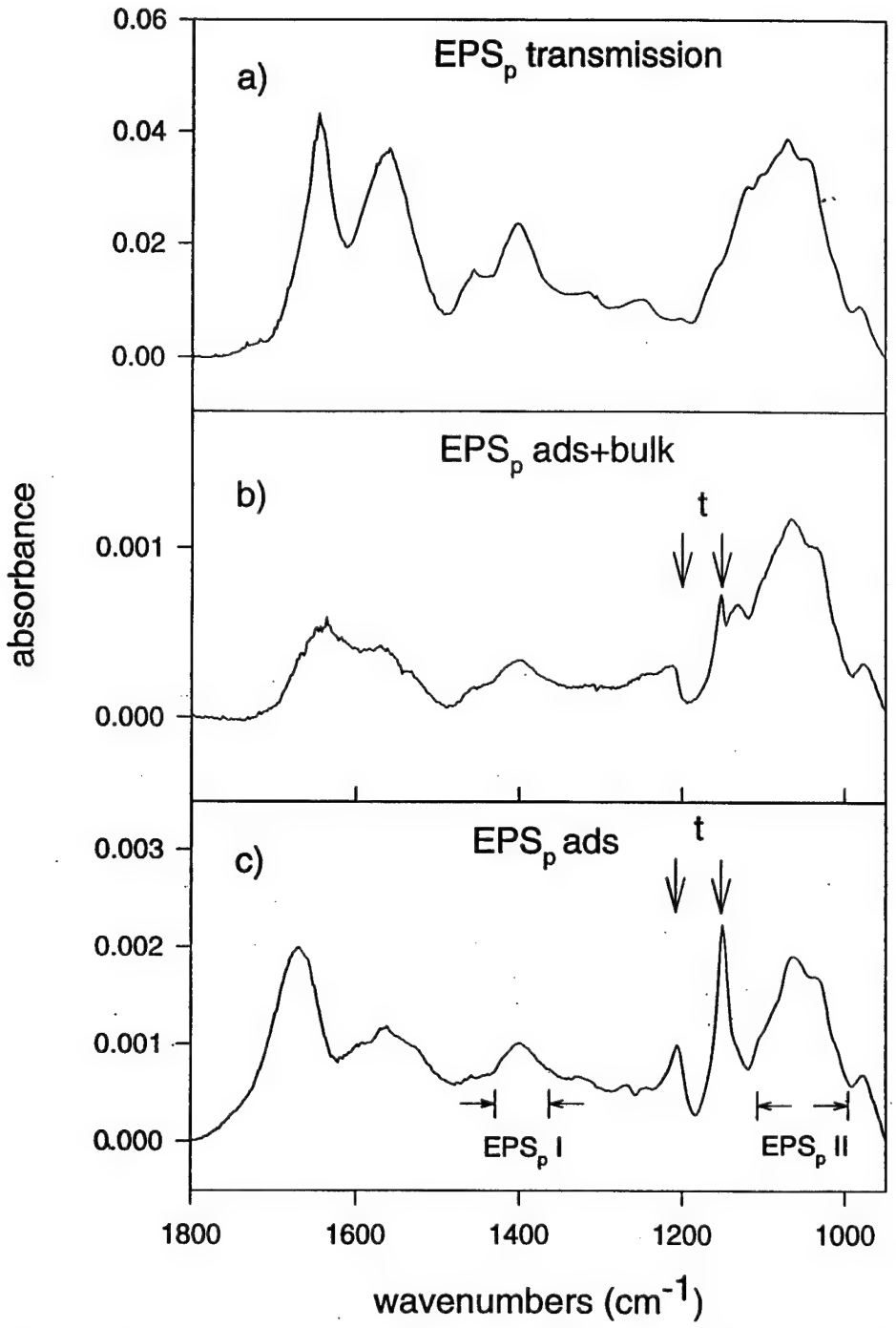

Fig. 4 a = IR transmission spectrum of EPS_p (30 mg·ml^{-1}); b = ATR spectrum of 0.2 mg·ml^{-1} EPS_p in the flow chamber; positions of bands emanating from the Teflon O-rings are indicated; c = ATR spectrum of adsorbed EPS_p at the end of the rinse period. Spectral features (EPS_p I and II) used to follow the adsorption reaction are indicated.

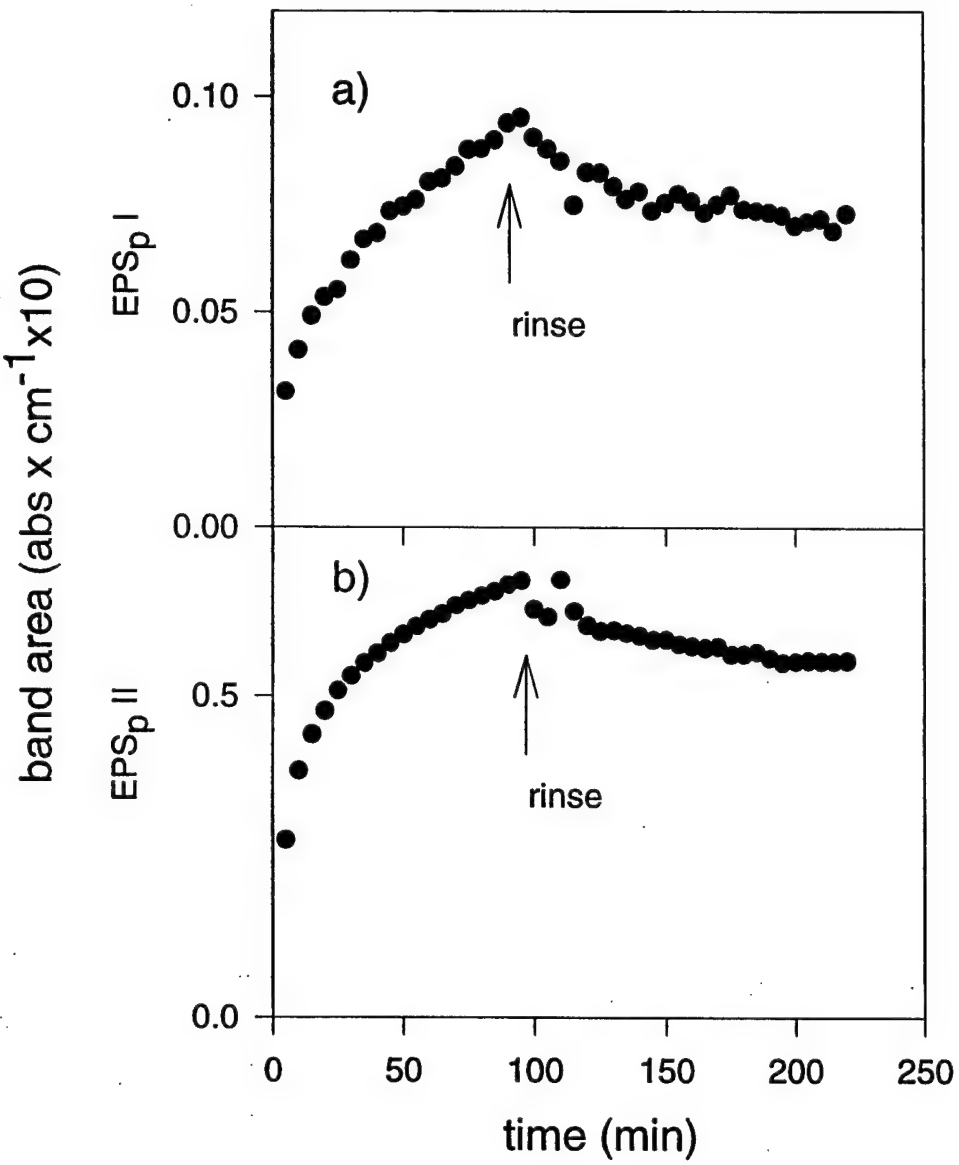

Fig. 5 Time course of adsorption and desorption of EPS_p based on areas of spectral features. a = EPS_p I; b = EPS_p II.

teflon bands at 1200 cm^{-1} and 1150 cm^{-1} (which emanate from the O-rings) than other spectral features. In addition, the wide spectral feature named EPS_p II is located within the prospective carbohydrate region. For the adsorbed material (Fig. 4c) this spectral feature appears to be composed primarily of bands centered at 1060 cm^{-1} and 1033 cm^{-1}. Vibrations near 1030 cm^{-1} have been assigned to C-O-H deformations or C-O stretch of the pyranose ring (Cael *et al.*, 1975; Parker, 1983; Ishida & Griffiths, 1993b).

Polysaccharides containing N-acetyl groups such as hyaluronic acid have bands near 1070 cm^{-1} (Parker, 1983). The spectral feature named EPS_p I, centered at 1395 cm^{-1}, cannot be given an unambiguous assignment. Carboxylate salts commonly have a symmetric stretch in this region (L-Vien *et al.*, 1991) with an accompanying asymmetric stretch in the region from 1650–1540 cm^{-1}. However, for uronic acids this latter band is typically located near 1600 cm^{-1} and is prominent (Parker, 1975). Proteins normally display a band in this region. However, as mentioned above, for low surface coverages of EPS_p, the putative amide II band centered at 1561 cm^{-1} becomes undetectable, while EPS_p I remains conspicuous. At these low surface coverages, it becomes impossible to distinguish the band centered at 1646 cm^{-1}, (another candidate for the asymmetric carboxylate stretch), from the strong background water absorbance at 1640 cm^{-1}.

Figure 5 shows the time course of EPS_p adsorption/desorption from the substratum based on the areas of EPS_p I and II (Fig. 4c). Although there is some desorption after the rinse is initiated, a major fraction of the material is retained on the surface at the end of the rinse period.

EPS Binding Curves

In order to construct binding curves for the various EPS preparations, the areas of pertinent spectral features at the end of the rinse period have been plotted against the bulk concentration to which the substratum was exposed. The binding curves have been fit with a Langmuir model (Eqn 2). Parameters (K^{-1} and Γ) obtained from the Langmuir fits to binding curves are listed in Table 2. Binding curves presented below (Figs 6, 7a, 7b) have been plotted in terms of area of the spectral feature *vs* total concentration of bulk EPS. To obtain the parameters K^{-1} and Γ, ordinate and abscissa values must be converted to surface coverage and concentration of the specific EPS component, respectively (see Methods). Using the total carbohydrate content of EPS_p for these estimates yields maximum estimates of K^{-1} and Γ.

The binding curve for the protein fraction of EPS_c (amide II band *vs* bulk concentration) is shown in Figure 6. The fit to the Langmuir model is shown by the dotted line. The adsorbed quantity at a 1 $mg \cdot ml^{-1}$ bulk concentration exhibits an extent of variability not observed at lower concentrations. The mean of these five adsorption experiments is indicated by the open square symbol.

Table 2 Parameter fits to the Langmuir model (Eqn 2). Data are presented in Figures 6 and 7. See text for conversion of spectral features to surface coverage (Γ). Lower values of K^{-1} imply greater binding affinity.

	Hyphomonas EPS[a]			*Literature (proteins)*		
parameter[b]	Amide II *(EPS_c)*	EPS_p I	EPS_p II	i	ii	iii
Γ ($\mu g.cm^{-2}$)	0.179 ± 0.019	0.143 ± 0.015	0.143 ± 0.017	0.281 ± 0.010	0.5	0.25
K^{-1}($mg.ml^{-1}$)	0.049 ± 0.015	0.270 ± 0.047	0.033 ± 0.010	0.017 ± 0.002	0.103	0.006

i = mussel adhesive protein on germanium; binding curve previously published (Suci & Geesey, 1995)
ii = bovine serum albumin on methylated surface (estimated from Fig. 5), Koltisko & Walton, 1985
iii = gamma-globulin on silicone rubber (Watkins & Robertson, 1977);
[a]Identified by IR spectral feature
[b]Fits for EPS_p I and II are to data points for bulk concentrations < 5$mg \cdot ml^{-1}$

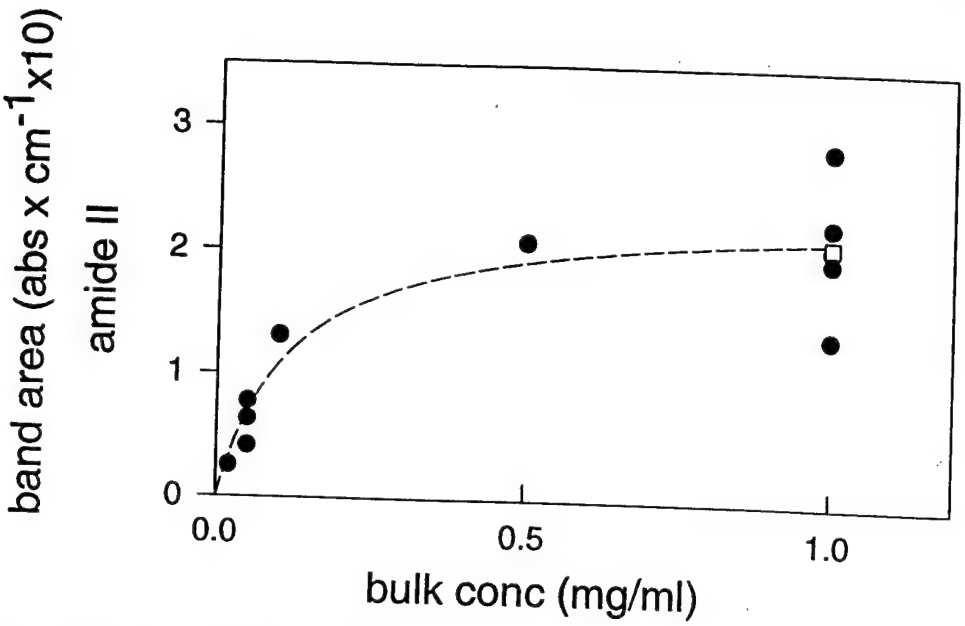

Fig. 6 Binding curve of the EPS_c protein fraction. □ = the position of the average of the five data points at 1 mg·ml^{-1} bulk concentration; --- = the Langmuir fit.

The binding curves for EPS_p are shown in Figure 7. Areas of spectral features named EPS_p I and II (Fig. 4c), determined at the end of the rinse period, have been plotted against the total bulk concentration to which the substratum was exposed. For each plot two fits of the Langmuir model are indicated. The broken line is the fit to all data points, while the dotted line is the fit to data points for bulk concentration below 5 mg·ml^{-1}. The mean value for data points at 5 mg·ml^{-1} bulk concentration is designated by an open square. The variation in the areas of EPS_p II at this concentration is extreme. An obvious explanation is that the extent of adsorption varies sensitively with the degree of surface contamination. However, the extent of adsorption at this relatively high bulk concentration is uncorrelated to general hydrocarbon contamination estimated by absorbances in the CH_2 and CH_3 stretch region between 2980 and 2820 cm^{-1} immediately before the adsorption was initiated (data not shown). It is possible that a small fraction of the adhesive protein, which resides in the EPS_p after the purification, begins to compete with the polysaccharide components for adsorption sites above a certain threshold concentration which is just barely achieved at 5 mg·ml^{-1} bulk concentration of total EPS_p. However, this does not explain the enhancement of adsorption above the mean for two experiments.

Interaction Between Proteins and Polysaccharides

Conditioning the germanium substratum with EPS_c impedes adsorption of the putative polysaccharides in EPS_p. This is indicated by results presented in Figure 8. Germanium IREs were first exposed to EPS_c, and then rinsed as described above. Substrata which had different degrees of surface coverage of EPS_c were then exposed to a 0.1 mg·ml^{-1} bulk concentration of EPS_p. This second adsorption was performed with the same protocol as

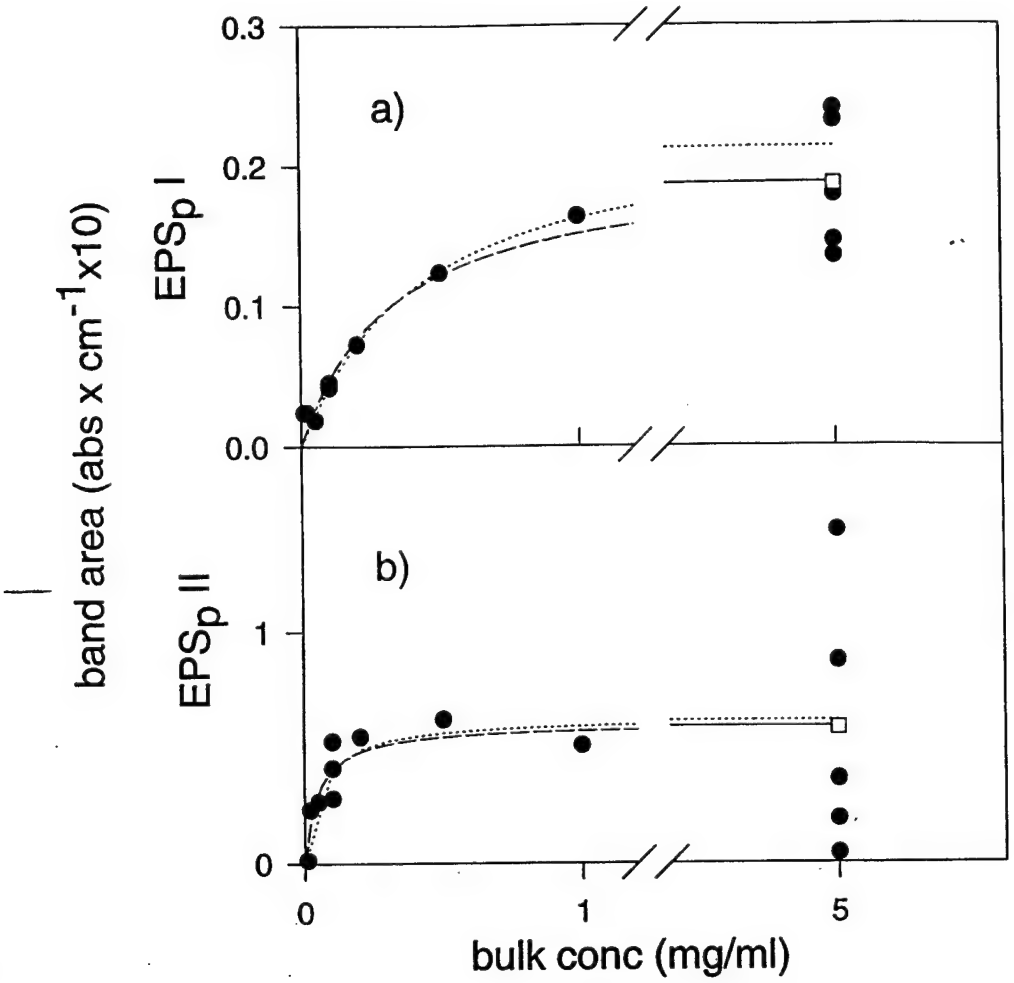

Fig. 7 a, b = binding curves for putative polysaccharide fractions of EPS_p □ = the position of the average of the five data points at 5 mg·ml^{-1} bulk concentration; — = the Langmuir fit to all data points; ... = the fit to data points for bulk concentrations < 5 mg·ml^{-1}.

for adsorption experiments to the clean substratum (100 min adsorption/120 min rinse). (The adsorption attained a plateau during the 100 min time period). The results are summarized in Figure 8 in which the areas of the spectral feature EPS_p II at the end of the second rinse period are plotted against the amount of pre-adsorbed protein from EPS_c (amide II area). (Results for EPS_p I are similar). The negative correlation between surface coverage of pre-adsorbed EPS_c and area of the spectral feature EPS_p II is apparent.

In order to see whether the protein from the EPS_c would displace the putative polysaccharides (from which spectral features EPS_p I and II emanate), EPS_p was adsorbed at a concentration of 1 mg.ml^{-1} using the standard protocol. The surface conditioned with EPS_p was then exposed to a 1 mg·ml^{-1} bulk concentration of the EPS_c. Figure 9 shows the time course of the change in the amide II band (Fig. 9a) and in EPS_p II (Fig. 9b) during

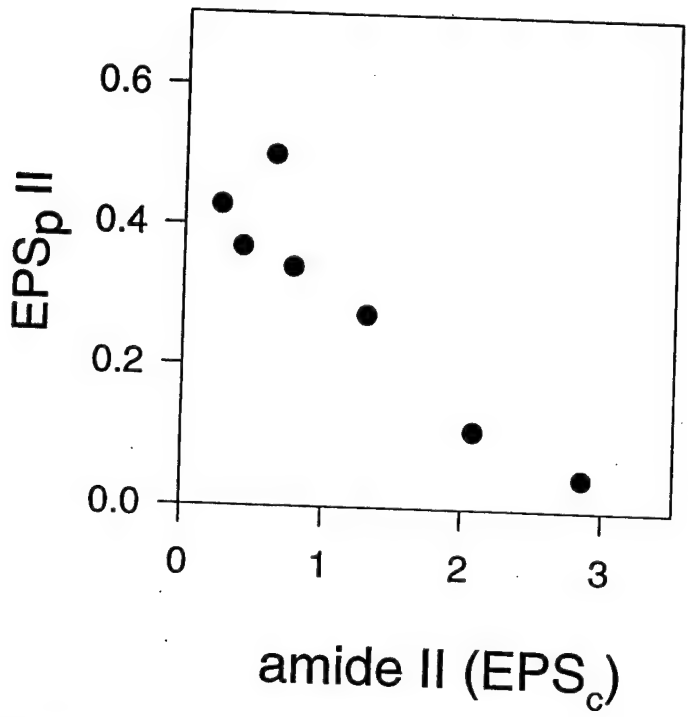

Fig. 8 Relation between surface coverage of pre-adsorbed protein from EPS_c and putative polysaccharide fraction from EPS_p (EPS_p II) adsorbed onto the conditioned substratum.

this second adsorption and the rinse. The solid line through the initial data points in Figure 9a is an exponential fit as described in Methods. This empirical fit allows assignment of a "time constant" to the adsorption kinetics (τ in Eqn 3) of 100 min. The average τ value for adsorption of protein from EPS_c onto a clean substratum is 40 ± 10 min (5 experiments).

Pre-adsorbed material from EPS_p is not displaced by the protein fraction from EPS_c. There is little change in the area of EPS_p II (Fig. 9b) and the insert reveals that the material remaining on the surface resembles the material adsorbed on a clean germanium substratum from EPS_p: the peak at 1060 cm^{-1}, the shoulder at 1034 cm^{-1} and the small peak at 976 cm^{-1} are evident. Although the rate of adsorption is slower, the empirical fit to Eqn 2 indicates that, if the same general trend in the time course of adsorption is followed, the protein will eventually reach a plateau area of 0.208 abs·cm^{-1} or 4 mA peak height above baseline (A_p in Eqn 2), which is in the range for adsorption to a clean substratum after the rinse period (mean for 4 experiments: 0.257 ± 0.505 abs.cm^{-1}) (see also Fig. 6).

DISCUSSION

Characterization of adsorption behavior is one approach which has been used to investigate the potential adhesive role of EPS matrix components (Pringle & Fletcher,

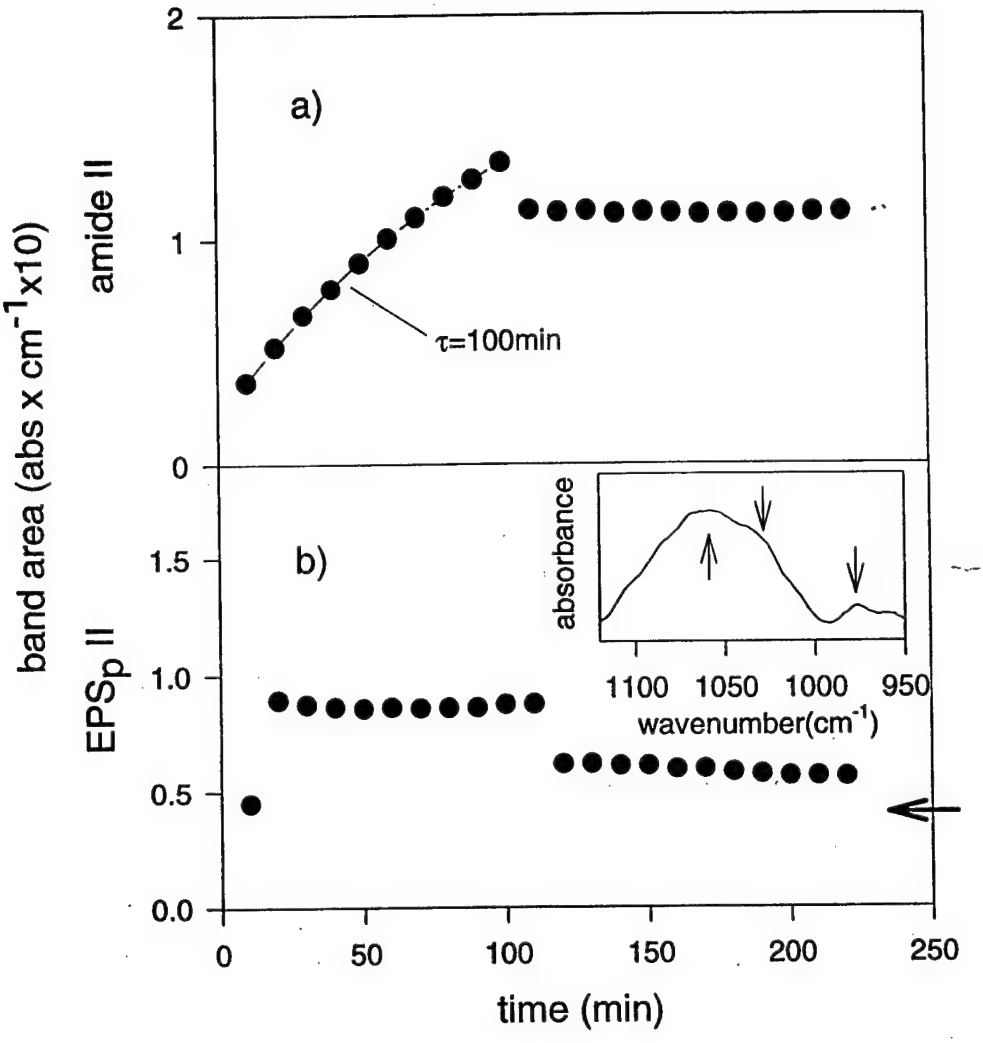

Fig. 9 a = time course of binding of protein for EPS_c onto substratum conditioned with EPS_p at 1 $mg \cdot ml^{-1}$ with time constant indicated (see text); b = change in area of EPS_p during protein binding; arrow indicates area of this region before exposure to protein; insert is difference spectrum of this region at the end of the rinse period with characteristic features indicated.

1986). In order to make definite structure/function assignments these studies must be supplemented with data acquired using other methods *e.g.* direct observation (Fletcher & Floodgate, 1973) or footprint analysis (Neu, 1992). In this context, adsorption studies can indicate interactions between biomolecules and surfaces which merit scrutiny.

In this report, adsorption behavior of crude EPS (EPS_c) from biofilms of *Hyphomonas* MHS-3 has been compared to EPS from which a large portion of the protein, DNA and

RNA has been removed (EPS_p). The protein dominates the adsorption process for EPS_c. Removal of the Protease K accessible protein allows adsorption of two putative polysaccharide components to be detected. In terms of adsorption behavior, the interaction between protein and polysaccharide in the EPS is apparently antagonistic; they appear to compete for the same sites on the substratum. It is apparent from the data that even EPS_p consists of a mixture of biomolecules. It is likely that the chaotic adsorption behavior at 5 $mg \cdot ml^{-1}$ bulk concentration (Fig. 7b) can be attributed to interactions between minor components of this mixture which begin to exert an influence at some threshold concentration. However, the nature of the critical governing interactions remains illusive.

Characterization of adsorption behavior yields an estimate of affinity for the surface of the various molecular species. The Langmuir model has been applied here to allow a quantitative appraisal of binding affinity, with the understanding that its application is not rigorous. Intuitively, it might be expected that an adsorbent with a strong affinity for a surface would adsorb out of relatively dilute bulk solutions and would have a high density of coverage at saturation. The parameters K^{-1} and Γ listed in Table 2 reflect these adsorption tendencies. In addition, this approach allows comparison of adsorption behavior with results of other investigators, some of whom have applied the Langmuir model to quantify irreversible adsorption behavior (Pringle & Fletcher, 1986; Watkins & Robertson, 1977).

Using the parameters obtained from the Langmuir fit as an index of binding affinity, both the protein fraction from the EPS_c and the putative polysaccharide fraction of EPS_p corresponding to the spectral feature EPS_p II are quite sticky. The EPS component responsible for the spectral feature EPS_p I (which cannot be unambiguously assigned) is somewhat less sticky. This assessment has been made based on a comparison with typical values for globular blood proteins (Brash & Horbett, 1987), which are conventionally considered to be strong adsorbents, from comparison to adsorption data for an EPS from another marine biofilm forming organism (Pringle & Fletcher, 1986), and from data collected in the authors' laboratory on the adsorption of adhesive protein from *Mytilus edulis* (Suci & Geesey, 1995).

It is notable that the *Hyphomonas* EPS contains at least one adhesive protein and at least one adhesive polysaccharide. The literature indicates that, in general, proteins adsorb strongly to most surfaces. However, it is important to mitigate this generalization with the qualification that the majority of research in this respect has been done on globular blood proteins, which may have inherently adhesive properties.

Polysaccharides are not considered to be universally strong adsorbents. Results indicate that presence of a preformed polysaccharide rich capsule may impede initial cell attachment to hydrophobic surfaces (Wrangstadh *et al.*, 1986; Rosenberg & Kjelleberg, 1986) or enhance binding preferentially to hydrophilic surfaces (Shea & Smith-Somerville, 1994). The uronic acid-containing polysaccharide, alginate, adsorbs only weakly to both germanium and polystyrene (Ishida & Griffiths, 1993b, Suci & Geesey, 1995). This suggests that affinity for hydrophilic surfaces is not a universal characteristic of functionalized polysaccharides, and must be conferred by appropriate molecular architecture. It has been proposed that polysaccharides functionalized with methyl or acetyl groups may exhibit protein-like adsorption behavior as a result of the consequent hydrophobic domains (Christensen *et al.*, 1985). Extracellular polysaccharides produced after cell attachment could presumably attain sufficient concentration to confer an extent of adhesion originating purely from their viscosity (Humphrey *et al.*, 1979). The *Hyphomonas* polysaccharide responsible for the spectral feature EPS_p II adsorbs from dilute solutions which suggests that it may have been specially synthesized as a primary adhesive EPS component.

Although chemical characterization of bacterial EPS has revealed that it is typically composed of significant amounts of both protein and carbohydrate (Humphrey *et al.*, 1979; Abu *et al.*, 1991), there are few studies which have investigated the interaction between the protein and polysaccharide EPS components in mediating adhesion of bacteria to surfaces. The SDS-PAGE banding pattern suggests that many EPS_c proteins originate from processes related to cell lysis which occur during biofilm development. There is some slight evidence for the presence of specialized EPS matrix proteins. Collectively these proteins do not appear to perform the clear function of serving to mediate adhesion between the substratum and (structural) polysaccharides. However, the possibility remains that there may be particular proteins contained within this set which do serve this function.

The proteins contained within EPS_c do not readily displace the adhesive EPS_p polysaccharide fraction. In contrast, they adsorb either to unoccupied sites on the substratum or to the bound polysaccharides. This leads to the possibility that they may serve to pin these polysaccharides more tenaciously to the surface. This type of interaction has been observed between macromolecules adsorbing to substrata (Johnson & Granick, 1992).

Acknowledgement

This work was supported by Office of Naval Research Grant N00014-93-1-0168, a grant from 3M, and Cooperative Agreement ECD-8907039 between the National Science Foundation and Montana State University. One of us (BF) received support from the Danish Technical Research Council (Grant # 5.26.16.22).

References

Abu G O, Weiner R M, Rice J, Colwell R R (1991) Properties of an extracellular adhesive polymer from the marine bacterium, *Shewanella colwelliana*. *Biofouling* **3**: 69–84

Allison, D G, Sutherland, I W (1987) The role of exopolysaccharides in adhesion of freshwater bacteria. *J Gen Microbiol* **133**: 1319–1327

Andrade J D (1985) Principles of protein adsorption. In: Andrade J D (ed) *Surface and Interfacial Aspects of Biomedical Polymers, Vol 2, Protein Adsorption*. Plenum Press, New York, pp 1–80

Bandekar J, Krimm S (1980) Vibrational analysis of peptides, polypeptides, and proteins. VI. Assignment of ß-turn modes in insulin and other proteins. *Biopolymers* **19**: 31–36

Blumenkrantz N, Asboe-Hansen G (1973) A new method for quantitative determination of uronic acids. *Anal Biochem* **54**: 484

Brash J L, Horbett T A (1987) *Proteins at Interfaces: Physicochemical and Biochemical Studies*. ACS symposium series 343, American Chemical Society, Washington, DC

Busscher H J, Bellon-Fontaine M-N, Mozes N, Van der Mei H C, Sjollema J, Cerf O, Rouxhet P G (1990) Deposition of *Leuconostoc mesenteroides* and *Streptococcus thermophilus* to solid substrata in a parallel plate flow cell. *Biofouling* **2**: 55–63

Cael J J, Koenig J L, Blackwell J (1975) Infrared and raman spectroscopy of carbohydrates. VI. Normal coordinate analysis of V-amylose. *Biopolymers* **14**: 1885–1903

Christensen B E, Kjosbakken J, Smidsrod O (1985) Partial chemical characterization of two extracellular polysaccharides produced by marine periphytic *Pseudomonas* sp. strain NCMB 2021. *Appl Environ Microbiol* **50**: 837–845

Cooksey K E (1992) Extracellular polymers in biofilms. In: Melo L F, Bott T R, Fletcher M, Capdeville B (eds) *Biofilms: Science and Technology*. Kluwer, The Netherlands, pp 137–147

Costerton J W, Cheng K J, Geesey G G, Ladd T I, Nickel J C, Dasgupta M, Marrie T J (1987) Bacterial biofilms in nature and disease. *Ann Rev Microbiol* **41**: 435–464

Croes C L, Moens S, van Bastelaere E, Vanderleyden J, Michiels K W (1993) The polar flagellum mediates *Azospirillum brasilense* adsorption to wheat roots. *J Gen Microbiol* **139**: 2261–2269

DeBeer D, Stoodley P, Roe F, Lewandowski Z (1993) Oxygen distribution and mass transport in biofilms. *Biotechnol Bioeng* **43**: 1131–1138

Dexter S C, Sullivan Jr J D, Williams III J, Watson W (1975) Influence of substrate wettability on the attachment of marine bacteria to various surfaces. *Appl Microbiol* **30**: 298–308

Doyle R J, Rosenberg M (1990) *Microbial Cell Surface Hydrophobicity*: American Society for Microbiology, Washington, D C

Dubois M, Gilles K A, Hamilton J K, Rebers P A, Smith F (1956) Colorimetric method for determination of sugars and related substances. *Anal Chem* **28**: 350–356

Fink D J, Hutson T B, Chittur K K, Gendreau R M (1987) Quantitative surface studies of protein adsorption by infrared spectroscopy: II. Quantification of adsorbed and bulk proteins. *Anal Biochem* **165**: 147–154

Fletcher M, Floodgate G D (1973) An electron microscope demonstration of an acidic polysaccharide involved in the adhesion of a marine bacterium to solid surfaces. *J Gen Microbiol* **74**: 325–334

Fletcher M, Loeb G I (1979) Influence of substratum characteristics on the attachment of a marine pseudomonad to solid surfaces. *App Environ Microbiol* **37**: 67–72

Geesey G G (1982) Microbial exopolymers: ecological and economic considerations. *ASM News* **48**: 9–14

Holmström C, Kjelleberg S (1994) The effect of external biological factors on settlement of marine invertebrate and new antifouling technology. *Biofouling* **8**: 147–160

Hoyle B D, Jass J, Costerton J W (1990) The biofilm glycocalyx as a resistance factor. *J Antimicrob Chemother* **26**: 1–5

Humphrey B A, Dickson M R, Marshall K C (1979) Physicochemical and *in situ* observations on the adhesion of gliding bacteria to surfaces. *Arch Microbiol* **120**: 231–238

Ishida K P, Griffiths P R (1993a) Comparison of the amide I/II intensity ratio of solution and solid-state proteins sampled by transmission, attenuated total reflectance, and diffuse reflectance spectrometry. *App Spectrosc* **47**: 584–589

Ishida K P, Griffiths P R (1993b) Investigation of polysaccharide adsorption on protein conditioning films by attenuated total reflection infrared spectrometry. *J Colloid Interface Sci* **160**: 190–200

Jann K, Jann B (1990) Bacterial adhesins. In: *Curr Top Microbiol Immunol* **151**: Springer-Verlag, New York

Johnson H E, Granick S (1992) New mechanism of nonequilibrium polymer adsorption. *Science* **255**: 966–968

Kintner P K, Van Buren J P (1982) Carbohydrate interference and its correction in pectin analysis using m-hydroxydiphenyl method. *J Food Sci* **47**: 756–760

Knutzen K, Lyman D J (1985) Surface infrared spectroscopy. In: Andrade J D (ed) *Surface and Interfacial Aspects of Biomedical Polymers, Vol 1, Surface Chemistry and Physics*. Plenum Press, New York, pp 197–247

Koltisko B, Walton A (1985) Chromatographic analysis of protein adsorption. In: Andrade J D (ed) *Surface and Interfacial Aspects of Biomedical Polymers, Vol. 2, Protein Adsorption*. Plenum Press, New York, pp 217–239

Korber D R, James G A, Costerton J W (1994) Evaluation of fleroxicin activity against established *Pseudomonas fluorescens* biofilms. *Appl Environ Microbiol* **60**: 1663–1669

Krimm S (1962) Infrared spectra and chain conformation of proteins. *J Mol Biol* **4**: 528–540

Lange W (1976) Speculation on a possible essential function of the gelatinous sheath of blue-green algae. *Can J Microbiol* **22**: 1181–1185

Lowry O H, Rosebrough N J, Farr A L, Randall R J (1951) Protein measurement with the folin reagent. *J Biol Chem* **193**: 265–275

L-Vien D, Colthup N B, Fateley W G, Grasselli J G (1991) *The Handbook of Infrared Characteristic Frequencies of Organic Molecules*. Academic Press Incorporated, New York pp 139

Miyazawa T, Blout E R (1961) The infrared spectra of polypeptides in various conformations: amide I and II bands. *J Amer Chem Soc* **83**: 712–719

Miyazawa T, Shimanouchi T, Mizushima S-I (1958) Normal vibrations of N-methylacetamide. *J Chem Phys* **29**: 611–616

Moore W H, Krimm S (1976) Vibrational analysis of peptides, polypeptides, and proteins II. β-poly(L-alanine) and β-poly(L-alanyl)glycine. *Biopolymers* **15**: 2465–2483

Neu T R (1992) Microbial "footprints" and the general ability of microorganisms to label surfaces. *Can J Microbiol* **38**: 1005–1008

Nevskaya N A, Chirgadze Y N (1976) Infrared spectra and resonance interactions of amide-I and II vibrations of α-helix. *Biopolymers* **15**: 637–648

Parker F S (1983) Carbohydrates. In: *Applications of Infrared, Raman, and Resonance Raman in Biochemistry*. Plenum Press, New York, pp 315–347

Pitt W G (1987) Protein adsorption on polyurethanes. Ph D Thesis, University of Wisconsin, Madison, WI

Pitt W G, Cooper S L (1988) Albumin adsorption on alkyl chain derivatized polyurethanes: I. the effect of C-18 alkylation. *J Biomed Mat Res* **22**: 359–382

Pringle J H, Fletcher M, Ellwood D C (1983) Selection of attachment mutants during the continuous culture of *Pseudomonas fluorescens* and relationship between attachment ability and surface composition. *J Gen Microbiol* **129**: 2557–2569

Pringle J H, Fletcher M (1986) Adsorption of bacterial surface polymers to attachment substrata. *J Gen Microbiol* **132**: 743–749

Quintero E J, Weiner R M (1995a) Physical and chemical characterization of the polysaccharide capsule of the marine bacterium, *Hyphomonas* strain MHS-3. *J I M*, (submitted)

Quintero E J, Weiner R M (1995b) Evidence for the adhesive function of the exopolysaccharide of *Hyphomonas* strain MHS-3 in its attachment to surfaces. *App Environ Microbiol* **61**: 1897–1903

Read R R, Costerton J W (1987) Purification and characterization of adhesive exopolysaccharides from *Pseudomonas putida* and *Pseudomonas fluorescens*. *Can J Microbiol* **33**: 1080–1090

Rosenberg M, Kjelleberg S (1986) Hydrophobic interactions: role in bacterial adhesion. *Adv Microbial Ecol* **9**: 353–393

Shapiro A L, Vinuela E, Maizel J V (1967) Molecular weight estimation of polypeptide chains by electrophoresis in SDS-polyacrylamide gels. *Biochem Biophys Res Comm* **28**: 815–818

Shea C, Smith-Somerville H E (1994) The effects of phenotype variability on the adhesion properties of *Deleya marina*. *Biofouling* **8**: 13–25

Shen N, Dagasan L, Sledjeski D, Weiner R M (1989) Major outer membrane proteins unique to reproductive cells of *Hyphomonas jannaschiana*. *J Bacteriol* **171**: 2226–2228

Suci P A, Geesey G G (1995) Investigation of alginate binding to germanium and polystyrene substrata conditioned with mussel adhesive protein. *J Coll Int Sci* **172**: 347–357

Taillandier E, Liquier J, Taboury J A (1985) Infrared spectral studies of DNA conformations. In: Clark R J H, Hester R E (eds) *Advances in Infrared and Raman Spectroscopy, Vol 12*. John Wiley and Sons, New York, pp 65–114

Tetz V V, Rybalchenko O V, Savkova G A (1993) Ultrastructure of the surface film of bacterial colonies. *J Gen Microbiol* **139**: 855–858

Vincent P, Pignet P, Talmont F, Bozzi L, Fournet B, Guenennec C, Jeanthon C, Prieur D (1994) Production and characterization of an exopolysaccharide excreted by a deep-sea hydrothermal vent bacterium isolated from the polychaete annelid *Alvinella pompejana*. *Appl Environ Microbiol* **60**: 4134–4141

Watkins R W, Robertson C R (1977) A total internal reflection technique for the examination of protein adsorption. *J Biomed Mat Res* **11**: 915–938

Wrangstadh M, Conway P L, Kjelleberg S (1986) The production of an extracellular polysaccharide during starvation of a marine *Pseudomonas* sp. and the effect thereof on adhesion. *Arch Microbiol* **145**: 220–227

Biofouling, 1996, Vol. 10, pp. 17–30
Reprints available directly from the publisher
Photocopying permitted by license only

INFLUENCE OF PROTEIN CONDITIONING FILMS ON BINDING OF A BACTERIAL POLYSACCHARIDE ADHESIN FROM *HYPHOMONAS* MHS-3

B FRØLUND[1,2], P A SUCI[†2], S LANGILLE[3], R M WEINER[3] and G G GEESEY[2,4]

[1]*Danish Technological Institute, Plastics Technology, Teknologiparken, 8000 Aarhus C, Denmark* [2]*Center for Biofilm Engineering, Montana State University, MT 59717, USA*
[3]*Department of Microbiology, University of Maryland, College Park, MD 20742, USA*
[4]*Department of Microbiology, Montana State University, MT 59717, USA*

(Received 23 November 1995; in final from 1 March 1996)

A putative polysaccharide adhesin which mediates non-specific attachment of *Hyphomonas* MHS-3 (MHS-3) to hydrophilic substrata has been isolated and partially characterized. A polysaccharide-enriched portion of the extracellular polymeric substance (EPS_p) from MHS-3 was separated into four fractions using high performance size exclusion chromatography (HPSEC). Comparison of chromatograms of EPS_p from MHS-3 and a reduced adhesion strain (MHS-3 rad) suggested that one EPS_p fraction, which consisted of carbohydrate, served as an adhesin. Adsorption of this fraction to germanium (Ge) was investigated using attenuated total reflection Fourier transform infrared (ATR/FT-IR) spectrometry. Binding curves indicated that the isolated fraction had a relatively high affinity for Ge when ranked against an adhesive protein from *Mytilis edulis*, mussel adhesive protein (MAP) and an acidic polysaccharide (alginate from *Macrocystis pyrifera*). Spectral features were used to identify the fraction as a polysaccharide previously reported to adsorb preferentially out of the EPS_p mixture. Conditioning the Ge substratum with either bovine serum albumin (BSA) or MAP decreased the adsorption of the adhesive polysaccharide significantly. Conditioning Ge with these proteins also decreased adhesion of whole cells.

KEYWORDS: extracellular polymeric substances, adhesion, marine bacterium, conditioning films

INTRODUCTION

Bacterial colonization of surfaces can be engineered for useful purposes, *e.g.* in wastewater treatment (Bryers & Characklis, 1990), or can lead to deleterious consequences, *e.g.* pathogenesis (Evans *et al.*, 1993), persistent implant-associated infections (Gristina, 1987), or fouling of industrial machinery (Väisänen *et al.*, 1994). Specific protein/ligand interactions have been found to mediate adhesion in some specialized ecosystems. Examples include adhesion of pathogens to host tissues (Jann & Jann, 1990), of oral bacteria to components of the pellicle (Clark *et al.*, 1989), and of cellulolytic bacteria to cellulose (Salamitou *et al.*, 1994). It seems reasonable to suppose that, in general, adhesion of bacteria to inert surfaces is a more generic phenomenon, *i.e.* not likely to involve interaction between ligands and customized binding pockets. However, there is evidence that specialized biomolecules have evolved to serve as primary (non-specific) adhesins to inert surfaces (Rosenberg *et al.*, 1982; Bar-ness *et al.*, 1988; Bashan & Levanony, 1988; Zottola, 1991; Yun *et al.*, 1994) and that the molecular architecture of extracellular components may be fashioned for adhesion to (Shea &

† Corresponding author

Smith-Somerville, 1994), or detachment from, inert surfaces (Pringle *et al.*, 1983; Wrangstadh *et al.*, 1986).

Various approaches have been taken in order to investigate the biochemistry of adhesion to inert (or inanimate) surfaces including inhibition assays (Merker & Smit, 1988; Quintero & Weiner, 1995), footprint analysis (Nue, 1992), enzyme treatment (Paul & Jeffrey, 1985) and adsorption assays (Pringle & Fletcher, 1986; Bidle *et al.*, 1993). Adsorption of organic compounds probably begins immediately after a material is placed in any natural water (Baier *et al.*, 1983). Interactions between this initial "conditioning film" and compounds proximal to the interface continue as the fouling process progresses (Baty *et al.*, 1996b). Many of these compounds will be biopolymers introduced by members of the fouling community. The more adhesive compounds may become part of the adsorbed film which eventually mediates the adhesive bond anchoring the fouling community to the substratum. Adsorption studies can help elucidate which factors determine the composition and binding properties of this interfacial film.

Surface associated microorganisms (biofilms) are typically embedded in a matrix of extracellular polymeric substance(s) (EPS) (Costerton *et al.*, 1987; Cooksey, 1992). The EPS matrix is often composed primarily, but not exclusively, of polysaccharides. It typically contains a mixture of biomolecules including a significant protein fraction (Humphrey *et al.*, 1979; Abu *et al.*, 1991; Vincent *et al.*, 1994). Therefore, the EPS components from one organism can present a complex set of interaction possibilities at an interface. It has been found that the EPS from *Hyphomonas* MHS-3 (MHS-3) contains at least one polysaccharide component which binds strongly to a clean Ge surface, and that this binding appeared to be blocked by conditioning the surface with intrinsic EPS proteins (Suci *et al.*, 1995). In order to further characterize these interactions, the most adhesive polysaccharide EPS component has been isolated using high performance size exclusion chromatography (HPSEC) and its adsorption behavior has been studied on Ge, and Ge conditioned with proteins expected to confer widely different surface properties to the substratum *viz.* a globular blood protein (bovine serum albumin) (BSA) and proteins from the adhesive plaque of *Mytilis edulis* (mussel adhesive protein) (MAP) (Waite, 1990). BSA inhibits cell adhesion in many cases and is used to block non-specific binding sites (Goding, 1983). In contrast, MAP promotes adhesion of a variety of cell types (Benedict & Picciano, 1987; Notter, 1988) and has been shown to enhance alginate adsorption in seawater (Suci & Geesey, 1995). The adhesion behavior of MHS-3 whole cells has also been characterized on these surfaces.

MATERIALS AND METHODS

Bacterial Strains and Cell Culturing

MHS-3 was isolated from shallow water sediments in Puget Sound, WA. A reduced adhesion strain (MHS-3 rad) was isolated on the basis of distinct colony morphology when cultured on marine agar plates (Quintero & Weiner, 1995). Cultures of MHS-3 and MHS-3 rad were grown in Marine Broth 2216 (37.4 g l^{-1}) (Difco Laboratories, Detroit, MI) at 25°C on a rotating shaker at 100 revs min^{-1}. Teflon™ mesh was introduced into the culture vessels to provide greater surface area for attached growth (mesh opening, 1.8 mm, thread diameter, 0.5 mm, Tetko, Incorporated, Briarcliff, NY). The attached cells and associated EPS were harvested from a culture in which the suspended cell population had just entered stationary phase. The medium was poured off and the biofilm was removed from the teflon mesh and the sides of the culture vessel walls by scraping.

EPS Extraction

The EPS was extracted in two steps. The cell suspension was centrifuged for 20 min at 16,000xg, and the "loosely bound" EPS in the supernatant was precipitated with 4 volumes of ice cold 2-propanol. The more "tightly bound" EPS was extracted from the cell pellet. The cell pellet was blended in a Waring blender in a minimum volume of 10 mM EDTA, 3% NaCl for 1 min at 4°C. The suspension was centrifuged for 15 min at 16000xg and the EPS from the supernatant was precipitated using 2-propanol as described above.

EPS Purification

A crude EPS preparation was obtained by pooling the two EPS fractions and resuspending in a minimum volume of distilled water (dH_2O). They were then dialyzed for 12 h against dH_2O and lyophilized. Polysaccharide-enriched EPS (EPS_p) was prepared by a published protocol (Read & Costerton, 1987). EPS was dissolved in a minimum volume of 0.1 M $MgCl_2$, and DNase and RNase were added to a final concentration of 0.1mg ml^{-1}, followed by incubation at 37°C for 4 h. Protease K was added to 0.1 mg ml^{-1} and incubated at 37°C overnight. Residual protein was removed with a hot phenol extraction, followed by a chloroform extraction. The preparation was dialyzed for 12 h against dH_2O and lyophilized. The EPS_p preparations were stored desiccated at room temperature.

HPSEC fractionation of EPS_p was performed using a Hewlet Packard 1090 liquid chromatograph equipped with an on-line diode array UV-VIS detector (Shodex OHpack B-2004 column). The mobile phase was 0.5 M NaCl, 0.05 M Na_2HPO_4 at pH 7.0 in dH_2O. EPS_p was dissolved in mobile phase at a concentration of 1 mg ml^{-1} and filtered through a 0.22 μm millipore filter. The injected sample volume was 1 ml. The column was run at room temperature at a flow rate of 0.9 ml min^{-1}. Separated EPS_p fractions were collected post column and concentrated in 0.01 M NaCl using ultrafiltration (Amicon 8010 stirred ultrafiltration cell, Amicon 5YM5 membrane). The concentrated fractions were stored at –40°C.

Chemical Analysis of EPS

Neutral hexoses were determined using the phenol sulfuric acid assay with glucose as the standard (Dubois *et al.*, 1956). Proteins were estimated using the Lowry procedure with BSA as standard (Lowry *et al.*, 1951). Total organic carbon (TOC) was analyzed using a Dohrmann DC 80 total organic carbon analyzer.

MHS-3 lipopolysaccharide (LPS) was identified using a monoclonal antibody (Busch, 1993) and Western blots. Polyacrylamide gels were run on a "Mighty Small II SE 250" mini-gel apparatus from Hoeffer Scientific with a 8% Tris/glycine separating gel at pH 8.8 and 4% Tris/glycine stacking gel at pH 6.8 (acrylamide/bisacrylamide ratio was 37.5:1). Running buffer was 3.0 g l^{-1} Tris Base, 14.4 g l^{-1} glycine and 1 g l^{-1} SDS in dH_2O. Sample buffer was 1.52 g Tris Base, 20 ml glycerol, 2.0 g SDS, 1.0 mg bromphenol blue and 80 ml dH_2O (pH 6.8). Aliquots (10 μl) of sample were mixed with an equal volume of sample buffer. The mixture was loaded on individual wells and electrophoresis carried out at 30 mA/gel for 1.5 h. Electroblotting was for 2 h onto a nitrocellulose filter (2117 multiphor II electrophoresis unit from Pharmacia) in buffer consisting of 2.93 g glycine, 5.81 g Tris Base, 0.375 g SDS and 200 ml methanol dissolved in 800 ml dH_2O. After washing in 20 ml of 5% skim milk for 0.5 h, the nitrocellulose was incubated at 25°C overnight with anti-LPS monoclonal antibody

diluted 1:1000 in 20 ml skim milk. The nitrocellulose was washed three times in a PBS-Tween solution (8.0 g l^{-1} NaCl, 2 g l^{-1} KCl, 1.15 gl^{-1} Na_2HPO_4, 0.2 g l^{-1} KH_2PO_4 and 0.5 ml l^{-1} Tween-20 at pH 7.4), then incubated at 25°C for 2 h with a 1:1000 diluted horseradish peroxidase labelled goat anti-mouse IgG antiserum. The nitrocellulose was again washed three times in PBS-Tween and placed in a developing solution containing 1.0 ml Tris buffer at pH 8.0, 20 mg 4-choro-1-napthol and 5 µl 50% H_2O_2.

Surface Preparation

Single crystal, cylindrical germanium (Ge) internal reflection elements (IRE) (Spectra Tech, Stamford, CT) were cleaned by ultrasonication in a base bath (saturated KOH in isopropyl alcohol) for 10 min. Following the base bath were two rinses in ultrapure water followed by a gentle scrubbing with undiluted Micro™ cleaning solution using cotton swabs. The cleaning solution was flushed off in a hard stream of ultrapure water. The IRE was then subjected to the following rinses, which consisted of a 10 min ultrasonication in each liquid: ultrapure water (2×), ethyl alcohol, chloroform and dichloromethane. The advancing contact angle of Ge surfaces cleaned by this protocol is between 10° and 20°, and Auger electron spectroscopy (Phi 595 scanning Auger microprobe) indicated that the elemental composition of the first few monolayers was 9.11 ± 1.38 carbon, 6.51 ± 2.01 oxygen and 83.92 ± 2.24 Ge.

Adsorption Protocol

All adsorption experiments were conducted using synthetic seawater as the aqueous solvent (w/v), *viz.* 2.3% NaCl, 0.024% Na_2CO_3, 0.033% KCl, 0.4% MgCl. $6H_2O$, 0.066% $CaCl_2$. $2H_2O$, pH adjusted to 8.0 with HCl. For seawater lacking divalent cations the NaCl was increased to 3.29% to elevate its ionic strength to that of the seawater containing divalent cations. This preparation was used for adsorption experiments with alginate, which is not soluble in the presence of divalent cations.

For adsorption experiments the cylindrical IRE was positioned within a stainless steel flow chamber (Circle Cell™, Spectra Tech). Details have been described elsewhere (Suci & Geesey, 1995). A simple flow through system was used to deliver solutions into the flow chamber. Teflon valves (Cole-Parmer, Niles, IL) served to shuttle the appropriate solution into tubing leading to the flow chamber. All tubing leading into the flow chamber as well as the fittings were teflon (0.08cm I D).

Before each adsorption experiment the surface was exposed to flowing synthetic seawater for 20 min. A vial containing approximately 1 ml of the appropriate substance was inserted into the flow system and the contents immediately pumped through a short section of leader tubing and through the flow chamber for 105 s. Flow was then stopped to allow adsorption. Adsorption was performed under these static conditions to conserve purified polysaccharide. Flow was then resumed and the surface was rinsed with synthetic seawater. Binding curves were obtained as step isotherms (Hlady *et al.*, 1985). At each bulk concentration the adsorption reaction was preformed for 60 min under quiescent conditions followed by a 30 min rinse with synthetic seawater. For conditioning with proteins, adsorption was for 60 min under quiescent conditions at 0.1 mg ml^{-1} for MAP and 0.5mg ml^{-1} for BSA followed by a 60 min rinse as above.

FT-IR Spectrometry

During the course of each experiment infrared (IR) spectra were acquired periodically using a Perkin Elmer Model 1800 Fourier transform infrared (FT-IR) spectrophotometer.

Experimental details are described elsewhere (Suci & Geesey, 1995). FT-IR measurements were made in a temperature controlled room (25 ± 1°C). For experiments in which the substratum was conditioned with BSA or MAP, the spectrum acquired immediately before the initiation of second adsorption reaction was used as the background.

Langmuir Fit

The binding curves were fit to a Langmuir model. The equation describing Langmuir adsorption is:

$$A = A_s\,[((1/Kc_b)+1)^{-1}] \qquad \text{Eqn 1}$$

where K is the binding (association) constant, C_b is the concentration of the substance in bulk solution, A is the absorbance (or band area in abs cm^{-1}) and A_s is the (estimated) saturation value of the absorbance (projected plateau for large bulk concentrations). Best fits for the parameters K and A_s were obtained by nonlinear regression using the software provided with the SigmaPlot™ application (Jandell Scientific, Corte Madera, CA). A_s is then converted to surface coverage (Γ) as described below.

Theoretical justification for application of the Langmuir model relies on demonstration of reversible adsorption. In the present case the adsorbed components analyzed are essentially irreversibly bound. There is no rigorous theoretical model which applies to the case of irreversible adsorption (Andrade, 1985). The use of the Langmuir model in the present context is intended to be empirical; it serves to quantify the data in terms of affinity of the adsorbate for the surface for comparison purposes.

Estimation of Surface Coverage

Surface coverage of the protein was estimated using a published correlation based on the area of the amide II band (Pitt & Cooper, 1988). Surface coverage of polysaccharide was estimated by comparing absorbances obtained in transmission mode with those obtained in the ATR mode using a previously published expression (Suci *et al.*, 1995). For the MHS-3 adhesive polysaccharide this estimate was based on transmission spectra of EPS_p, since concentrated quantities of the purified polysaccharide component sufficient to obtain transmission spectra were not available. Using the mass of the EPS_p for this estimate gives values of Γ which are maximum. By assuming that the K^{-1} value of the purified polysaccharide is the same as that of the purified EPS_p component, the proportion of EPS_p which is contributed by the purified polysaccharide can be estimated, and thereby a minimum estimate for Γ can be calculated.

Cell Adhesion Assay

Aliquots (6 ml) of an early stationary phase culture were centrifuged for 10 min at 1000 ×g in order to remove cell aggregates. The supernatant was centrifuged for 10 min at 12000 ×g and the cell pellet was resuspended in synthetic seawater. Ge fragments were cleaned using the protocol described above. Fragments conditioned with BSA or MAP were prepared by adsorption under stagnant conditions for 60 min (0.1 mg ml^{-1} protein) followed by a rinse in synthetic seawater. Ge fragments were exposed to the cell suspension for 30 min and then gently rinsed using liquid displacement. For each

experiment 3 fragments (Ge, Ge conditioned with BSA and Ge conditioned with MAP) were placed in the same cell suspension. Cells remaining on the surface were fixed for 30 min in 5% glutaraldehyde and stained with 0.1 mg ml^{-1} DAPI (4, 6 -diaminodino-2-phenylindole). Attached cells were counted using epifluoresence microscopy using an Olympus BX60 microscope.

RESULTS

The chromatogram of EPS_p reveals four baseline separated peaks. The associated fractions will be referred to as fractions 1 through 4 in order of elution (Fig. 1, Table 1). Chromatographic variations between batches were primarily in fractions 3 and 4. A peak position was not assigned for fraction 3, since it split clearly into at least two components in some chromatograms.

Chemical analysis of the four eluted fractions is presented in Table 1. Fractions 1 and 2 contain primarily polysaccharides, with negligible protein. Monoclonal antibody labelling of Western blots indicated that fraction 1 contains MHS-3 lipopolysaccharide (LPS). Fraction 3 contains a mixture of polysaccharides and proteins. Fraction 4 contains negligible amounts of both polysaccharides and proteins. The TOC content for this fraction was barely above background detection, despite the large relative area of the associated chromatographic peak, indicating that it is composed primarily of salts.

A comparison of chromatograms of EPS_p from MHS-3 and MHS-3 rad (Fig. 1) suggested that fraction 2 contained the capsular polysaccharide which was previously reported to serve as an adhesin (Quintero & Weiner, 1995). The chromatograms closely resemble each other in terms of both number of baseline separated peaks and peak positions. However, the ratio of fraction 2 to fraction 1 was considerably reduced for MHS-3 rad (0.25) compared to the wild type (1.85+/–1.23).

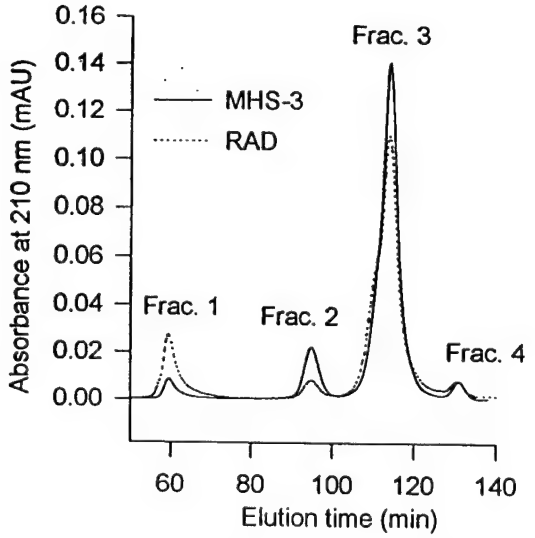

Fig. 1 HPSEC chromatograms of EPS_p from *Hyphomonas* MHS-3 (—) and *Hyphomonas* MHS-3 rad (....).

Table 1 Chemical composition of *Hyphomonas* MHS-3 EPS_p HPSEC fractions

	Peak Position[a] (min)	TOC (mg l^{-1})	Neutral Hexoses (mg l^{-1})	Protein (mg l^{-1})	Mab[b]
Fraction 1	59.4 ± 0.4[c]	5.3 ± 0.2	10.6 ± 0.1	0.0 ± 0.0	+
Fraction 2	94.8 ± 0.2	10.2 ± 0.1	27.6 ± 1.7	0.7 ± 0.0	–
Fraction 3	na[d]	19.5 ± 0.5	6.3 ± 1.7	19.2 ± 1.0	–
Fraction 4	130.3 ± 1.1	3.3 ± 0.3	0.9 ± 0.5	1.2 ± 0.8	nt[e]

[a] = from 4 different EPS_p batches; [b] = monoclonal antibody reactivity; [c] = standard deviation; [d] = not assigned; [e] = not tested.

It had been previously reported that EPS_p contained at least one adhesive polysaccharide which adsorbed preferentially out of the mixture (Suci *et al.*, 1995). Figure 2 shows ATR/FT-IR spectra of the carbohydrate C-O stretch region from this polysaccharide component of EPS_p and from fraction 2 polysaccharide (fr2PS), each adsorbed to Ge. The spectra exhibit very similar features with primary or secondary maxima at 972, 1033, 1064, 1080 and 1132 cm^{-1}. This strongly suggests that the component which adsorbs preferentially out of EPS_p has been isolated in fraction 2. Since it adsorbs preferentially out of the mixture this implicates it as the most adhesive component in the EPS_p matrix with respect to a Ge substratum.

Figure 3 shows the kinetics of adsorption of fr2PS onto the Ge substratum. The process was followed by computing areas of the spectral feature shown in Figure 2. It can be seen that the adsorption was essentially complete after 60 min. The rinse was begun at 100 min. There is a small amount of desorption during the rinse period, especially during

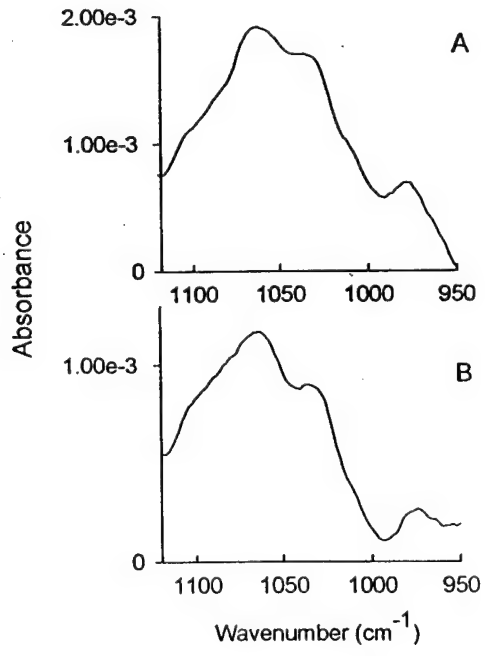

Fig. 2 ATR/FT-IR spectra of the carbohydrate C-O stretch region of EPS_p (A), and fr2PS (B), adsorbed to Ge.

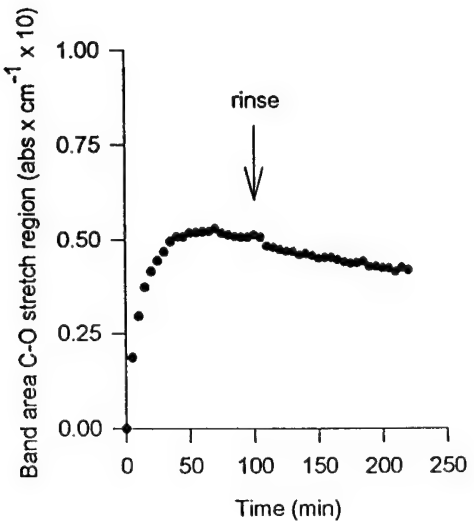

Fig. 3 Kinetics of adsorption of fr2PS onto Ge. Rinse was initiated at 100 min.

the first 10 min, but adsorption is essentially irreversible. Langmuir fits to binding curves were used to measure the "stickiness" of fr2PS with respect Ge. The Langmuir fit yields two parameters, *viz.* surface coverage (Γ) and bulk concentration to reach half saturation (K^{-1}), where a high Γ and low K^{-1} indicate a relatively sticky substance. In order to place this quantitation in context, Γ and K^{-1} have been obtained for an adhesive protein mixture from *M. edulis* (MAP) and an acidic polysaccharide (kelp alginate) using an identical protocol as for fr2PS (Table 2). According to this ranking the fr2PS has an adhesive quality (or "stickiness") comparable to MAP. The acidic polysaccharide, alginate, is relatively non-adhesive with respect to Ge.

The effect of two different protein conditioning films on the adsorption behavior of fr2PS was examined. Binding curves were obtained using a protocol identical to that used to obtain binding curves on clean Ge. Binding curves obtained by ATR/FT-IR for conditioned and unconditioned substrata are presented in Figure 4. It is evident from the binding curves that the affinity of fr2PS for both conditioned substrata is severely depressed. The Langmuir model did not converge when attempting to fit data for Ge conditioned with BSA or MAP, precluding a quantitative comparison of the Γ and K^{-1} values. There was no indication of any loss of the protein conditioning film during the

Table 2 Binding parameters for Langmuir fit to binding curves of fraction 2 polysaccharide, MAP, and alginate to Ge. A lower value of K^{-1} and a higher value of Γ implies greater stickiness.

	Fraction 2	MAP	Alginate
Γ ($\mu g\ cm^{-2}$)	0.158 ± 0.009^a 0.029 ± 0.017^b	0.305 ± 0.016	0.039 ± 0.003
K^{-1} ($mg\ l^{-1}$)	0.018 ± 0.002	0.024 ± 0.003	0.738 ± 0.179

[a] = estimated minimum value; [b] = estimated maximum value.

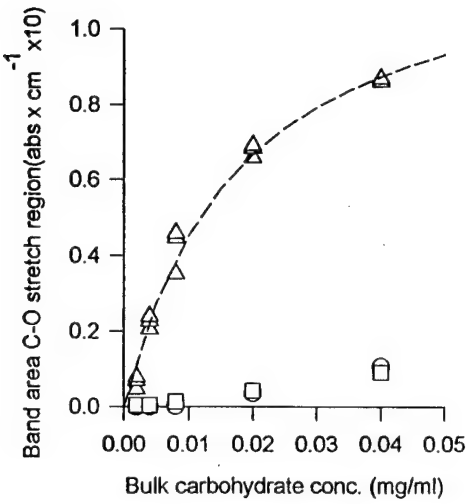

Fig. 4 Binding curves of fr2PS adsorbed on Ge, (△), Ge conditioned with MAP (□) and Ge conditioned with BSA (○). Broken line = Langmuir model fit to three data sets for unconditioned Ge.

acquisition of the step isotherm. Any such loss would be evident from a change in prominent amide bands located at approximately 1650 and 1550cm^{-1} (Suci & Geesey, 1995).

The ATR/FT-IR spectra of the absorbed fr2PS on Ge and Ge conditioned with protein are shown in Figure 5. The absorbances are low and very close to background noise. However, differences in the adsorbed material from fr2PS between the two conditioned substrata are revealed. The spectrum of the absorbed EPS_p on BSA resembles the spectrum obtained on Ge, suggesting that the same components are adsorbed. The spectrum of adsorbed components on MAP bares less resemblance to the spectrum on clean Ge, suggesting adsorption of a trace contaminant.

The large differences in the affinity of fr2PS for clean Ge and Ge conditioned with proteins offered an opportunity to see whether the adsorption behavior of fr2PS could be extrapolated to whole cell adhesion behavior (Fig. 6). The results showed that MHS-3 attaches to a much greater extent to clean Ge than to Ge conditioned with MAP or BSA. Thus, the cells show the same preference for unconditioned Ge that fr2PS displays in its adsorption behavior. The number of cells attached to Ge after the 30 min exposure period and the rinse was significantly larger than cells attached to Ge conditioned with BSA (2 sample t-test, $P < 0.95$). The number of cells attached to Ge conditioned with BSA was significantly larger than cells attached to Ge conditioned with MAP (2 sample t-test, $p < 0.95$).

DISCUSSION

It has previously been demonstrated that MHS-3 rad lacks diffuse capsular material which is present on MHS-3 (Quintero & Weiner, 1995). The capsular material binds gold labelled *Bauhinia purpurea* lectin (BPA) and calcofluor, both of which reduce MHS-3 attachment to the level observed in MHS-3 rad. Thus, the capsular material has been suggested to be both a polysaccharide and an adhesin. MHS-3 EPS, isolated from

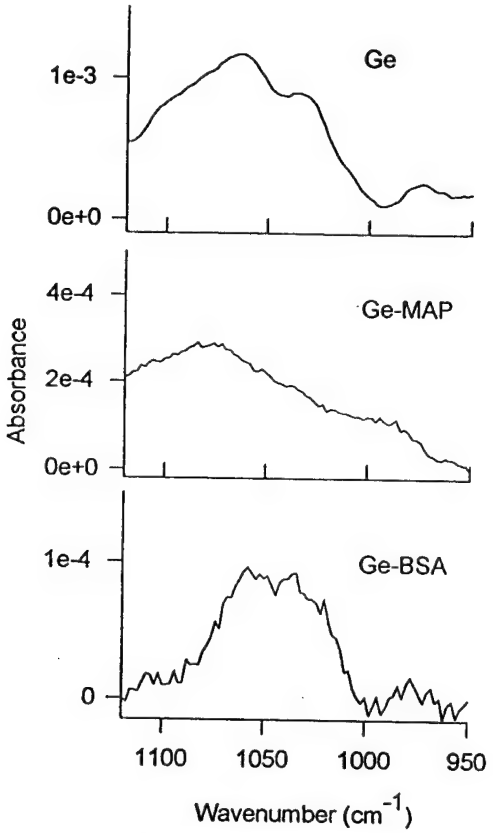

Fig. 5 Spectra of fr2PS adsorbed to Ge, and Ge conditioned with MAP (Ge-MAP), and BSA (Ge-BSA).

biofilms and flocs, has been reported to contain an adhesive polysaccharide which adsorbs preferentially out of a mixture from which the protease K accessible proteins have been removed (EPS_p) (Suci *et al.*, 1995). Using HPSEC, an adhesive polysaccharide fraction has been isolated and identified as the same substance which adsorbed preferentially out of the EPS_p mixture. This isolated adhesin is referred to as fraction 2 polysaccharide (fr2PS).

One significant implication is that a subclass of EPS molecules mediate MHS-3 adhesion to hydrophilic substrata. fr2PS is apparently dispersed throughout the EPS matrix of the biofilm since HPSEC of the more loosely associated and EDTA extracted EPS yielded similar chromatograms (data not shown). This was also indicated by labelling MHS-3 microcolonies with BPA lectin and calcofluor (Quintero & Weiner, 1995). On individual planktonic cells fr2PS is located integrally, extending from the cell envelope to a distance of approximately 0.2 μm (Quintero & Weiner, 1995). It may be that this polysaccharide functions both to mediate initial adhesion and as an EPS matrix polymer to anchor the biofilm to the substratum. Previously, it was found that calcofluor inhibited long term (5 d) biofilm formation (Quintero & Weiner, 1995).

Isolation of the adhesin in research quantities has allowed characterization of its adsorption behavior. It has been found that its "stickiness" (assessed by surface

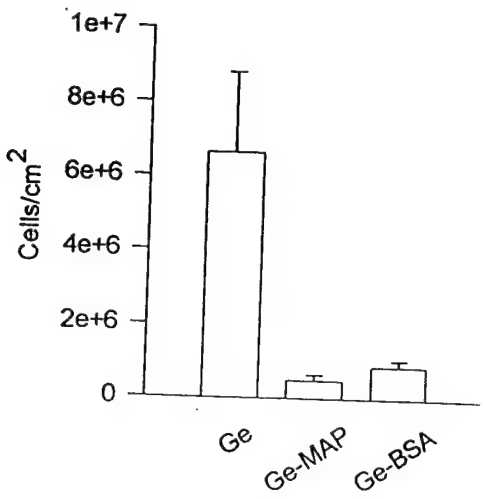

Fig. 6 Adhesion assays for MHS-3 on Ge, Ge conditioned with MAP, and Ge conditioned with BSA. Error bars designate standard deviation for 4 independent assays.

coverage and affinity) with respect to a hydrophilic surface is comparable with a protein mixture which constitutes the resin of a natural thermoset composite (MAP) (Waite, 1990). The driving forces behind non-specific adsorption of globular blood proteins have been well studied (Andrade, 1985; Brash & Horbett, 1987; Haynes *et al.*, 1994). Interactions responsible for adsorption of marine proteins are just beginning to be investigated (Baty *et al.*, 1996a). There is only speculation concerning structural features, molecular bonds, *etc.* which promote binding of adhesive polysaccharides (Allison, 1994) and fr2PS should provide a good model system in this respect.

It was found previously that proteins in a crude MHS-3 EPS preparation competed with the adhesive polysaccharide(s) for interfacial binding sites (Suci *et al.*, 1995). It appears from the results presented here that this polysaccharide binds poorly to substrata conditioned with two proteins which have completely different properties. BSA is a globular blood protein having a rich secondary structure (Peters, 1985) and a net negative charge at pH 8.0. It has been hypothesized that presentation of one of three, hydrated, negatively charged domains to the aqueous phase creates an interface which is unfavorable for bacterial attachment (Al-Makhlafi *et al.*, 1994). Mefp-1, the primary component of MAP, is densely populated with lysine residues which are protonated at this pH and is reported to have an open conformation in solution with little secondary structure (Waite, 1990). It is sold commercially as a coating to enhance cell adhesion (Cell-Tak, Collaborative Biomedical Products, Bedford, MA). Previously, it was found that MAP enhanced adsorption of kelp alginate above that found on clean Ge (Suci & Geesey, 1995). It was concluded that the driving force for adsorption was primarily electrostatic, even at the relatively high ionic strength of seawater. Conditioning with BSA was found to have little effect on the adsorption of alginate when compared to clean Ge.

The cumulative results presented here and in two other publications (Quintero & Weiner, 1995; Suci *et al.*, 1995) suggest the following interpretation. MHS-3 has evolved a capsular extracellular polysaccharide (fr2PS) that binds *via* non-electrostatic interactions. It has been suggested on the basis of inhibition assays that hydrogen bonding is involved (Quintero & Weiner, 1995). Hydrogen bonds involving both organic acids

and bases can form with mineral surfaces (oxides) in marine sediments (Thurman, 1985). Therefore, this may be a common adhesive molecular strategy of marine organisms which occupy these environments.

It seems likely that the EPS matrix of most marine biofilms is composed of a large portion of proteins, some which reach the substratum and adsorb tenaciously; this is the case for MHS-3 (Suci *et al.*, 1995). Thus, in general, the first microorganisms which colonize a surface condition it with a film which consists partially of adsorbed protein. The molecular bonds which are established between fr2PS and the Ge surface (an oxide) form poorly, or not at all, with adsorbed proteins. Therefore, the adhesive polysaccharide (fr2PS) may be the implement for a binding strategy which is selective for relatively pristine mineral surfaces that have not been previously colonized. This would be consistent with the proposed niche it fills in the succession of microfouling as a primary colonizer (Quintero & Weiner, 1995). An interesting research direction could be initiated by posing the question: to what extent do the different adhesive strategies of a variety of microorganisms occupying a similar niche determine the ecology of the local microfouling process?

Acknowledgements

This work was supported by Office of Naval Research Grant N00014–93–1–0168, a grant from 3M, and Cooperative Agreement ECD-8907039 between the National Science Foundation and Montana State University. One of us (BF) received support from the Danish Technical Research Council (Grant #5.26.16.22) and one of us (PAS) received support from the Whitaker Foundation.

References

Abu G O, Weiner R M, Rice J, Colwell R R (1991) Properties of an extracellular adhesive polymer from the marine bacterium, *Shewanella colwelliana. Biofouling* **3**: 69–84

Allison D G (1994) Exopolysaccharide synthesis in bacterial biofilms. In: Wimpenny J, Nichols W, Stickler D, Lappin-Scott H (eds) *Bacterial Biofilms and their Control in Medicine and Industry*. Bioline, Cardiff, UK, pp 25–30

Al-Makhlafi H, McGuire J, Daeschel M (1994) Influence of preadsorbed milk proteins on adhesion of *Listeria monocytogenes* to hydrophobic and hydrophilic silica surfaces. *Appl Environ Microbiol.* **60**: 3560–3565

Andrade J D (1985) Principles of protein adsorption In: Andrade J D (ed) *Surface and Interfacial Aspects of Biomedical Polymers, Vol 2, Protein Adsorption.* Plenum Press, New York, pp 1–80

Baier R E, A E Meyer, V A DePalma, R W King, M S Fornalik (1983) Surface microfouling during the induction period. *J Heat Trans* **105**: 618–624

Bar-ness R, Avrahamy N, Matsuyama T, Rosenberg M (1988) Increased cell surface hydrophobicity of a *Serratia marcescens* NS 38 mutant lacking wetting ability. *J Bacteriol* **170**: 4361–4364

Bashan Y. Levanony H (1988) Active attachment of *Azospirillum brasilense* Cd to quartz sand and to a light-textured soil by protein bridging. *J Gen Microbiol* **134**: 2269–2279

Baty A M, Suci P A, Tyler B J, Geesey G G (1996a) Investigation of mussel adhesive protein adsorption on polystyrene and poly (octadecyl methacrylate) using angle dependent XPS, ATR/FT-IR and AFM. *J Colloid Interface Sci* **177**: 307–315

Baty A M, Frølund B, Geesey G G, Langille S, Quintero E J, Suci P A, Weiner R M (1996b) Adhesion of biofilms to inert surfaces: a molecular level approach directed at the marine environment. *Biofouling* **10**: 111–121

Benedict C V, Picciano P T (1987) Adhesives from marine mussels. In: Hemingway R W (ed) *Adhesives from Renewable Resources*, ACS Symposium Series, ACS, Washington, DC pp 466–483

Bidle K, Wickman H, Fletcher M (1993) Attachment of a *Psuedomonas*-like bacterium and *Bacillus coagulans* to solid surfaces and adsorption of their S-layer proteins. *J Gen Microbiol* **139**: 1891–1897

Brash J L, Horbett T A (1987) Proteins at Interfaces: Physicochemical and Biochemical Studies. ACS Symposium Series 343, American Chemical Society, Washington, DC

Bryers J B, Characklis W G (1990) Biofilms in water and wastewater treatment. In: Characklis W G, Marshall K C (eds) *Biofilms* John Wiley & Sons, New York, pp 671–696

Busch K A (1993) Specificity of a monoclonal antibody against *Hyphomonas* MHS-3 polysaccharide. M S Thesis, University of Maryland, College Park

Clark W B, Beem J E, Nesbitt W E, Cisar J O, Tseng C C, Levine M J (1989) Pellicle receptors for *Acinomyces viscosus* type I fimbriae *in vitro*. *Infect. Immun.* **57**: 3003–3008

Cooksey K E (1992) Extracellular polymers in biofilms, In: Melo L, Bott T R, Fletcher M, Capdeville B (eds) *Biofilms: Science and Technology*. Kluwer, The Netherlands, pp 137–147

Costerton J W, Cheng K J, Geesey G G, Ladd T I, Nickel J C, Dasgupta M, Marrie T J (1987) Bacterial biofilms in nature and disease. *Annu Rev Microbiol* **41**: 435–464

Dubois M, Gilles K A, Hamilton J K, Rebers P A, Smith F (1956) Colorimetric method for determination of sugars and related substances. *Anal Chem* **28**: 350–356

Evans D G, Karjalainen T K, Evans D J, Jr., Graham D Y, Lee C-H (1993) Cloning, nucleotide sequence and expression of a gene encoding an adhesin subunit protein of *Helicobacter pylori*. *J Bacteriol* **175**: 674–683

Goding J W (1983) *Monoclonal Antibodies: Principles and Practice* Academic Press, Incorporated, London pp 162

Gristina A G (1987) Biomaterial-centered infection: microbial adhesion *vs.* tissue integration. *Science* **237**: 1588–1595

Haynes C A, Sliwinsky E, Norde W (1994) Structural and electrostatic properties of globular proteins at a polystyrene-water interface. *J Collold Interface Sci* **164**: 394–409

Hlady V, Van Wagenen R A, Andrade J D (1985) Total internal reflection intrinsic fluorescence applied to protein adsorption. In: Andrade J D (ed) *Surface and Interfacial Aspects of Biomedical Polymers, Vol 2, Protein Adsorption*. Plenum Press, New York, pp 81–118

Humphrey B A, Dickson M R, Marshall K C (1979) Physicochemical and in situ observations on the adhesion of gliding bacteria to surfaces. *Arch Microbiol* **120**: 231–238

Jann K, Jann B (1990) Bacterial adhesins. In: Jann K, Jann B (eds) *Curr Top Microbiol Immunol* **151**: Springer-Verlag, New York, pp. 1-209

Loosdrecht M C M, Lyklema J, Norde W, Zehnder A J B (1990) Influences of interfaces on microbial activity. *Microbiol Rev* **54**: 75–87

Lowry O H, Rosebrough N J, Farr A L, Randall R J (1951) Protein measurement with the folin reagent. *J Biol Chem* **193**: 265–275

Merker R I, J Smit (1988) Characterization of the adhesive holdfast of marine and freshwater caulobacters. *Appl Environ Microbiol* **54**: 2078–2085

Notter M F (1988) Selective attachment of neural cells to specific substrates including Cell-Tak, a new cellular adhesive. *Exp Cell Res* **177**: 237–246

Neu T R (1992) Microbial "footprints" and the general ability of microorganisms to label surfaces. *Can J Microbiol* **38**: 1005–1008

Paul J H, Jeffrey W H (1985) Evidence for separate adhesion mechanisms for hydrophilic and hydrophobic surfaces in *Vibrio proteolytica*. *Appl Environ Microbiol* **50**: 431–437

Peters T, Jr (1985) Serum albumin, *Adv Protein Chem* **37**: 161–245

Pitt W G, Cooper S L (1988) Albumin adsorption on alkyl chain derivatized polyurethanes: I. the effect of C-18 alkylation. *J Biomed Mater Res* **22**: 359–382

Pringle J H, Fletcher M, Ellwood D C (1983) Selection of attachment mutants during the continuous culture of *Pseudomonas fluorescens* and relationship between attachment ability and surface composition. *J Gen Microbiol* **129**: 2557–2569

Pringle J H, Fletcher M (1986) Adsorption of bacterial surface polymers to attachment substrata. *J Gen Microbiol* **132**: 743–749

Quintero E J, Weiner R M (1995) Evidence for the adhesive function of the exopolysaccharide of *Hyphomonas* MHS-3 in its attachment to surfaces. *Appl Environ Microbiol* **61**: 1897–1903

Read R R, Costerton J W (1987) Purification and characterization of adhesive exopolysaccharides from *Pseudomonas putida* and *Pseudomonas fluorescens*. *Can J Microbiol* **33**: 1080–1090

Rosenberg M, Bayer E A, Delarea J, Rosenberg E (1982) Role of thin fimbriae in adherence and growth of *Acinetobacter calcoaceticus* RAG-1 on hexadecane. *Appl Environ Microbiol* **44**: 929–937.

Salamitou S, Lemaire M, Fujino T, Ohayon H, Gounon P, Beguin P, Aubert J-P (1994) Subcellular localization of *Clostridium thermocellum* ORF3p, a protein carrying a receptor for the docking sequence borne by the catalytic components of the cellulosome. *J Bacteriol* **176**: 2828–2834

Shea C, Smith-Somerville H E (1994) The effects of phenotype variability on the adhesion properties of *Deleya marina*. *Biofouling* **8**: 13–25

Suci P A, Frølund B, Quintero E R, Weiner R M, Geesey G G (1995) Adhesive extracellular polymers of *Hyphomonas* MHS-3: interaction of polysaccharides and proteins. *Biofouling* **9**: 95–114

Suci P A, Geesey G G (1995) Investigation of alginate binding to germanium and polystyrene substrata conditioned with mussel adhesive protein. *J Colloid Interface Sci* **172**: 347–357

Thurman E M (1985) *Organic Geochemistry of Natural Waters*. Martinus Nijhoff, Boston, pp 382

Väisänen O M, Nurmiaho-Lassila E-L, Marmo S A, Salkinoja-Salonen M S (1994) Structure and composition of biological slimes on paper and board machines. *Appl Environ Microbiol* **60**: 641–653

Vincent P, Pignet P, Talmont F, Bozzi L, Fournet B, Guênennec C, Jeanthon C, Prieur D (1994) Production and characterization of an exopolysaccharide excreted by a deep-sea hydrothermal vent bacterium isolated from the polychaete annelid *Alvinella pompejana*. *Appl Environ Microbiol* **60**: 4134–4141

Waite J H (1990) Marine adhesive proteins: natural composite thermosets. *Int J Biol Macromol* **12**: 139–144

Wrangstadh M, Conway P L, Kjelleberg S (1986) The production of an extracellular polysaccharide during starvation of a marine *Pseudomonas* sp. and the effect thereof on adhesion. *Arch Microbiol* **145**: 220–227

Yun C, Ely B, Smit J (1994) Identification of genes affecting production of the adhesive holdfast of a marine caulobacter. *J Bacteriol* **176**: 796–803

Zottola E A (1991). Characterization of the attachment matrix of *Pseudomonas fragi* attached to non-porous surfaces. *Biofouling* **5**: 37–55

Biofouling, 1996, Vol. 10(1–3), pp. 111–121
Reprints available directly from the publisher
Photocopying permitted by license only

ADHESION OF BIOFILMS TO INERT SURFACES: A MOLECULAR LEVEL APPROACH DIRECTED AT THE MARINE ENVIRONMENT

A M BATY[1], B FRØLUND[2], G G GEESEY[1], S LANGILLE[3], E J QUINTERO[4], P A SUCI[†1] and R M WEINER[3]

[1]*Center for Biofilm Engineering, Montana State University, MT 59717, USA*
[2]*Danish Technological Institute, Plastics Technology, Teknologiparken, 8000 Aarhus C, Denmark*
[3]*Department of Microbiology, University of Maryland, College Park, MD 20742, USA*
[4]*Oceanix Bioscience Corporation, 7170 Standard Drive, Hanover, MD 21076, USA*

(Received 23 December 1995; in final form 1 March 1996)

Protein/ligand interactions involved in mediating adhesion between microorganisms and biological surfaces have been well-characterized in some cases (*e.g.* pathogen/host interactions). The strategies microorganisms employ for attachment to inert surfaces have not been so clearly elucidated. An experimental approach is presented which addresses the issues from the point of view of molecular interactions occurring at the interface.

KEYWORDS: fouling, molecular interactions, adhesin, marine

FEASIBILITY AND POTENTIAL FRUITS OF THE APPROACH

Communities of bacteria which have colonized a surface present a fascinating subject for microbiological investigation. The conceivable extent of the organizational complexity of these surface-associated communities has only recently become apparent. For example, cells in a biofilm are typically embedded in a matrix of extracellular polymeric substances (EPS) (Costerton *et al.*, 1987; Cooksey, 1992) commonly referred to as "slime". Recent studies suggest that this heterogeneous network of bioploymers may serve in some cases to optimize biofilm architecture such that oxygen transport (DeBeer *et al.*, 1993) or nutrient utilization (Wolfaardt *et al.*, 1994) are facilitated. There is even some hint that for some biofilms the three dimensional lattice can metamorphose in response to toxins (Korber *et al.*, 1994). Studies reveal that bacteria adapt by utilizing networks of regulatory genes which respond to a host of environmental stimuli (Parkinson, 1993; Deretic *et al.*, 1994; Loewen & Hengge-Aronis, 1994). If these findings are viewed in the light of evidence for cell-to-cell communication, effected at the level of genetic regulation (Passador *et al.*, 1993; Piper *et al.*, 1993), for an expanding number of bacterial species (Klotz, 1993), the implication that there may be some points for comparison of many biofilms with specialized tissues in multicellular organisms becomes reasonable (Jackson *et al.*, 1986; Kaiser & Losick, 1993).

Despite the complex nature of biofilms, a molecular level (biochemical) approach toward understanding their adhesion to inert surfaces should be tractable. The framework

† Corresponding author

for analyzing and understanding adsorption of biomolecules to engineered materials has been established, primarily in literature concerning blood compatibility (Andrade, 1985; Bohnert & Horbett, 1986; Brash & Horbett, 1987; Krisdhasima *et al.*, 1993; Haynes & Norde, 1995). Methods for EPS isolation and purification are available (Troy, 1979; Read & Costerton, 1987; Henningson & Gudmestad, 1993). Adhesion inhibition assays conventionally used to investigate specific adhesion mediated by protein/ligand interactions (Jann & Jann, 1993) may be applicable in some cases (Merker & Smit, 1988; Quintero & Weiner, 1995). Biomolecules involved in attachment of cells to inert surfaces have been classified according to general type (proteins or polysaccharide) by utilizing proteolytic enzymes and surfactants (Paul & Jeffrey, 1985). Detailed biochemical characterization of adhesin remnants left by displaced microorganisms ("footprints") (Neu, 1992) is becoming increasingly feasible as sophisticated surface analysis techniques are adapted for analysis of biological samples (Mantus *et al.*, 1993). In at least one case, genetic determinants of a non-specific holdfast have been characterized (Yun *et al.*, 1994). The fruits of a molecular level approach can be relevant to understanding particular aspects of even extremely complex surface-associated ecosystems such as climax marine fouling communities; *i.e.* it can be expected that these communities will be anchored to the substratum *via* contributions from at least the most adhesive biomolecules expressed by the primary colonizers. This is a testable hypothesis since exchange reactions at interfaces can be characterized (Koltisko & Walton, 1985).

At a molecular (reductionist or biochemical) level the adhesive relationship between a developing fouling community and the inert surface can be simplified to an investigation of interfacial interactions among adsorbed and impinging biopolymers. A number of interactions between solution phase and preadsorbed biomolecules are possible. These include displacement (or exchange) (Vroman & Adams, 1986), intercalation to unoccupied sites, which may promote "pinning" of the preadsorbed species (Johnson & Granick, 1992), or binding to moieties on the preadsorbed film (Suci & Geesey, 1995). There may be no direct, simple correspondence between adhesive properties and interactions of isolated biomolecules, and the molecular interactions which mediate adhesion of a fouling community. For example, the simplest fouling community consists of single cells attached to a substratum. Even for this simple case, the molecular interactions of an adhesin with a surface can be altered by the tether or anchor to the cell in a number of ways. For example functional groups involved in securing the adhesin to the cell will be less likely to participate in binding to the surface; the stereochemistry of the adhesin may be altered, reducing the entropy gain upon binding. However, despite the possible caveats, adsorption behavior of biomolecules has been positively correlated to whole cell adhesion behavior and used to identify potential adhesins (Pringle & Fletcher, 1986; Bidle *et al.*, 1993).

Less reductionistic frameworks for interpreting adhesion behavior are available (Busscher *et al.*, 1989). The application of DLVO theory, which can adequately account for observed cell adhesion behavior in some cases, essentially ignores individual molecular interactions (Van Loosdrecht *et al.*, 1989). Similarly, some cell adhesion behavior can be predicted on the basis of cell-surface hydrophobicity (Rosenberg & Kjelleberg, 1986; Stenström, 1989). A molecular level approach may provide a basis for interpreting patterns of adhesion behavior which do not conform easily to the predictions of either of these more global schemes (McEldowney & Fletcher, 1986). In addition, when combined with isolation and biochemical analysis of EPS components, it allows examination of a number of related questions. Have certain biomolecules evolved to serve as non-specific adhesins (Yun *et al.*, 1994)? Do particular classes of biomolecules mediate adhesion to inert surfaces having similar properties (Paul & Jeffrey, 1985)? Is

molecular architecture crafted by organisms to promote either adhesion to, or detachment from (Wrangstadh *et al.*, 1986) inert surfaces?

MARINE CONDITIONING FILMS

The interfacial interactions between biomolecules and the surface which were outlined above will probably begin before the first encounter between microbes and an engineered surface placed in the marine environment. It is well known that biomaterials in contact with blood will be coated rapidly with intrinsic proteins (Gendreau *et al.*, 1981). Similarly, adsorption of salivary components onto oral surfaces creates the organic biopolymer film (the pellicle) to which bacteria eventually attach (Kolenbrander & London, 1993). The macromolecular content of the sea is considerably more dilute than that of blood or the oral cavity. Estimates of dissolved organic carbon (DOC) are in the range of 0.5 to 1.0 mg l^{-1} in the open sea and can be ten times higher in coastal waters (Thurman, 1985; Benner *et al.*, 1992). However, organic "conditioning" films apparently form quickly on materials placed in seawater (Loeb & Neihof, 1975; 1977; Kristoffersen *et al.*, 1982).

Definitive biochemical characterization of marine conditioning films is lacking, except for a study suggesting incorporation of proteinaceous material (Baier *et al.*, 1983), and a study indicating that the composition of the film is site specific (Little, 1985). However, there is indirect evidence supporting the supposition that the films may consist of a large proportion of biopolymeric material regardless of the site. Much of the organic material in the sea is in the form of colloids which range in size from 5–200 nm (Wells & Goldberg, 1994). There is evidence that a substantial portion of the carbohydrates are in the form of polysaccharides (Pakulski & Benner, 1994). The total amino acid content ranges from 0.06 to 0.24 mg l^{-1} with the combined fraction being on average five times as high as the free amino acids on a mass per volume basis (Thurman, 1985). This suggests that many of the amino acids are also incorporated into biopolymers. Polymers tend to have high affinity isotherms (Cohen Stuart *et al.*, 1982). This implies that, given enough time, even very dilute solutions will saturate the surface binding sites. This prediction has been verified experimentally for adsorption of bovine serum albumin (BSA) on stainless steel (Van Enckevort *et al.*, 1984).

EXPERIMENTAL APPROACH

A number of biomolecules have been selected as model compounds, *viz.* mussel adhesive protein (MAP) from *Mytilis edulis*, an adhesive polysaccharide (fraction 2 polysaccharide (fr2ps)) from the marine bacterium, *Hyphomonas* MHS-3 (MHS-3), alginate from *Macrocystis pyrifera* and the globular blood protein, bovine serum albumin (BSA). Interactions between these biomolecules and germanium (Ge), polystyrene (PS), and poly (octadecyl methacrylate) (POMA) surfaces in contact with synthetic seawater are being investigated.

Both MAP and BSA adsorb tenaciously to both hydrophobic and hydrophilic substrata. MAP constitutes the resin of a natural thermoset adhesive with which *M. edulis* anchors itself to a variety of substrata (Waite, 1990), and is sold commercially as a coating to enhance cell adhesion (Benedict & Picciano, 1987; Notter, 1988). BSA is often used to block nonspecific binding sites (Goding, 1983), and in many cases reduces cell attachment (*e.g.* Pratt-Terpstra *et al.*, 1987; Tamada & Ikada, 1993). Evidence has been

presented that fr2ps is a polysaccharide adhesin which mediates attachment of MHS-3 to (at least) hydrophilic substrata (Quintero & Weiner, 1995; Frølund *et al.*, 1996). Alginate is a linear copolymer composed of the uronic acids α-L-guluronic and β-D-mannuronic acid (Cotrell & Kovacs, 1977). Derivatives of this polysaccharide are the primary exopolysaccharides produced by mucoid strains of *Pseudomonas aeruginosa* (Evans & Linker, 1973). Uronic acids constitute a significant fraction of the EPS of several marine pseudomonads (Uhlinger & White, 1983; Christensen *et al.*, 1985) and are a common component of extracellular and cell surface biopolymers of most marine bacteria studied to date (Sutherland, 1980; Christensen, 1989).

Thus far, investigations have been confined to a relatively simple system, *i.e.* interaction of a solution phase polysaccharide with a preadsorbed (irreversibly bound) protein film coating a submerged substratum. The complementary experiment has also been performed. *i.e.* exposure of a preadsorbed polysaccharide film to solution phase protein. These types of dual adsorption experiments are particularly compatible with the technique of attenuated total reflection Fourier transform infrared (ATR/FT-IR) spectrometry (Ishida & Griffiths, 1993). The term "irreversibly bound" requires explanation. Although it has a precise thermodynamic meaning (Norde *et al.*, 1986), it has been used (in an operational sense) to describe an adsorbed species (usually macromolecular) which cannot be rinsed from a surface (Bohnert & Horbett, 1986). The term is used here in the latter (less precise) sense.

Alginate does not adsorb with great affinity to Ge (Ishida & Griffiths, 1993). However, preconditioning Ge substrata with MAP enhances alginate adsorption (Suci & Geesey, 1995). The driving force for adsorption in synthetic seawater (pH 8) appears to be primarily electrostatic, conferred by interaction of protonated lysine residues of the MAP and the negatively charged carboxylate functionalities of the alginate. As expected, conditioning Ge with BSA, which has an isoelectric point (IEP) of approximately 5, does not enhance alginate adsorption. The data suggest that once the alginate has penetrated the electrostatic double layer, it forms additional bonds with MAP which involve pyranose ring atoms. According to the FT-IR diagnostic, the interaction of alginate with preadsorbed MAP was not affected by the underlying substratum (Ge *vs* PS); both the type(s) of bonding, and the extent of adsorption per surface coverage of MAP were the same regardless of whether the underlying substratum was Ge or PS.

Whereas MAP enhances alginate adsorption to Ge, conditioning Ge with MAP, BSA or intrinsic MHS-3 EPS proteins depresses adsorption of fr2ps, the putative MHS-3 adhesin (Suci *et al.*, 1995; Frølund *et al.*, 1996). The molecular characteristics of MAP and BSA are in most ways contrasting. MAP is rich in lysine and DOPA residues, has an open conformation (Williams *et al.*, 1989) and has an IEP above 10. BSA has ample secondary and tertiary structure, and has a net negative charge at pH 8 (Peters, 1985). Adsorption of fr2ps was reduced to a similar extent (compared to unconditioned Ge) on Ge conditioned with MAP and BSA, which suggests that electrostatic repulsion is not a dominant factor in excluding fr2ps from the conditioned substrata. Adsorption of MHS-3 cells to Ge conditioned with MAP or BSA was also depressed (Frølund *et al.*, 1996), implying that interactions characterized at the molecular level are relevant to the functioning of the adhesin *in situ*.

MHS-3 ADHESION TO PS AND POMA SUBSTRATA CONDITIONED WITH MAP

The question of whether adhesion-mediating substratum properties are "transferred" through a protein conditioning film has been posed by a number of investigators (*e.g.*

Pratt-Terpstra *et al.*, 1987; Schakenraad *et al.*, 1989; Busscher *et al.*, 1990; Ranieri *et al.*, 1993; Tamada & Ikada, 1993; Al-Makhlafi *et al.*, 1994). Substrata may exert their influence on cell adhesion in the presence of a preadsorbed film in the trivial sense, due to incomplete coverage of the original surface by the film, or the original substrata may select for different subsets of proteins from a mixture used to form the film (Tamada & Ikada, 1993). Alternatively, the substrata may influence properties of the adsorbed state of a protein (or proteins) in the film differently, thus inducing different film structures (Pratt-Terpstra *et al.*, 1987; Busscher *et al.*, 1990; Al-Makhlafi *et al.*, 1994). It is generally accepted that proteins which are irreversibly adsorbed alter their conformation to reach the final adsorbed state (Norde *et al.*, 1986; Haynes & Norde, 1995). Measurements indicate that different substrata induce different kinds of conformational changes in proteins (Bohnert & Horbett, 1986; Pitt & Cooper, 1988; Banovac *et al.*, 1994; Haynes & Norde, 1995). It has been proposed that the adsorbed protein film structure may be partially determined by the balance between cohesive (protein/protein) and adhesive (protein/surface) forces (Taylor *et al.*, 1994).

A detailed study of the absorbed film structure of MAP on PS and POMA using atomic force microscopy (AFM), X-ray photoelectron spectrometry (XPS) and ATR/FT-IR has been performed (Baty *et al.*, 1995). The adsorbed film exhibits markedly different surface topography on PS and POMA (Fig. 1). The fibrous network observed on the POMA surface indicates that the proteins have formed aggregates upon adsorption, while on the PS surface the largest resolvable structures approach the size of an individual mefp-1 molecule (the primary component of MAP). These results suggest that on the PS surface, protein/surface interactions dominate, while on the POMA surface, protein/protein interactions determine the supramolecular structure. XPS and ATR/FT-IR data are consistent with this interpretation. Recent studies indicate that the structural differences are preserved in the hydrated state (Baty *et al.*, unpublished).

It might be anticipated that these distinctly different adsorbed film structures would induce comparatively large differences in cell adhesion behavior. In the case of MHS-3 this prediction is not supported by the data. Preliminary results from ATR/FT-IR adsorption studies indicate that fr2ps adsorbs quite differently to unconditioned PS and POMA, but that these differences are mitigated by conditioning with MAP; the spectra are somewhat difficult to interpret due to the large background signal from the polymer films (data not shown). The results of MHS-3 whole cell adhesion assays are much less ambiguous (Fig. 2). It is apparent that the MAP conditioning film masks the underlying substratum properties, at least with respect to numbers of cells attaching within the 30 min exposure period.

It is well known that conditioning with BSA can inhibit adsorption of other biomolecules and reduce cell adhesion. (Note, however, that adsorption onto certain substrata can reverse this latter trend (Ranieri *et al.*, 1993)). At anionic and hydrophobic surfaces BSA is thought to assume a surface orientation which presents a negatively charged domain (one of three) to the aqueous phase (Andrade *et al.*, 1990). This surface orientation could be expected to exclude many bacterial strains which are generally considered to have net negatively charged cell envelopes. The reduced adsorption of fr2ps and reduced adhesion of MHS-3 cells to MAP requires a different explanation. MAP is rich with lysine residues which are protonated at the pH of the synthetic seawater (8.0). These lysine residues are apparently available for binding to solution phase biopolymers since they enhance alginate binding in seawater as described above.

The reduced cell adhesion on conditioned surfaces cannot be accommodated, at least in a simple way, within a framework of hydrophobic/hydrophilic tendencies. Although the extent of cell adhesion to POMA, PS and Ge surfaces appears to indicate a preference

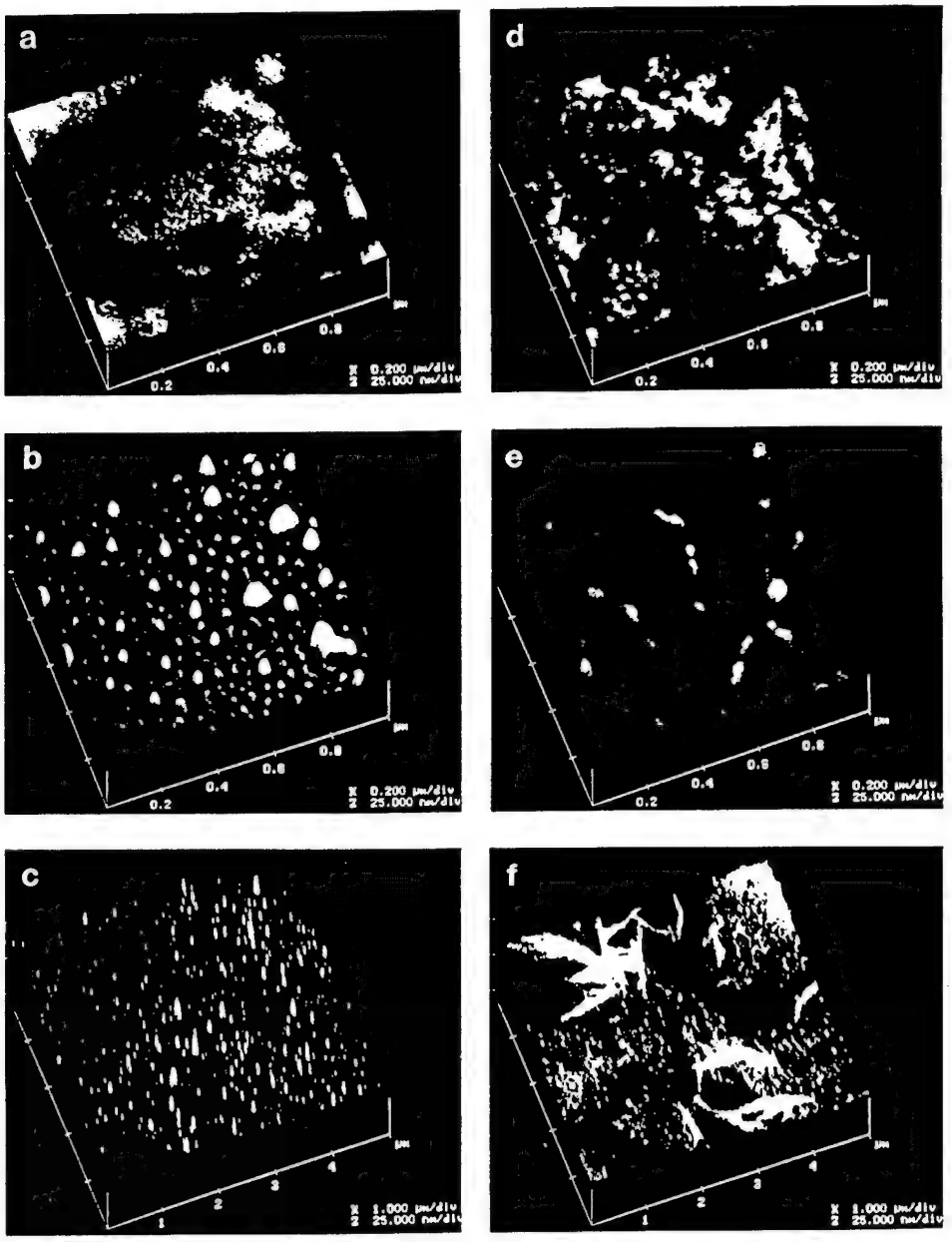

Fig. 1 a,d; b,e; c,f = AFM contour images, Underlying substratum is PS (left side) or POMA (right side). a = 1 μm × 1 μm area of PS before protein adsorption; b = 1 μm × 1 μm area of MAP adsorbed to PS; c = 5 μm × 5 μm area of MAP adsorbed to PS; d = 1 μm × 1 μm area of POMA before protein adsorption; e = 1 μm × 1 μm area of MAP adsorbed to POMA; f = 5 μm × 5 μm area of MAP adsorbed to POMA. Protein adsorption was performed in a 50 μg ml^{-1} solution of MAP for 60 min followed by a rinse using fluid displacement (Baty *et al.*, 1995; with permission, *J Colloid Interface Sci*). (see Color Section.)

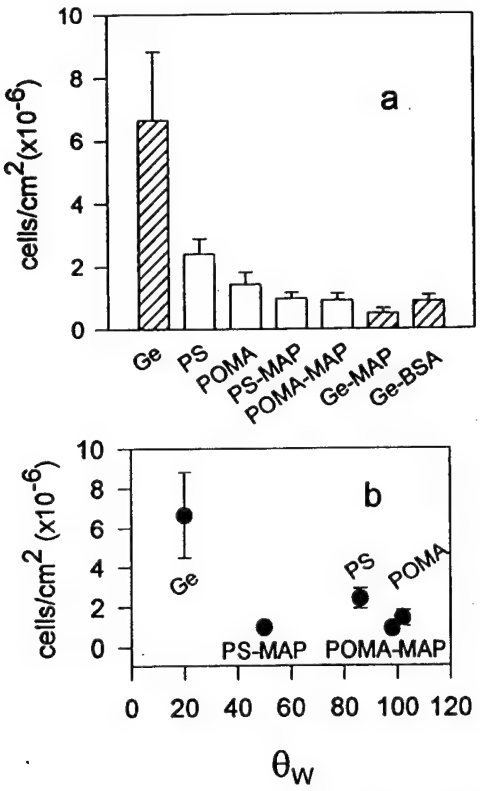

Fig. 2 a = adhesion of MHS-3 cells onto various substrata. Substrata conditioned with MAP or BSA are indicated by hyphenation (*e.g.* PS-BSA). Error bars are standard deviations. Cross hatched bars indicate data presented previously (Frølund *et al.*, 1996). For new data (bars not cross-hatched) PS > POMA > PS > MAP = POMA-MAP, based on 2 sample t-test (0.95). Experimental details are described in Baty *et al.* (1995) and Frølund *et al.* (1996). Polymer films (PS and POMA) were spun cast onto Ge coupons. Preadsorption of MAP and BSA was for 60 min under static conditions. Substrata were exposed to washed MHS-3 cells for 30 min and then rinsed in synthetic seawater. Attached cells were stained and observed using epifluorescence microscopy. b = advancing water contact angles for some of the surfaces obtained using the sessile drop method *vs* number of adhered cells.

for hydrophilic substrata with unconditioned surfaces (Fig. 2b), the conditioned surfaces are exceptions to this trend. The high contact angle obtained for the POMA-MAP surface is thought to result from interaction of the water drop with portions of the substratum which are exposed when MAP coalesces into aggregates upon dehydration (Baty *et al.*, 1995; unpublished). If this interpretation is correct, then both the PS and POMA surfaces conditioned with MAP may exhibit similar hydrophilicities (mildly hydrophilic) in the hydrated state.

It may be that the exclusion of fr2ps from both BSA and MAP results from steric repulsion, a phrase which is used to explain protein exclusion from self assembled monolayers of oligo (ethylene oxide). These films can exclude both solution phase proteins (Prime & Whitesides, 1993) and whole cells (Lopez *et al.*, 1993). The effect has been compared to steric stabilization of colloids by adsorption of a hydrophilic polymer at the water/colloid interface (Prime & Whitesides, 1991). Steric repulsion between

adsorbed protein films can be measured using the surface-force apparatus (Nylander *et al.*, 1994), and the phrase has been invoked to explain the exclusion of methylated BSA from preadsorbed films of BSA (Staunton & Quiquampoix, 1994). Many proteins saturate the surface at monolayer coverage which means they exclude at least themselves from the interface (Malmsten, 1994; Nylander *et al.*, 1994). This exclusion occurs even though the adsorbed proteins might be expected to have altered conformations which would promote binding of their solution phase counterparts.

The similar extent of (reduced) cell adhesion on the PS and POMA surfaces conditioned with MAP suggest that the molecular interactions involved are unaffected by a pronounced difference in adsorbed (conditioning) film supramolecular structure. This result is reminiscent of the phenomenon of protein and cell exclusion reported for oligo (ethylene oxide) films, *i.e.* the effect is robust in the sense that the ethylene glycol chains need not be individually grafted to the surface to produce the exclusion, but can be graft-polymerized *via* plasma polymerization (Lopez *et al.*, 1992). This deposition process produces films with more chemical heterogeneity than self-assembled films (Johnston & Ratner, 1995). (Plasma polymerized films are normally highly cross-linked).

The analogy drawn above may be superficial when examined closely. The putative MHS-3 adhesin, fr2ps, is thought to be located in a diffuse capsular envelope on the mother cell (Quintero & Weiner, 1995). Mineral surfaces can participate in hydrogen bonding with both organic acids and bases (Thurman, 1985) and it has been postulated that MHS-3 capsular polysaccharide binds to substrata primarily through hydrogen bonding (Quintero & Weiner, 1995). In theoretical treatments of steric repulsion associated with oligo (ethylene oxide) films hydrogen bonding is not explicitly considered (Jeon & Andrade, 1991). This may leave an opening for some interesting studies.

SUMMARY AND CONCLUSIONS

In general biofilms are complex communities of interacting microbes. Despite this complexity a molecular level approach to investigating interactions which mediate adhesion of fouling communities to inert surfaces is tractable. Experimental methodologies and associated interpretative tools are available. The interface between the biofilm and the inert surface provides a clear focus for investigation of adsorption behavior of biomolecules. Such studies can yield useful information about adhesins involved, molecular architectures which may promote adhesive (or non-adhesive) interactions, and information about interactions between biomolecules at the interface.

References

Al-Makhlafi H, McGuire J, Daeschel M (1994) Influence of preadsorbed milk proteins on adhesion of *Listeria monocytogenes* to hydrophobic and hydrophilic silica surfaces *Appl Environ, Microbiol* **60**: 3560–3565

Andrade J D (1985) *Surface and Interfacial Aspects of Biomedical Polymers Vol 2, Protein Adsorption.* Plenum Press, New York

Andrade J D, Hlady V, Wei A-P, Gölander C-G (1990) A domain approach to the adsorption of complex proteins: preliminary analysis and application to albumin, *Croat Chem Acta* **63**: 527–538

Baier R E, A E Meyer, DePalma V A, King R W, Fornalik M S (1983) Surface microfouling during the induction period. *J Heat Trans* **105**: 618–624

Banovac F, Saavedra S S, Truskey G A (1994) Local conformational changes of vitronectin upon adsorption on glass and silane surfaces, *J Colloid Interface Sci* **165**: 31–40

Baty A M, Suci P A, Tyler B J, Geesey G G (1995) Investigation of mussel adhesive protein adsorption on polystyrene and poly (octadecyl methacrylate) using angle dependent XPS, ATR/FT-IR and AFM. *J Colloid Interface Sci* **177**: 307–315

Benedict C V, Picciano P T (1987) Adhesives from marine mussels In: Hemingway R W (ed) *Adhesives from Renewable Resources*. ACS Symposium Series, ACS, Washington DC, p 466–483

Benner R, Pakulski J D, McCarthy M, Hedges J I, Hatcher P G (1992) Bulk chemical characterization of dissolved organic matter in the ocean. *Science* **255**: 1561–1564

Bidle K, Wickman H, Fletcher M (1993) Attachment of a *Psuedomonas*-like bacterium and *Bacillus coagulans* to solid surfaces and adsorption of their S-layer proteins. *J Gen Microbiol*, **139**: 1891–1897

Bohnert J L, Horbett T A (1986) Changes in fibronectin and albumin interactions with polymers indicated by decreases in detergent elutability. *J Colloid Interface Sci* **111**: 363–377

Brash J L, Horbett T A (1987) *Proteins at Interfaces: Physicochemical and Biochemical Studies*. ACS Symposium Series 343, ACS, Washington, DC

Busscher H J, Bellon-Fontaine M-N, Mozes N, Van der Mei H C, Sjollema J, Cerf O, Rouxhet P G (1990) Deposition of *Leuconostoc mesenteroides* and *Stretococcus thermophilus* to solid substrata in a parallel plate flow cell. *Biofouling* **2**: 55–63

Busscher H J, Weerkamp A H, Van der Mei H C, Van Steenberghe D, Quirynen M, Pratt I H, Marechal M, Rouxhet P G (1989) Physico-chemical properties of oral streptococcal cell surfaces and their relation with adhesion to solid substrata *in vitro* and *in vivo*. *Colloids Surf* **42**: 345–353

Christensen B E, (1989) The role of extracellular polysaccharides in biofilms. *J Biotechnol* **10**: 181–202

Christensen B E, Kjosbakken J, Smidsrod O (1985) Partial chemical characterization of two extracellular polysaccharides produced by marine periphytic *Pseudomonas* sp. strain NCMB 2021. *Appl Environ Microbiol* **50**: 837–845

Cohen Stuart M A, Fleer G J, Bijsterbosch B H (1982) The adsorption of poly (vinyl pyrrolidone) onto silica I. Adsorbed amount *J Colloid Interface Sci* **90**: 310–320

Cooksey K E (1992) Extracellular polymers in biofilms. In: Melo L F, Bott T R, Fletcher M, Capdeville B (eds) *Biofilms: Science and Technology*. Kluwer, The Netherlands, pp 137–147

Costerton J W, Cheng K J, Geesey G G, Ladd T I, Nickel J C, Dasgupta M, Marrie T J (1987) Bacterial biofilms in nature and disease. *Annu Rev Microbiol* **41**: 435–464

Cotrell I W, Kovacs P (1977) Algin. In: Graham P (ed) *Food Colloids*. AVI Publishing Company, Westport, CT, pp 438–463

DeBeer D, Stoodley P, Roe F, Lewandowski Z (1993) Oxygen distribution and mass transport in biofilms. *Biotechnol Bioeng* **43**: 1131–1138

Deretic V, Schurr M J, Boucher J C, Martin D W (1994) Conversion of *Pseudomonas aeruginosa* to muciody in cystic fibrosis: environmental stress and regulation of bacterial virulence by alternative sigma factors. *J Bacteriol* **176**: 2773–2780

Evans L R, Linker A (1973) Production and characterization of the slime polysaccharide of *Pseudomonas aeruginosa*. *J Bacteriol* **116**: 915–924

Frølund B, Suci P A, Langille S, Weiner R M, Geesey G G (1996) Influence of protein conditioning films on binding of a bacterial polysaccharide adhesin from *Hyphomonas* MHS-3. *Biofouling* 10: 17–30

Gendreau R M, Winters S, Leininger R I, Fink D, Hassler C R, Jakobsen R J (1981) Fourier transform infrared spectroscopy of protein adsorption from whole blood: *ex vivo* dog studies. *Appl Spectrosc* **35**: 353–357

Goding J W (1983) *Monoclonal Antibodies: Principles and Practice*. Academic Press, Incorporated, London pp 162

Haynes C A, Norde W (1995) Structures and stabilities of adsorbed proteins *J Colloid Interface Sci* **169**: 313–328

Henningson P J, Gudmestad N C (1993) Comparison of exopolysaccharides from mucoid and nonmucoid strains of *Calvibacter michiganensis* subspecies *sepedonicus*. *Can J Microbiol* **39**: 291–296

Ishida K P, Griffiths P R (1993) Investigation of polysaccharide adsorption on protein conditioning films by attenuated total reflection infrared spectrometry. *J Colloid Interface Sci* **160**: 190–200

Jackson E R, Johnson D, Nash W G (1986) Gene networks in development *J Theor Biol* **119**: 379–396

Jann K, Jann B (1993) Bacterial adhesins. *Curr Top Microbiol Immunol* **151**: pp. 1–209

Jeon S I, Andrade J D (1991) Protein-surface interactions in the presence of polyethylene oxide II. Effect of protein size. *J Colloid Interface Sci* **142**: 159–166

Johnson H E, Granick S, (1992) New mechanism of nonequilibrium polymer adsorption. *Science* **255**: 966–968

Johnston E, Ratner B D (1995) Characterization of RF plasma-deposited oligo (glyme) films by XPS and SSIMS. *ACS Polymer Preprints* **36**: 87–88 (#572)

Kaiser D, Losick R (1993) How and why bacteria talk to each other. *Cell* **73**: 873–885

Klotz M G (1993) The importance of bacterial growth phase for in planta virulence and pathogenicity testing: coordinated stress response regulation in fluorescent pseudomonads? *Can J Microbiol* **39**: 948–957

Kolenbrander P E, London J (1993) Adhere today, here tomorrow: oral bacterial adherence. *J Bacteriol* **175**: 3247–3252

Koltisko B, Walton A (1985) Chromatographic analysis of protein adsorption In: Andrade J D (ed) *Surface and Interfacial Aspects of Biomedical Polymers Vol 2, Protein Adsorption*. Plenum Press, New York, pp 217–239

Korber D R, James G A, Costerton J W (1994) Evaluation of fleroxicin activity against established *Pseudomonas fluorescens* biofilms. *Appl Environ Microbiol* **60**: 1663–1669

Krisdhasima V, Vinaraphong P, McGuire J (1993) Adsorption kinetics and elutability of α-lactalbumin, β-lactoblobulin, and bovine serum albumin at hydrophobic and hydrophilic interfaces. *J Colloid Interface Sci* **161**: 325–334

Kristoffersen A, Rölla G, Skjorland K, Glantz P O, Ivarsson B (1982) Evidence for the formation of organic films on metal surfaces in seawater. *J Colloid Interface Sci* **86**: 196–203

Little B (1985) Factors influencing the adsorption of dissolved organic matter from natural waters. *J Colloid Interface Sci* **108**: 331–340

Loeb G I, Neihof R A (1975) Marine conditioning films. *Adv Chem Ser* **145**: 319–335

Loeb G I, Neihof R A (1977) Adsorption of an organic film at the platinum-seawater interface. *J Mar Res* **35**: 283–291

Loewen P C, Hengge-Aronis R (1994) The role of the sigma factor σ^s (KatF) in bacterial global regulation. *Annu Rev Microbiol* **48**: 53–80

Lopez G P, Albers M W, Schreiber S L, Carrol R, Peralta E, Whitesides G M (1993) Convenient methods for patterning the adhesion of mammalian cells to surfaces using self-assembled monolayers of alkanethiolates on gold. *J Am Chem Soc* **115**: 5877–5878

Lopez G P, Ratner B D, Tidwell C D, Haycox C L, Rapoza R J, Horbett T A (1992) Glow discharge plasma deposition of teraethylence glycol dimethyl ether for fouling-resistant biomaterial surfaces. *J Biomed Mater Res* **26**: 415–439

Malmsten M (1994) Ellipsometry studies of protein layers adsorbed at hydrophobic surfaces. *J Colloid Interface Sci* **166**: 333–342

Mantus D S, Ratner B D, Carlson B A, Moulder J F (1993) Static secondary ion mass spectrometry of adsorbed proteins. *Anal Chem* **65**: 1431–1438

McEldowney S, Fletcher M (1986) Variability of the influence of physicochemical factors affecting bacterial adhesion to polystyrene substrata. *Appl Environ Microbiol* **52**: 460–465

Merker R I, Smit J (1988) Characterization of the adhesive holdfast of marine and freshwater caulobacters. *Appl Environ Microbiol* **54**: 2078–2085

Neu T R (1992) Microbial "footprints" and the general ability of microorganisms to label surfaces. *Can J Microbiol* **38**: 1005–1008

Norde W, MacRitchie F, Nowicka G, Lyklema J (1986) Protein adsorption at solid-liquid interfaces: reversibility and conformation aspects. *J Colloid Interface Sci* **112**: 447–456

Notter M F (1988) Selective attachment of neural cells to specific substrates including Cell-Tak, a new cellular adhesive. *Exp Cell Res* **177**: 237–246

Nylander T, Klekicheff P, Ninham B W (1994) The effect solution behavior of insulin on interactions between adsorbed layers of insulin. *J Colloid Interface Sci* **164**: 136–150

Pakulski J D, Benner R (1994) Abundance and distribution of carbohydrates in the ocean. *Limnol Oceanogr* **39**: 930–940

Parkinson, J S (1993) Signal transduction schemes in bacteria. *Cell* **73**: 857–871

Passador L, Cook J M, Gambello M J, Rust L, Iglewski B H (1993) Expression of *Pseudomonas aeruginosa* virulence genes requires cell-to-cell communication. *Science* **260**: 1127–1130

Paul J H, Jeffrey W H (1985) Evidence for separate adhesion mechanisms for hydrophilic and hydrophobic surfaces in *Vibrio proteolytica*. *Appl Environ Microbiol* **50**: 431–437

Peters T, Jr (1985) Serum albumin. *Adv Protein Chem* **37**: 161–245

Piper K R, von Bodman S B, Farrand S K (1993) Conjugation factor of *Agrobacterium tumefaciens* regulates Ti plasma transfer by autoinduction. *Nature* **362**: 448–450

Pitt W G, Cooper S L (1988) Albumin adsorption on alkyl chain derivatized polyurethanes: I. the effect of C-18 alkylation. *J Biomed Mater Res* **22**: 359–382

Pratt-Terpstra I H, Weekramp A H, Busscher H J (1987) Adhesion of oral streptococci from a flowing suspension to uncoated and albumin-coated surfaces. *J Gen Microbiol* **133**: 3199–3206

Prime K L, Whitesides G M (1991) Self-assembled organic monolayers: model systems for studying adsorption of proteins at surfaces. *Science* **252**: 1164–1167

Prime K L, Whitesides G M (1993) Adsorption of proteins onto surfaces containing end-attached oligo (ethylene oxide): a model system using self-assembled monolayers. *J Am Chem Soc* **115**: 10714–10721

Pringle J H, Fletcher M (1986) Adsorption of bacterial surface polymers to attachment substrata. *J Gen Microb* **132**: 743–749

Quintero E J, Weiner R M (1995) Evidence for the adhesive function of the exopolysaccharide of *Hyphomonas* strain MHS-3 in its attachment to surfaces. *Appl Environ Microbiol* **61**: 1897–1903

Ranieri, J P, Bellamkonda R, Jacob J, Vargo T G, Gardella J A, Aebischer P (1993) Selective neuronal cell attachment to a covalently patterned monoamine on fluorinated ehtylene propylene films. *J Biomed Mater Res* **27**: 917–925

Read R R, Costerton J W (1987) Purification and characterization of adhesive exopolysaccharides from *Pseudomonas putida* and *Pseudomonas fluorescens*. *Can J Microbiol* **33**: 1080–1090

Rosenberg M, Kjelleberg S (1986) Hydrophobic interactions: role in bacterial adhesion. *Adv Microb Ecol* **9**: 353–393

Schakenraad J M, Noordmans J, Wildevuur Ch R H, Arends J, Busscher H J (1989) The effect of protein adsorption on substratum surface free energy, infrared absorption and cell spreading. *Biofouling* **1**: 193–201

Staunton S, Quiquampoix H (1994) Adsorption and conformation of bovine serum albumin on montmorillonite: modification of the balance between hydrophobic and electrostatic interactions by protein methylation and pH variation. *J Colloid Interface Sci* **166**: 89–94

Stenström T A (1989) Bacterial hydrophobicity, an overall parameter for the measurement of adhesion potential to soil particles. *Appl Environ Microbiol* **55**: 142–147

Suci P A, Geesey G G (1995) Investigation of alginate binding to germanium and polystyrene substrata conditioned with mussel adhesive protein. *J Colloid Interface Sci* **172**: 347–357

Sutherland I W (1980) Polysaccharides in the adhesion of marine and fresh water bacteria. In: Berkeley R C W, Lynch J M, Melling J, Vincent B (eds) *Microbial Adhesion to Surfaces*. Ellis Horwood, Chichester, UK, pp 329–338

Tamada Y, Ikada Y (1993) Effect of preadsorbed proteins on cell adhesion to polymer surfaces. *J Colloid Interface Sci* **155**: 334–339

Taylor G T, Troy P J, Nullet M, Sharma S K, Liebert B E (1994) Protein adsorption from seawater onto solid substrata: II. behavior of bound protein and its influence on interfacial properties. *Mar Chem* **47**: 21–39

Thurman E M (1985) *Organic Geochemistry of Natural Waters*. Martinus Nijhoff, Boston

Troy II F A (1979) The chemistry and biosynthesis of selected bacterial capsular polymers. *Annu Rev Microbiol* **33**: 519–560

Uhlinger D J, White D C (1983) Relationship between physiological status and formation of extracellular polysaccharide glycocalyx in *Pseudomonas atlantica*. *Appl Environ Microbiol* **45**: 64–70

Van Enckevort H J, Dass D V, Langdon A G (1984) The adsorption of bovine serum albumin at the stainless-steel/aqueous solution interface. *J Colloid Interface Sci* **98**: 138–143

Van Loosdrecht M C M, Lyklema J, Norde W, Zehnder A J B (1989) Bacterial adhesion: a physicochemical approach. *Microb Ecol* **17**: 1–15

Vroman L, Adams A L (1986) Adsorption of proteins out of plasma and solutions in narrow spaces. *J Colloid Interface Sci* **111**: 391–402

Waite J H (1990) Marine adhesive proteins: natural composite thermosets. *Int J Biol Macromol* **12**: 139–144

Wells M L, Goldberg E D (1994) The distribution of colloids in the north atlantic and southern oceans. *Limnol Oceanogr* **39**: 286–302

Williams T, Marumo K, Waite J H, Henkens R W (1989) Mussel glue protein has an open conformation. *Arch Biochem Biophys* **269**: 415–422

Wolfaardt G M, Lawrence J R, Robarts R D, Caldwell S J, Caldwell D E (1994) Multicellular organization in a degradative biofilm community. *Appl Environ Microbiol* **60**: 434–446.

Wrangstadh M, Conway P L, Kjelleberg S (1986) The production of an extracellular polysaccharide during starvation of a marine *Pseudomonas* sp. and the effect thereof on adhesion. *Arch Microbiol* **145**: 220–227

Yun C, Ely B, Smit J (1994) Identification of genes affecting production of the adhesive holdfast of a marine caulobacter. *J Bacteriol* **176**: 796–803

Microbial Cell Fingerprinting-- Development of TOF-SIMS for the Study of Microbial Cell Surfaces

Patrick C. Schamberger, Frank Caccavo, Jr.,
Fintan van Ommen Kloeke, Gill G. Geesey

Center for Biofilm Engineering
409 Cobleigh Hall
Montana State University
Bozeman, MT 59717

Abstract for Surfaces in Biomaterials conference
Sept. 4→7, 1996, Phoenix, Az.

P.C. Schamberger

Notes

Introduction

Time-of-Flight Secondary Ion Mass Spectrometry (TOF-SIMS) has been applied to the study of biomolecules (1,2,3). To date, the study of biomolecules has been limited to constructing model surfaces (i.e. silver) on which a biomolecule is adsorbed to determine its fragmentation pattern in a dry state. This project demonstrates the utility of TOF-SIMS as an analytical tool to study microorganisms (bacteria) in marine environments. Using the cold probe technique, the analysis of bacteria in biofilms in an hydrated environment is possible.

This project involves developing TOF-SIMS, which is an analytical technique. No changes to the spectrometer will be made, therefore, one must only construct samples for analysis by TOF-SIMS and model samples to aid in the interpretation. The approach is to use the TOF-SIMS, and a cold probe on a TOF-SIMS where applicable, to analyze a series of bacteria. The three goals of this project are to determine if the TOF-SIMS ion fragmentation pattern of a cell surface results in a "fingerprint" spectrum that can be used to identify a particular bacterium. If one does obtain a unique fingerprint of a bacterium, an attempt to determine the cell surface molecules responsible for adhesion can be made. Lastly, evaluating the use of the cold probe technique to study microbes in a biofilm will be made.

Ion fragmentation patterns obtained in the TOF-SIMS are unique to the molecules from which the ions and ion fragments are obtained (4). The different properties of microbial cell surfaces should be reflected by a unique molecular composition. Therefore, one should be able to identify ion fragments unique to each different molecule on a microbe surface to form a "fingerprint" spectrum of the microbe. This spectrum could then be used to determine the presence or absence of a particular microbe in a biofilm. Using the cold probe technique we propose to develop a protocol for analysis of a biofilm in its native hydrated state. Specifically, this project would develop TOF-SIMS to study biofilm populations that have developed on surfaces in the natural environment.

Experimental

Samples

Cell samples were obtained by transferring the cells from colonies on agar plates to a cleaned, oxidized silver substrate. The silver substrate (Johnson Matthey, Alfa Aesar, Ward Hill, MA 99.9% silver foil) was cleaned by immersion for 5 minutes in an ultrasound bath of the following solvents: hexane, chloroform, tetrahydrofuran, and methanol (all Fisher Scientific, Fair Lawn, NJ, HPLC grade solvents). After cleaning the coupon was etched (oxidized) in concentrated HNO_3 (Fisher Scientific, Fair Lawn NJ, reagent grade) then rinsed in nanopure water.

The following cell types were analyzed:

- *Hyphomonas*, strain MHS-3, wild type strain
- *Hyphomonas*, strain MHS-3, reduced adhesive strain
- ***Pseudomonas aeruginosa***
- *Enterococcus faecium*, parent
- *Enterococcus faecium*, L-form
- *Shewanella alga*, strain BrY, wild type
- *Shewanella alga*, strain BrY, reduced adhesive

The cells were allowed to air dry overnight before analysis.

TOF-SIMS

The instrument used to collect the TOF-SIMS spectra was a Charles Evans & Associates (now PHI-Evans) T-2000 TRIFT TOF-SIMS. The primary ion source was an 11 keV cesium ion source with an average ion current of 2 pA (measured on Si) for 150 seconds, with a 156 ps pulse width, 10 kHz repetition rate, corresponding to 5.7×10^{13} ions/cm^2, within a static SIMS ion dosage. The ion beam was rastered using a scatter raster pattern in a 65μ by 65μ area. Charge compensation was accomplished using a 24 V, 4 nA (pulsed current) beam of electrons, pulsed out of phase with the ion gun every five ion gun cycles. A 3 kV sample bias was placed at the sample stage to act as the secondary ion extraction field. Ions were detected in ion counting mode. A 1 kV post-accelerating voltage was applied at the detector. Positive and negative ion spectra were obtained.

Results and Discussion

For simplicity, positive ion mass spectra are being presented in this paper. In some cases, negative ion spectra aids in identifying cells and cell surface molecules and will be discussed in the presentation. In general, it is easier to obtain higher mass fragments of positive ions due to the nature of the ion formation mechanisms.

Marine system, Wild Type and Reduced Adhesive *Hyphomonas* cells

Figure 1 shows the positive ion spectra of *Hyphomonas* Wild Type (1A) and Reduced Adhesive mutant (1B) cells. Notice that the spectra appear to be identical. Unfortunately, salt ion interference (from the marine saline conditions necessary to grow the cells) prevented the observation of higher mass ions. The region from 100 to 200 m/z is useful in identifying classes of adhesive molecules. The peaks observed at 110 and 120 m/z are indicative of proteins on the surface. These ions, as well as peaks at 112, 115, and 136 can be used to identify the presence of proteins. Figure 1C shows the spectrum for a typical protein, Bovine Serum Albumin (BSA) and is included as a protein model compound.

Estuarine system, Wild Type and Reduced Adhesive *Shewanella alga* strain BrY cells

Figure 2 shows the positive ion TOF-SIMS spectra for the Wild Type (Figure 2A) and Reduced Adhesive mutant (Figure 2B) of *Shewanella alga* strain BrY cells. In this region (100-200 m/z), the cells can be distinguished from each other. The Wild Type cells have mass fragments that do not indicate proteins or polysaccharides necessarily, but may be from aliphatic compounds. The higher mass region of the Reduced Adhesive strain (Fig. 2B) contains mass fragments that indicate the presence of proteins (110, 120, and 130 m/z) as discussed above, as well as peaks that indicate polysaccharides (107, 113, 165 and 181 m/z). The peak at 181 m/z is most likely a glucose+H^+ ion, and the peak at 165 m/z is most likely the 181 ion fragment with the loss of an oxygen.

This data suggests an adhesion mechanism that is through a lipid moiety. Additional work must be done to confirm this hypothesis and falls outside of the scope of this project. However, in a preliminary fashion, this demonstrates the ability to define the type of molecule responsible for adhesion by TOF-SIMS in certain instances.

Note also the peak at 197 m/z. This peak is observed in both cell types and may be an indicator of the *Shewanella alga* cells in general. This observation must be repeated. As an additional test, cells will be grown under different conditions to see if growth conditions effect the fingerprint spectra.

Distinctive bacterial cell fingerprints, *Shewanella*, *Pseudomonas* and *Enterococcus* cells

Figure 3--A,B,C shows representative spectra for *Pseudomonas aeruginosa*, *Enterococcus faecium*--parent strain, and *Enterococcus faecium*--L-form strain in the mass region from 100 to 200 m/z. These spectra demonstrate that differences between cell types can be observed in this region. *Shewanella*, *Pseudomonas* and *Enterococcus* cells can be distinguished from in this region, although there are overlapping peaks as well. The parent and L-form of the *Enterococcus* cell can also be distinguished. In this region, the following fingerprint peaks can be assigned: *Shewanella*--Wild Type 121, 125, 141, 197; *Shewanella*--Reduced Adhesive 113, 197; *Pseudomonas* 159, 172, 186; *Enterococcus*--parent 140, 176; and *Enterococcus*--L-form 154, 184. One should also note that the indicator peaks for proteins (110, 120) are present on the *Pseudomonas* (also on the *Enterococcus*--parent in as a small spectral component). The indicator peaks for polysaccharide (165, 181) are present on all three cell surfaces shown on Figure 3.

While the results obtained in the mass region 100 to 200 m/z indicate the ability to fingerprint these cell types, unique higher mass ions have been observed for the *Pseudomonas* and both *Enterococcus* cells. These ions appeared in the region from 200 to 400 m/z and are shown on Figure 5.

For the *Pseudomonas aeruginosa* cell (Fig. 4A), note the fingerprint ion mass fragment peaks between 244 and 300 m/z, centered at 272 m/z. The fragments 244, 272 and 300 differ by 28 a.m.u. and are related to each other through a loss of $CH_2.CH_2$ units or CO, both common mass spec. ion loss fragments. 260 and 288 are related in this fashion also.

For the *Enterococcus faecium--parent* cell (Fig. 4B), the ion fragment fingerprint spectra are different. 304, 332 and 365 m/z ion fragments are indicators of this cell surface. (Note that 304 and 332 also differ by 28 a.m.u.)

For the *Enterococcus faecium--L-form* cell (Fig. 4C), a mutant of the parent, the 365 m/z fragment is common to the parent cell. This peak may be used to fingerprint all *Enterococcus* cells. More data will be collected to see if this is the case including the effect of growth conditions. However, the peaks at 206, 224, and 246 can be used to distinguish this cell from the parent. The mass differences between these fragments are not 28 in this case; but rather, have a mass difference of 18. This indicates the 206 peak is most likely related to the 224 peak through the loss of a water molecule.

Cell wall extracts may aid in identifying each peak in the TOF-SIMS spectra of a particular cell. This type of work may be useful in the future towards unraveling a recognition sequence responsible for adhesion. However, this work currently falls outside of the scope of this project.

In summary, this data suggests the ability of TOF-SIMS to distinguish:

1.) Different genera of bacterial cells.

2.) Mutants of the same species of bacterial cells.

References

(1) Clark, M.B., Jr.; Gardella, J.A., Jr. *Anal. Chem.* **62** (8), 1990, pp.870-875.

(2) Benninghoven, A.; Hagenhoff, B.; Niehuis, E. *Anal. Chem.* **65** (14), 1993, p. 635A

(3) Mantus, D.S.; Ratner, B.D.; Carlson, B.A.; Moulder, J.F. *Anal. Chem.* **65** (10), 1993, pp. 1431-1438.

(4) Benninghoven, A.; Hagenhoff, B.; Niehuis, E. *Anal. Chem.* **65** (14), 1993, p. 631A

Acknowledgments

The authors wish to thank Jo Rayner and Hillary Lappin-Scott of Exeter University; Exeter, England; and Ken Runnion and Joan Comble of JK Research, Bozeman, MT for providing various cell samples. We proudly acknowledge the Office of Naval Research, Biological & Biomedical Science and Technology Division, for funding this project, Award # 96PR03095-00.

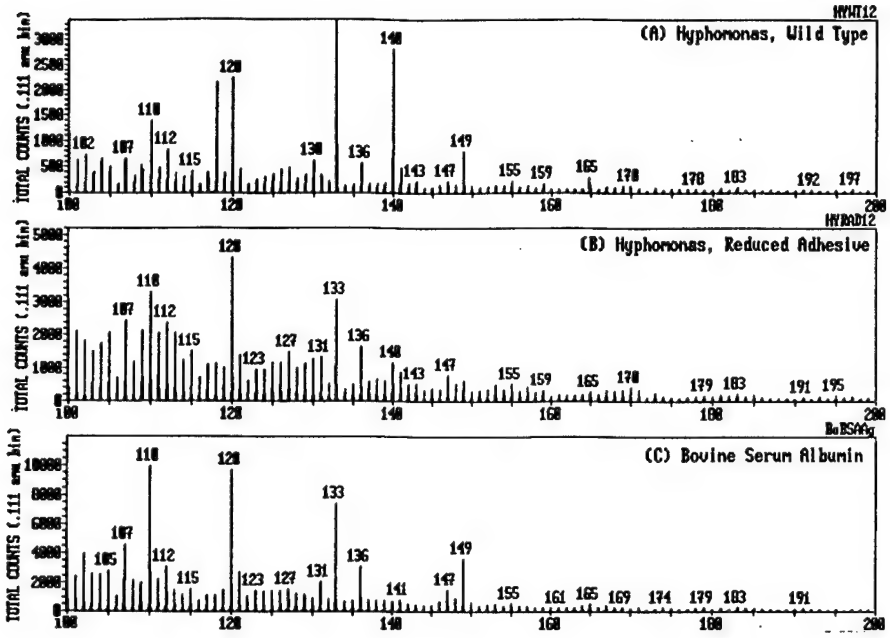

Figure 1-- Positive ion TOF-SIMS spectra (100 to 200 m/z) of:
(A) *Hyphomonas* Wild Type cells
(B) *Hyphomonas* Reduced Adhesive
(C) Bovine Serum Albumin

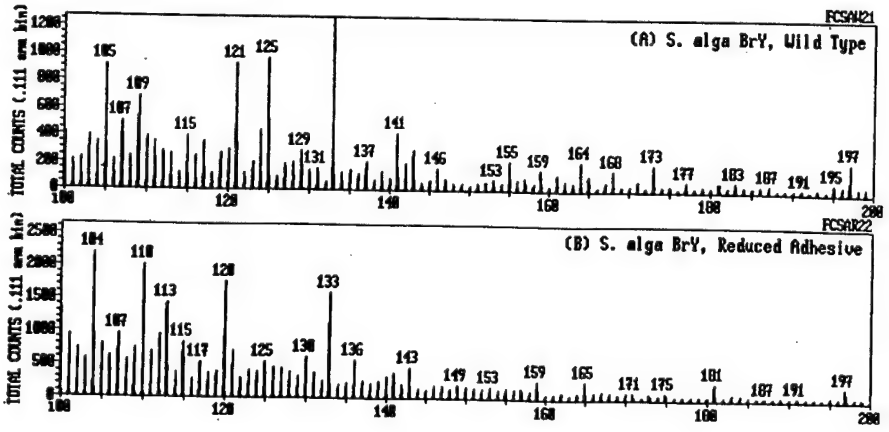

Figure 2-- Positive ion TOF-SIMS spectra (100 to 200 m/z) of:
(A) *Shewanella alga* strain BrY Wild Type cells
(B) *Shewanella alga* strain BrY Reduced adhesive cells

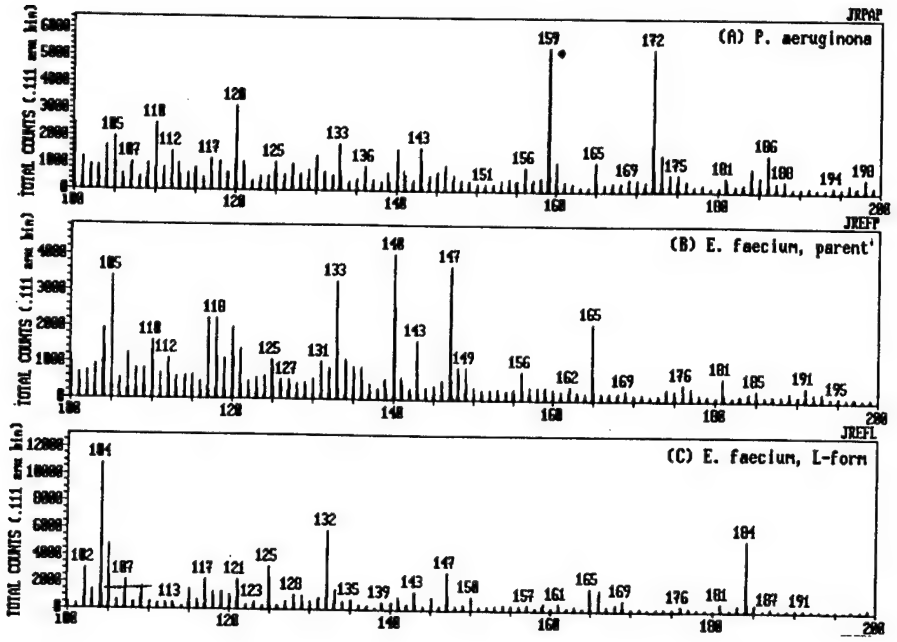

Figure 3– Positive ion TOF-SIMS spectra (100 to 200 m/z) of:
(A) *Pseudomonas aeruginosa* cells
(B) *Enterococcus faecium*, parent cells
(C) *Enterococcus faecium*, L-form cells

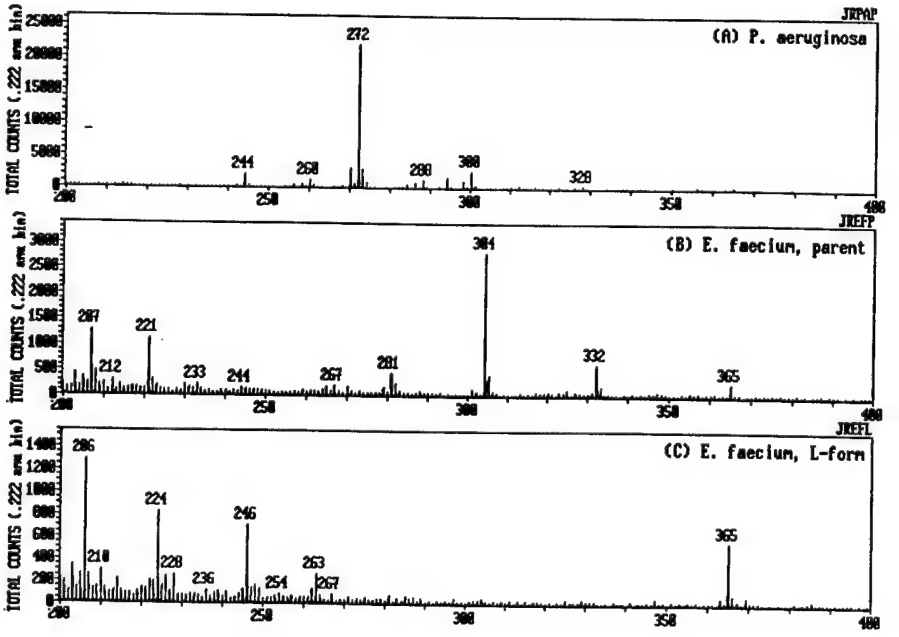

Figure 4– Positive ion TOF-SIMS spectra (200 to 400 m/z) of:
(A) *Pseudomonas aeruginosa* cells
(B) *Enterococcus faecium*, parent cells
(C) *Enterococcus faecium*, L-form cells

JOURNAL OF COLLOID AND INTERFACE SCIENCE 177, 307–315 (1996)
ARTICLE NO. 0036

Investigation of Mussel Adhesive Protein Adsorption on Polystyrene and Poly(octadecyl methacrylate) Using Angle Dependent XPS, ATR-FTIR, and AFM

ACE M. BATY,*‡ PETER A. SUCI,* BONNIE J. TYLER,*‡ AND GILL G. GEESEY*†,[1]

*Center For Biofilm Engineering, 409 Cobleigh Hall, Montana State University, Bozeman, Montana 59717; †Department of Microbiology, 109 Lewis Hall, Montana State University, Bozeman, Montana, 59717; and ‡Department of Chemical Engineering, 306 Cobleigh Hall, Montana State University, Bozeman, Montana, 59717

Received April 17, 1995; accepted June 28, 1995

The irreversible adsorption of mussel adhesive proteins (MAP) from the marine mussel *Mytilus edulis* has been investigated on polystyrene (PS) and poly(octadecyl methacrylate) (POMA) surfaces using angle resolved X-ray photoelectron spectroscopy (XPS), attenuated total reflection Fourier transform infrared (ATR-FTIR) spectrometry, and atomic force microscopy (AFM). Angle resolved XPS was used to quantify the elemental composition with depth of the upper 90 Å of the surface, and AFM was used to obtain the surface topography. The adsorption pattern of MAP, revealed by AFM images, is distinctly different on the two polymer surfaces and suggests that the substratum influences protein adhesion. The depth profiles of MAP, obtained from angle resolved XPS, show differences in nitrogen composition with depth for MAP adsorbed to PS and POMA. Infrared spectra of hydrated adsorbed MAP revealed significant differences in the amide III region and in two bands which may originate from residues in the tandemly repeated sequences of MAP. This data demonstrates that the chemistry of the polymer film that is present at the protein–polymer interface can influence protein–protein and protein–surface interactions.

Key Words: mussel adhesive protein; protein adsorption; XPS; ATR-FTIR; AFM.

INTRODUCTION

In the marine environment, microorganisms adhere tenaciously to virtually every known solid surface. Despite many years of research effort, the molecular interactions that are responsible for microbial adhesion and fouling of surfaces remain obscure. An understanding of these interactions would contribute to the development of surfaces that resist colonization of microorganisms. One reason why the molecular interactions are not understood is because microbial adhesion to surfaces is a multifactorial process that involves many types of bonding (1). To further complicate the situation, it has been shown that prior to microbial adhesion, a proteinaceous conditioning film forms on the surface of the substratum (2). This conditioning film imparts a uniform net negative charge to the surface and masks the substratum properties (3). The microorganisms attach to the conditioning film through adhesive structures composed of proteinaceous and exopolysaccharide molecules. Therefore, any serious study of microbial adhesion to submerged surfaces must include the characterization of molecular interactions with the conditioning film. Since the conditioning film which forms on the surface in the marine environment is still poorly defined, simplification of its composition is essential in order to provide for a degree of control that will enable the interactions at these surfaces to be characterized. The goal of this research is to characterize the interactions these proteins have when they are associated with two polymer surfaces displaying different functionalities, as is illustrated in Fig. 1.

The mussel adhesive proteins (MAP), which contain *Mytilus edulis* foot proteins one and two (MeFP-1 and MeFP-2), were used as a model protein conditioning film. MeFP-1 and MeFP-2 have a highly conserved repeat pattern. The MeFP-1 protein has a well-characterized structure consisting of repeating hexa- and decapeptide motifs and has an open conformation with very little secondary structure (4, 5). These qualities make this protein an ideal model conditioning film since the open conformation and repeat pattern makes the functional groups fully accessible for surface interactions. MeFP-1 and MeFP-2 also have novel compositions, with elevated levels of 3,4-dihydroxyphenyl-L-alanine (L-DOPA) and 4- and 3-mono- and di-transhydroxyproline (Hyp). These functional groups may confer an adhesive character to the proteins by enabling interactions using quinone redox chemistry (6, 7). However, these protein–surface interactions have yet to be demonstrated. Characterization of the specific protein–surface interactions is a prerequisite to the understanding of microbial attachment and fouling of surfaces.

MATERIALS

Adsorbates, Solvents, and Substrates

Purified MAP from *Mytilus edulis* was obtained from Swedish Bioscience Laboratory (Floda, Sweden) and stored

[1] To whom correspondence should be addressed.

0021-9797/96 $12.00

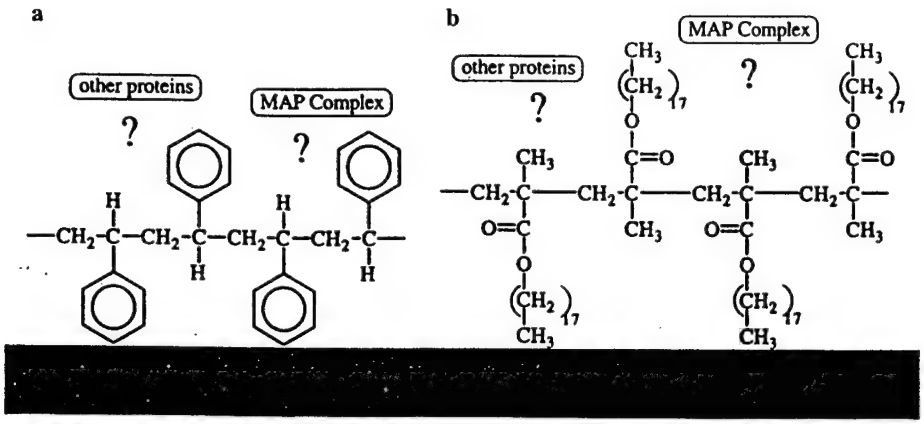

FIG. 1. Schematic diagram of the interactions being investigated between the MAP proteins (MeFP-1 and MeFP-2) and between the protein and polymer surfaces of (a) polystyrene and (b) poly(octadecyl methacrylate).

desiccated at −40°C. The amino acid composition according to the supplier is (per 1000 residues): 83 Asp, 74 Thr, 97 Ser, 64 Glu, 69 Pro, 132 Gly, 68 Ala, 50 Val, 25 Ile, 29 Leu, 30 Tyr, 12 Phe, 27 His, 115 Lys, 41 Arg, 41 Hyp, and 70 3,4-dihydroxy-L-phenylalanine (L-DOPA). Acetic acid-urea polyacrylamide gel electrophoresis (PAGE) indicated that the MAP preparation consisted of 80% of the two L-DOPA containing proteins, MeFP-1 and MeFP-2, in equal quantities. Two non-L-DOPA containing proteins contributed 20% of this preparation. The protocol for the PAGE was performed using previously described methods and the identification of MeFP-1 (130 kD) and MeFP-2 (45 kD) were made according to previously published results (8). Both MeFP-1 and MeFP-2 contain the unusual catecholic functionality L-DOPA.

Dichloromethylsilane (Aldrich 97%) was used as received. Hexadecane (Aldrich 99+%) was purified by passage through Super I Basic Alumina (Fisher Scientific) five times. All solvents including chloroform, ethanol, and toluene (Aldrich) were HPLC grade.

Optically smooth germanium (111) wafers (Exotic materials Inc., Costa Mesa, CA), 2.54 cm in diameter and 1-mm thick, were cut into 1 cm × 1 cm pieces using a diamond tipped stylus and spin coated with either polystyrene (PS) or poly(octadecyl methacrylate) (POMA) for the X-ray photoelectron spectroscopy (XPS) and atomic force microscopy (AFM) studies. For the attenuated total reflection Fourier transform infrared (ATR-FTIR) spectroscopy studies cylindrical germanium internal reflection elements (IRE) (Spectra Tech, Stamford, CT) were used.

PS (Aldrich Secondary Standard) was prepared as a 1.5% (w/v) solution in toluene. POMA (Aldrich) was prepared as a 1.5% (v/v) solution in toluene.

PREPARATION OF SUBSTRATUM

Ge Cleaning Procedure

The germanium crystals were immersed in an ultrasonic bath of a cleaning solution that was a mixture of isopropyl alcohol saturated with potassium hydroxide for 10 min. The crystals were then removed and immediately placed in an ultrasonic bath of ultra pure water. They were then gently scrubbed with undiluted Micro cleaning solution using cotton swabs. The crystals were rinsed in a hard stream of ultra pure water and immersed in a series of ultrasonic solvent baths, for 5 min each in ultra pure water (twice), ethanol, and chloroform. The crystals were then immediately dried under a stream of hydrocarbon free, dry nitrogen and transferred to an inert atmosphere (dry N_2) chamber, prior to silanization. The above cleaning procedure was performed immediately before the silanization reaction to prevent any adsorbed materials from contaminating the surface.

Auger electron spectroscopy, using a Phi Model 595 scanning Auger microprobe, indicated that the composition of the outermost surface region of the germanium substratum, when cleaned by this protocol, was 9.1 ± 1.4% carbon, 6.5 ± 2.0% oxygen, and 83.9 ± 2.2% germanium.

Silanization Procedure

The germanium crystals were silanized with dichloromethylsilane to improve the adhesion of the polymer films and to prevent film delamination in aqueous solution. All silane monolayers were prepared under an inert atmosphere of dry N_2. Monolayers of dichloromethylsilane were formed by immersing clean Ge crystals into a freshly prepared solution of dichloromethylsilane in *n*-hexadecane. All glassware used was cleaned with "piranha" solution, consisting of a 70:30 mix of concentrated H_2SO_4 and 30% H_2O_2, respectively. [WARNING: Piranha solution reacts violently, even explosively with organic materials (9).] Individual solutions were prepared by mixing a solution that was 5×10^{-3} *M* dichloromethylsilane in *n*-hexadecane. Each solution was stirred for 5 min before a germanium crystal was introduced. The reaction vessel was then capped and stored at room temperature for 12 h. Upon removal from the silane solution, the crystals were immediately rinsed with 50 ml of chloroform. They were then removed from the inert atmosphere

and extracted in a sohxlet extractor with hot chloroform for 30 min to remove any excess silane. They were then cured in an oven at 112°C for 3 h. Contact angle measurements were performed with water to estimate the quality of the silane film. Surfaces with contact angles less than 100° proved inadequate for polymer adhesion and were discarded.

Preparation of Polymer Surfaces

PS and POMA polymer films were spin cast onto presilanized, germanium fragments for the XPS and AFM studies. PS was used as a 1.5% (w/v) solution in toluene and POMA was used as a 1.5% (v/v) solution in toluene. Presilanized germanium crystals were completely covered with polymer solution and then immediately spin cast at 3500 rpm for 2 min. The polymer films were dried at room temperature for 24 h.

For the ATR-FTIR studies the cylindrical germanium IRE were silanized as described above. PS and POMA were dip coated onto germanium IRE at a speed of 0.5 cm/s.

X-ray photoelectron spectroscopy (Surface Science Instruments, Model SSX-100, 600-μm diameter spot size, monochromatized aluminum $K\alpha$ source) of the polymer films indicated that the films were continuous (i.e., no germanium or silane was detected). Recent AFM images acquired in the Fluid Tapping mode and cold-probe XPS analysis indicate that the spin cast polymer surfaces are stable when hydrated (manuscript in preparation).

Protein Adsorption Protocol

For the XPS and AFM studies the polymer coated germanium substrata were placed in a glass flow cell with entrance and exit tubing ports to allow for protein adsorption and subsequent rinse. For ATR-FTIR adsorption experiments, the polymer coated germanium IRE were placed within a stainless steel flow chamber (Circle Cell, Spectra Tech, Stamford, CT). Fluid was introduced and displaced through entrance and exit ports at each end of the Circle Cell.

All protein films were deposited onto freshly prepared polymer surfaces after the 24 h drying period. A stock solution of 1 mg/ml MAP was prepared in dilute HCl (pH 2.5) with deionized double distilled water, deaerated with N_2. The stock solution was stored at 5°C. A 50 μl aliquot of this solution was added to 0.45 ml of dilute HCl (pH 2.5). For the XPS and AFM studies this mixture was delivered into the flow cell containing the substratum that was to undergo protein adhesion. MAP was allowed to adsorb by raising the pH to 8.0 by delivering a 0.5 ml aliquot of a pH 10.9 solution into the reaction chamber, bringing the concentration of the protein to 50 μg/ml. For the ATR-FTIR studies a 50 μg/ml MAP solution was prepared as above before delivery into the flow cell. After a 1 h adsorption, the substratum was rinsed of any unadsorbed protein by flowing an aqueous solution at pH 8.0 through the reaction chamber at a rate of 100 ml/min for 3 min. The ATR-FTIR Circle Cell was rinsed at a rate of 0.5 ml/min for 60 min. The samples were removed and dried in hydrocarbon free dry air overnight.

SURFACE CHARACTERIZATION

Atomic Force Microscopy Imaging

All surfaces were imaged using a Nanoscope III AFM (Digital Instruments, Inc., Santa Barbara, CA) with a 350D scanner and a 3-101 optical head. The instrument was used in contact mode using square pyramid microfabricated silicon nitride cantilevers which were 100 μm in length and had a spring constant of 0.38 N/m. The images were recorded using 1 μm × 1 μm and 5 μm × 5 μm scan areas at 512 scans per area with a scan rate of 2 s^{-1}. All images were acquired in air and were stable with time and reproducible.

Angle Resolved X-Ray Photoelectron Spectroscopy

XPS spectra were obtained from a Surface Science Instrument Model SSX-100 spectrometer. A 5 eV flood gun was used to offset charge accumulation on the samples. A 600-μm diameter spot size was scanned using a monochromatized Aluminum $K\alpha$ X-ray source at 350 W and pass energies between 25.0 eV (resolution 1) and 150 eV (resolution 4). Elemental composition was calculated on peak areas from the C 1*s*, N 1*s*, and O 1*s* core levels. Relative peak areas were calculated by fitting the high resolution C 1*s*, N 1*s*, and O 1*s* peaks with Gaussian functions. Before the variable angle study was conducted an initial survey at 80° (from the surface) was completed. Depth profiles were performed using variable angle XPS data collected at takeoff angles of 10°, 22°, 35°, and 80°. The elemental compositions at the initial 80° survey were compared with the final 80° angle study to ensure no X-ray damage had occurred during analysis. The data were collected with the wide angle acceptance lens masked with a 12° slit. The binding energy scale was referenced by setting the CHx peak maximum in the C 1*s* spectrum to 285.0 eV (10).

ATR-FTIR Spectrometry

The time course of MAP adsorption in a hydrated state was followed by ATR-FTIR spectrometry. During the time course of each experiment infrared (IR) spectra were acquired every 5 min. A Perkin Elmer Model 1800 Fourier transform infrared (FT-IR) spectrophotometer equipped with a liquid N_2 cooled, medium range mercury–cadmium–telluride detector (5000–580 cm^{-1}) was used to collect the ATR-FTIR spectra. Interferograms were double-sided, apodization was a weak Beer–Norton function, and the range was 4000–700 cm^{-1} with an interval of 1 cm^{-1} and nominal resolution of 2 cm^{-1}; 50 interferograms were averaged per spectrum. Water vapor bands were removed by subtraction of a pure water vapor spectrum; fluctuations in intensity of the strong water band at 1640 cm^{-1} resulted in the appearance of this band in the difference spectra. This residual

water absorption band was removed by subtracting out a pure water spectrum using the ratio of areas of the absorption water band centered at 2120 cm^{-1} as a normalization factor (11). Variation in absorbance values resulting from slight differences in alignment of the flow chamber on the optical bench and coating with polymer films were normalized by using the area of the water absorption band at 1640 cm^{-1} (area: 1540 to 1740 cm^{-1}) as an internal standard (12). Areas of spectral features were computed for the region bounded by the data curve and a linear baseline drawn between the two endpoints of the integration.

Protein surface coverage was estimated based on area of the amide II band using published correlations. Adsorption conditions of Fink *et al.* (12) resemble approximately those here (saline solution, pH 7.4 on germanium). Extinction coefficients for solution phase bovine serum albumin compare favorably with our estimates (within 80%). Fink *et al.* (12) obtained correlations for adsorbed human albumin, immunoglobulin, and fibrinogen. Using their data, a factor for conversion of amide II areas to surface coverage in $\mu g/cm^2$ can be estimated. This conversion factor is 0.26 ± 0.12 $\mu g/cm^2$ per unit area amide II ($abs \cdot cm^{-1}$).

RESULTS

Atomic Force Microscopy Imaging

MAP adsorbed to clean PS and POMA from a solution with a bulk protein concentration of 50 $\mu g/ml$ was imaged using AFM. Figure 2 shows AFM contour images of 1 $\mu m \times 1$ μm areas of the two substrata before MAP adsorption (2a, 2d) and 1 $\mu m \times 1$ μm (2b, 2e) and 5 $\mu m \times 5$ μm (2c, 2f) areas after MAP adsorption. Before MAP adsorption, the polymer surfaces are extremely smooth with almost no surface features and with RMS surface roughness values of 1.035 and 0.546 nm for PS and POMA, respectively.

Adsorption of MAP to the PS surface resulted in the formation of closely packed, repeating structures as shown in Fig. 2b. Cross-sectional analysis of these features shows an average height of 9.48 ± 3.05 nm and a width of 33.02 ± 7.82 nm. The 5 $\mu m \times 5$ μm scan area, shown in Fig. 2c, reveals that the features observed at high magnification cover larger areas of the surface, suggesting that the surfaces are homogeneous and have continuous protein coverage. In contrast, MAP adsorbed to the POMA surface displays very different protein features that appear to be linearly ordered as revealed in the 1 $\mu m \times 1$ μm scan area in Fig. 2e. Cross-sectional analysis reveals that these features have an average height of 2.45 ± 1.35 nm and a width of 68.4 ± 3.91 nm. The 5 $\mu m \times 5$ μm scan area, shown in Fig. 2f, shows the protein features on this surface to be very heterogeneous, with larger more complex fibrous structures. These features extend 19.36-nm high and 179.69 nm in width, with some as long as 2.4 μm. Because of the heterogeneous nature of MAP on this surface it is difficult to determine whether the surface coverage of the protein is continuous based on this technique.

Angle Resolved X-Ray Photoelectron Spectroscopy

Angle dependent XPS of the surfaces studied in Fig. 2 further reveals the differences in MAP adsorption to PS and POMA surfaces. A detailed examination of the C 1*s* region of clean PS and POMA and of MAP adsorbed to PS and POMA at takeoff angles of 80° and 10° are given in Fig. 3. Each peak is contributed by different chemical groups. The C 1*s* peak at a binding energy of 291.6 eV is attributed to the pi–pi* transition in the aromatic rings of the polystyrene. The peak at 288.5 eV arises from the N—C=O and O—C=O functionalities on the protein and in the methacrylate chain, respectively. The C 1*s* peak at a biding energy of 286.6 eV is attributed to the C—N and C—O functionalities in the protein and the C—O—C functionality of the POMA. The dominant peak in both sets of spectra is at 285.0 eV. This peak originates from the aliphatic carbon in both the polymers and the protein.

Comparing the C 1*s* regions of MAP adsorbed to PS at 80° and 10° takeoff angles reveals a decrease in the aliphatic peak at 285.0 eV and disappearance of the peak associated with the pi–pi* transition. The disappearance of the pi–pi* transition and the decrease in the aliphatic peak relative to the 286.6 and 288.5 eV peaks from the protein indicates that at a takeoff angle of 10° the signal from the PS has disappeared from the spectra and signal intensity arises only from the protein. The C 1*s* region of MAP adsorbed to POMA reveals an increase in the peak at 286.6 eV relative to the 285.0 eV peak at the lower takeoff angle. This also indicates a greater contribution from the protein to this C 1*s* spectra.

The elemental compositions at the different angles were used with the calculated escape depths for each angle to gain insight on the elemental depth distribution of the proteins adsorbed to the polymer surfaces. The escape depths were calculated using parameters for organic compounds to calculate the inelastic mean free path and subsequently the escape depth using equations previously defined (13). Table 1 indicates that nitrogen is increasing with depth when MAP is adsorbed to PS, whereas, this trend is reversed on POMA. This indicates that MAP adsorbed to the polystyrene surface shows a nitrogen distribution that is enriched at the surface of the adsorbed protein film. In contrast, the MAP adsorbed to the POMA surface displays a depth profile that shows the nitrogen enrichment from the adsorbed protein at a maximum at the polymer surface.

ATR-FTIR Spectrometry

Figures 4a and 4b show ATR-FTIR spectra of MAP adsorbed onto PS and POMA polymer films after the 60 min rinse period. The time course of adsorption/desorption was followed based on the areas (1591 to 1493 cm^{-1}) of the amide II band (indicated by (iii) in Figs. 4a and 4b). This

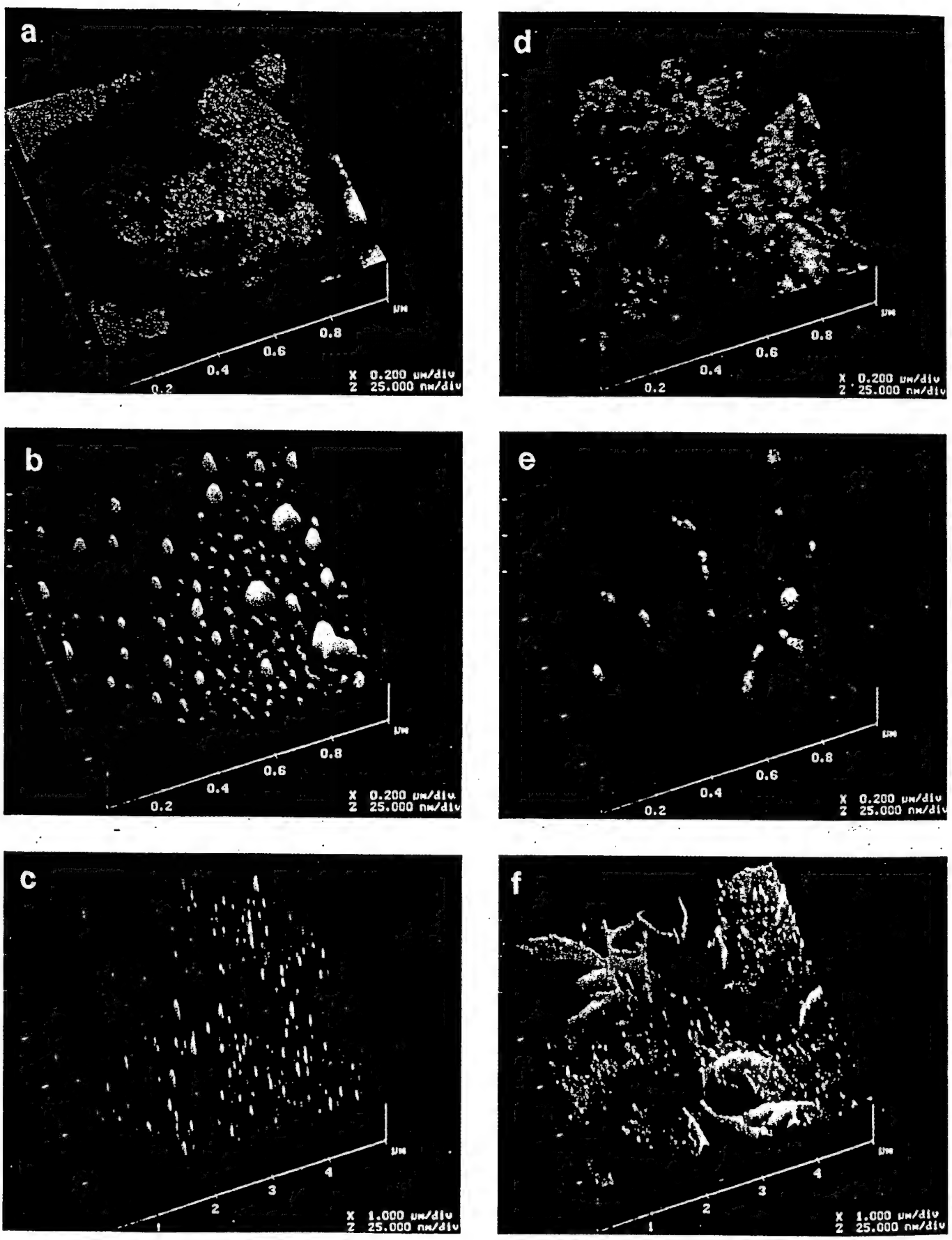

FIG. 2. AFM contour images of (a) 1 μm × 1 μm area of PS before protein adsorption, (b) 1 μm × 1 μm area of MAP adsorbed to PS, (c) 5 μm × 5 μm area of MAP adsorbed to PS, (d) 1 μm × 1 μm area of POMA before protein adsorption, (e) 1 μm × 1 μm area of MAP adsorbed to POMA, and (f) 5 μm × 5 μm area of MAP adsorbed to POMA.

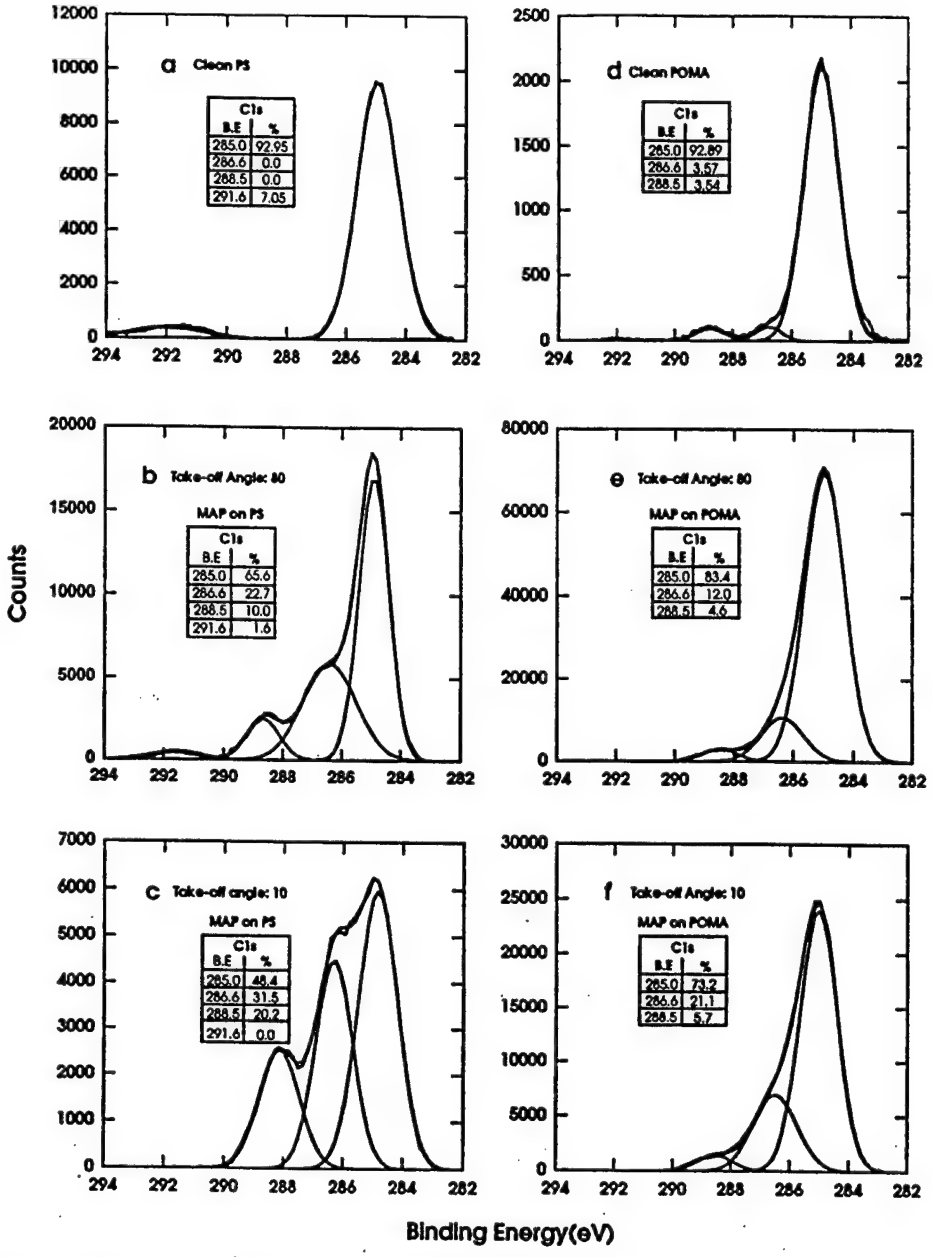

FIG. 3. C 1*s* spectra of clean PS (a) and POMA (d) and of MAP adsorbed to PS (b,c) and POMA (e, f) at takeoff angles of 80° and 10°.

is shown in Fig. 4c for each of the two surfaces (PS and POMA). Adsorption appears to be irreversible. The surface coverage of MAP at the end of the rinse period on PS and POMA surfaces, estimated from the correlations specified in the Methods section, is 0.045 ± 0.021 and 0.066 ± 0.031 $\mu g/cm^2$, respectively.

Comparison of the spectra presented in Figs. 4a and 4b reveals a number of differences in spectral features. (Features are indicated in Figs. 4a and 4b by lower case Roman numerals.) A band centered at 1740 cm^{-1} (i) is evident in MAP on POMA which does not appear in the spectrum of MAP on PS (although there is a slight band centered at 1730 cm^{-1} in this spectrum). The amide I band (ii) is centered at 1645 and 1654 cm^{-1} in the MAP on PS and POMA, respectively. Spectral features in the region from 1300 to 1200 cm^{-1} (iv) are typically attributed to amide III vibrations which are sensitive to protein secondary structure (14–16) and less obscured by the large water band centered at 1640 cm^{-1} than the amide I and II bands. In this region the spectrum of MAP on PS and POMA differ significantly. Distinct features centered at 1150 (v) and 1083 cm^{-1} (vi) in both spectra are unusual for adsorbed proteins. The band centered at 1150 cm^{-1} is especially prominent in the MAP on POMA.

DISCUSSION

The results presented here, demonstrate that the functional groups that are present at a polymer surface can influence

TABLE 1

Sample	Take-off angle	Escape depth	Mean atomic percent[a]		
			C	O	N
MAP adsorbed to PS	80	84.3	78.8 ± 6.3	13.5 ± 4.4	6.2 ± 3.2
	35	49.1	76.5 ± 7.5	15.8 ± 3.5	7.5 ± 3.6
	22	32.1	74.3 ± 8.4	16.0 ± 4.8	8.5 ± 4.3
	10	14.9	72.8 ± 8.5	16.7 ± 4.6	8.9 ± 4.2
MAP adsorbed to POMA	80	84.3	90.6 ± 1.5	6.2 ± 1.6	1.5 ± 0.1
	35	49.1	92.1 ± 0.6	6.6 ± 0.3	1.0 ± 0.1
	22	32.1	92.7 ± 0.4	6.5 ± 0.1	0.6 ± 0.1
	10	14.9	94.8 ± 0.6	4.7 ± 0.9	0.5 ± 0.5

[a] Taken from three separately prepared surfaces.

protein–protein and protein–surface interactions. The protein–surface interactions that can occur in the polymer–protein systems studied here are limited to two categories: one surface capable of undergoing MAP–surface pi–pi bond overlap interactions (PS) and one with no favorably energetic MAP–surface interactions (POMA). The PS surface provides a hydrophobic surface with an aromatic character and a medium surface free energy, and the POMA surface provides a hydrophobic low energy surface with an aliphatic functionality.

There are four mechanisms that have been proposed to play important roles in MAP–MAP and MAP–surface interactions: hydrogen bonding, metal-ligand complexes, Michael-type addition compounds derived from *o*-quinones, and charge transfer complexes (17). Olivieri *et al.* (18) have collected data that suggests that MAP can orient itself toward oxide surfaces enabling the L-DOPA residues to interact with the surface through hydrogen bonding. Hansen *et al.* (19) have recently found that MAP interacts with stainless steel by complexing and binding with surface metals. The Michael-type addition compounds are driven by the catechol oxidase enzyme that is cosecreted with the proteins in the natural system (20). In the system studied here, there are no divalent cations or metal ions to provide metal–ligand complexation. There are no enzyme driven reactions because the catechol oxidase does not survive the purification procedures for the MAP proteins and there are no functionalities present on the surface to allow hydrogen bonding interactions. However, at an elevated pH of 8 (approximately that of sea water and the pH during adsorption) the catechol functionality on the L-DOPA can undergo a spontaneous reverse dismutation to the *o*-quinone that is capable of interacting through a quinhydrone charge-transfer complex, illustrated in Fig. 5. The PS surface that displays an aromatic functionality would inhibit this MAP–MAP interaction because of the ability of PS to undergo pi–pi overlap interactions with the aromatic functionality of PS and the aromatic side chains of the MAP. The resulting surface topography after MAP adsorption to PS reveals homogeneous, repeating structures that would suggest this type of MAP–surface interaction. Furthermore, the dimensions of these features on the PS surface are representative of individual MeFP-1 and MeFP-2 molecules (21). In order to maximize the pi–pi interactions with the surface, the MAP will orient the aromatic side chains facing the polymer surface. This reasoning is supported by the decreasing nitrogen composition with depth in the XPS data. Since there are no energetically favorable MAP interactions with the POMA surface, the catecholic functional groups of the adsorbed protein are free to interact with each other and form charge-transfer complexes, as shown in Fig. 5. In this case the adsorption of the protein on a surface that appears to have no favorably energetic mechanisms for interactions is most likely driven by van der Waals forces, arising from the cross-linked protein with the surface. This results in the aggregated protein structures and the apparent linear order of the protein shown in the AFM images on this polymer surface. Furthermore, the smaller linear features on the POMA surface are representative of cross-linked MeFP-1 and MeFP-2 on the surface (21). The larger, fibrous structures on the POMA could arise from aggregated or cross-linked MAP. In either case, the AFM images suggest that the differences in surface chemistry on these two polymer surfaces strongly influence protein adsorption. Recent images obtained under fully hydrated conditions by AFM in Tapping Mode suggest that dehydration is not responsible for the gross differences observed by MAP on these surfaces.

When MAP adsorption to PS and POMA was evaluated under hydrating conditions by ATR-FTIR, spectral differences further suggested different protein interactions with the chemically distinct polymers. Differences in IR spectral features in the amide III region of proteins have been attributed to differences in secondary structure (14–16). Although it is difficult to make specific assignments unless the

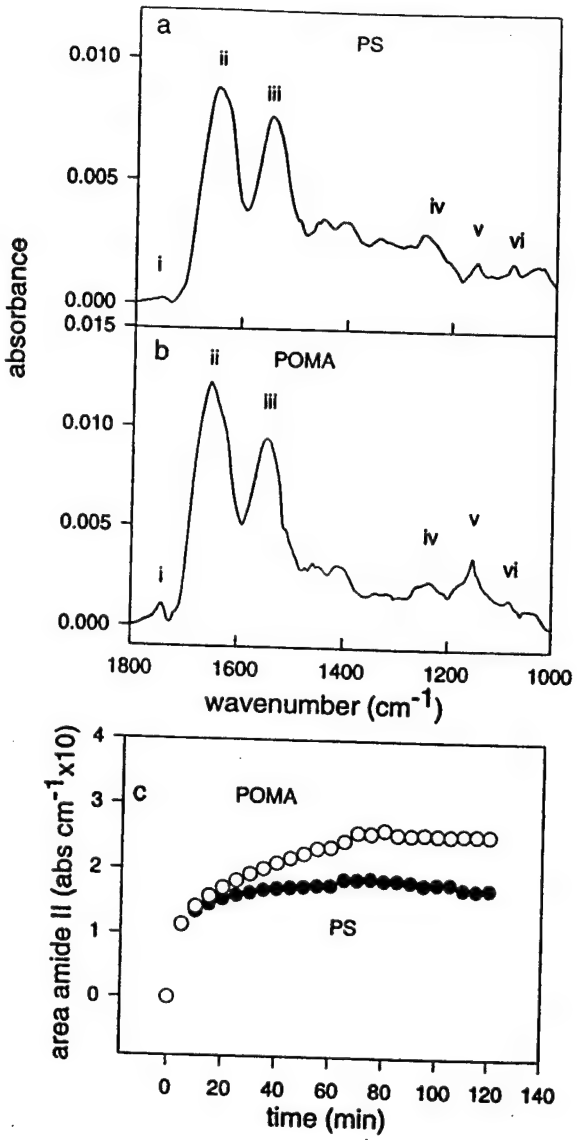

FIG. 4. ATR-FTIR spectra of adsorbed MAP to PS (a) and POMA (b). Roman numerals indicate spectral features discussed in the text. (c) Time course of adsorption (60 min) and rinse (60 min) followed by the area of the amide II band (iii). Open circles represent PS and closed circles POMA.

proteins consist entirely of one domain, differences observed in this amide III region (1200–1300 cm^{-1}) do indicate a difference in the hydrogen bonding pattern between the amide linkages of MAP on the PS and POMA surface. Therefore, the IR results are consistent with the XPS and AFM data which indicate that MAP organization and/or orientation are different on the PS and POMA surfaces. Of the three methodologies used, ATR-FTIR has the least spatial resolution. Since these spectral differences represent an average over the entire IRE surface (approx. 2.5 cm^2) it is unlikely that the phenomenon is confined to a small region of the surface.

The bands centered at 1150 and 1083 cm^{-1} may originate from residues whose repetitive motif results in resonance summation at particular frequencies, making them visible above the background. An attempt to identify these bands as arising from specific residues by comparison with ATR-FTIR spectra of aqueous solutions of various compounds has so far been unsuccessful. Nevertheless, there is a resemblance between the contrasting spectral features which appear for MAP on PS and POMA and those reported for adsorption of the blood plasma protein, fibronectin, on a series of functionalized polyurethanes (15). Notably, differences were observed in the amide III and I regions, and a band appeared to varying degrees in the 1720–1740 cm^{-1} region. The latter band arises from the carbonyl group and appears when a carboxylate functionality is protonated (i.e., salt to acid form) (22). For fibronectin, the appearance of this band was most prominent for the polyurethanes having the most hydrophobic functionalities. It was hypothesized that the acidic residues of the adsorbed protein entered a region of low dielectric constant proximal to the hydrophobic surface, shifting the equilibrium toward the protonated form. The MAP protein MeFP-2 is rich in acidic residues and it is speculated that it may mediate bridging between MeFP-1 (21). It is possible that the highly interconnecting pattern observed in the AFM images of MAP adsorbed to POMA results from this crosslinking reaction of MeFP-1 with MeFP-2.

Some degree of caution is necessary in interpreting the spectral features in the region from 1200 to 1300 cm^{-1} as arising purely from the amide III resonance frequencies. Both L-DOPA and tyrosine exhibit bands in this region. In fact, the band at approximately 1250 cm^{-1} has been previously attributed to the L-DOPA residues (18, 23). Therefore, the differences in this region for MAP on PS and POMA may indicate differences in the interaction between these residues and the polymer functional groups. These differences in protein–surface interactions between an aromatic surface (PS) and an aliphatic surface (POMA) are also indicated by the contrasting shape of the bands centered at 1150 and 1083 cm^{-1}.

The research presented here demonstrates that the functional groups that are present on the PS and POMA polymer surfaces will influence MAP–MAP and MAP–surface interactions. The XPS, AFM, and ATR-FTIR data demonstrates that differences in surface interactions can be correlated through these complementary analytical techniques.

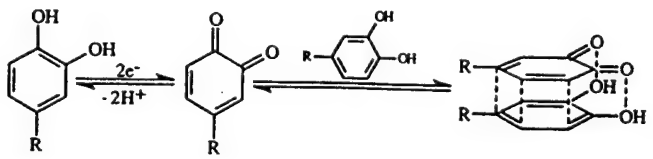

FIG. 5. Quinhydrone-charge transfer complex of the catechol functionality of MAP.

ACKNOWLEDGMENTS

The authors gratefully acknowledge Joe A. Gardella Jr. and Pat Schamberger at SUNY Buffalo and Deborah Leach-Scampavia at NESA/BIO at the University of Washington for help with the XPS measurements. Also, thanks are extended to Kevin Siedlecki at MSU and Barney Drake and Clint Calahan at Imaging Services Inc. in Santa Barbara, CA for their help in AFM imaging. This work was sponsored by the Office of Naval Research under Grant N0014-93-1-0168, and the NSF under cooperative agreement EEC 8907039 and a grant to Gill G. Geesey from 3M.

REFERENCES

1. McEldowney, S., and Fletcher, M., *Appl. Environ. Microbiol.* **52,** 460 (1986).
2. Baier, R. E., *in* "Adsorption of Microorganisms to Surfaces" (G. Bitton and K. C. Marshall, Eds.), p. 59. Wiley, New York, 1980.
3. Marshall, K. C., *ASM News* **58,** 202 (1992).
4. Waite, J. H., T. J. Housley, and M. L. Tanzer., *Biochemistry* **24,** 5010 (1985).
5. Taylor, S. W., Ross, M. M., Shabanowitz, J., Hunt, D. F., and Waite, J. H., *J. Am. Chem. Soc.* **116,** 10803 (1994).
6. Vogler, H., Z. *Naturfosch.* **386,** 1130 (1982).
7. Matsuda, H., Osaki, K., and Nitta, I., *Nippon Kogokukai Bull.* **31**(5), 611 (1958).
8. Waite, J. H., and C. V. Benedict, *Methods Enzymol.* **107,** 397 (1984).
9. Dobbs, D. A., Bergman, R. G., and Theopold, K. H., *Chem. Eng. News* **68**(17), 2 (1990).
10. Ratner, B. D., and Castner, D. G., *in* "Surface Analysis-Techniques and Applications" (J. C. Vickerman and N. M. Reed, Eds.), p. 163. Wiley, Chichester, UK, 1994.
11. Dousseau, F., Therien, M., and Pezolet, M., *Appl. Spectrosc.* **43,** 538 (1989).
12. Fink, D. J., Hutson, T. B., Chittur, K. K., and Gendreau, R. M., *Anal. Biochem.* **165,** 17 (1987).
13. Seah, M. P., Dench, W. A., Heydon and Son Ltd., *Surf. Interface Anal.* **2**(6) (1980).
14. Kaiden, K., Matsui, T., and Tanaka, S., *Appl. Spectrosc.* **41,** 180 (1987).
15. Jakobsen, R. J., and Wasacz, F. M., *in* "Proteins at Interfaces: Physiochemical and Biochemical Studies" (J. L. Brash and T. A. Horbett, Eds.), p. 339. Am. Chem. Soc., Washington, DC, 1987.
16. Pitt, W. G., Spiegelberg, S. H., and Cooper, S. L., *in* "Proteins at Interfaces: Physiochemical and Biochemical Studies" (J. L. Brash and T. A. Horbett, Eds.) p. 324. Am. Chem. Soc., Washington, DC, 1987.
17. Waite, J. H., *Int. J. Adhes. Adhes.* **7,** 9 (1987).
18. Olivieri, M. P., Loomis, R. E., and Baier, R. E., *Biomaterials* **13,** 1000 (1992).
19. Hansen, D. C., Luther III, G. W., and Waite, J. H., *J. Colloid Interface Sci.* **168,** 206 (1994).
20. Waite, J. H., *Int. J. Biol. Macromol.* **12,** 139 (1989).
21. Rzepecki, L. M., Hansen, K. M., and Waite, J. H., *Biol. Bull.* **183,** 123 (1992).
22. Parker, F. S. (Ed.), *in* "Applications of Infrared, Raman, Resonance Raman in Biochemistry. Chapter 8, Carbohydrates" p. 315. Plenum, New York, 1983.
23. Olivieri, M. P., Loomis, R. E., Meyer, A. E., and Baier, R. E., *J. Adhes. Sci. Technol.* **4,** 197 (1990).

Adsorption of Adhesive Proteins from the Marine Mussel, *Mytilus edulis*, on Polymer Films in the Hydrated State Using Angle Dependent X-ray Photoelectron Spectroscopy and Atomic Force Microscopy

Ace M. Baty,[†,‡] Pam K. Leavitt,[⊥] Christopher A. Siedlecki,[∥] Bonnie J. Tyler,[†,‡] Peter A. Suci,[†] Roger E. Marchant,[∥] and Gill G. Geesey*[,†,§]

Center for Biofilm Engineering, 366 EPS Building, P.O. Box 173980, Montana State University, Bozeman, Montana 59717, Department of Chemical Engineering, 306 Cobleigh Hall, Montana State University, Bozeman, Montana 59717, Department of Microbiology, 109 Lewis Hall, Montana State University, Bozeman, Montana 59717, Department of Biomedical Engineering, Case Western Reserve University, Cleveland, Ohio 44106, and Physical Electronics Inc., Eden Prairie, Minnesota 55344

Received November 5, 1996. In Final Form: July 23, 1997[⊗]

The adsorption of mussel adhesive protein (MAP) from the marine mussel *Mytilus edulis* has been investigated on polystyrene (PS) and poly(octadecyl methacrylate) (POMA) surfaces using angle dependent X-ray photoelectron spectroscopy (XPS) and atomic force microscopy (AFM). AFM images previously published in the dehydrated state using contact mode are compared with images acquired in the hydrated state using fluid Tapping Mode to assess the contribution that hydration has on the architecture of the adsorbed proteins. To further characterize the adsorbed protein layer, XPS analysis was performed at liquid nitrogen (LN_2) temperature without dehydrating the samples and at room temperature after the surfaces were dehydrated. The differences observed upon dehydration can be attributed to the strength of the interactions between MAP and the two surfaces. The AFM and XPS data indicate that adsorbed MAP is stabilized on the surface of the PS through interactions that prevent the protein layer from being disrupted upon dehydration. The adsorbed MAP on the POMA surface is representative of a loosely bound protein layer that becomes highly perturbed upon dehydration.

Introduction

The marine mussel, *Mytilus edulis*, produces a series of adhesive proteins that allow the organism to attach to a variety of surfaces in an underwater environment.[1] These proteins serve to support and bind components of the adhesive holdfast composed of byssal threads.[2,3] The ability of *M. edulis* to form a tenacious adhesive bond rapidly at a solid−liquid interface entails more than just depositing these proteins on the surface. Before adhering to a surface, the mussel foot first explores and then scrubs the prospective surface by cavitation. Phenolic proteins and collagen are then injected into the already cavitated mussel foot by phenol and collagen glands, forming the plaque that is attached to the surface.[4]

Despite the complexities involved, attempts to fabricate a biomimetic version of the mussel adhesive proteins (MAP) adhesive are underway. MAP has seen recent interest in the biomedical community as a tissue adhesive. MAP has been studied for its ability to fix chondrocyte allografts internally.[5,6] The protein has also been used in experimental epikeroplasty in laboratory animals, and as an adhesive agent to increase cellular attachment to substrata.[7,8] Recent studies have also indicated that MAP enhances the attachment of osteoblasts and epiphyseal cartilage cells to substrata.[9] However, commercial uses for MAP have been limited due to the lack of understanding of how these proteins function as an adhesive. The practical application of MAP as a biocompatible adhesive has not yet been realized, as the actual anchoring mechanism is poorly understood. Despite MAPs tenacious adhesive action in the natural environment, this function has not been duplicated with the purified proteins.

The byssal threads of *M. edulis* are comprised of a collagenous matrix that is bound with a series of phenolic proteins. There have been four proteins identified in the byssal threads that are thought to serve these structural and adhesive functions: *M. edulis* foot proteins (MeFP), 1, 2, 3, and 4, collectively termed mussel adhesive proteins (MAP). It has been suggested that MeFP-1 serves as one of the initial adhesive components as well as a protective varnish on the surface of the byssal thread.[10,11] MeFP-1 is a 130 kDa protein consisting of highly conserved tandemly repeated decapeptide sequences.[12] MeFP-1 has extensive hydroxylation of tyrosine to 3,4-dihydroxyphenyl-L-alanine (L-DOPA) and of proline to hydroxyproline.[12,13] This protein is one of the first proteins described to contain

* Author to whom correspondence should be sent Center For Biofilm Engineering, 366 EPS Building, P.O. Box 173980, MSU, Bozeman, MT 59717.
† Center for Biofilm Engineering, MSU.
‡ Department of Chemical Engineering, MSU.
§ Department of Microbiology, MSU.
∥ Department of Biomedical Engineering, Case Western Reserve University.
⊥ Physical Electronics Inc.
⊗ Abstract published in *Advance ACS Abstracts*, October 1, 1997.

(1) Waite, J. H. *Int. J. Biol. Macromol.* **1990**, *12*, 139−144.
(2) Young, G. A.; Crisp, D. J. In *Adhesion 6*; Allen, K. W., Ed.; Applied Science Publishers: Oxford, U.K., 1982; p 19.
(3) Waite, J. H. *J. Biol. Chem.* **1983**, *258*, 2911−2915.
(4) Waite, J. H. *Int. J. Adhes. Adhes.* **1987**, *7*, 9−14.
(5) Pitman, M. I.; Menche, D.; Song, E. K.; Ben-Yishay, A.; Gilbert, D.; Grande, D. A. *Bull. Hosp. J. Dis. Orthopedic Institute* **1989**, *49* (2), 213−220.
(6) Grande, D. A.; Pitman, M. I. *Bulletin of the Hospital for Joint Diseases Orthop. Inst.* **1988**, *48* (2), 140−148.
(7) Robin, J. B.; Picciano, P.; Kusleika, R. S.; Salazar, J.; Benedict, C. *Arch. Ophthalmol.* **1988**, *106* (7), 973−977.
(8) Olivieri, M. P.; Rittle, K. H.; Tweden, K. S.; Loomis, R. E. *Biomaterials* **1992**, *13* (4), 201−208.
(9) Fulkerson, J. P.; Norton, L. A.; Gronowicz, G.; Picciano, P.; Massicotte, J. M.; Nissen, C. W. *J. Orthop; Res.* **1990**, *8* (6), 793−798.
(10) Waite, J. H. *Biol. Rev.* **1983**, *58*, 209.
(11) Benedict, C. V.; Waite, J. H. *J. Morphol.* **1986**, *189*, 171−181.
(12) Waite, J. H.; Housley, T. J.; Tanzer, M. L. *Biochemistry* **1985**, *24*, 5010−5014.

S0743-7463(96)01072-4 CCC: $14.00

DOPA in its primary sequence and is one of the few proteins found in nature that contains hydroxyprolines in noncollagenous sequences.[14] The β-turn structure, imparted by the hydroxyprolines, contributes a slight circular dichroism to the protein. MeFP-1 has no other secondary structure.[15]

It is believed that MeFP-2 serves a structural function, binding the collagen fibers within the byssal threads. MeFP-2 is a 42–47 kDa protein consisting of at least three repeating motifs.[16] In contrast to MeFP-1, MeFP-2 contains 6–7 mol % of the disulfide containing amino acid cystine, indicating considerable secondary structure. A similar foot protein, MgFP-2, from the closely related mussel *Mytilus galloprovincialis* has been shown to harbor internal repeats that display a high degree of homology with epidermal growth factors.[17] MeFP-3 is thought to play a role as an initial surface primer, and the function of MeFP-4 is still uncertain.

Although the biochemistry of the adhesive plaque has been extensively and elegantly characterized, relatively little work has been done to characterize the molecular interactions between components and surfaces.[18,19] A greater understanding of how MAP binds to surfaces is essential in developing MAP as a useful adhesive. To effectively understand the complex series of interactions that occurs with these proteins, it is necessary to characterize the role that each plays in the development of the adhesive bond. For this study, two components of MAP have been selected in an effort to define the protein–surface and protein–protein interactions that mediate the adhesive interactions. Once these interactions are defined, the other components of the natural adhesive can be investigated in light of these results.

The goal of this study was to investigate the adsorption of MeFP-1 and MeFP-2 (MAP_{1-2}) to polystyrene (PS) and poly(octadecyl methacrylate) (POMA) surfaces in the hydrated state using cold probe techniques in variable angle X-ray photoelectron spectroscopy (XPS) and atomic force microscopy (AFM) using fluid Tapping Mode. The adsorption of MAP_{1-2} is interpreted in light of the known surface chemistry of PS and POMA and the known biochemistry of MAP_{1-2}. Surfaces were also dehydrated at room temperature and analyzed using variable angle XPS to assess the contribution that hydration has on the adsorbed protein layer. XPS was used to quantify the elemental composition with depth of the adsorbed protein, and AFM was used to provide information about the architecture of the adsorbed protein film on the polymer surfaces.

Materials and Methods

Adsorbates, Solvents, and Substrates. MAP_{1-2} used in this study consists of two of the *M. edulis* foot proteins, (MeFP-1 and -2). Purified MAP_{1-2} from *M. edulis* was obtained from Swedish Bioscience Laboratory (Floda, Sweden) and stored desiccated at −40 °C. The amino acid composition according to the supplier is (per 1000 residues) as follows: 83 Asp, 74 Thr, 97 Ser, 64 Glu, 69 Pro, 132 Gly, 68 Ala, 50 Val, 25 Ile, 29 Leu, 30 Tyr, 12 Phe, 27 His, 115 Lys, 41 Arg, 41 Hyp, and 70 3,4-dihydroxy-L-phenylalanine (DOPA). Acetic acid–urea polyacrylamide gel electrophoresis (PAGE) indicated that the preparation consisted of approximately 80% of the two DOPA-containing proteins: MeFP-1 and MeFP-2 in equal quantities.[19] The rest of the mixture (20%) is comprised of lower molecular weight collagenic material. The protocol for the PAGE was performed using previously described methods, and the identification of MeFP-1 (130 kDa) and MeFP-2 (45 kDa) was made according to previously published results.[20]

Pure polystyrene (PS) (Aldrich Secondary Standard) and poly(octadecyl methacrylate) (POMA) (Aldrich) were dissolved in toluene for spin casting. PS was prepared as a 1.5% w/v solution in toluene. POMA was prepared as a 1.5% v/v solution in toluene. Bulk PS substrata were obtained from Plaskolite Inc. (Columbus, OH). All solvents, methanol, hexanes, and toluene (Aldrich), were obtained as HPLC grade.

Preparation of Polymer Surfaces. PS and POMA polymer films were spin cast onto 1 cm × 1 cm PS fragments for all XPS and AFM studies. PS substrata were cleaned prior to spin casting by a solvent rinse, for 5 min each, in methanol and hexanes.[21] Clean PS substrata were completely covered with 2.0 mL of polymer solution and then immediately were spin cast at 3500 rpm for 2 min. The polymer films were dried at room temperature for 24 h.

The underlying PS substrata contained trace constituents (<1% Zn, <2% Si, and <2% O) that distinguished it from the pure, spin cast PS and POMA obtained from Aldrich. These trace contaminants were used as indicators to determine purity and homogeneity of the spin cast polymer films. XPS and time-of-flight secondary ion mass spectrometry of the spin cast polymer films indicated that the films were continuous (i.e., no contaminants from the underlying polymer substratum were detected through the spin cast films). Given the limitations of variable angle XPS, an exact film thickness is difficult to determine. However, it is possible to calculate an estimated film thickness by calculating the inelastic mean free path and subsequently the escape depth of the photoelectrons. For both the PS and POMA surfaces the Zn, Si, and O impurities in the underlying PS substrata were used to gauge film thickness. The estimated film thickness of these spin cast films is approximately 10–20 nm.

Protein Adsorption Protocol. All protein films were deposited onto freshly prepared polymer surfaces that had undergone a 24 h drying period. A stock solution of 1 mg/mL of MAP_{1-2} was prepared in dilute HCl (pH 2.9) with deionized, double-distilled water, deaerated with N_2. The stock solution was maintained at pH 2.9 to prevent catechol oxidation to quinone that occurs above pH 8.5. The stock solution was stored at 5 °C. The polymer-coated substrata were placed in glass cells with entrance- and exit-tubing ports to allow for protein adsorption and subsequent rinse without exposure to the air. All glassware used was cleaned with "piranha" solution, consisting of a 70:30 mix of concentrated H_2SO_4 and 30% H_2O_2, respectively. [WARNING: Piranha solution reacts violently, even explosively with organic materials.][22]

For the XPS studies, a 50 μL aliquot of the stock solution was delivered into the glass cell containing the substratum, followed immediately by a 0.95 mL aliquot of a pH 9.2 solution (Millipore water adjusted with NaOH). The final concentration of protein was 50 μg/mL at pH 8.5. At this pH quinone formation from catechols is favored. After 1 h, the substratum was rinsed of any residual protein by flowing an aqueous solution at pH 8.5 (Millipore water adjusted with NaOH) through the reaction chamber at a rate of 100 mL/min for 1.5 min.

For the hydrated AFM studies, a much lower protein concentration was used to ensure submonolayer coverage on the substratum, so that the spatial distribution of the nucleation events could be resolved. For these experiments a 2 μL aliquot of the 1 mg/mL stock MAP_{1-2} solution was diluted in ≈1.0 mL of deionized double-distilled water at pH 2.9 to make a solution

(13) Waite, J. H.; Tanzer, M. L. *Biochem. Biophys. Res. Commun.* **1980**, *96* (4), 1554–1561.
(14) Taylor, S. W.; Ross, M. M.; Shabanowitz, J.; Hunt, D. F.; Waite, J. H. *J. Am. Chem. Soc.* **1994**, *116*, 10803–10804.
(15) Williams, T.; Marumo, K.; Waite, J. H.; Henkens, R. W. *Arch. Biochem. Biophys.* **1989**, *269*, 415.
(16) Rzepecki, L. M.; Hansen, K. M.; Waite, J. H. *Biol. Bull.* **1992**, *183*, 123–137.
(17) Inoue, K.; Takeuchi, Y.; Miki, D.; Odo, S. *J. Biol. Chem.* **1995**, *270* (12), 6698–6701.
(18) Baty, A. M.; Suci, P. A.; Tyler, B. J.; Geesey, G. G. *J. Coll. Int. Sci.* **1996**, *177*, 307–315.
(19) Suci, P. A.; Geesey, G. G. *J. Colloid Interface Sci.* **1995**, *172*, 347–457.
(20) Waite, J. H, and C. V Benedict *Methods in Enzymology* **1984**, 107, 397–413.
(21) Vargo, T. G.; Thompson, P. M.; Gerenser, L. G.; Valentini, R. F.; Aebischer, P.; Hook, D. J.; Gardella, J. A. *Langmuir* **1992**, *8*, 131.
(22) Dobbs, D. A.; Bergman, R. G.; Theopold, K. H. *Chem. Eng. News* **1990**, *68* (17), 2.

that was 2 μg/mL of MAP_{1-2}. A 25 μL aliquot of this solution was then delivered into the flow cell along with ≈1.0 mL of a dilute NaOH solution at pH 9.2, bringing the concentration of MAP_{1-2} to 25 ng/mL and the pH to 8.5. After 1 h, the substratum was rinsed of any residual protein by flowing an aqueous solution at pH 8.5 (Millipore water adjusted with NaOH) through the reaction chamber at a rate of 100 mL/min for 1.5 min.

Surface Characterization

Angle-Resolved X-ray Photoelectron Spectroscopy. Since protein adhesion to surfaces occurs in an aqueous environment, any reliable chemical analysis of the structure of the adsorbed proteins must be performed in the hydrated state. Therefore, cryostage sample-handling techniques must be employed during the analysis of a hydrated surface in ultrahigh vacuum in an effort to preserve the adsorbed species in their hydrated state. A hydrated surface can be frozen at liquid nitrogen (LN_2) temperatures and loaded onto a cold stage where the sample can be kept at LN_2 temperatures during analysis.[23,24] The structure of the adsorbed molecules at the surface are preserved at LN_2 temperature.

XPS spectra were obtained with a Physical Electronics instrument Model 5600 spectrometer (Physical Electronics, Eden Prairie, MN). A 5 eV flood gun was used to offset charge accumulation on the samples. An 800 μm diameter area was analyzed using a monochromatized Al Kα X-ray source at 350 W and a pass energy of 11.750 eV. For cold probe analysis, wet surfaces were removed from the glass cell after protein adsorption, rinsed, and mounted in the sample introduction chamber. The chamber was quickly purged with nitrogen, and the sample was immediately brought into contact with a liquid nitrogen cold finger before the sample could dehydrate. The sample remained in contact with the cold finger for 30 min, followed by immediate sample transfer to the cold stage in the analytical chamber. Most of the ice that formed on the surface when the sample was frozen quickly sublimed in the high-vacuum environment of the introduction chamber, leaving residual frozen water around the adsorbed protein molecules. The cold stage was maintained at −120 °C during analysis. Samples that were dehydrated at room temperature were removed from the final rinse and dried under an atmosphere of pure, dry N_2 in the sample introduction chamber of the XPS. Before the variable angle study was conducted, an initial 80° (near normal) high-resolution spectrum was collected. Depth profiles were performed using variable angle XPS data collected at take-off angles of 15°, 22°, 35°, and 80° from the surface. The elemental compositions at the initial 80° survey were compared with the final 80° angle study to ensure no X-ray damage of the surface had occurred during analysis. An abundance of carbon, nitrogen, and oxygen was calculated from high-resolution C_{1s}, N_{1s}, and O_{1s} peak areas by fitting the data with Gaussian functions. The binding energy scale was referenced by setting the CH_x peak maximum in the C_{1s} spectrum to 285.0 eV.[25]

The relative atomic concentrations at the different take-off angles were used with the calculated escape depths of the photoelectrons for each angle to gain insight on the elemental depth distribution of the proteins adsorbed to the polymer surfaces. The escape depths were calculated using parameters for organic compounds to calculate the inelastic mean free paths and subsequently the escape depths using equations previously defined.[26]

Atomic Force Microscopy Imaging. In order to image hydrated biological molecules on a surface using AFM, a mode of operation called fluid Tapping Mode was used. In fluid Tapping Mode the AFM cantilever is oscillated vertically at a set high frequency during $x-y$ raster scanning.[27] As the probe tip contacts the surface, its oscillations are dampened. Since the tip only intermittently "taps" the surface, this mode of operation is characterized by overall weak tip−sample interactions. This allows minimal disturbance of the adsorbed molecules during imaging.

All surfaces were imaged using a Bioscope AFM (Digital Instruments, Inc., Santa Barbara, CA). The instrument was used in fluid Tapping Mode using thin-legged, triangular, microfabricated silicon nitride cantilevers which were 100 μm in length, with nominal spring constants of 0.38 N/m and integrated pyramidal tips. The samples were attached to the fluid cell using a cyanoacrylate adhesive and dried in a laminar flow hood. The images were recorded as 1 μm × 1 μm and 2 μm × 2 μm scan areas with 512 × 512 data points/scan area. Images were recorded at scan rates of 0.8−6.1 μm/s. Scan rates were optimized to minimize hysteresis between the forward and return traces of the probe. All images were stable with time and reproducible. For analysis, images were low-pass filtered, flattened to remove sample tilt, and planefit to remove sample bow arising from hysteresis in the piezocrystal.

Results

Atomic Force Microscopy Imaging. MAP_{1-2} adsorbed to clean PS and POMA from solutions with bulk protein concentrations of 25 ng/mL were imaged in fluid Tapping Mode using AFM. Figures 1a and 1b show AFM 3-D surface images of 1 μm × 1 μm areas of the PS and POMA substrata before MAP_{1-2} adsorption. Before MAP_{1-2} adsorption, the PS and POMA surfaces are extremely smooth with few surface features and root-mean-square (rms) surface roughness values of 0.52 ± 0.13 nm and 1.06 ± 0.08 nm, respectively. Figure 2 shows AFM 3-D surface images of 1 μm × 1 μm areas of PS and POMA substrata after MAP_{1-2} adsorption. Adsorption of MAP_{1-2} to the PS surface resulted in the formation of closely packed, repeating structures as shown in Figure 2a. Cross-sectional analysis of these features revealed a near monolayer structure, making it difficult to differentiate between adjoining protein structures. The heights of these features are less than 1 nm. MAP_{1-2} adsorbed to the POMA surface displays very different protein features that appear to be linearly ordered as revealed in the 1 μm × 1 μm scan area in Figure 2b. An additional scan performed at a right angle to the first showed these features to rotate 90°, indicating that the linear features observed were not an artifact of the AFM probe tip rastering across the surface. Cross-sectional analysis reveals that these features have an average height of 5.0 ± 0.7 nm with lateral dimensions of 67 ± 17 nm (minor axis) and 177 ± 26 nm (major axis).

The 2 μm × 2 μm scan area of MAP adsorbed to PS, shown in Figure 3a, reveals that the features observed at high magnification cover larger areas of the surface, suggesting that the surfaces are homogeneous and have continuous protein coverage. The 2 μm × 2 μm scan area of MAP_{1-2} adsorbed to POMA, shown in Figure 3b, shows that the protein features on POMA are also very homo-

(23) Ratner, B. D.; Weathersby, P. K.; Hoffman, A. S.; Kelly, M. A.; Sharpen, L. H. *J. Appl. Poly. Sci.* **1978**, *22*, 643−664.
(24) Ratner, B. D.; Castner, D. G. *Colloids Surf., B* **1994**, *2*, 343−345.
(25) Ratner, B. D.; Castner, D. G. In *Surface Analysis-Techniques and Applications*; Vickerman, J. C., Reed, N. M., Eds.; John Wiley & Sons: Chichester, U.K. 1994; p 163.
(26) Seah, M. P.; Dench, W. A. *Surf. Interface Anal.* **1979**, *1*, 2−11.
(27) Drake, B.; Prater, C. B.; Weisenhorn, A. L.; Gould, S. A. C.; Albrecht, T. R.; Quate, C. F.; Cannell, D. S.; Hansma, H. G.; Hansma, P. K. *Science* **1989**, *243* (4898), 1586−1589.

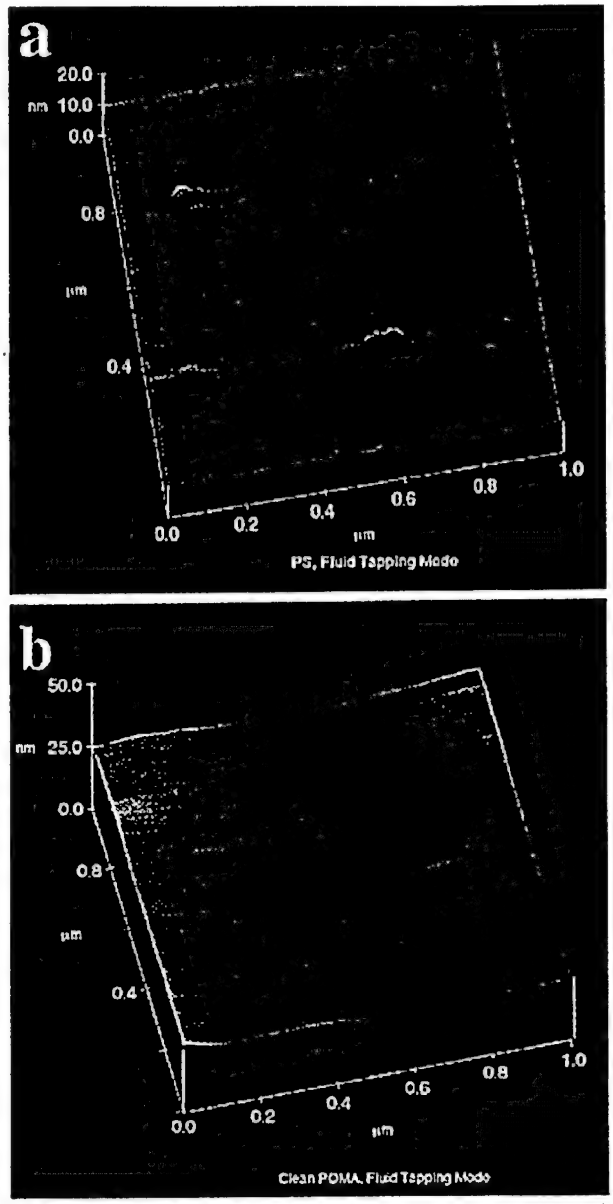

Figure 1. Fluid Tapping Mode AFM surface images of 1 μm × 1 μm area of PS (a) and POMA (b) before protein adsorption.

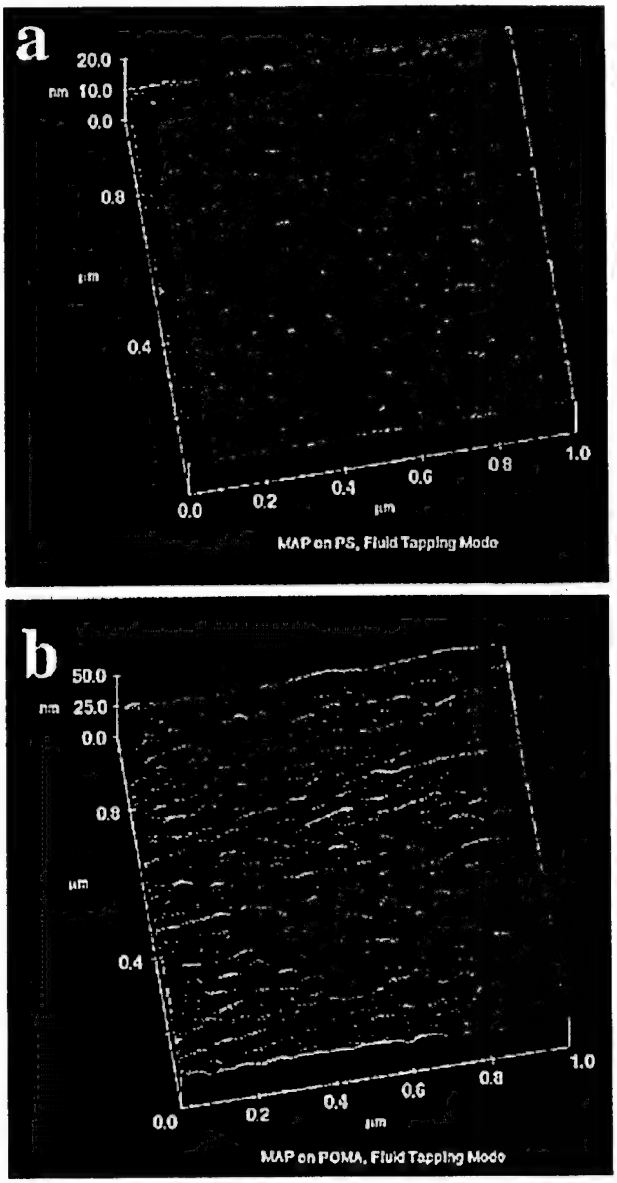

Figure 2. Fluid Tapping Mode AFM surface images of 1 μm × 1 μm area of MAP_{1-2} adsorbed to PS (a) and POMA (b).

geneous. However, there appears to be larger protein domains covering the surface, which might suggest extensive aggregation of the adsorbed protein. These features extend 6.2 ± 1.7 nm in height with lateral dimensions of 173 ± 35 nm (minor axis), with major axis values extending up to 760 nm.

Angle-Resolved X-ray Photoelectron Spectroscopy. Angle dependent XPS, performed at room temperature and LN_2 temperature, of the surfaces studied in Figures 1, 2, and 3 reveals further differences in MAP_{1-2} adsorption to PS and POMA surfaces. A detailed examination of the C_{1s} region of clean PS and POMA at a 30° take-off angle and at LN_2 temperature is shown in Figure 4. MAP_{1-2} adsorbed to PS at take-off angles of 80° and 22° at LN_2 temperature and at 22° at room temperature are given in Figure 5. MAP_{1-2} adsorbed to POMA at a takeoff angle of 80° and 22° at LN_2 temperature and at 22° at room temperature are given in Figure 6. Each peak component under these C_{1s} regions represents different carbon bonds. The C_{1s} component at a binding energy of 291.0–291.6 eV is attributed to the $\pi-\pi^*$ transition in the aromatic rings of the polystyrene. There is no detectable $\pi-\pi^*$ C_{1s} component of MAP_{1-2}. Even though these proteins have considerable aromatic character, their pi-electron systems are not dense enough to form an observable peak. The C_{1s} component at 288.0–288.8 eV arises from the N–C=O and O–C=O functionalities on the protein and the methacrylate chain, respectively. The C_{1s} component at a binding energy of 286.2–287.0 eV is attributed to the C–N and C–O functionalities in the protein and the C–O–C functionality of the POMA. The dominant C_{1s} component in both sets of spectra is at 285.0 eV. This peak originates from the aliphatic carbon in both the polymers and the protein.

The C_{1s} region of MAP_{1-2} adsorbed to PS, at LN_2 temperature at a take-off angle of 80° (Figure 5a), reveals a decrease in the aliphatic component at 285.0 eV and an increase in the 286.2 and 288.2 eV C_{1s} components when compared to clean PS (Figure 4a). This indicates MAP_{1-2} contribution to the C_{1s} region. At a take-off angle of 22° at LN_2 temperature (Figure 5b), there is a shift in the C_{1s} component at 286.2 eV toward 286.8 when compared to the spectrum collected at 80°. This peak shift suggests

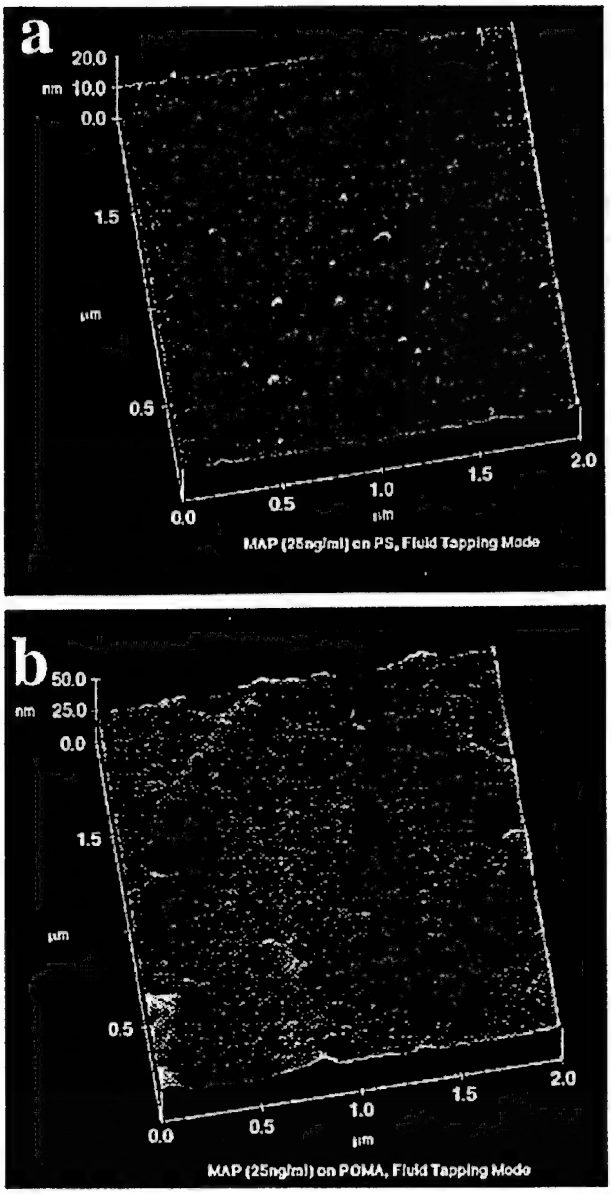

Figure 3. Fluid Tapping Mode AFM surface images of 2 μm × 2 μm area of MAP_{1-2} adsorbed to PS (a) and POMA (b).

an increase in the signal from the C−O functionalities, as opposed to the C−N functionalities, that are present on the protein. There is more sample charging at the lower take-off angles on the surfaces analyzed at LN_2 temperature. This can be seen in the broader peak components in both sets of spectra obtained at LN_2. However, charging does not account for the peak shift observed between 286.2 and 286.8 eV since not all of the peak components are shifted. There is also an increase in the intensity of the 286.8 and 288.2 eV C_{1s} components, as compared to the spectrum at 80°, indicating that at the angle approaching glancing, the signal from the PS is decreasing while that of the adsorbed protein is increasing. The C_{1s} region of MAP_{1-2} adsorbed to PS and dehydrated at room temperature (Figure 5c) shows an increase in the 291.6 eV C_{1s} component that is attributed to the $\pi-\pi^*$ transition of the aromatic rings of the PS. There is also a decrease in the peak area of the 286.8 and 288.1 eV components from the adsorbed protein, as compared to the surfaces analyzed at LN_2 temperature. This indicates that PS is contributing to the spectra more when the surface is analyzed after dehydration at room temperature than when the surface

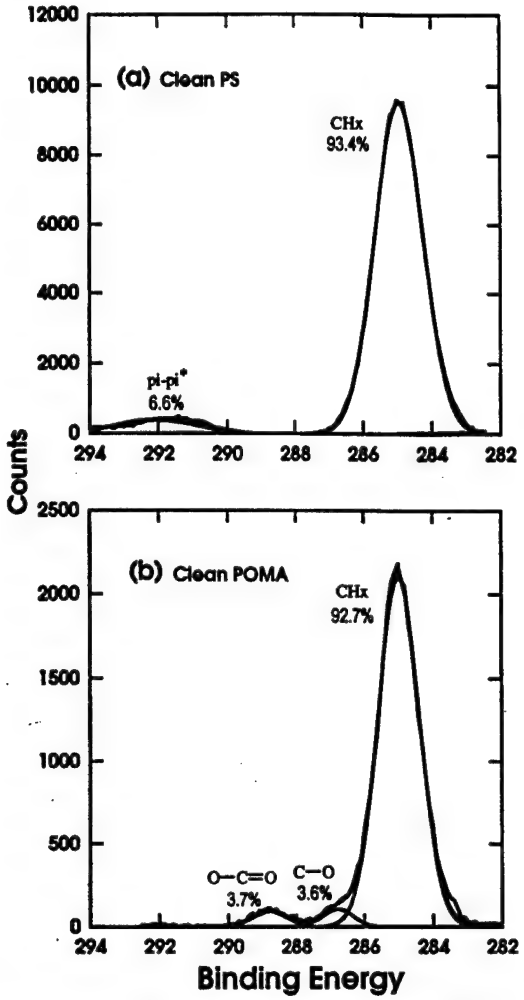

Figure 4. C_{1s} XPS spectra of clean PS (a) and POMA (b) at take-off angles of 30° at LN_2 temperature.

is analyzed at LN_2 temperature. Furthermore, a peak at 289.0 eV (acid or ester functionality) appears in the spectra upon dehydration. This functionality is not part of the MAP_{1-2} or the underlying PS substrata. It is unclear whether this species is present in the MAP_{1-2} mixture and migrated to the surfaces upon dehydration or adsorbed to the surface during dehydration.

The C_{1s} region of MAP_{1-2} adsorbed to POMA, at LN_2 temperature at a take-off angle of 80° (Figure 6a), reveals a shift in the C_{1s} component at 286.7 and 288.8 eV (clean POMA) toward 286.1 and 288.3 eV, respectively. This is a result of an increase in the signal from the C−N functionalities that are present from the adsorbed protein. There is also a decrease in the aliphatic component at 285.0 eV and an increase in the 286.1 and 288.3 eV C_{1s} components when compared to those of clean POMA (Figure 4b). This also indicates MAP_{1-2} contribution to the C_{1s} region. At a take-off angle of 22° at LN_2 temperature (Figure 6b), there is a shift in the 286.1 and 288.3 eV components back to 286.7 and 288.8 eV, respectively. This could be a result of an increase in the signal from the C−O functionalities that are present from the adsorbed protein. However, there is no significant increase in the area of the peaks which are attributed to the protein. The fact that the AFM images show homogeneous coverage and there is no significant difference in these peak areas at the two different take-off angles suggest that the adsorbed protein layer on the POMA is much less densely packed than on the PS surface, where

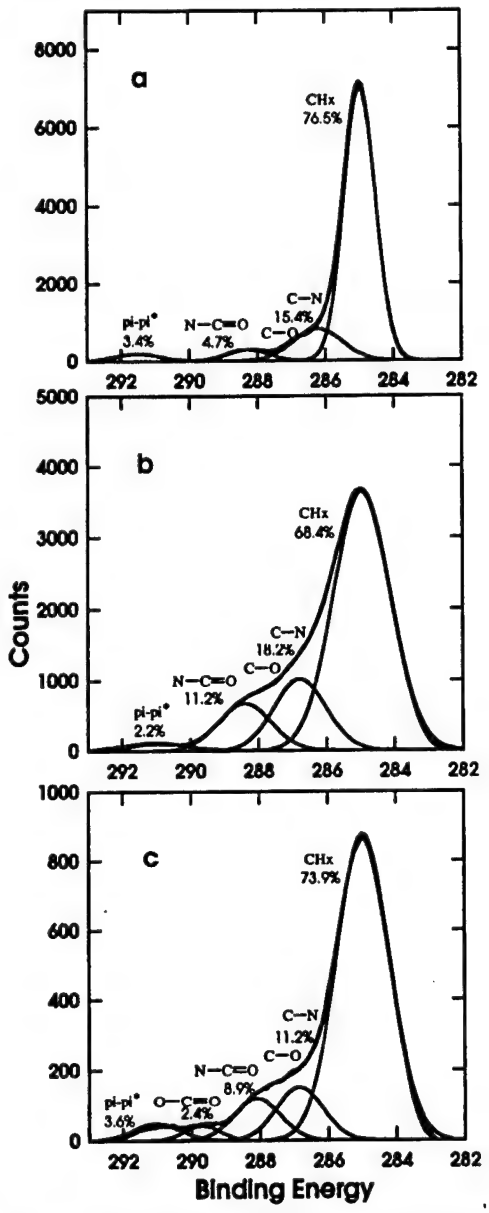

Figure 5. C_{1s} XPS spectra of MAP_{1-2} adsorbed to PS at 80° (a) and 22° (b) takeoff angles at LN_2 temperature and at 22° take-off angles (c) at room temperature.

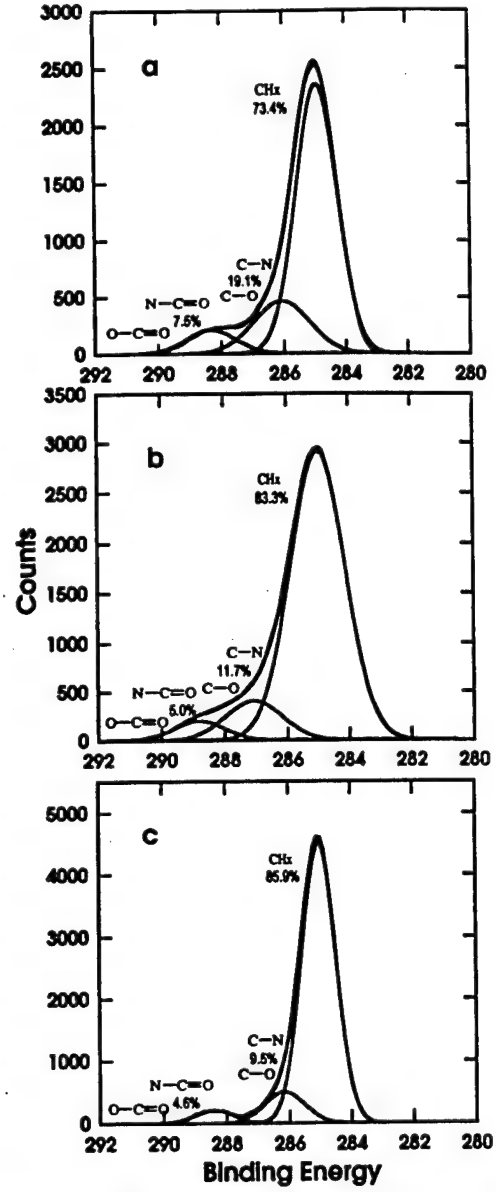

Figure 6. C_{1s} XPS spectra of MAP_{1-2} adsorbed to POMA at 80° (a) and 22° (b) take-off angles at LN_2 temperature and at 22° take-off angles (c) at room temperature.

the signal intensity at the 22° take-off angle (LN_2) appears to be contributed primarily by MAP_{1-2}. However, these data are difficult to interpret due to the insufficient knowledge, to date, concerning the analyses of biological surfaces at LN_2 temperature using XPS. The C_{1s} region of MAP adsorbed to POMA and dehydrated at room temperature (Figure 6c) shows a decrease in the 286.5 and 288.5 eV components and is approaching a pure POMA spectrum. This indicates that more of the POMA is contributing to the spectra when the surface is dehydrated at room temperature than when it is at LN_2 temperature during analysis. It was also observed that at LN_2 temperature the high-resolution C_{1s} peak components were broader than the same spectra taken at room temperature. This might be attributed to less efficient charge compensation at LN_2 temperatures at the lower take-off angles. How this would affect signal intensity is currently unknown.

Figure 7 shows a plot of the atomic concentration of MAP_{1-2} adsorbed to PS (Figure 7a) and POMA (Figure 7b) at take-off angles of 80°, 35°, 22°, and 15°, corresponding to sampling depths of 84.3, 49.1, 32.1, and 22.2 Å, respectively. The atomic concentrations when analyses were performed at LN_2 temperature and when the samples were dehydrated at room temperature are shown. At all depths, on both PS and POMA exposed to MAP_{1-2}, the atomic concentration of nitrogen and oxygen was lower when the samples were dehydrated and analyzed at room temperature as compared to the surfaces analyzed at LN_2 temperature. This suggests that more of the substratum is contributing to the spectra upon dehydration of the adsorbed MAP_{1-2}, which decreases the relative signal intensity of the adsorbed MAP_{1-2}. When MAP_{1-2} adsorbed to PS was analyzed at LN_2 temperature and room temperature, the surface dehydrated at room temperature experienced an average 2.6% loss in nitrogen and a 1.9% loss in oxygen. Furthermore, the atomic concentrations for MAP_{1-2} adsorbed to PS, when analyzed at LN_2 and room temperature after dehydration converge at the 80° take-off angle. This indicates that the same amount of protein is being sampled on the surface at the 80° take-off

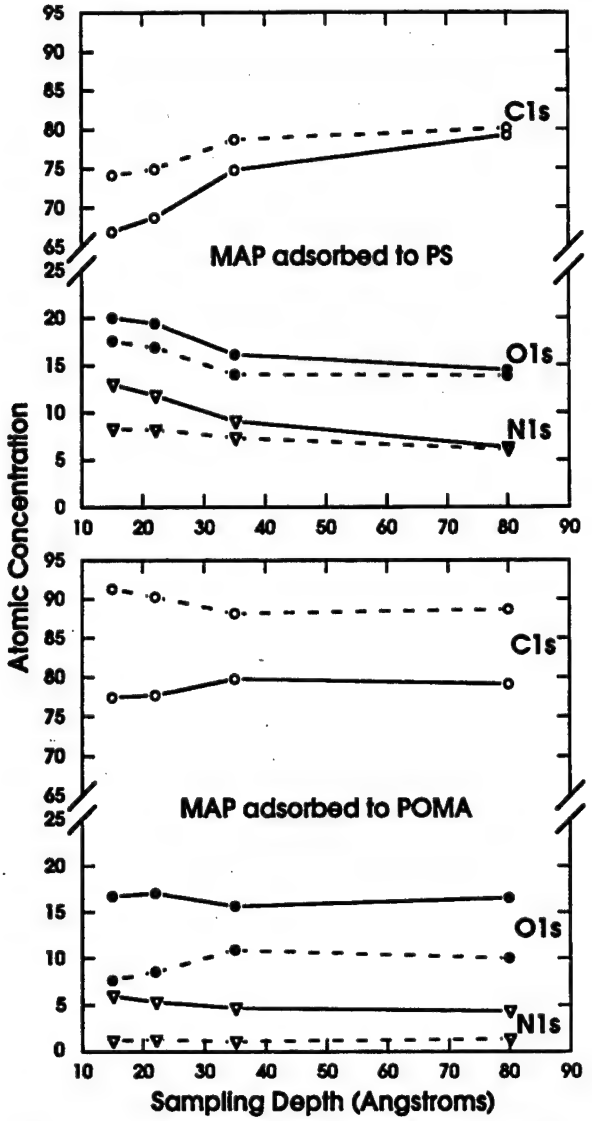

Figure 7. Summary of angle-resolved XPS data of MAP_{1-2} adsorbed to PS (top) and POMA (bottom) at LN_2 temperature (solid line) and room temperature (broken line).

angle regardless of whether water is present. In contrast, when MAP_{1-2} adsorbed to POMA was analyzed at LN_2 temperature and at room temperature after dehydration, the surface experienced a loss of nitrogen and oxygen upon dehydration of 3.9% and 7.2%, respectively. Furthermore, the atomic concentrations for the LN_2 and room temperature studies do not converge at the 80° take-off angle for MAP_{1-2} adsorbed to POMA. This suggests that upon the removal of water the protein architecture is more perturbed on the POMA surface than on the PS surface.

Discussion

The study of the adsorption behavior of proteins has primarily been focused on globular proteins. Theories concerning the adsorption process of globular proteins have stressed the importance of structural rearrangements, electrostatic interactions, and the displacement of interfacial water as the processes of primary importance.[28-30] However, specific functional group chemistry is not generally discussed as a contributing factor in adsorption. The results presented here indicate that the adsorption behavior of MAP_{1-2} is influenced by both functional group chemistry and the displacement of ordered water from the interface. The relative contribution of these two factors depends upon the surface chemical properties of the substratum. The data indicate that protein–surface as well as protein–protein interactions, with specific functional groups on MAP_{1-2}, play significant roles in driving adsorption to polymer surfaces that display different chemical properties. This is consistent with MAP_{1-2}'s role as a component of a multifunctional adhesive used by *M. edulis*.

The MAP_{1-2}-surface interactions that are available in the polymer–protein system studied here are constrained by the surface chemical properties of PS and POMA as well as the aqueous environment. PS provides a hydrophobic surface with an aromatic character and a medium surface free energy (88° water contact angle). Possible interactions that could occur on this surface would be a $\pi-\pi$ overlap between the DOPA residues in MAP_{1-2} and the aromatic rings of PS and cation–π interactions between the protonated amines of the lysines and the π-face of the styrene rings. In contrast, the POMA surface provides a hydrophobic low-energy surface (104° water contact angle) with an aliphatic functionality. Interactions with specific functional groups are not likely to occur between MAP_{1-2} and a POMA surface because there are no functional groups on POMA that would mediate such interactions. Interactions involving the ester functionalities of POMA are sterically hindered by the C_{18} hydrocarbon chains and are unavailable for interactions with MAP_{1-2}, as indicated by the high water contact angle.

We have previously presented AFM images of MAP_{1-2} adsorbed to PS and POMA after dehydration at room temperature.[18] Comparison with the present images obtained under hydrated conditions reveals that the architecture of the adsorbed protein on both PS and POMA surfaces is perturbed as a result of dehydration. The instability of MAP_{1-2} adsorbed to the POMA surface, following dehydration, is reflected by the increased relief of the protein film and the lateral displacement and aggregation of the proteins on the surface, as seen in the AFM images (previously published). In contrast to the POMA surface, the stability of MAP_{1-2} adsorbed to the PS surface is not as dependent on the presence of water. Although MAP_{1-2} adsorbed to PS gains relief as a result of dehydration, it does not undergo lateral displacement or aggregation. These results suggest that the presence of water is not as important in stabilizing the interactions between MAP_{1-2} and PS as between MAP_{1-2} and POMA.

XPS data also revealed that hydration played a significant role in MAP_{1-2}–surface interactions on both PS and POMA. The increase in relief of the protein film on both surfaces is due to the collapse of the protein matrix upon removal of water by dehydration. This results in greater signal intensity from the underlying substratum for both PS and POMA. This is reflected in the reduced atomic concentration of the protein, as indicated by nitrogen and oxygen, when surfaces were dehydrated and analyzed at room temperature as compared to analysis at LN_2 temperature. The XPS evidence that dehydration resulted in a greater decrease in atomic concentration of MAP_{1-2} on POMA than on PS supports the AFM observation that POMA permitted more lateral surface displacement of MAP than PS. The reorientation of MAP_{1-2} on POMA as a result of dehydration was sufficient to cause shifts in atomic concentrations of MAP_{1-2} at all XPS take-off angles used in these studies. Dehydration-induced

(28) Haynes, C. A., Sliwinsky, E., Norde, W. *J Colloid Interface Sci.* **1994**, *164*, 394–409.
(29) Ball, R. A.; Jones, R. A. L. *Langmuir* **1995**, *11*, 3542–3548.
(30) Haynes, C. A.; Norde, W. *J. Colloid Interface Sci.* **1995**, *169*, 313–328.

shifts in atomic concentration were only observed at the shallower sampling depths on PS. The lateral displacement and reorientation on the POMA surface upon dehydration reflect the instability of the MAP_{1-2}–POMA interaction in the absence of water and reveal, again, the importance of specific functional group interactions in stabilizing protein adsorption to the PS surface.

It is hypothesized here that the aromatic residues of MAP_{1-2} are not involved in adsorption on the POMA surface, and therefore, are free to interact with other functional groups within MAP_{1-2}. There are several interactions that have been proposed to play important roles in protein–protein interactions on the basis of the chemistry of MAP_{1-2}, including hydrogen bonding, metal–ligand complexes, the formation of Michael-type addition compounds derived from *o*-quinones, and charge transfer complexes.[1] Recently, cation–π interactions have also been shown to occur with high-binding enthalpies in systems containing cations and aromatic rings.[31] In the system studied here three of these interactions could be responsible for the protein–protein interactions in MAP_{1-2}: hydrogen bonding, charge transfer interactions between the aromatic residues of MAP_{1-2}, and cation–π interactions. Charge transfer interactions are promoted at an elevated pH, above 8.5 (the pH during adsorption). At this pH the catechol functionality on the DOPA can undergo a spontaneous reverse dismutation to the *o*-quinone that is capable of interacting through a quinhydrone charge transfer complex that is stabilized by π–π overlap interactions. Cation–π interactions can be considered an electrostatic interaction between the protonated amines of the lysines and the π-face of the aromatic amino acids in the protein. Michael-type additions between the protonated amines of the lysines and the quinones have not been shown to occur spontaneously with these proteins. However, there is a catechol oxidase found in the natural adhesive holdfast that catalyzes the oxidation of catachols to quinones which is believed to promote this cross-linking reaction. The possibility of this type of cross-linking occurring in the system described here is unlikely since the enzyme is not present. Thus, the charge transfer complex that is stabilized by π–π overlap interactions and cation–π interactions are the most likely candidates for causing the aggregation of MAP_{1-2} on the POMA surface. Evidence for this behavior was demonstrated by AFM and is shown schematically in Figure 8.

In the case of MAP_{1-2} adsorption to POMA, water likely provides the driving force for adsorption through the displacement of interfacial water. For human blood plasma albumin and bovine pancreas ribonuclease adsorption to PS, it has been shown that in the absence of dominant enthalpic interactions between specific groups of the surface and the protein, the proteins affect the overall adsorption by dehydrating or displacing water from the surface.[32] On a surface like the POMA surface this type of interaction would be the dominant protein–surface interaction. Such adsorption increases the entropy of the system providing the driving force for adsorption. This type of protein–surface interaction results in a tenaciously bound protein layer with no specific functional group interactions between the surface and the adsorbed MAP_{1-2}, as long as the driving force provided by the surrounding aqueous environment is present. Thus, aggregation of the adsorbed protein is favored by the lack of potential interactions between the protein and the substratum.

When MAP_{1-2} is adsorbed on PS, aggregation is not observed, rather individual, tightly packed structures resembling individual protein molecules project from the surface. Since the PS surface has considerable aromatic character, the adsorbed MAP_{1-2} may interact with the aromatic rings of PS through π–π overlap interactions and cation–π interactions further strengthening the interaction with the substratum and reducing the likelihood of protein–protein interactions, as shown in Figure 8. The adsorption of a series of aromatic compounds has been previously studied, and it was found that the orientation of the adsorbed aromatic domains followed several rules.[33] In the absence of chemisorbable functional groups that interfere with the aromatic framework, and in the absence of bulky electronegative constituents on the aromatic framework, the *o*-quinones were found to adsorb parallel to the surface when π–π overlap interactions were involved in adsorption. Likewise, the DOPA residues in MAP_{1-2} may orient themselves parallel to the aromatic rings of PS to facilitate π–π overlap interactions. The protonated amines of the lysines may also interact with the π-face of the styrene rings through cation–π interactions, and they may interact with the aromatic amino acids of MAP_{1-2} to facilitate protein–protein interactions. In the case of MAP_{1-2} adsorption to PS, water may provide the initial driving force for adsorption through the displacement of interfacial water, but binding is then reinforced through these specific functional group interactions between the proteins and the surface. It should also be noted that at the lower take-off angles at LN_2 temperature, charge buildup on these insulating surfaces may not have been sufficiently compensated. The extent to which uncompensated charge buildup on the surface and/or the presence of frozen water affects signal intensity is uncertain and remains to be determined. Furthermore, it is currently uncertain what the concentrations of Mefp-1 and Mefp-2 are on the surface. A study that has yet to be undertaken is a set of solution depletion experiments to measure the amount of protein adsorbed to the surface by measuring the residual left in the bulk. This may provide further insight into the differences between adsorption of MAP_{1-2} on these polymer surfaces.

Conclusions

The LN_2 temperature XPS analysis and hydrated AFM images demonstrate that differences in substratum chemistry will influence protein adsorption. The data support the hypothesis that interactions requiring the presence of water are more important in stabilizing MAP_{1-2} films on POMA than on PS. Interactions between specific functional groups on MAP_{1-2} and PS, possibly involving π–π overlap between DOPA residues of MAP_{1-2} and the aromatic rings of PS and cation–π interactions between the protonated amines of lysine and the π-face of the styrene rings stabilize MAP_{1-2} films on this substratum during dehydration. These results offer insight into the types of molecular interactions that control surface adsorption of biological molecules in aqueous environments. This research also shows that when MAP_{1-2} is subjected to dehydration on a surface, changes in the structure of the adsorbed protein film can be detected by XPS and AFM, demonstrating the role of water in stabilizing interactions that mediate MAP_{1-2} adsorption to PS and POMA surfaces. However, the magnitude of the change depends on what types of interactions mediate protein adsorption to the surface. From the present study it appears that irreversible protein adsorption involving

(31) Dougherty, D. A. *Science* **1996**, *271*, 163–167.
(32) Norde, W., Lyklema, J. *J. Colloid Interface Sci.* **1979**, *71*, 350–366.
(33) Soriaga, M. P., Hubbard, A. T. *J. Am. Chem. Soc.* **1982**, *104*, 2735–2742.

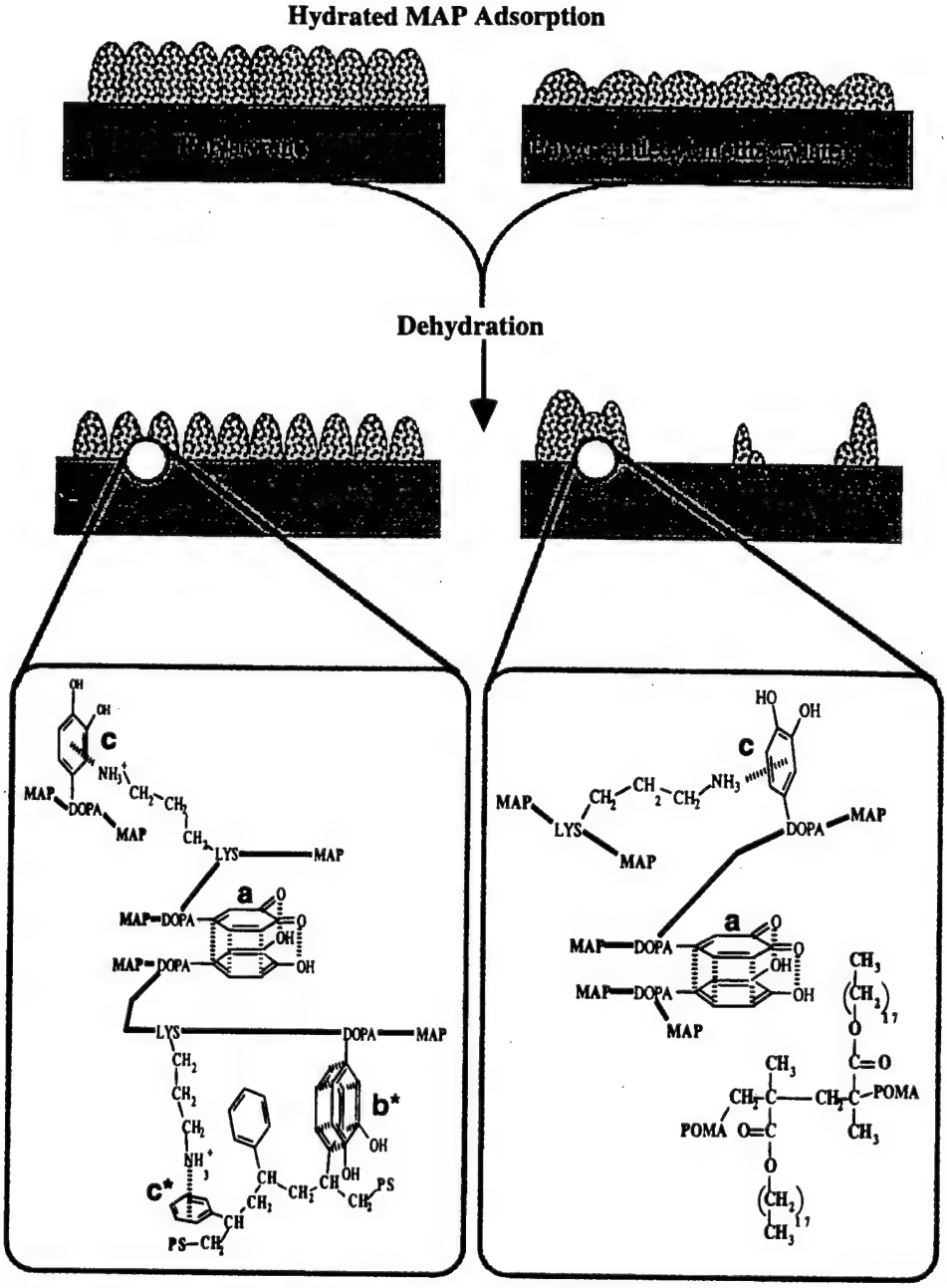

Figure 8. Schematic representation of the AFM images observed as related to the mechanisms available for adsorption: a = quinhydrone charge transfer complex, b = $\pi-\pi$ overlap interactions, c = cation$-\pi$ interactions, * = protein−surface interactions (hydorgen-bonding interactions not shown).

specific functional group interactions will experience much less disruption upon dehydration than interactions that only require the presence of water as the driving force for adsorption.

Acknowledgment. The authors gratefully acknowledge the Interfacial Chemical Analysis Lab at Montana State University for their guidance and expertise in surface analysis and the Murdock Charitable Trust for a grant to obtain the instrumentation used for this research. Also, thanks are extended to Dr. Herbert Waite at the University of Delaware for his insight into the mussel adhesive proteins. Thanks are also extended to Dr. Larry Davis at Physical Electronics Inc. in Minneapolis, MN for his generous gift of many hours of instrument time. The authors also acknowledge the Center for Cardiovascular Biomaterials at Case Western Reserve University for the use of their AFM facilities. This research was supported by the Office of Naval Research under Grant N0014-93-1-0168 and N0014-95-11086, a grant to Dr. Gill G. Geesey from 3M and the NSF under cooperative agreement EEC 8907039.

LA9610720

Weiner, R., S. Langille, G. Geesey and E. Quintero. 1997. Function of bacterial (Hyphomonas spp.) capsular exopolysaccharide in biofouling, pp. 373-386, In Saxena (ed), Recent Advances in Marine Science and Technology, PACON International, Honolulu, HA.

RECENT ADVANCES IN MARINE SCIENCE AND TECHNOLOGY, 96

Edited by

Narendra Saxena
Professor of Civil Engineering
University of Hawaii
Honolulu, Hawaii, U.S.A.

PACON INTERNATIONAL
1997

June 1997

Published by
PACON International
P.O. Box 11568
Honolulu, Hawaii 96828
U.S.A.

ISBN 0-9634343-2-2 (this volume)
ISBN 0-9634343 (series)

Printed in the United States of America

FUNCTION OF BACTERIAL (*HYPHOMONAS SPP.*) CAPSULAR EXOPOLYMERS IN BIOFOULING

Ronald Weiner[1], Stephen Langille[1], Gill Geesey[2] and Ernesto Quintero[3]

[1]Department of Microbiology, University of Maryland
College Park, MD. USA

[2]Department of Microbiology, Montana State University
Bozeman, MT, USA

[3]Oceanix Corporation
Hanover, MD, USA

ABSTRACT

The build-up of biotic communities on surfaces exposed to fresh and marine water can have deleterious effects and is termed biofouling. It results in billions of dollars annual damage and/or degraded performance to pipes, ships and other structures. Bacteria are believed to initiate biofouling and maintain a crucial role in macrobiotic colonization. It is because the pelagic region (mid ocean) is so limited in nutrients that bacteria have developed "ingenious" survival strategies to colonize immersed surfaces which provide enhanced nutrition. They adhere under very adverse conditions. Biofouling bacteria are among the oldest forms of life on this planet. A key to controlling fouling and on obtaining marine coatings and cements is to understand how these bacteria adhere.

It is widely held that bacteria behave like charged colloidal particles when approaching a surface and must pass through a repulsive boundary. They synthesize a variety of adhesive tethers for this purpose (adhesins). This report reviews the complicated and costly biofouling processes and focuses on the complex polysaccharide capsules that function as adhesins of a group of pioneer fouling bacteria (*Hyphomonas spp.*).

INTRODUCTION

Microbial Adhesion and Biofouling

Biofouling and succession of colonizing organisms

Clean surfaces quickly become coated with biotic communities when immersed in seawater. There is an ordered sequence for such colonization. Initially, the substratum becomes coated by organic matter (Lis and Sharon, 1986). Then pioneer bacteria, normally oligotrophic (low nutrient feeders), attach to the surface and begin to grow forming microcolonies within several hours (Corpe, 1973; Marshall et al., 1971). Pioneer bacteria are crucial in initiating the

development of the subsequent complex biotic community and their initial attachment is a key step in the whole process. The survival strategy of these pioneer adherent bacteria is to "bioform" the oligotrophic constraints of the pelagic region (requiring active heterotrophs to adapt a K survival mode), to a richer nutrient niche permitting the r-survival mode. The modified nutrient rich surface now becomes available for colonization by many different species. Diatoms, fungi, protozoans, micro-algae and other microorganisms attach to the surface, forming what is termed the primary slime layer (Skerman, 1956). However the resulting biofilm (immobilized cells at a substratum in an organic polymer matrix), when formed on man-made structures, may cause corrosion deterioration and promote increased fluid frictional resistance resulting in energy losses and reduced system performance. Furthermore, this primary microbial colonization is often a prerequisite for the final stage of succession in which large organisms, viz., invertebrates, attach and grow on the surface (Crisp and Ryland, 1960; Zobell and Allen, 1935)(biofouling), further deteriorating system performance and often integrity. For example it was reported that corrosion alone has cost the US economy $167 billion (US Dept of Commerce, 1986) with corrosion prevention over $100 billion (Wall Street J., 1991) annually.

Physicochemistry of bacterial adhesion

Several related theories govern the probability of bacterial attachment to a substratum in aqueous environments (Marshall, 1988). Each states that the adhesion of microorganisms to surfaces is influenced by long-range, short-range, and hydrodynamic forces. The DLVO (letters after first initials of last names of its proposers) theory assumes that interaction between two objects is comprised of an attractive component, governed by Van der Waals forces, and a potential repulsive component due to overlap of electrical double layers associated with charged groups (Loeb, 1985). These yield two distances at which a particle may be attracted to the substratum. At a primary minimum (ca 1nm), attractive forces are strong; at the secondary minimum (ca 15 nm), forces are weaker. These distances are divided by an intermediate repulsion barrier. Microorganisms may accumulate at the secondary minimum and much of the strategy in surface colonization is concerned with remaining at the secondary minimum and overcoming the repulsive barrier to reach the primary minimum (Okuyawa et al., 1980). Microorganisms synthesize a variety of tethers for this purpose. All have narrow diameter and sufficient length to minimize and "break through" the repulsive layer (Costerton et al., 1985). Such structures have been reported (Costerton et al., 1985) to include long fibular, capsular polysaccharide (CP), pili and flagella, each of which could form an adhesive bridge minimizing electrostatic repulsion (Hammond et al., 1984).

A second, Stern, theory predicts that there will be a net charge distribution at any solid surface and that as a consequence, counter ions are held closely at the surface forming a Stern layer while the rest of the ions are less restricted forming a diffuse ionic zone (Loeb, 1985). This model, probably less applicable in a marine habitat, also predicts a double layer of attractive domains sandwiching a repulsive barrier and would require similar structures to function as tethers as would the DLVO model. The thermodynamic model considers adhesion equilibria in terms of system free energy (Marshall, 1985) with zones of attraction and repulsion approximately those of the other models.

Once the bacteria are attached to the surface, multiple events can transpire to carry it to the primary minimum at which multiple bonds of a more permanent nature may be formed between the organism and substratum. This attachment is generally considered to involve hydrophobic bonds of outer membrane components of Gram negative bacteria or more likely capsular extracellular polymers which form the cement-like biofilm. The roles of bacterial capsules (see below) in this process have been discussed with the conclusion that "much more information is required" (Christensen, 1989; Marshall, 1985).

Adhesins

The term adhesin was originally coined to denote specific bonding molecules to receptors on cell surfaces (Ofek et al., 1985). In this paper, biopolymers that mediate non-specific adhesion on marine surfaces are also referred to as adhesins. As noted above, adhesins include proteinaceous flagella, fimbriae (Swanson et al., 1985) and capsular extracellular polymeric substances (EPS), possibly the capsular polysaccharide (CP) component. EPS is a focus of this report (see below). *Hyphomonas* MHS-3, *Caulobacter crescentus*, *Seliberia stellata* (Hood and Schmidt, 1996) and Asticcacaulis biprosthecum are bacteria that make extracellular polymer holdfast (localized "sticky" capsule) and fimbriae at the same pole (Merker and Smit, 1988; Ong et al., 1990). A lectin domain on some fimbriae adheres them to specific cell surface carbohydrates. They may also attach nonspecifically to inanimate surfaces: i.e. since many fimbriae have a low pI and are relatively hydrophobic, they may adhere via salt bridges or hydrophobic bonds.

Capsular Extracellular Polymeric Substances (EPS)

Capsules normally surround bacteria external to the envelope but can also be more localized as in a holdfast. Many are pure polysaccharide (CP; capsular polysaccharide) while a few covalently or otherwise bind a protein (Wrangstadh et al., 1990) and/or fatty acid residues (Sar and Rosenberg, 1988). Consequently, unless the capsule is known to be composed of pure polysaccharide (CP), the term capsular extracellular polymeric substances (EPS) is used.

Bacterial surface polysaccharides have considerable heterogeneity, from the simple α 1-4 linked, unbranched glucose polymers called dextrans, to the highly complex, branched, and substituted heteropolysaccharides made up of oligosaccharide repeating subunits such as xanthan and colanic acid (Christensen et al., 1985). CP can also be substituted with pyruvate, acetate, formate, sulfate, phosphate and other groups (Jann and Westphal, 1975). Two identical sugars can bond to form 11 different disaccharides whereas two identical amino acids can form only one dipeptide. Additionally, CP contain a wide variety of sugars, (Bhattacharjee et al., 1984). Furthermore, the non-carbohydrate side groups that are found in bacterial CP adds to their heterogeneity that, as a consequence of all of these considerations, far exceeds that of proteins (Sutherland, 1982).

Investigations for Model Fouling Bacteria

Fouling films are comprised of complex multispecies communities and a number of species are considered to be primary colonizers. Among these *Hyphomonas* serves as an excellent model to

define the specific roles of the extracellular polymeric substances (EPS) in marine biofouling processes because: 1) it participates in both early colonization of surfaces and subsequent biofilm development; 2) it elaborates proteinaceous fimbriae and capsular polysaccharides at times coincident with cell attachment to surfaces; 3) synthesis of both EPS structures are temporally and polarly regulated; 4) EPS-deficient progeny (rad strain) are "spontaneously" produced (at a rate of 10^{-10} for *Hyphomonas* isolate MHS-3); 5) "footprints" (see below) of *Hyphomonas* spp. left behind on a previously colonized surface can be detected and chemically characterized.

Nearly all underwater marine surfaces are colonized; all support heterogenous populations; no one species appears to be the "linchpin" of the process; and not all species are found in diverse habitats. *Hyphomonas* is important not only as a model, but in nature as well (Baier et al., 1983; Railkin, 1994). It is hypothesized that *Hyphomonas* swarmer cells are chemotactically attracted to both uncolonized conditioning films and biofilm on marine substrata by the concentration of amino acids there. This triggers its differentiation into reproductive cells that synthesize adhesin(s). While adhesion science is still rather empirical (Strausberg and Link, 1990), it may be speculated that EPS or (and?) fimbriae (in the case of strain MHS-3) would tether the cell at the secondary minimum. Given the luxury of time, enough cells would penetrate to the primary minimum where EPS would partition out of the water column and onto the solid substratum, forming hydrogen bonds, not with water but with the surface. This process would continue resulting in a buildup of biofilm which becomes a sink for nutrients and begins to attract a constantly increasing menagerie of other pelagic voyagers.

Life Cycle and Morphogenesis of Hyphomonas

Hyphomonas, like other prosthecate, budding bacteria, has a biphasic life cycle (Wali et al.; Fig. 1) The progeny, swarmer cell, is dispersive (motile) by means of a single flagellum. It can chemotactically sense favorable areas such as nutrient rich surfaces, sometimes nearby; but it also has the capability to form distant colonies, because it is well adapted to survive in the oligotrophic pelagic zone (Emala and Weiner, 1983). It has a low metabolic rate (Emala and Weiner, 1983), polyhydroxybutyrate storage reserves, and is microspherical (0.4μm diameter), all properties of deep sea survival cells (Morita, 1985). The prosthecate reproductive stage is morphologically and physiologically equipped to establish, maintain, and survive in marine biofilms. The prosthecate form is larger than the swarmer cell (the main body being a prolate spheroid 1-2μm long, with a prosthecum 1-2μm long, 0.2μm wide).

As the prosthecum emerges from one pole, a "holdfast" has been reported to be synthesized from the other (Moore, 1981). A polar adhesin arrangement would allow the stalk to extend toward regions of richer nutrient and oxygen level. Reproductive budding at the distal tip of the stalk allows the progeny to either escape to the water column to establish a new community, or to settle nearby to extend the existing community. It is interesting that the "holdfast" survival strategy of another genus of procaryotes, *Caulobacter*, may be an example of converging evolution, with the polysaccharide, however, synthesized on the opposite pole (tip of the stalk) so that the reproductive cell body faces upward, with the stalk serving as the anchor (Merker and Smit, 1988).

Physiology of Hyphomonas

By virtue of their specialized physiologies as well as morphologies, motile swarmer cells are well adapted for survival in the oligotrophic water column, while the periphytic, prosthecate, reproductive cell is suited to establish, maintain, and survive in marine biofilms. For heterotrophic growth our laboratory has demonstrated a functional Krebs cycle (Devine and Weiner, 1990) and proteases (Shi et al., 1989), showing that reproductive stages, growing in microbial films, use protein and amino acids for energy (Shi et al., 1988). It was also shown that "autotrophically maintained" *Hyphomonas* assimilates copious quantities of CO_2 (Weiner et al., 1997) growing with repeated transfers in water containing only salts, reduced sulfur, and 10% CO_2. They will not multiply without sulfur and CO_2. Such physiological plasticity confers unusual ability for primary surface colonization. Once a biofilm is established, it would be beneficial to switch to heterotrophic metabolism for rapid multiplication using the accumulating organic material that may be sequestered by the growing biofilm.

RECENT DEVELOPMENTS AND DISCUSSION

Temporal and Spatial Synthesis of EPS Adhesin

The precise timing of EPS synthesis and localization for both strains MHS-3 (Quintero, 1994) and VP-6 (Langille, 1996) has been determined. Using monoclonal antibodies (Busch, 1993) against *Hyphomonas* MHS-3 lipopolysaccharide (LPS) as a negative stain (EPS would sterically hinder the approach of the mAb to its LPS target) in immuno-electron microscopy, we determined that MHS-3 synthesizes EPS only during its adherent (Quintero and Weiner, 1995) reproductive stage and only at the main body of the reproductive cell. No EPS could be detected on the prosthecum. This was also demonstrated probing with gold-labeled *Bauhinia purpurea* lectin and thin sections of polycationic ferritin-stained cells (Quintero and Weiner, 1995) (Fig. 2).

Purification (gel permeation), lectin binding studies (see below) and fine structure micrographs revealed a very different EPS profile for VP-6 than for MHS-3. VP-6 was recently been shown to synthesize two different EPS. One (termed "capsule") surrounds the entire cell, including the prosthecum and the bud (Fig. 3), during all developmental stages; the other is (termed "holdfast") is localized and temporal, being synthesized at one pole of the reproductive cell (Fig. 4) and only during the reproductive stage (Fig. 1, Stages D-F). Structure follows function as MHS-3 does not form rosettes, typical of the hyphomicrobia (i.e. reproductive cells stick to one another with stalks pointing outward in a floral pattern) while VP-6 does form rosettes. The entire capsule of MHS-3 may serve as holdfast, structurally and functionally. Since MHS-3 produces more holdfast adhesin than other species it is an important source of this kind of polymer which is a potentially useful commercial bioadhesive or underwater coating.

MHS-3 produces one cell in 10^{10} replications that does not synthesize EPS (rad; Quintero and Weiner, 1995). Among all *Hyphomonas* strains, empirically examined, it also produces the most extensive and adhesive EPS. One may speculate that the rad variant may allow a small number

of reproductive cells to be free of the rare biofilm subject to nutrient depletion, toxin build up or excessive predation.

Purification and Physical Adhesin Properties

The chemical and structural analysis are further along for strain MHS-3 than for VP-6. VP-6 capsular EPS is pyruvylated; MHS-3 EPS is not (Quintero et al., 1990). Crude EPS of MH3 elutes in 5 peaks on an analytical HPLC column (6FC column, 10^4 to $2x10^6$ size separation, polystyrene-divinylbenzene packing). Fraction two is the adhesin. The capsular EPS of VP-6 has a much larger molecular weight than that of MHS-3 (500,000 MW to 60,000 MW respectively) and is composed of much larger percentage of uronic acids (Quintero et al., 1990). When the purified EPS of MHS-3 is fractionated by gel permeation chromatography, a single peak is resolved which, remains homogeneous after second dimension anion exchange chromatography. The peak is the putative adhesin. Rad mutants do not yield such polymer. We take this to mean that *Hyphomonas* MHS-3 capsule, "holdfast", and EPS are one and the same (Fig. 2). No protein appears to be tightly associated with this structure. On the other hand, from Commassie blue-stained SDS-PAGE VP-6 capsule putatively contains a tightly associated protein. The holdfast appears to be pure CP which like other holdfasts consists partly of N-acetyl galactosamine (from lectin analysis). This arrangement is similar to that of *S. stellata* (Hood and Schmidt, 1996) which also may be a primary colonizer with a biphasic life cycle.

The Adhesins

Functionally (in adhesion) there are interesting differences and similarities between both strains. MHS-3 synthesizes long, thin fimbriae at the same pole and about the same time as it synthesizes capsule; VP-6 does not (manusc. in prep). Preliminary studies have been carried out to evaluate the importance of the proteinaceous components in adhesion of prosthecate bacteria. Prosthecate MHS-3 attach, even after treatment with protease, at the pole where EPS is deposited. These initial observations suggest that either proteins do not participate in adhesion of *Hyphomonas* MHS-3 to an inanimate surface or that they are protected from or resistant to protease treatment in the presence of the CP. However no protein is detected in the purified adhesin fraction either. VP-6 on the other hand has reduced ability to adhere after protease treatment, from Coomasie blue stained gels, because of the degradation of the capsular associated proteins (manusc. in prep).

Recent experiments in our laboratory support the necessity for CP in the adhesion of *Hyphomonas* MHS-3 to surfaces. The lectin, *Bauhinia purpurea* (BPA), specific for the CP (Quintero and Weiner, 1995), was found to interfere with cell adhesion (Quintero and Weiner, 1995). Furthermore, the rad strain (CP deficient) synthesizes fimbriae and does not adhere. Thus it appears that CP but not necessarily fimbriae must be present in order for the adhesive process to occur. We have also identified lectins specific for VP-6 holdfast (coral tree) and capsule (sweet pea) and have made monoclonal antibodies (mAb) to the capsular associated protein (Langille, 1996). In preliminary studies these specific reacting agents (not other lectins or mAb) appear to interfere with adhesion (Langille, 1996).

Consistent with the above, a preliminary ATR/FT-IR investigation of the adsorption properties of the crude exopolysaccharide fraction of VP-6 indicated that there was protein present. By contrast, the purified MHS-3 adhesin was shown to form amide bonds in footprint experiments. Therefore, as in the case of other bacteria with adhesive polar CP the adhesive component is possibly an NAG (putatively uronic acid) moiety.

Microbial Footprints

Detection of the adhesive molecules responsible for anchoring bacterial cells to substrata has been achieved through microscopic observations of the "footprints" left on a surface after removal of the surface-associated bacterial cells by one of a variety of techniques. Bacteria, removed by shear force (Marshall et al., 1971), enzymes (Paul and Jeffrey, 1985) or ultrasonication (Neu and Marshall, 1991), leave behind on the substratum the polymers that presumably are responsible for cell adhesion. Surface-sensitive, chemical analytical techniques such as attenuated total reflection infrared spectrometry (ATR/FT-IR) are ideally suited to identify the types of molecules that form the footprints (see Fig. 5). The nature and types of adhesive bonds are revealed. Thus, a chemical analysis of the footprints represents a powerful approach to identifying and characterizing microbial adhesins.

Time-of-flight secondary ion mass spectrometry (ToF-SIMS) is a new surface-sensitive, chemical analytical technique (Niehuis et al., 1989) that developed out of static secondary ion mass spectrometry (S-SIMS)(Fig. 5). ToF-SIMS provides chemical information on chain branching, cross-linking and conformation of polymers in the adsorbed state and has the added advantage of high spatial resolution to investigate the chemistry of a small area containing a footprint. ToF-SIMS provides a spatially-resolved mass spectrum of the molecules located within the top 10-20 angstroms of a surface (Meyer et al., 1992). Spatial resolution ranges from 0.2 mm-12 mm and detection limits are on the order of ppm to ppb. Furthermore, if the primary ion flux is maintained at £10^{13} atoms/cm^2, organic material such as the adhesive compounds of interest here can be characterized from the fragmentation pattern generated from the mass spectrum. To date, ToF-SIMS has been used to conduct microanalysis of membrane surfaces, molecular microanalysis in soft tissue, microanalysis of peptide diffusion in polymer and patterned arrays (Shamberger et al., 1996). This new instrumentation is, thus, ideally suited to elucidate the chemical identity of the constituents of microbial footprints, and hence, the adhesive molecules excreted by surface fouling microorganisms.

Commercial Promise of the Adhesins

There is a promising beginning to the potential commercialization of MHS-3 adhesin. There is a general purpose growth medium (Marine Broth (MB)), synthetic media (Havenner et al., 1979)(Medium G) and a commercial, low cost medium (Manyak and Weiner, 1994) (LD). We have grown MHS-3 in a fermenter with the finding that there is a higher yield of cells and polymer in the fermentor than in flask culture. The adhesins may have value as underwater surface coatings and as bioadhesives since they are relatively non-immunogenic (MacLeod and Krauss, 1950).

SUMMARY

To control biofouling, it is necessary to understand the primary adhesive interaction between pioneer colonizing bacteria and the substratum. There are apparently several species specific mechanisms involved. One bacterial strategy for adhesin is the synthesis of amino sugar polymeric adhesins. These can be demonstrated by agents that specifically bind these moieties and consequently interfere with the adhesive process. They can be characterized by new spectrometry technology.

ACKNOWLEDGEMENTS

We thank P. Suci and B. Frolund for their contributions to this study. We acknowledge A. Snyder for technical assistance and S. Payne for editing the manuscript. This work was supported by grants from the Office of Naval Research (ONR), the Maryland Industrial Partnerships (MIPS) and Oceanix Corp.

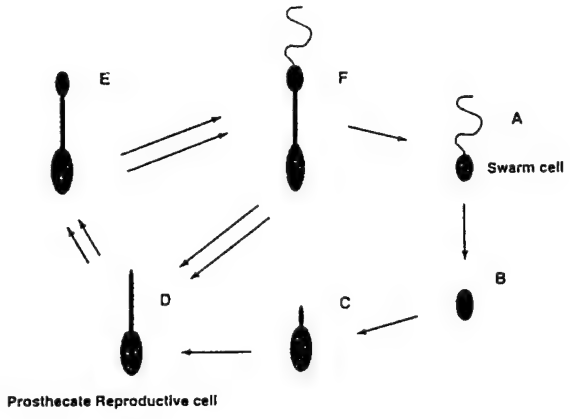

Figure 1. Biphasic life cycle of *Hyphomonas*. Single arrows designate swarm cycle (pelagic form). Double arrows designate reproductive cycle (Adherant, biofilm form).

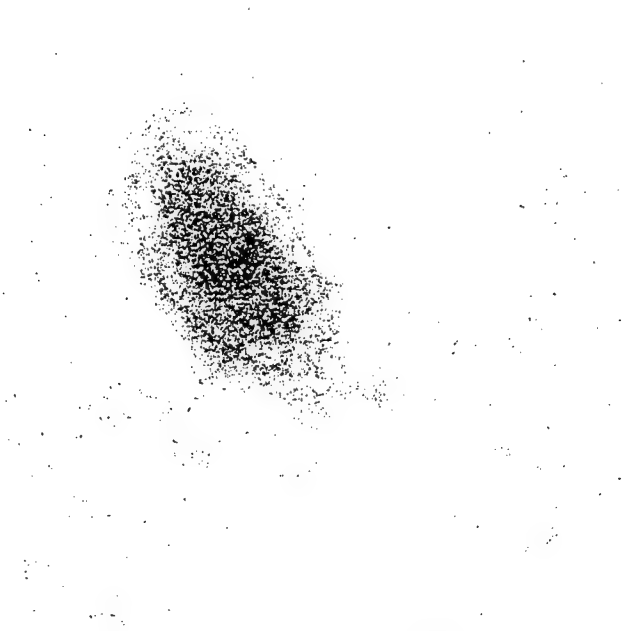

Figure 2. Holdfast capsule of *Hyphomonas*. MHS-3 capsule labelled with *Bauhinia purpurea* lectin. In this electron micrograph, the cell is approx. 2µm.

Figure 3. Electron micrograph of *Hyphomonas*. VP-6 showing capsule (surronding entire cell), stained with cationic cerritin. Bar represents one µm.

Figure 4. Electron Micrograph of *Hyphomonas* VP-6 showing holdfast. Hostfast (arrow) is clearly visable without staining and other procedures that could induce artifacts.

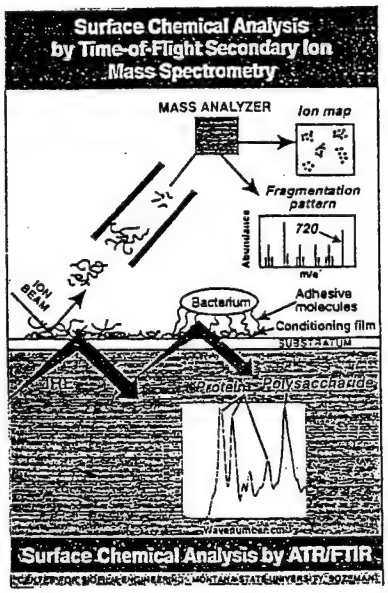

Figure 5. Diagram depicting emerging technologies to determine the nature of bioadhesins and the bonds they form on immersed substrata.

REFERENCES

Baier, R., A. Meyer, V. DePalma, R. King, M. Fornalik. 1983. Surface microfouling during the induction period. *J. Heat Trans.* **105**:618-624.

Bhattacharjee, A. K., J. E. Bennett, and C.P.J. Glaudemans. 1984. Capsular polysaccharides of *Cryptococcus neoformans. Rev. of Infect. Diseas.* **6**:619-624.

Busch, K. 1993. Specificity of a monoclonal antibody against *Hyphomonas* MHS-3 polysaccharide. M.S. thesis, 93 pp. MD: University of Maryland.

Christensen, B., J. Kjosbakken and O. Smidsrod. 1985. Partial chemical and physical characterization of two extracellular polysaccharides produced by marine periphytic *Pseudomonas* sp. strain NCMB 2021. *Appl. and Environ.* **50**:837-845.

Christensen, B.E. 1989. The role of extracellular polysaccharides in biofilms. *J. Biotechnol.* **10**:181-202.

Corpe, W.A. 1973. Microfouling: the role of primary film forming bacteria. In: Proceedings of the Third International Congress on Marine Corrosion Fouling. R.F. Ackjer, B.F. Brown, J.R. DePalma and W.P. Iverson, eds. Evanston, IL: Northwestern Univ. pp. 598-609.

Costerton, J. W., T. Marrie, and K-J. Cheng. 1985. Phenomena of bacterial adhesion. In Bacterial adhesion. D. Savage and M. Fletcher, eds. NY: Plenum Pres. pp. 3-43.

Crisp, D. J. and J. S. Ryland. 1960. Influence of filming and of surface texture on the settlement of marine organisms. *Nature* **185**:119.

Devine, R. A. and R. M. Weiner. 1990. *Hyphomonas* species metabolize amino acids using Krebs cycle enzymes. *Microbios.* **62**:137-153.

Emala, M. A. and R. M. Weiner. 1983. Modulation of adenylate energy charge during the swarmer cycle of *Hyphomicrobium neptunium. J. Bacteriol.* **153**:1558-1561.

Hammond, S. M., P. A. Lambert, and A. N. Rycroft. 1984. The bacterial cell surface. Kent, GB: Croon Helm Ltd.

Havenner, J., B. McCardell and R. Weiner. 1979. Development of defined, minimal and complete media for the growth of *Hyphomicrobium neptunium. Appl. Environ. Microbiol.* **38**:18-23.

Hood, M. and J. Schmidt. 1996. Examination of *Seliberia stellata* exopolymers using lectin assays. *Microb. Ecol.* **31**:281-290.

Jann, K., and O. Westphal. 1975. Microbial polysaccharides. In: The antigens. Michael Sela (ed.). Academic Press. New York, San Francisco and London. vol. 3. pp. 1-110.

Langille, S. 1996. Adhesive capsules of *Hyphomonas* VP-6. Ph.D. Thesis. (In prep.)

Lis, H. and N. Sharon. 1986. Lectins as molecules and as tools. *Ann. Rev. Biochem.* **55**:35-67.

Loeb, G. I. 1985. Properties of non-biological surfaces and their characterization. In: Bacterial adhesion. D. Savage and M. Fletcher, eds. NY:Plenum Press. pp. 111-129.

Macleod, C. M., and M. R. Krauss. 1950. Relation of virulence of pneumococcal strains for mice to the quantity of capsular polysaccharide formed in vitro. *J. Exp. Med.* **92**:1-9.

Manyak, D. and R. Weiner. 1994. Fermentation of marine bacteria for production of novel biomaterials. In: Abst. Gen. Meet. Amer. Chem. Soc. San Diego.

Marshall, K. C. 1985. Mechanisms of bacterial adhesion at solid-water interfaces.. In: D. Savage and M. Fletcher (ed.) Bacterial adhesion. NY: Plenum Publishing Corp. pp. 133-160.

Marshall, K. C. 1988. Adhesion and growth of bacteria at surfaces in oligotrophic habitats. *Can. J. Microbiol.* **34**:503-506.

Marshall, K. D., R. Stout and R. Mitchell. 1971. Selective sorption of bacteria from seawater. *Can. J. Microbiol.* **17**:1413-1416.

Merker, R. and J. Smit. 1988. Characterization of the adhesive holdfast of marine and freshwater Caulobacters. *Appl. Environ. Microbiol.* **54**:2078-2085.

Meyer, K., B. Hagenhoff, M. Deimel, and A. Benninghoven. 1992. Quantification of molecular secondary ion mass spectrometry by internal standards. *Org. Mass Spectr.* **27**:1148-1150.

Moore, R.L. 1981. The biology of *Hyphomicrobium* and other prosthecate, budding bacteria. *Annu.Rev. Microbiol.* **35**:567-594.

Morita, R. Y. 1985. Starvation and miniaturization of heterotrophs, with special emphasis on maintenance of the starved viable state. In: Bacteria in their natural environments. M. Fletcher and G. D. Floodgate, eds. Society for General Microbiology Publication #16. Academic Press. pp. 111-130

Neu, T. R. and K. C. Marshall. 1991. Microbial "footprints"-a new approach to adhesive polymers. *Biofouling* **3**:101-112.

Niehuis, E., P. N. T. van Velzen, J. Lub, T. Heller and A. Benninghoven. 1989. High mass resolution time-of-flight secondary ion mass spectrometry. *Surface Interface Anal.* **14**:135-142.

Ofek, I., H. Lis, and N. Sharon. 1985. Animal Cell Surface Membranes. pp. 71-80. In: Bacterial adhesion, D. Savage and M. Fletcher, eds. NY:Plenum Press.

Okuyawa, K. S. Arnott, R. M. Moorhouse, M.D. Walkinshaw, E.D.T. Atkins, and C. Wolf-Ullish. 1980. *Am. Chem. Soc. Symp. Ser.* **141**:411-419.

Ong, C., M. Wong and J. Smit. 1990. Attachment of the adhesive holdfast organelle to the cellular stalk of Caulobacter crescentus. *J. Bacteriol.* **172**:1448-1456.

Paul, J. H. and W. H. Jeffrey. 1985. Evidence for separate adhesion mechanisms for hydrophilic and hydrophobic surfaces in Vibrio proteolytica. *Appl. Environ. Microbiol.* **50**:431-437.

Quintero. E. 1994. Characterization of adhesion and biofilm formation by the marine procaryote MHS-3. Ph.D. Thesis. 200p. MD:University of Maryland.

Quintero, E., G. Geesey and R. Weiner. 1990. Characterization of adhesive exopolysaccharides of new species of *Hyphomonas*. In: Abst. of Annu. Meeting of Amer. Soc. Microbiol. p. 263.

Quintero, E. and R. Weiner. 1995. Evidence for the adhesive function of the exopolysaccharide of *Hyphomonas* MHS-3 in its attachment to surfaces. *App. Environ. Microbiol.* **61**:1897-1903..

Railkin, A. 1994. Self-assembly of marine microfouling communities. *Dokl. Biol. Sci.* **337**:349-357.

Sar, N., and E. Rosenberg. 1988. Fish skin bacteria: production of friction-reducing polymers. *Microbial Ecol.* **17**:27-38.

Shamberger, P., F. Caccavo, F. von Ommen Kloche and G. Geesey. 1996. Microbial cell fingerprinting - Development of ToF-SIMS for the study of microbial cell surfaces. Abst. of Surfaces and Biomaterials Conference. Phoenix.

Shi, J., V. E. Coyne and R. Weiner. 1989. Characterization of the exoproteases of the hydrothermal vent bacterium *Hyphomonas* jannaschiana VP3. 89th Annual Meeting of the American Society for Microbiology, New Orleans, Louisiana. Abst. of Ann. Meeting. p. 253.

Shi, J., V. E. Coyne and R. M. Weiner. 1988. Characterization of extracellular alkaline protease activity in the budding, hydrothermal vent bacterium *Hyphomonas* jannaschiana. 1st International Symposium on Marine Molecular Biology. Baltimore, Maryland.

Skerman, T. M. 1956. The nature and development of primary films on submerged surfaces in the sea. N. Zealand, *J. Sci. Technol. B.* **38**:44-57.

Strausberg, R. and R. Link. 1990. Protein-based medical adhesives. *Tibtech.* **8**:53-57.

Sutherland, I.W. 1982. Biosynthesis of microbial exopolysaccharides. In: Advances in Microbial Physiology. vol. 23. A.H. Rose and J.G. Morris (eds). NY: Academic Press.

Swanson, J. S., Bergstrom, K. Robbins, O. Barrera, D. Corwin, J.M. Koomey. 1985. Gene conversion involving the pilin structural gene correlates with pilus^{+}--pilus^{-} changes in Neisseria gonorrhoea. *Cell* **47**:267-276.

U.S. Department of Commerce, Natl. Bureau of Stds., and Cooperative Research Opportunities at NBS. 1986. Washington, D. C.: U.S. Govt. Print. Off.

Wali, R. M., G. R. Hudson, D. A. Danald and R. M. Weiner. 1980. Timing of swarmer cell cycle morphogenesis and macromolecular synthesis by Hyphomicrobium neptunium in synchronous culture. *J. Bacteriol.* **144**:406-412.

Wall Street J. April 19, 1991.

Weiner, R., L. Dagasan and J. Tuttle. 1997. Evidence for chemolithotrophic metabolism in *Hyphomonas*. Appl. and Environ. Microbiol. (In prep).

Wrangstadh, M., U. Szewzyk, J.Ostling, and S. Kjelleberg. 1990. Starvation-specific formation of aperipheral exopolysaccharide by a marine Pseudomonas sp., Strain S9. *Appl. Environ. Microbiol.* **56**:2065-2072.

Zobell, C. E. and E. C. Allen. 1935. The significance of marine bacteria in the fouling of submerged surfaces. *J. Bacteriol.* **29**:230-251.

APPLIED AND ENVIRONMENTAL MICROBIOLOGY, Aug. 1998, p. 2906–2913
0099-2240/98/$04.00+0

Vol. 64, No. 8

Spatial and Temporal Deposition of *Hyphomonas* Strain VP-6 Capsules Involved in Biofilm Formation

STEPHEN E. LANGILLE AND RONALD M. WEINER*

Department of Microbiology, University of Maryland, College Park, Maryland

Received 23 February 1998/Accepted 12 May 1998

***Hyphomonas* strain VP-6 is a prosthecate bacterium isolated from the Guayamas vent region and is a member of a genus of primary and common colonizers of marine surfaces. It adheres to solid substrata as a first step in biofilm formation. Fine-structure microscopy and the use of specific stains and lectins reveal that it synthesizes two different extracellular polymeric substances (EPS). One is a temporally synthesized, polar holdfast EPS, and the other is a capsular EPS that is present during the complete life cycle and surrounds the entire cell, including the prosthecum. The timing and location of *Hyphomonas* strain VP-6 EPS elaboration correlate with adhesion to surfaces, suggesting that the EPS serves not only as the biofilm matrix but also as a primary adhesin. The temporality and polarity of VP-6 EPS expression substantially differ from those properties of *Hyphomonas* strain MHS-3 EPS expression.**

This paper reports on a relationship between adhesion and capsule synthesis in the prosthecate, budding, marine bacterium *Hyphomonas* strain VP-6. There are two separate, but equally important, steps in the adhesion of bacteria at liquid-solid interfaces (15). The first is primary, reversible adhesion that occurs when the cell initially approaches a surface (15, 20). Bacteria have evolved structures designed to span the electrical repulsion barrier between them and a surface, including fimbriae, pili, flagella, and surface polysaccharides. The lengths and diameters of these appendages dictate that they are less susceptible to charge repulsion than are whole cells (14). Adhesion at this stage occurs through van der Waals forces, hydrophobic bonds, and electrostatic interactions (6). After primary adhesion, a cell displays Brownian and/or flagellum-mediated motion but can become easily detached from the surface (14). It is believed that chemotactic sensors are employed by the cells to determine if the attachment site is suitable for growth (10). Should the organism colonize, primary reversible attachment becomes secondary, permanent adhesion. This step is time dependent and may involve the production of additional extracellular polymers (6). At this point, Brownian motion ceases and cells cannot be removed from the surface without the application of significant shear force (14).

Some studies have shown that surface polysaccharides are responsible for the primary adhesion of cells to surfaces (4, 18, 23). However, most report that other structures are involved in primary adhesion. The identity of the polymer responsible for permanent adhesion of cells to surfaces is also a major topic of debate (8). However, it is generally accepted that capsular extracellular polymeric substances (EPS; polysaccharide-based polymers, possibly associated with proteins or lipids) are the main components of biofilm matrixes, serving as the glue that holds the conglomerates of cells together (5, 14). In this context, it is important to understand where and when biofouling bacteria produce surface polysaccharides as well as how many and what types of surface polysaccharides they produce.

Bacteria have evolved various types of surface polysaccharides that mediate adhesion to surfaces (7, 16, 18, 28). The holdfast is an extracellular structure that is usually spatially confined to a single pole of the cell (21). It is typically composed of heteropolysaccharide (18) and has been reported to be a tenacious adhesive (18). While the holdfast does not function as a complete EPS capsule (which serves as a nutrient sink and protects from predation and desiccation), its synthesis does not require nearly as much energy as that required by a full capsule, which needs as much as 62% of that used by the cell at any moment (6).

Electron microscopy has proven to be a powerful tool for investigating surface polysaccharide-mediated adhesion by microorganisms. A study by Marshall and Cruickshank (16) showed that species of *Hyphomicrobium* and *Flexibacter* use holdfasts to mediate adhesion to surfaces. Likewise, Fletcher and Floodgate (7) showed that *Pseudomonas* strain NCMB 2021 produces two separate types of EPS during the adhesion process. One is a hydrophilic polymer involved in primary adhesion, while the other is a hydrophobic EPS produced subsequent to the first polymer, believed to solidify the organism's attachment to a surface. Thus, scanning and transmission electron microscopy (SEM and TEM, respectively) may be used to elucidate the number of adhesive polymers, their locations on a cell, and their function in the adhesion process.

Plant lectins are also effective tools for investigating surface polysaccharide production. Soybean and wheat germ agglutinins were used to probe the locations of EPS on *Rhizobium japonicum* (29) and *Seliberia stellata* (9), respectively. Merker and Smit (18) used wheat germ agglutinin to label the holdfast of *Caulobacter crescentus*, and workers in our laboratory have used *Bauhinia purpuria* lectin to label the EPS of another strain of *Hyphomonas* (17), designated MHS-3.

Hyphomonas spp. have a relatively complex biphasic life cycle. A swarm cell is planktonic and specialized for survival in the pelagic zone, while a prosthecate cell is adherent and adapted for survival in more nutrient-rich biofilms. In a prior study of *Hyphomonas* strain MHS-3, we showed that it has a single EPS holdfast that is less localized than other holdfasts in that it covers the entire main body of the reproductive cell (23). The MHS-3 holdfast is expressed coincidentally with formation of prosthecal outgrowth (23, 24). Treatment with specific lectins inhibited adhesion. Here we report on the spatial and temporal production of surface polysaccharides by *Hyphomonas* strain VP-6 and show that its synthesis and spatial arrange-

* Corresponding author. Mailing address: Department of Microbiology, University of Maryland, College Park, Md. Phone: (301) 405-5446. Fax: (301) 314-9489. E-mail: RW19@umail.umd.edu.

ment are very different than those of MHS-3. We show that VP-6 synthesizes two EPS structures. One, a holdfast, is expressed during a limited stage of growth and only at one pole. The other, a capsular EPS, is constitutively expressed and surrounds the entire cell.

(A portion of these results was presented at the 96th General Meeting of the American Society for Microbiology (12) and were used by S. Langille in partial fulfillment of the Ph.D. requirements of the University of Maryland, College Park.)

MATERIALS AND METHODS

Strains, culture conditions, and chemicals. *Hyphomonas* strain VP-6 was isolated from the Guayamas Basin hydrothermal vent region by H. Jannasch (Woods Hole Oceanographic Institute). VP-6 was stored and enumerated on marine agar (55.1 g/liter) and cultivated aerobically in marine broth 2216 (MB; 37.4 g/liter; Difco Laboratories, Detroit, Mich.) at 25°C. All chemicals were purchased from Sigma Chemical Company (St. Louis, Mo.) or Fisher Biologicals (Melvin, Pa.), unless otherwise noted.

TEM. TEM was done on a JEM 100CX transmission electron microscope operating at 80 kV with collodion-coated 200-mesh copper grids (EY Labs, San Mateo, Calif.). Middle-logarithmic-phase broth cultures were used for all experiments. Cells used for rosette and holdfast visualization were layered on grids for 1 min and then passed through 3 drops of distilled water (dH_2O), blotted dry, and stained for 15 s in a drop of 1% uranyl acetate. EPS were stained with cationic ferritin. The cells were centrifuged and washed once with sterile phosphate-buffered saline (PBS; 8.0 g of NaCl, 2.0 g of KCl, 1.2 g of Na_2HPO_4, 0.2 g of KH_2PO_4/liter of dH_2O [pH 7.2]). Cells were resuspended in PBS, incubated for 1 h with 1.0 mg of cationic ferritin per ml, washed twice with PBS, and layered on collodion-coated copper grids. Ruthenium red staining was done essentially according to the method of Luft (13). Briefly, the culture was harvested in mid-logarithmic phase and resuspended in a 0.5-mg/ml solution of ruthenium red dissolved in PBS containing 0.9% glutaraldehyde. After 1 h, cells were washed twice with PBS, layered onto collodion-coated grids, and stained for 15 s with 1% uranyl acetate.

SEM. SEM was done on an Amray 1820D scanning electron microscope operating at 20 kV. Cells attached to surfaces were visualized by coating glass coverslips with MB for 5 min and then layering mid-logarithmic-phase cultures on the coverslips for 60 min. Attached cells were then dehydrated in a graded series of ethanol solutions (75, 90 and 100, 100 and 100%) for 5 min each and dried in a Denton DCP-1 critical-point drying apparatus. Each coverslip was glued to an aluminum stub (EY Labs) with silver paint (Ted Pella Inc., Redding, Calif.) and evaporation coated with gold-palladium.

FITC-conjugated lectin EPS probes. Cells were harvested during mid-logarithmic phase, washed once in sterile PBS, and resuspended in PBS along with 50 μg of fluorescein isothiocyanate (FITC)-labeled sweet pea lectin (SPL), coral tree lectin (CTL), or *Griffonia simplicifolia* (GSII) lectin for 1 h. Cells were then washed three times in sterile PBS and photographed with a Zeiss Axiophot microscope by incident light fluorescence microscopy.

Orientation of adhesion. One hundred-microliter samples of a mid-logarithmic-phase culture were layered onto glass coverslips precoated with MB. Coverslips were incubated in a humid chamber at 25°C and then washed after 5, 15, 30, 60, 120, or 240 min with 10 ml of artificial seawater (23.0 g of NaCl, 0.24 g of Na_2CO_3, 0.33 g of KCl, 4.0 g of $MgCl_2 \cdot 6H_2O$, 0.66 g of $CaCl_2 \cdot H_2O$/liter of dH_2O). The number and orientation of cells attached to 80-μm^2 areas of the coverslip were determined at each time point with a Zeiss Axiophot light microscope (objective, numerical aperture 1.32) and an ocular micrometer. We used 30 samples, from which the mean and standard deviation were calculated.

Culture synchronization. A modification of the size-sorting procedure of Wali et al. (32) was used to synchronize VP-6 cultures. One liter of early- to mid-logarithmic-phase culture was centrifuged at 13,000 × *g* for 5 min. The supernatant was passed through a 0.6-μm-pore-size membrane (Poretics Corp., Livermore, Calif.) and then centrifuged at 16,000 × *g* for 30 min. The pellet, consisting of swarm cells, was then resuspended in 30 ml of MB and shaken at 100 rpm at 25°C. Aliquots (1.5 ml) were taken every 20 min for 6 h. Twenty microliters of culture from each time point was layered directly onto a collodion-coated copper grid and stained with 1% uranyl acetate for 15 s. The remaining culture sample from each time point was frozen at −80°C. Aliquots from each time point were thawed and labeled with cationic ferritin.

RESULTS

VP-6 produces a polar holdfast. The first indication that VP-6 produces holdfasts came from its ability to form rosettes consisting of three or more cells attached at a common pole, with prostheca radiating outward (Fig. 1A). Closer inspection revealed fibrous material at the tip of the mother cell, distal to the prosthecum, which mediated intercellular adhesion (Fig. 1B and C). Holdfasts were approximately 30 nm wide at the base of the cell, fanning out to a width of approximately 200 nm. The holdfast enlarges with cell maturation, reaching a length of up to 300 nm. The CTL, specific for galactose-β-1,4-*N*-acetylglucosamine linkages, bound holdfasts, as determined by immunofluorescence microscopy (Fig. 2). Note the pinpoint labeling pattern of CTL-treated cells (Fig. 2B) compared to that of control cells (Fig. 2D).

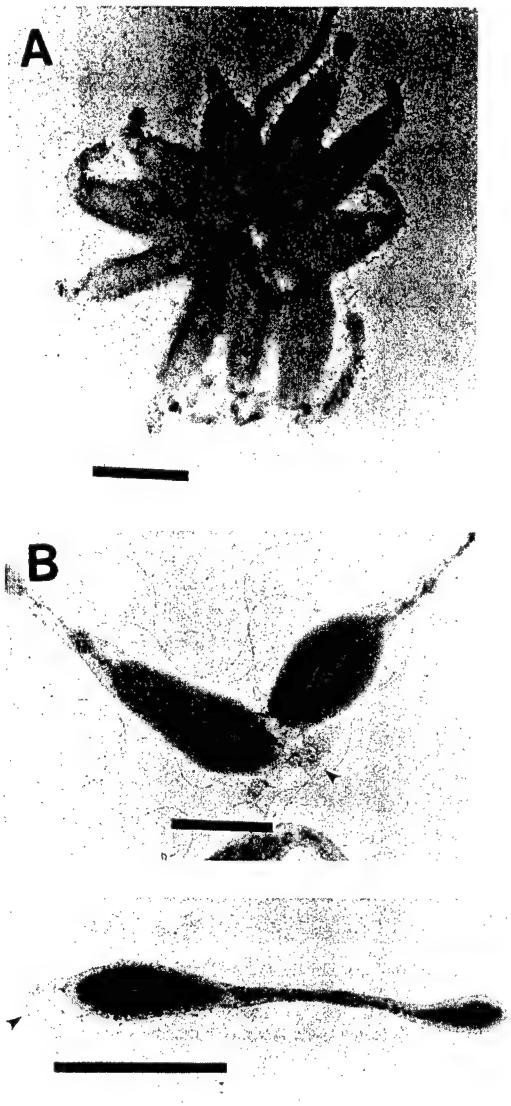

FIG. 1. Holdfast production. Middle-logarithmic-phase VP-6 cells were layered on copper grids and stained with uranyl acetate. Shown are a rosette (A), two cells attached by the fibrous holdfast (arrowhead) (B), and a single cell with a holdfast (arrowhead) (C). Bar = 1 μm.

Evidence for a VP-6 capsular EPS. Ruthenium red staining, specific for acidic polysaccharides (1), revealed that VP-6 produces a rough acidic capsular EPS that surrounds the entire budding reproductive cell (Fig. 3). Cationic-ferritin-stained cells (Fig. 4) and specific lectin immunoprobes corroborated these results. EPS were viewed on swarm, reproductive, and budding reproductive cells, which demonstrated constitutive production throughout the life cycle (Fig. 4). The thickness of capsular EPS ranged from approximately 100 nm on swarm

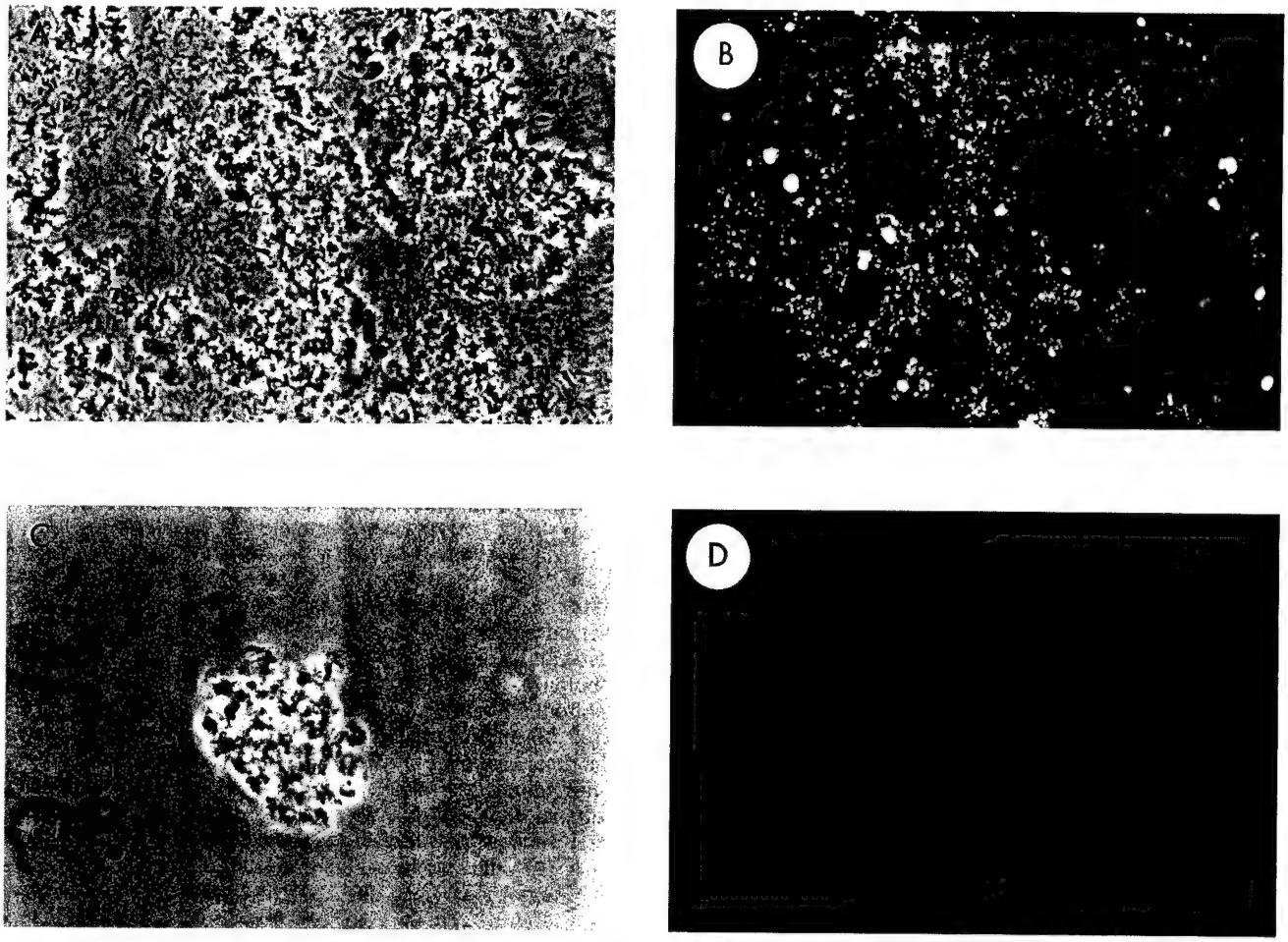

FIG. 2. VP-6 holdfasts labeled with FITC-conjugated CTL. Logarithmically growing cells were washed and resuspended in PBS with 50 μg of FITC-labeled CTL or *G. simplicifolia* lectin per ml. A phase-contrast image of VP-6 cells labeled with FITC-conjugated CTL (A) and the same preparation viewed with incident light fluorescence wavelengths (B) are shown. Notice the pinpoint fluorescence indicating the labeling of holdfast EPS. Also shown are control cells labeled with FITC-conjugated *G. simplicifolia* lectin (C) and the same cells viewed by incident light fluorescence (negative control) (D). Magnification, ×863.

FIG. 3. Budding, prosthecate VP-6 cell stained with Ruthenium Red. Logarithmically growing cells were suspended in a 0.5-mg/ml solution of ruthenium red dissolved in PBS containing 0.9% glutaraldehyde. After 1 h, cells were washed twice with PBS, layered on collodion-coated copper grids, and stained with uranyl acetate. Notice the rough capsular EPS covering the entire cell. Bar = 1 μm.

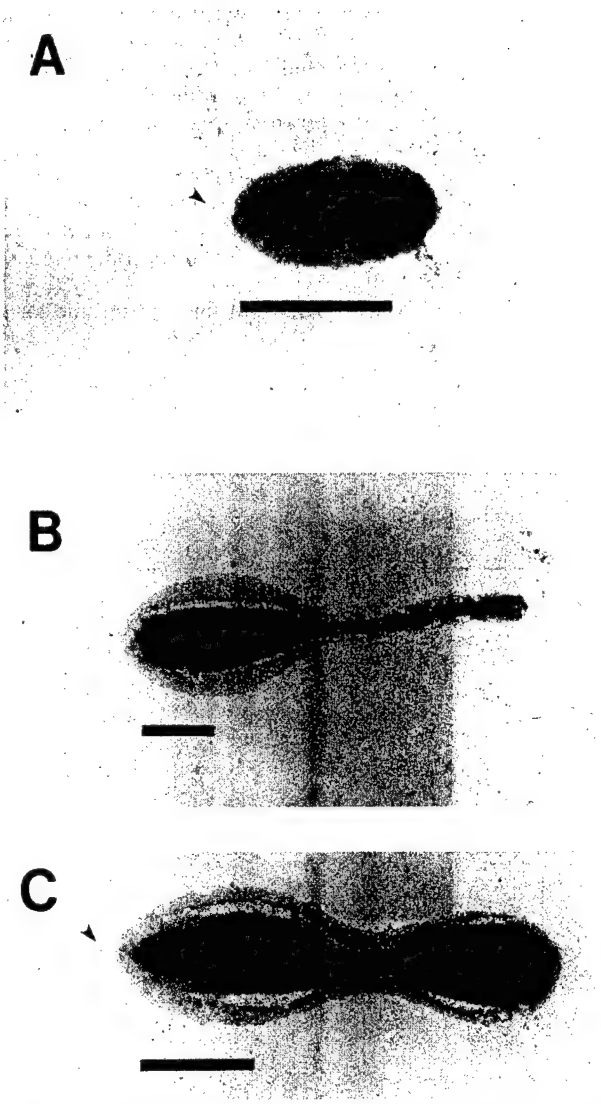

FIG. 4. Cationic-ferritin-labeled capsules. Cells were incubated in 1.0 mg of cationic ferritin/ml of dH_2O solution, washed, and layered on collodion-coated copper grids. Swarm (A), prosthecate reproductive (B), and budding reproductive (C) cells are shown. Notice that in all cases the entire cell is surrounded by capsular EPS. Arrowheads point to unlabeled holdfasts. Bar = 1 μm.

cells and buds to 300 nm on the prostheca and the main bodies of reproductive cells. Capsular EPS appeared to be tightly bound to cells and was not easily sheared during the multiple centrifugation and resuspension steps involved in the cationic-ferritin labeling process (Fig. 4). The holdfasts of VP-6 cells were not bound by cationic ferritin (Fig. 4). Holdfasts were not obvious on cationic-ferritin-labeled cells because they could not be stained with uranyl acetate.

Timing of EPS and holdfast production by VP-6. The timing of both EPS and holdfast expression was determined in synchronously growing populations. Figure 5 shows the stages in the morphogenesis of *Hyphomonas* strain VP-6. Swarm cells required 60 ± 10 min for maturation and the initiation of prosthecal outgrowth. Prosthecate cells formed buds at 150 ± 10 min. The reproductive cells shed buds at the distal tips of their prostheca after 210 ± 10 min. The holdfast and flagellum were synthesized at the same pole 180 ± 10 min into the cycle (Fig. 5D), indicating that individual swarm cells have both a flagellum and a holdfast when they are released from the reproductive cell. Synchronized populations expressed capsular EPS at every stage of the developmental cycle, as was revealed by TEM of cells labeled with cationic ferritin (Fig. 6).

Correlation of surface polysaccharide production and adhesion. The orientations of cells of *Hyphomonas* strain VP-6 during surface attachment and whether attachment varies with

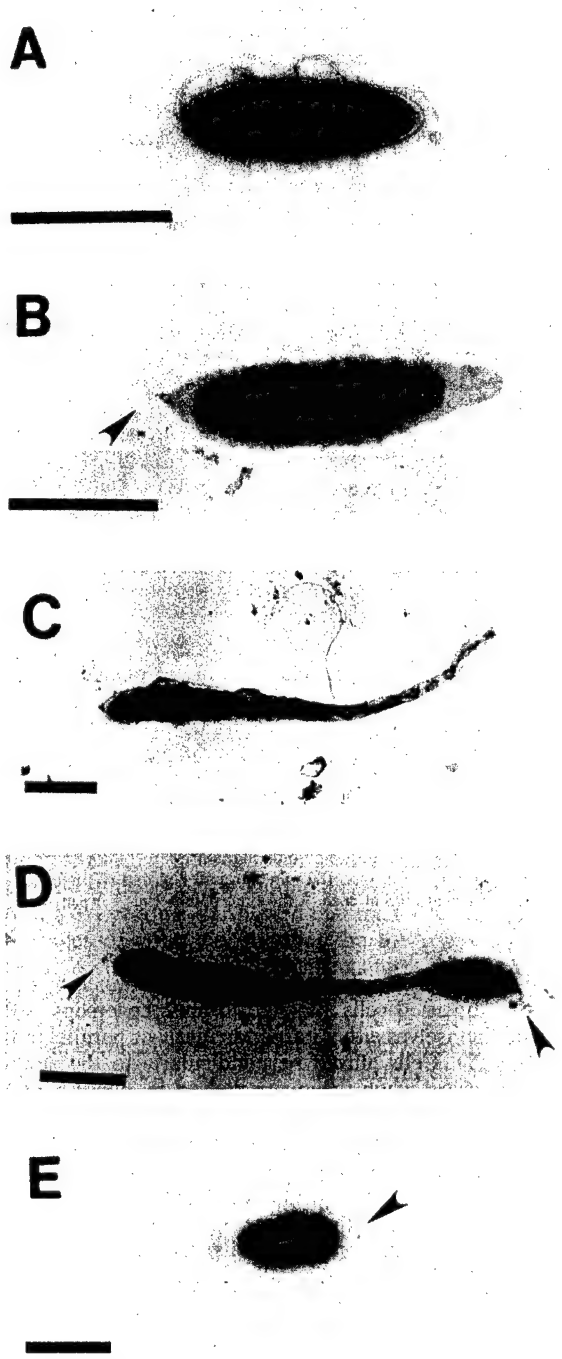

FIG. 5. Uranyl acetate-stained synchronized cultures. VP-6 was synchronized by using differential centrifugation and size sorting. Twenty microliters of culture from each time point was directly layered onto collodion-coated copper grids and stained with uranyl acetate. Shown are cells at 0 min (A), 60 min (B), 120 min (C), 180 min (D), and 240 min (E). Arrowheads point to holdfasts. Bar = 1 μm.

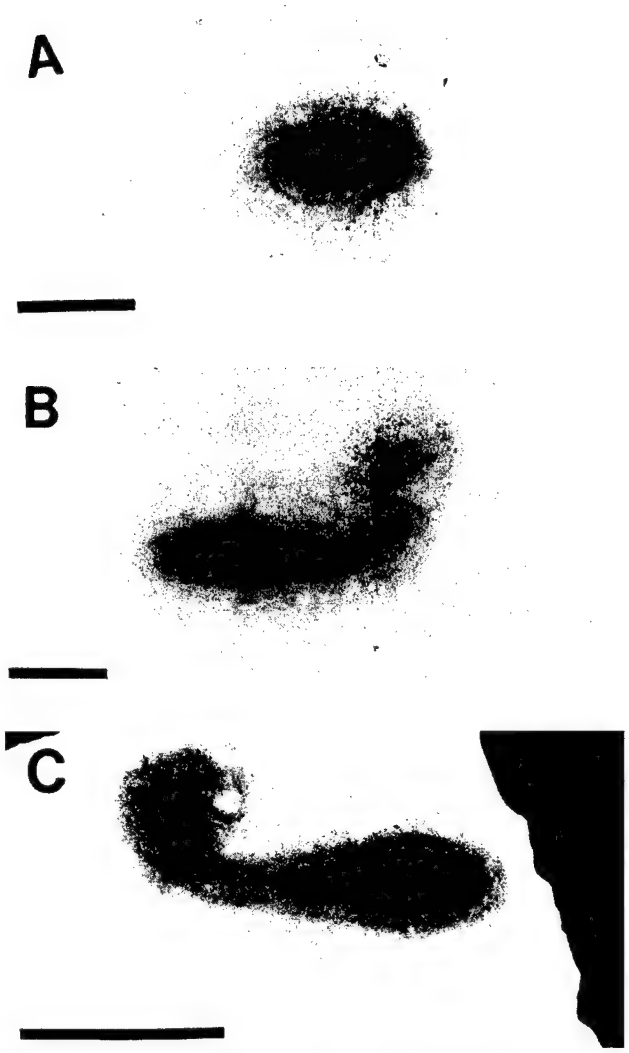

FIG. 6. Synchronized VP-6 cells labeled with cationic ferritin. Cells were removed from a synchronous culture, treated with a 1.0-mg/ml solution of cationic ferritin, washed, and layered onto collodion-coated copper electron micrograph grids. Cells shown in these photomicrographs were removed from the synchronous culture at 0 min (A), 180 min (B), and 360 min (C). Notice that VP-6 produced capsular EPS at each of the time points. Bar = 1 μm.

the location of surface polysaccharide were examined by SEM of critical-point dried cells attached to glass coverslips. VP-6 cells affixed themselves either perpendicularly or parallel to the surface (Fig. 7). Cells affixed perpendicularly to the surface appeared spherical when they were viewed by phase-contrast microscopy (Fig. 8). More of each cell that affixed itself parallel to the surface was visible in the plane of focus (Fig. 8A). The holdfasts, being polar, adhered cells at one pole so that they stood perpendicularly; the capsule, which surrounds the entire cell, adhered it parallel to the surface. As shown in Fig. 8B, the ratio of perpendicular to parallel cells decreased with time, suggesting that cells adhered initially via the holdfast and later predominately via the capsule.

DISCUSSION

An investigation of the spatial and temporal production of surface polysaccharides by *Hyphomonas* strain VP-6 shows that it produces two separate adhesive surface polysaccharides, both of which mediate cellular adhesion to surfaces. These polymers differ in their charges, structures, locations, and temporal levels of production. A holdfast is produced polarly and at a specific time during the life cycle, while a capsular EPS surrounds the entire cell during all morphogenic stages. Cells with holdfasts form rosettes by binding to one another by each holdfast (19, 31). The production of surface polysaccharide in VP-6 is very different from that in MHS-3, which produces a single EPS that surrounds the main body of the prosthecate cell and is synthesized only at reproductive-cell stages (24).

Electron microscopy is a useful tool for studying the loca-

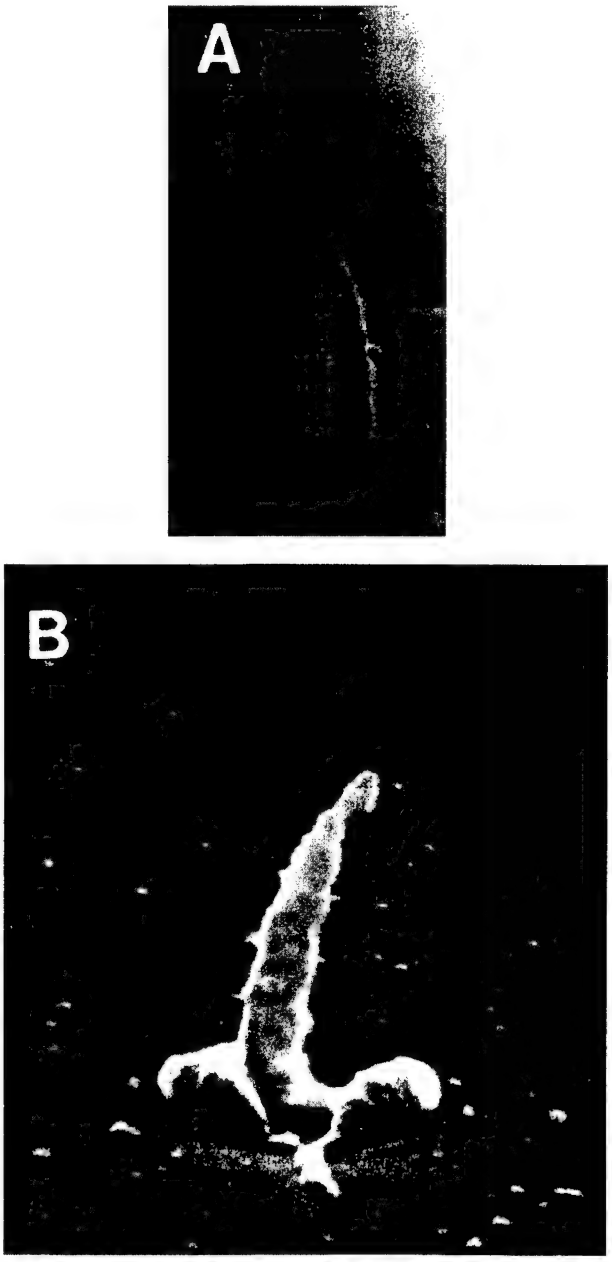

FIG. 7. Orientation of VP-6 cell attachment. Glass coverslips, coated with MB, were layered with logarithmically growing cells and viewed with an Amray 1820D scanning electron microscope. Notice that some VP-6 cells stand perpendicular to the surface (panel A and middle cell in panel B) but that others lie parallel to it (flanking cells in panel B). Bar = 1 μm.

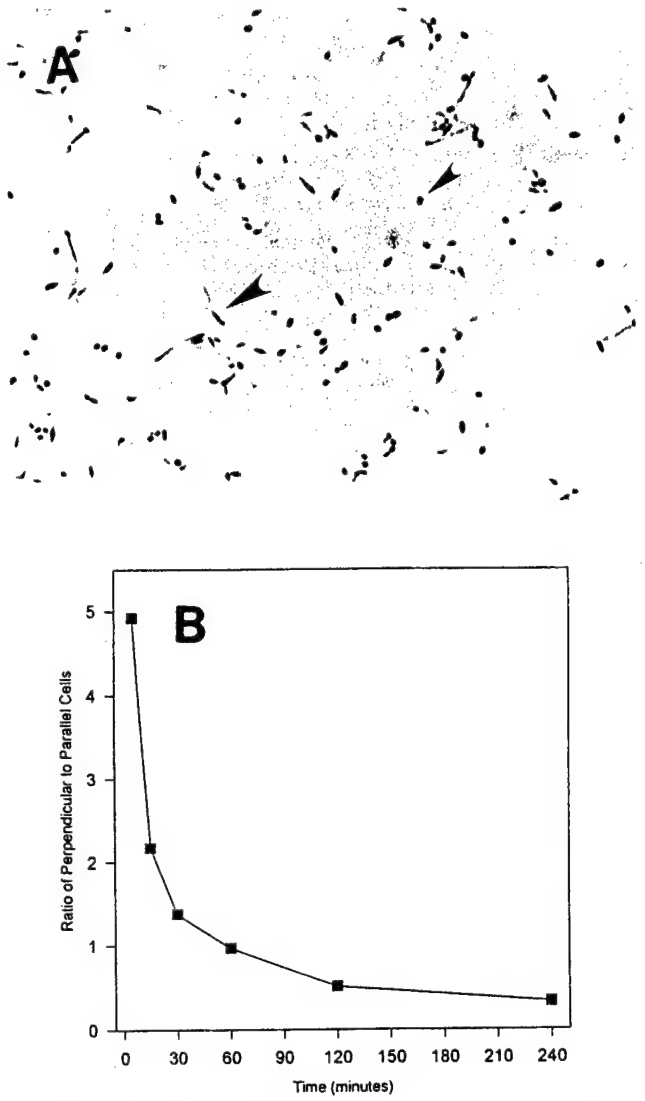

FIG. 8. Perpendicular versus parallel adhesion. (A) Phase-contrast image of VP-6 cells attached to a glass coverslip. Perpendicularly attached cells appear spherical (small arrowhead) and can be easily differentiated from those lying parallel to the surface (large arrowhead). Magnification, ×925. (B) Ratio of perpendicular to parallel cells relative to time of adhesion. The ratio of cells exhibiting perpendicular adhesion to those exhibiting parallel adhesion decreases with time.

tions and fine structures of surface polysaccharides on microbial cells. However, because surface polysaccharides are highly hydrated polymers (up to 99% water [26]), artifact formation during sample preparation is a legitimate concern. The major effect of dehydration is shrinking of the surface polysaccharides and loss of fine structure (26). However, negatively charged surface polysaccharides remain preserved, close to their original state, when they are treated with cationic ferritin or ruthenium red before the dehydration steps (1, 26). In addition, critical-point drying and chemical fixation, although not able to prevent shrinkage and artifact formation completely, have been used successfully in the observation of capsular material (26).

A number of aquatic bacteria have been shown to produce holdfasts. These include *Asticacaulis biprosthecum*, *C. crescentus*, *Flexibacter aurantiacus*, *Hyphomicrobium vulgarae*, *S. stellata*, species of *Thiothrix*, and *Hyphomonas* strains MHS-3 (9, 17, 18, 23, 31, 33) and VP-6 (this study). All of these organisms are believed to employ the holdfast for adhesion, and with the exception of MHS-3, which produces a less localized holdfast, all form rosettes in liquid culture. Unlike the holdfasts of *R. japonicum*, *A. biprosthecum*, *Thiothrix* species, *C. crescentus*, and *Hyphomonas* strain MHS-3, the VP-6 holdfast does not appear to be negatively charged, as was demonstrated by its inability to bind cationic ferritin (Fig. 4). This is surprising, because most adhesive surface polysaccharides carry a net negative charge (3). However, a neutral or positively charged holdfast may have the advantage of experiencing decreased repulsion by the negatively charged surface.

The VP-6 capsular EPS is a 550-kDa negatively charged polymer able to bind certain cationic metals and the carbohydrate-specific dye toluidine blue (11). The capsular EPS may measure up to 300 nm in thickness and is produced constitutively throughout the life cycle of the organism. Data presented both here and elsewhere (11) confirm that the EPS is used for adhesion and also probably serves as the biofilm matrix.

C. crescentus produces small amounts of a high-molecular-weight EPS believed to cover the entire cell; however, its function has not yet been determined (25). *S. stellata* also produces a second EPS in late growth stages (9) which contains an N-acetylated amino sugar. VP-6 EPS is produced constitutively during the entire life cycle and functions in cell adhesion (11). Thus, to the best of our knowledge, VP-6 is the first organism found to produce an adhesive holdfast and a second adhesive EPS concurrently. The reason for this apparent redundancy is not entirely clear but might be explained in the following way. The holdfast, either through its location on the cell or its chemical composition, is more specialized to make the initial adhesive bond. With time, the EPS exchanges hydrogen bonds with water for hydrogen bonds with the surface, thus slowly pulling the cell parallel to the surface. The selective advantage for this mechanism may be that cells lying parallel to the surface are more resistant to shear forces than cells attached perpendicularly, offering an advantage in turbulent environments. It is also possible that the EPS capsule may function primarily for protection, as a nutrient sink, or as the biofilm matrix and secondarily as an adhesin.

Staphylococcus epidermidis RP62A produces two extracellular polysaccharides known as capsular polysaccharide adhesin (CPA) and slime-associated antigen (SAA). Mutants for either CPA or SAA production showed that the CPA was used in the early stages of adhesion but that the SAA was involved in bacterial accumulation (27), a mechanism which might be mimicked by the holdfast and EPS of VP-6.

Capsular EPS surrounded the entire cell throughout the entire life cycle. However, SPL bound very weakly to the EPS of synchronized cells compared to its extent of binding to the EPS of a mid-logarithmic-phase culture. Thus, VP-6 may alter the composition of its capsular EPS as the culture ages. The exopolysaccharides of *Acinetobacter calcoaceticus* and *Klebsiella* sp. strain K32 varied in composition depending upon the available carbon source in the growth media (2). Similarly, *Pseudomonas atlantica* decreased the proportion of galactose and increased the proportion of uronic acids in its glycocalyx as the growth cycle progressed (30). VP-6 may similarly alter the composition of its capsular EPS, with one type being produced during lag and early-logarithmic growth phases (as would be the case in a synchronized culture) and another being produced as nutrients become depleted from the media in middle- to late-logarithmic phase (two-day culture). VP-6 also synthesizes a capsular EPS-associated 64-kDa protein (11). Perhaps that protein is synthesized only in older cultures, by modifying

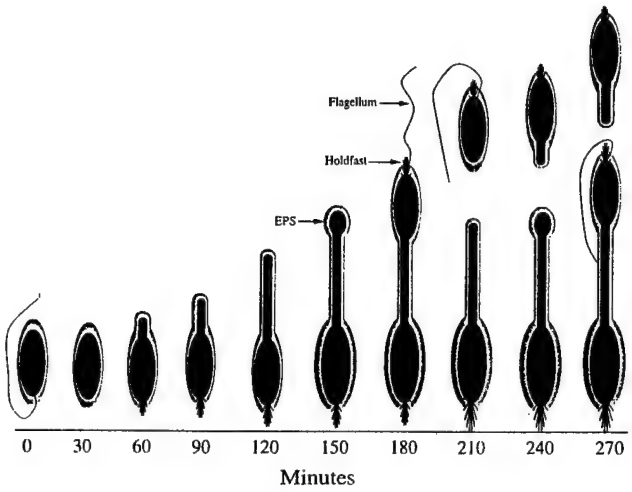

FIG. 9. Morphogenesis of VP-6 cells. Culture synchronization, electron microscopy, and incident light fluorescence microscopy were used to delineate morphogenesis. Prosthecum and holdfast production begins at 60 ± 10 min. The holdfast and flagellum are produced on a developing swarm cell after 180 ± 10 min. The swarm cell separates from the bud after 210 ± 10 min.

the orientation of EPS and making it a more suitable SPL ligand.

Figure 9 outlines the morphological development of VP-6 in a synchronous culture. An encapsulated and flagellated swarm cell sheds its flagellum after 30 ± 10 min and begins to produce a prosthecum and holdfast at 60 ± 10 min. Prosthecum elongation continues for the next 60 ± 10 min, with bud formation taking place at 150 ± 10 min. The holdfast and flagellum form on the bud after 180 ± 10 min, and separation of the swarm cell from the reproductive cell occurs at 210 ± 10 min. Reproductive cells continue to produce buds during the time that swarm cells begin the process of prosthecum elongation and, eventually, bud formation. Thus, VP-6 required 210 ± 10 min from the swarm cell stage to the release of the first progeny. Swarm cell maturation required 29%, prosthecal elongation required 43%, and swarm cell maturation required 29% of the developmental cycle. These values were 165 ± 15 min, 21%, 58%, and 21%, respectively, for MHS-3 (24).

The synchronized synthesis of holdfast by VP-6 and its use as an adhesin most closely resembles those properties of *C. crescentus*. Both produce holdfasts at the pole of the cell where the flagellum forms, and both organisms use holdfasts as a mechanism of swarm cell adhesion. The difference is that *C. crescentus* forms a prosthecum at the pole where the holdfast forms (22) while VP-6 forms a prosthecum at the opposite pole. In addition, *C. crescentus* does not produce a second adhesive EPS and therefore remains perpendicular to the surface while VP-6 initially binds perpendicularly but eventually lies parallel to the surface.

MHS-3 produces polar fimbriae at the tip of the reproductive cell distal to the prosthecum (22). Since the VP-6 holdfast and MHS-3 fimbriae are found on the same pole of the reproductive cell, parallels can be drawn between the two. Like fimbriae, the holdfast fibers may be of sufficient length (up to 300 nm) and diameter to breach the electrostatic repulsion barrier that exists between the cells and the surface. However, SEM of cells, attached to glass coverslips, shows that after moderate washing of the surfaces to remove loosely bound cells, remaining MHS-3 cells are attached via the holdfast, not the fimbriae. In contrast, VP-6 may use either the holdfast or the cell-surrounding EPS capsule to adhere strongly enough so that they are not removed by moderate shear forces. Thus, we postulate that the holdfast of VP-6 is primarily used in initial cell attachment to surfaces and that it can also function as a permanent adhesin. With *Hyphomonas*, *Caulobacter*, and a few other genera, temporal and spatial expression of capsule is a resource-conserving measure.

ACKNOWLEDGMENTS

We thank G. Geesey and E. Quintero for helpful insight and discussion and A. Snyder for technical assistance.

This work was supported in part by a subcontract from G. Geesey from the Office of Naval Research, Arlington, Va.

REFERENCES

1. **Bayer, M. E.** 1990. Visualization of the bacterial polysaccharide capsule. Curr. Top. Microbiol. Immunol. **150:**129–157.
2. **Bryan, B. A., R. J. Linhardt, and L. Daniels.** 1986. Variation in composition and yield of exopolysaccharides produced by *Klebsiella* sp. strain K32 and *Acinetobacter calcoaceticus* BD4. Appl. Environ. Microbiol. **51:**1304–1308.
3. **Christensen, B. E.** 1989. The role of extracellular polysaccharides in biofilms. J. Biotechnol. **10:**181–202.
4. **Christensen, B. E., J. Kjosbakken, and O. Smidsrod.** 1985. Partial physical and chemical characterization of two extracellular polysaccharides produced by marine, periphytic *Pseudomonas* sp. strain NCMB 2012. Appl. Environ. Microbiol. **50:**837–845.
5. **Costerton, J. W., G. G. Geesey, and K. J. Cheng.** 1978. How bacteria stick. Sci. Am. **120:**86–95.
6. **Decho, A. W.** 1990. Microbial exopolymer secretions in ocean environments: their role(s) in food webs and marine processes. Oceanogr. Mar. Biol. Annu. Rev. **28:**73–153.
7. **Fletcher, M., and G. D. Floodgate.** 1973. An electron-microscopic demonstration of an acidic polysaccharide involved in the adhesion of a marine bacterium to solid surfaces. J. Gen. Microbiol. **74:**325–334.
8. **Heilmann, C., C. Gerke, F. Perdreau-Remington, and F. Götz.** 1996. Characterization of Tn*917* insertion mutants of *Staphylococcus epidermidis* affected in biofilm formation. Infect. Immun. **64:**277–282.
9. **Hood, M. A., and J. M. Schmidt.** 1996. The examination of *Seliberia stellata* exopolymers using lectin assays. Microb. Ecol. **31:**281–290.
10. **Korber, D. R., J. R. Lawrence, H. M. Lappin-Scott, and J. W. Costerton.** 1995. Growth of microorganisms on surfaces, p. 15–45. *In* J. W. Costerton and H. M. Lappin-Scott (ed.), Microbial biofilms. Cambridge University Press, London, United Kingdom.
11. **Langille, S. L.** 1996. Capsular and holdfast extracellular polymeric substances of *Hyphomonas* strain VP-6 mediate adhesion to solid substrata. Ph.D. dissertation. University of Maryland, College Park.
12. **Langille, S. L., and R. M. Weiner.** 1996. Adhesive exopolysaccharide of *Hyphomonas* VP-6, abstr. I83, p. 160. *In* Abstracts of the 96th General Meeting of the American Society for Microbiology 1996. American Society for Microbiology, Washington, D.C.
13. **Luft, J. H.** 1971. Ruthenium Red and Violet: chemistry, purification, methods of use for electron microscopy and mechanism of action. Anat. Rec. **171:**374–378.
14. **Marshall, K. C.** 1992. Biofilms: an overview of bacterial adhesion, activity, and control at surfaces. ASM News **58:**202–207.
15. **Marshall, K. C.** 1976. Interfaces in microbial ecology. Harvard University Press, Boston, Mass.
16. **Marshall, K. C., and R. H. Cruickshank.** 1973. Cell surface hydrophobicity and the orientation of certain bacteria at interfaces. Arch. Mikrobiol. **91:**29–40.
17. **Melick, M., and R. M. Weiner.** Unpublished data.
18. **Merker, R. I., and J. Smit.** 1988. Characterization of the adhesive holdfast of marine and freshwater caulobacters. Appl. Environ. Microbiol. **54:**2078–2085.
19. **Mitchell, D., and J. Smit.** 1990. Identification of genes affecting production of the adhesion organelle of *Caulobacter crescentus* CB2. J. Bacteriol. **172:**5425–5431.
20. **Oliveira, D. R.** 1992. Physicochemical aspects of adhesion, p. 45–58. *In* L. F. Melo et al. (ed.), Biofilms—science and technology. Kluwer Academic Publishers, Dordrecht, The Netherlands.
21. **Ong, C. J., M. L. Y. Wong, and J. Smit.** 1990. Attachment of the adhesive holdfast organelle to the cellular stalk of *Caulobacter crescentus*. J. Bacteriol. **172:**1448–1456.
22. **Quintero, E. J.** 1994. Characterization of adhesion and biofilm formation by the marine prokaryote *Hyphomonas* MHS-3, p. 114–115. Ph.D. dissertation. University of Maryland, College Park.
23. **Quintero, E. J., and R. M. Weiner.** 1995. Evidence for the adhesive function of the exopolysaccharide of *Hyphomonas* strain MHS-3 in its attachment to surfaces. Appl. Environ. Microbiol. **61:**1897–1903.
24. **Quintero, E. J., K. Busch, and R. M. Weiner.** 1998. Spatial and temporal

deposition of adhesive extracellular polysaccharide capsule and fimbriae by *Hyphomonas* strain MHS-3. Appl. Environ. Microbiol. **64**:1246–1255.
25. **Ravenscroft, N., S. G. Walker, G. G. S. Dutton, and J. Smit.** 1991. Identification, isolation, and structural studies of extracellular polysaccharides produced by *Caulobacter crescentus*. J. Bacteriol. **173**:5677–5684.
26. **Roth, I. L.** 1977. Physical structure of surface carbohydrates, p. 5–26. *In* I. W. Sutherland (ed.), Surface carbohydrates of the prokaryotic cell. Academic Press, London, United Kingdom.
27. **Schumacher-Perdreau, F., C. Heilman, G. Peters, F. Gotz, and G. Pulver.** 1994. Comparative analysis of a biofilm forming *Staphylococcus epidermidis* strain and its adhesion-positive, accumulation-negative mutant M7. FEMS Microbiol. Lett. **117**:71–78.
28. **Sutherland, I. W.** 1983. Microbial exopolysaccharides—their role in microbial adhesion in aqueous systems. Crit. Rev. Microbiol. **10**:173–201.
29. **Tsein, H. C., and E. L. Schmidt.** 1981. Localization and partial characterization of soybean lectin binding polysaccharide of *Rhizobium japonicum*. J. Bacteriol. **145**:1063–1064.
30. **Uhlinger, D. J., and D. C. White.** 1983. Relationship between physiological status and formation of extracellular polysaccharide glycocalyx in *Pseudomonas atlantica*. Appl. Environ. Microbiol. **45**:64–70.
31. **Umbreit, T. H., and J. L. Pate.** 1978. Characterization of the holdfast region of wild-type cells and holdfast mutants of *Asticacaulis biprosthecum*. Arch. Microbiol. **118**:157–168.
32. **Wali, T. M., G. R. Hudson, D. A. Danald, and R. M. Weiner.** 1980. Timing of swarmer cell cycle morphogenesis and macromolecular synthesis by *Hyphomicrobium neptunium* in synchronous culture. J. Bacteriol. **144**:406–412.
33. **Williams, T. M., R. F. Unz, and J. T. Domain.** 1987. Ultrastructure of *Thiothrix* spp. and "type 021N" bacteria. Appl. Environ. Microbiol. **53**:1560–1570.

Recent Res. Devel. in Microbiology, 2 (1998)

Molecular level approach to microbial adhesion to inert surfaces

Peter A. Suci and Gill G. Geesey
Department of Microbiology and Center for Biofilm Engineering, Montana State University, Bozeman, MT 59717-3980, USA

Introduction

Many microbes spend all or part of their existence on surfaces. In many cases they have evolved specialized organs and appendages to promote the attachment process. In some instances, specific biomolecules have been assigned an adhesion function. At the molecular level, interactions between adhesive biomolecules and the substratum surface control the microbe's ability to first establish an initial association with the substratum as well as mediate a long-term association with the substratum. The focus of this review is the state of our understanding of molecular mechanisms responsible for microbial attachment to inert surfaces.

It is important is emphasize the association made here between "inert" and "molecular mechanisms". Investigations of adhesion of microbes to biological surfaces have demonstrated that, in general, adhesion is mediated by biomolecules with one or more binding sites for a restricted set of epitopes (1,2). The interactions, sometimes termed specific or stereo-specific interactions, which favor the bound over the unbound state are thought to be similar to those involved in enzyme/substrate or antibody/antigen associations. Interaction of microbial cells with inert surfaces has been widely investigated (3-5); however, with some exceptions, the approach used to investigate adhesion of microbes to inert surfaces differs profoundly from that taken in studies of adhesion to biological surfaces. Commonly, microbial adhesion to inert surfaces is considered to be driven by physicochemical properties of the cell envelope and the inert surface which can be characterized globally, without regard for the individual molecular composition of either.

Physicochemical approaches have been applied in diverse ecosystems including those associated with the oral cavity, the digestive tract, biomaterial-centered infections and industrial materials. In application of the Derjaguin-Landau-Verwey-Overbeck (DLVO) theory (6,7), microbes are treated as colloidal particles. In the simplest case, the colloid is represented

as a sphere and the surface as a plane, and the net effect of electrostatic and van der Waals forces on the potential energy of interaction is computed. The DLVO theory predicts that biological cells, whose envelopes typically have a net negative charge, cannot approach closer than the secondary energy minimum, about 10-20nm, from a typical (negatively charged) surface (8). Application of DLVO theory can adequately account for observed cell adhesion behavior in some cases (9). The prediction of relatively weak binding of a microbial cell at the secondary minimum, which can lead to stronger binding at the primary minimum, has served as a model for processes of reversible and irreversible attachment, respectively (10). Originating from the DLVO theory is the hypothesis that cells utilize appendages to breach the electrostatic barrier, in order to induce irreversible attachment (11).

The DLVO theory does not explicitly incorporate entropically driven adhesion forces which result from disordering of water. These hydrophobic effects can explain some adhesion behavior (12-16).

It is inaccurate to state that investigators have completely ignored the possibility that specific biomolecules have evolved in order to mediate adhesion to inert surfaces. However, it is fair to state that physicochemical approaches have dominated the literature. An argument can be made that these approaches have reached the limit of their power to predict cell adhesion behavior in specific instances. It is evident that in order to understand the influence of time-dependent, cell-regulated changes at the cell surface or molecular heterogeneity across the cell and substratum surface, a more reductionist approach must be taken. The purpose of this article is to provide a literature review for these types of studies.

Evidence for specialized adhesins for attachment to inert surfaces

Some of the earliest evidence that particular biomolecules serve to attach microbes to surfaces of inert substrata comes from the work of Floodgate (17) and Fletcher and Floodgate (18). Following the lead of an earlier study (10), they observed a fibrous material which appeared to anchor a marine bacterium to a cellulose ester filter. By combining histological staining and visualization by transmission electron microscopy they determined that a component of the fibers was acidic polysaccharide. It has become apparent that other types of biomolecules such as proteins reside in the extracellular matrix linking the bacterial cell to the substratum (19-21).

Existence of biomolecules which are specialized for attachment to surfaces of inert substrata can be demonstrated by selecting for adhesion-altered mutants. One method of selection is to exploit the enrichment for adhesion-altered mutants at various interfacial boundaries. Pringle et al. (22) described a method to separate mutant strains of a wild-type *Pseudomonas fluorescens* which had altered adhesion toward polystyrene from surfaces of this material submerged in a continuous culture apparatus. The primary finding was that production of an alginate-like acidic polysaccharide by the wild type and a mucoid strain inhibited attachment to both

polystyrene and treated (hydrophilic) polystyrene.

Other studies have shown that acidic exopolysaccharides promote cell adhesion to some surfaces. A mutant strain of the marine bacterium, *Deleya marina*, which produces rough colonies, lacks a uronic acid exopolysaccharide (23). Adhesion assays on hydrophobic and hydrophilic (chemically altered) polystyrene suggested that the acidic exopolysaccharide was involved in adhesion to the hydrophilic surfaces. The role of this exopolysaccharide in conferring adhesiveness toward hydrophilic surfaces was confirmed in a latter study (24).

Lectin-binding assays, treatment with lytic enzymes, and labeling with calcofluor provided evidence that the holdfast of a marine *Hyphomonas sp.* was primarily composed of polysaccharide, but that N-acetylglucosamine residues of this polysaccharide were involved in mediating cell adhesion to glass (25). Adsorption studies on a germanium substratum using the purified polysaccharide suggested that this putative polysaccharide adhesin had molecular properties catered to promoting strong interactions with mineral oxides (26).

Based on the limited data published to date, it appears that cell surface polysaccharides, when not in excess, promote cell attachment to hydrophilic surfaces. When the cell surface is depleted of polysaccharide, cells appear to attach more readily to hydrophobic surfaces. The absence of surface-localized polysaccharides may expose other biopolymers, such as proteins, which confer adhesiveness toward hydrophobic surfaces. It has long been known that proteins enriched in amino acids containing hydrophobic side chains confer a degree of hydrophobicity to the cell envelope and thus promote cell adhesion through hydrophobic interactions (27). Direct evidence for participation of a specific protein in hydrophobic adhesive interactions has been obtained from the bacterium, *Serratia marcescens* (28). The protein has been named serraphobin. It can be isolated from the culture supernatant of wild type strains, which adhere avidly to a hydrophobic interface (e.g., water/hexadecane), but is absent from that of an adhesion-deficient mutant. The adsorption behavior of this protein is consistent with its putative role in adhesion. Paul and Jeffrey (29) presented evidence for an adhesive role for proteins excreted by *Vibrio proteolytica* on polystyrene surfaces. Absence of long (primarily proteinaceous) fibrils on the pathogenic fungus, *Candida albicans*, exposes hydrophobic proteins which enhance adhesion of the cells to hydrophobic substrata (30). Adhesins which promote bonding to substrata through hydrophobic interactions have been termed "hydrophobins" (14).

One of the most well-characterized biomolecules mediating cell adhesion to surfaces (polystyrene) is fucoidin, a glycoprotein from the brown alga, *Fucus* (31). Fucoidan has significant sequence homology with vitronectin. Sulfonate functionalities associated with the oligosaccharide chain appear to be required for adhesion of the *Fucus* zygote to surfaces (32).

Localization of non-specific adhesins on the cell surface

Bioadhesive molecules may be

localized in specific areas of the cell surface, indicating that polarity is important to cell attachment to surfaces. *Caulobacter* spp. produce small quantities of holdfast material at the tip of a stalk structure (33). Marine *Hyphomonas* strains elaborate an adhesive polysaccharide around the mother cell but not around the stalk and daughter cell (25). Thus, control over production and cell surface localization of biomolecules appears to be an important part of the adhesion process.

Genetic basis of non-specific adhesion

Many adhesive bacteria in the marine environment produce extracellular polysaccharides after the initial attachment stage, particularly during microcolony growth (34). Vandevivere and Kirchman (35) showed that attachment to silica sand stimulated exopolysaccharide synthesis by a bacterium. Davies and Geesey (36) showed that cells of the bacterium *Pseudomonas aeruginosa,* up-expressed for a gene associated with extracellular polysaccharide synthesis, had a tendency to remain associated with a glass substratum longer than cells that were not expressing the gene. Synthesis of extracellular polysaccharide by the marine bacterium *Pseudoalteromonas (Pseudomonas) atlantica* is controlled by gene rearrangement of DNA on the chromosome (37). Whether this influences cell adhesion remains to be determined. Significant progress has been made in identifying the genes responsible for *Caulobacter* sp. holdfast production (38). The holdfast mediates adhesion between cells and adhesion to various inert substrata.

Biomolecules that promote detachment of cells from surfaces

Biopolymers may be produced not only to enhance cell adhesiveness toward various surfaces of inert substrata, but may also be produced to induce cell detachment from a surface. This has been demonstrated for *Pseudomonas* sp., strain S9 (39). This marine bacterium produces a neutral extracellular polysaccharide during starvation which causes the cells to be released from hydrophobic surfaces.

Summary and conclusions

The approach for investigating adhesion of microbes to inert, engineered or inert surfaces has been dominated by theories which treat the cells as objects having overall surface characteristics which can be used to predict adhesion behavior. Within the last twenty years it has become apparent that adhesion to biological tissues is regulated, in many cases, by adhesins which have evolved specialized stereo-specific binding pockets for particular ligands. The existence of biomolecules which have evolved to mediate adhesion to inert substrata is documented, especially for adhesion through hydrophobic interactions but, in general, is a less well studied area.

A molecular level approach to biological adhesion to inert substrata involves extensive laboratory investigation. At this stage of our understanding, an approach that utilizes model organisms in well-defined systems should be employed to maximize the chances of successfully identifying the biomolecules that mediate cell adhesion to inert substrata. The adhesive

biomolecules must be isolated and purified in sufficient quantities to allow characterization of their adsorption behavior. Finally, their adsorption behavior should be related to some aspect of the cell's adhesion behavior. Despite these labor-intensive manipulations, a molecular level approach to the investigation of cell adhesion to inert surfaces is tractable and may reveal that adhesins have evolved to employ a standard set of strategies to maximize bonding to particular substrata. The identification of these strategies could lead to new ideas for antifouling surface coatings or for molecular architectures for underwater biomimetic adhesives. At a more fundamental level, it may reveal the extent to which surface associated microbes have adapted to their environment at a biochemical level.

Acknowledgment

Preparation of this review was supported by the Office of Naval Research grant N00014-97-1-1062 and the National Science Foundation Grant EEC8907039.

References

1. Jann, K. & Jann, B. 1990. In: Jann, K, Jann, B. (Editors), *Currents Topics in Microbiology and Immunology* 151, 1, Springer-Verlag, New York
2. Salamitou, S., Lemaire, M., Fujino, T., Ohayon, H., Gounon, P., Beguin, P. & Aubert, J-P. 1994. J. Bacteriol. 176, 2828.
3. Fletcher, M. 1990. Methods in Microbiology 22, 251.
4. Mittelman, M.W. 1996. In: Fletcher, M., Savage, D., (Editors), Bacterial adhesion: molecular and ecological diversity, Page 89, Wiley-Liss, Inc., New York, NY
5. Rosenburg, M. 1991. Crit. Rev. Microbiol. 18, 159.
6. Derjaguin, B.V. & Landau, L. 1941. Acta Physicochim. USSR 14, 633.
7. Verwey, E.J.W. & Overbeck, J.Th.G. 1948. Theory of the stability of lyophobic colloids. Elsevier, Amsterdam.
8. Busscher, H.J. & Weerkamp, A.H. 1987. FEMS Microbiol. Rev. 46, 165.
9. Van Loosdrecht, M.C.M., Lyklema, J., Norde, W. & Zehnder, A.J.B. 1989. Microb. Ecol. 17, 1.
10. Marshall, K.C., Stout, R. & Mitchell, R. 1971. J. Gen. Microbiol. 68, 337.
11. Jones, G.W. & Isaacson, R. E. 1983.

Crit. Rev. Microbiol. 10, 229.

12. Dexter, S.C., Sullivan Jr., J.D., Williams III, .J & Watson, W., 1975. Appl. Microbiol. 30, 298.

13. Fletcher, M. & Loeb, G. I. 1979.. Appl. Environ. Microbiol. 37, 67.

14. Rosenberg, M. & Kjelleberg, S. 1986. Adv. Microb Ecol. 9, 353.

15. Busscher, H.J., Bellon-Fontaine, M.N., Mozes, N., Van der Mei, H.C., Sjollema, J., Cerf, O. & Rouxhet, P.G. 1990. Biofouling 2, 55.

16. Doyle, R J. & Rosenberg, M. 1990. Microbial Cell Surface Hydrophobicity, American Society for Microbiology, Washington, D.C.

17. Floodgate, G.D. 1972. Mem. Ist. Ital. Idrobiol. 29 Suppl., 309.

18. Fletcher, M. & Floodgate, G.D. 1973. J. Gen. Microbiol. 74, 325.

19. Humphrey, B.A., Dickson, M.R. & Marshall, K.C. 979. Arch. Microb. 120, 231.

20. Abu, G.O., Weiner, R.M. Rice J., & Colwell R R. 1991. Biofouling 3, 69.

21. Vincent, P., Pignet, P., Talmont, F., Bozzi, L., Fournet, B., Guenennec, C., Jeanthon, C., & Prieur, D. 1994. Appl. Environ. Microbiol. 60, 4134.

22. Pringle, J.H., Fletcher, M. & Ellwood, D.C. 1983. J. Gen. Microbiol. 129, 2557.

23. Shea, C., Nunley, J.W., Williamson, J.C. & Smith-Somerville, H.E. 1991. Appl. Environ. Microbiol. 57, 3107.

24. Shea C, Smith-Somerville, H.E. 1994. Biofouling 8,:13.

25. Quintero, E.J. & Weiner, R.M. 1995. Appl. Environ. Microbiol. 61, 1897.

26. Suci, P.A., Frølund, B, Quintero, E.R, Weiner, R. M, Geesey, G.G. 1995. Biofouling 9, 95.

27. Nesbitt, W.E., Doyle, R.J., Taylor, K.G. 1982. Infect Immun. 38, 637.

28. Bar-ness, R. & Rosenberg, M. 1989. J. Gen. Microbiol. 135, 2277.

29. Paul, J.H. & Jeffrey, W.H. 1985. Appl. Environ. Microbiol. 50, 431.

30. Hazen, K.C. & Glee, P.M. 1994. Can. J.

Microbiol. 40, 266.

31. Wagner,V.T., Leigh, B., & Quatrano, R.S. 1992. Proc. Natl. Acad. Sci. 89, 3644.
32. Crayton, M.A., Wilson, E., & Quatrano, R.S. 1974. *Dev. Biol.* 39,164.
33. Merker, R.I. & Smit, J. 1988. Appl. Environ. Microbiol. 54, 2078.
34. Corpe, W.A., Matsuuchi, L. & Armbruster, B. 1976. In: Sharpley, J.M. & Kaplan, A.M (Editors), Proceddings of the 3rd Internat. Biodegrad. Symp., Page 433, Applied Sciences Ltd., London.
35. Vandevivere, P. & Kirchman, D.L. 1993. Appl. Environ. Microbiol. 59, 3280.
36. Davies, D.G., & Geesey, G.G. 1995. Appl. Environ. Microbiol. 61, 860.
37. Bartlett, D.H., Wright , M.E. & Silverman, M. 1988. Proc. Natl. Acad. Sci. USA 85,:3923.
38. Yun, C., Ely, B. & Smit, J. 1994. J. Bacteriol. 176, 796.
39. Wrangstadh, M., Conway, P.L. & Kjelleberg, S. 1986. Arch. Mic*robiol.* 145, 2207.

APPLIED AND ENVIRONMENTAL MICROBIOLOGY, Apr. 1998, p. 1246–1255
0099-2240/98/$04.00+0

Vol. 64, No. 4

Spatial and Temporal Deposition of Adhesive Extracellular Polysaccharide Capsule and Fimbriae by *Hyphomonas* Strain MHS-3

ERNESTO J. QUINTERO, KATHRYN BUSCH, AND RONALD M. WEINER*

Department of Microbiology, University of Maryland, College Park, Maryland 20742

Received 25 August 1997/Accepted 7 January 1998

***Hyphomonas* strain MHS-3, a member of a genus of primary colonizers of surfaces immersed in marine water, synthesizes two structures that mediate adhesion to solid substrata, namely, capsular exopolysaccharide and fimbriae. Specific stains, gold-labelled lectins, and monoclonal antibodies, along with transmission electron microscopy of synchronized populations, revealed that both structures are polarly and temporally expressed. The timed synthesis and placement of the fimbriae and capsule correlated with the timing and locus of MHS-3 adhesion.**

Members of the marine bacterial genus *Hyphomonas* have a biphasic life cycle; swarm cells are planktonic entities, and prosthecate cells are sessile, benthic forms (14). These organisms are primary colonizers of surfaces in the marine environment (1, 3, 19, 38, 39, 42, 54) and are important because they adhere and form microcolonies (8, 33) which modify and enrich the surfaces. Thus, they can render a surface more suitable for subsequent attachment of heterotrophic bacteria, microalgae, fungi, and protozoans (13, 17). Such an adherent community can have profound effects on the subsequent colonization of the surface by invertebrates and on its ultimate performance (5, 12, 56, 57).

In order to adhere, bacteria produce extracellular adhesive structures that bridge repulsive electrostatic forces on submerged substrata. Functionally, these structures reduce the effective radius of interaction between the surface and the cell, thereby lowering the energy barrier (32, 40). Several types of proteinaceous structures may mediate transitory (primary) attachment of bacteria to surfaces. Among these are polar flagella (40, 61) and fimbriae (27, 40). Permanent cementation to surfaces requires the synthesis of exopolysaccharides (EPS) (9, 16, 32). EPS form the hydrated matrix in which multiple layers of cells and other materials become embedded, forming a biofilm (7). It has also been suggested that bacterial EPS are involved in primary adhesion (12), and more than 80% of the marine bacteria associated with deep-sea aggregates have EPS capsules (10).

The positions of polar structures in bacteria often correlate with physiological function (31). A number of different species of bacteria produce polar adhesive structures (holdfasts), leading to cell asymmetry and cell attachment in a distinct orientation. In *Thiothrix* spp., *Seliberia stellata*, and members of the prosthecate genera *Caulobacter* and *Asticcacaulis*, cells attach to inanimate surfaces and to one another (forming rosette-like aggregates) by polar production of fimbriae and EPS holdfasts (22, 30, 42, 51, 59). Several members of the prosthecate genus *Hyphomonas* and the related genus *Hyphomicrobium* also attach polarly to surfaces and form rosettes (36, 55). It has been theorized, but not demonstrated, that a *Hyphomicrobium* cell adheres via a polar holdfast opposite the prosthecum (35).

* Corresponding author. Mailing address: Department of Microbiology, University of Maryland, College Park, MD 20742. Phone: (301) 405-5435. Fax: (301) 314-9489. E-mail: rw19@umail.umd.edu.

Hyphomonas strain MHS-3 synthesizes copious amounts of an integral, capsule-like EPS, which is associated with flocculation in broth cultures and the formation of thick biofilms on both hydrophilic and hydrophobic surfaces. The MHS-3 EPS capsule has been observed only during the sessile stage (43), and its adhesive properties have been demonstrated (43, 47). The purified polymer has been partially characterized; one of its major components is galactosamine which appears to be acetylated (44). In this paper, we show that adhesive fimbriae and capsular EPS are expressed both polarly and temporally by MHS-3 and that the presence and location of these structures correlate with the previously reported timing and locus of cell adhesion (43).

MATERIALS AND METHODS

Bacterial strains, media, and chemicals. Wild-type *Hyphomonas* strain MHS-3 was isolated from shallow-water sediments in Puget Sound in Washington by J. Smit and was kindly given to R.M.W. Reduced-adhesion (rad) phase variants were isolated on the basis of their different colony morphology on agar plates and were named for their low adhesion to surfaces and low biofilm production. These strains were cultured in marine broth 2216 (MB) (54) (37.4 g/liter; Difco Laboratories, Detroit, Mich.) at 25°C. Marine agar contained MB and 2% (wt/vol) agar.

Electron microscopy stains and supplies were purchased from Electron Microscopy Sciences (Fort Washington, Pa.) or Sigma Chemical Co. (St. Louis, Mo.). Other chemicals and supplies were obtained from VWR Scientific (Bridgeport, N.J.). Copper grids (200 or 400 mesh) were used for electron microscopy; all grids were coated with collodion and then coated with carbon by using a type MED 10 deposition system (Balzers Union, Fürstentum, Liechtenstein).

Negative staining. Single drops of MHS-3 were placed on collodion-coated copper grids, cells were allowed to attach for 1 min, and the grids were blotted with filter paper. To negatively stain the cells, 5 drops of 1% uranyl acetate were placed on the grid (for <1 min) and then blotted. The stained cells were observed with a model JEM-100CX II transmission electron microscope (TEM) (JEOL Ltd., Tokyo, Japan).

Preparation of whole-cell antigen. Cultures (100 ml) of MHS-3 in the early stationary phase were pelleted by centrifugation (10,000 × *g*), resuspended in 100 ml of a sterile 3% NaCl solution containing 0.337% formaldehyde, incubated at 25°C for 30 min, washed once with 100 ml of 3% NaCl and twice with sterile 0.1 M phosphate-buffered saline (PBS), and resuspended in 0.1 M PBS at a concentration of approximately 1.25 mg (dry weight)/ml.

Immunization of mice. Six-week-old BALB/c mice were injected intraperitoneally (i.p.) with 0.2 ml of a 1:1 mixture of whole formalized cells (125 μg of dry wild-type cells) and complete Freund's adjuvant. The mice were boosted i.p. with whole cells mixed as described above in incomplete Freund's adjuvant five times at 2-week intervals. The serum antibody titer was monitored 3 days after each boost by performing an enzyme-linked immunosorbent assay (ELISA) (see below). If the antibody titer was sufficient (>10,000) after the sixth boost, the mice were sacrificed 3 days later.

Production of MAbs. The weak immunogen method of Lane et al. (28) was used for spleenocyte fusions to Sp2/O myeloma cells. Hybridomas were grown,

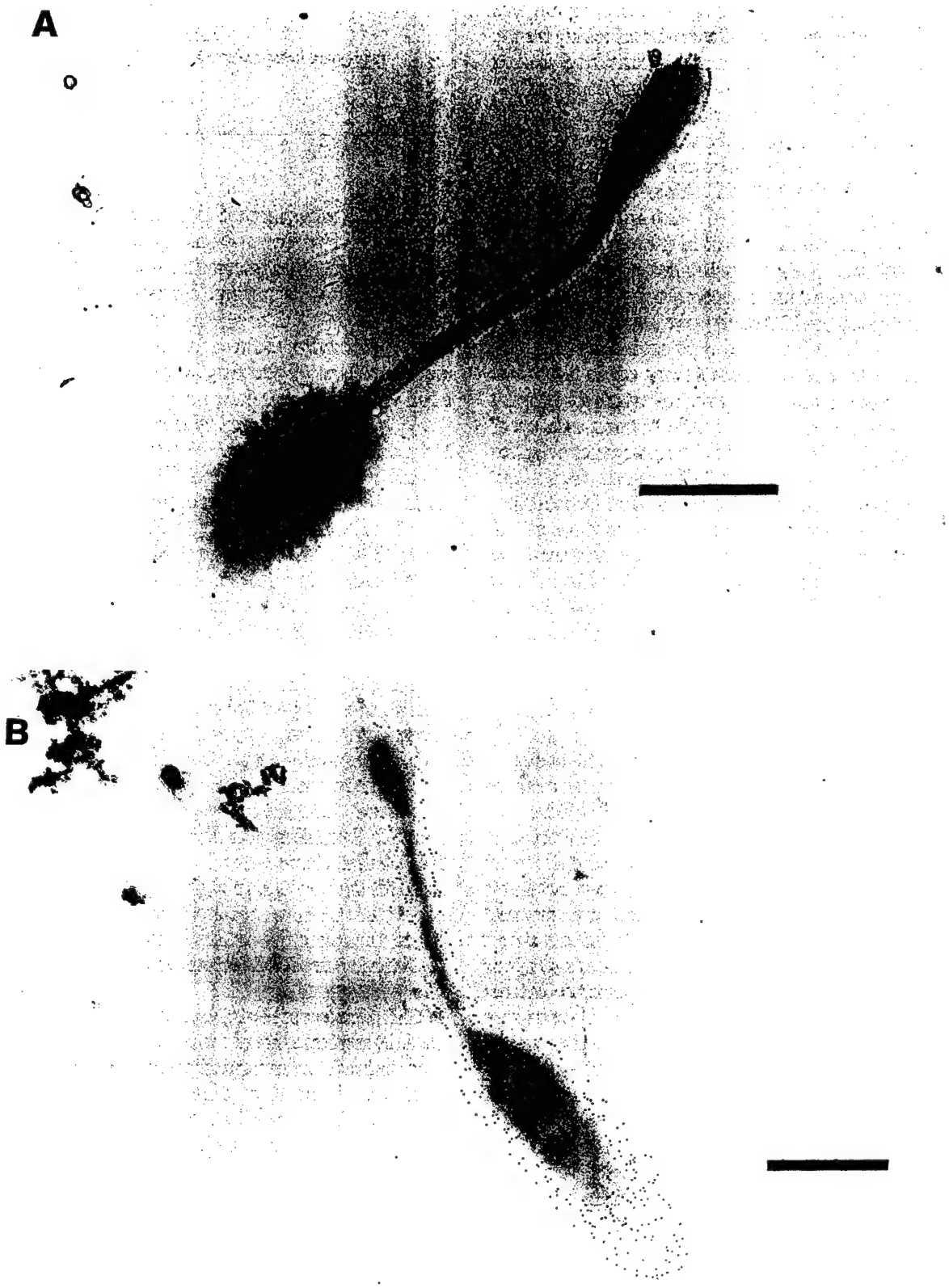

FIG. 1. Immunoelectron microscopy of *Hyphomonas* strain MHS-3 wild-type (A) and rad (B) whole cells. Anti-LPS MAb bound only the prosthecum and swarm cell in the wild-type strain (A); it labelled all the structures in the rad strain (B). Bars = 1 μm.

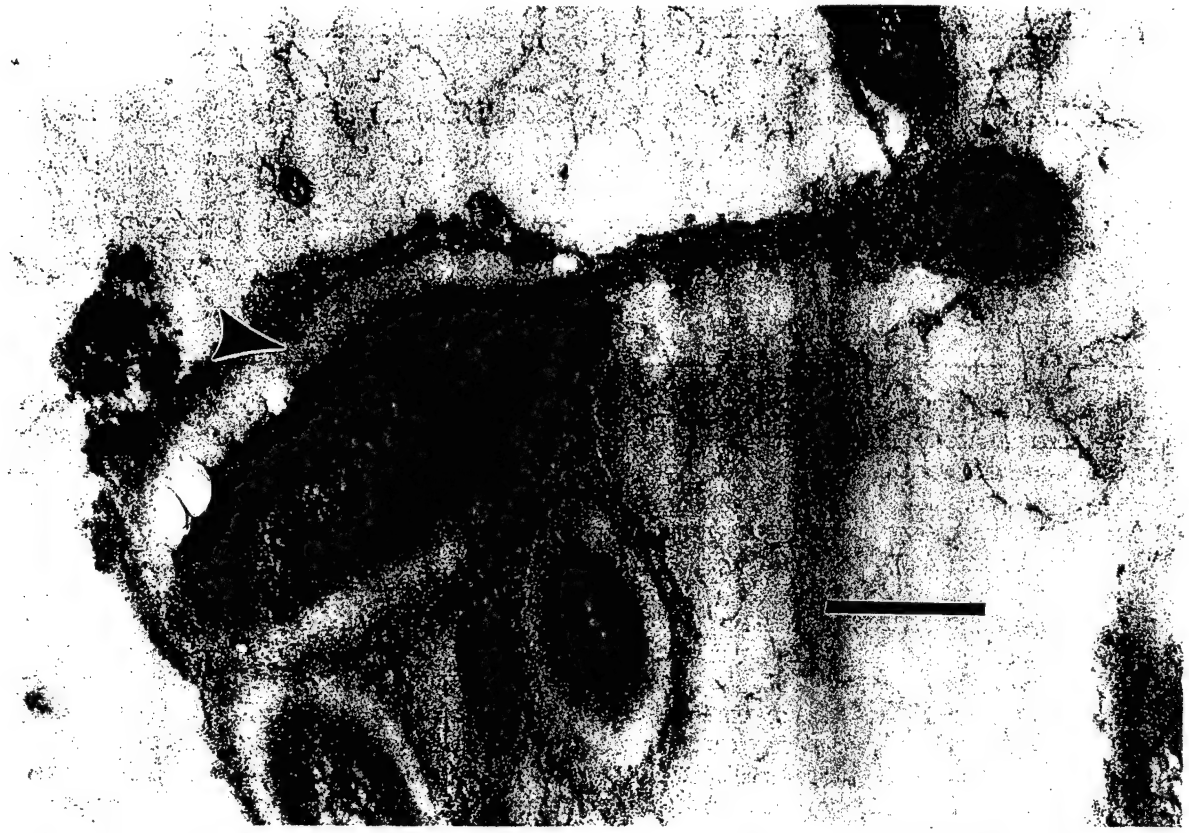

FIG. 2. Thin section of polycationic ferritin-treated *Hyphomonas* wild-type strain MHS-3. Note the presence of a spatially defined capsule on the body of the prosthecate reproductive cell (arrowhead). Bar = 0.5 μm.

screened, cloned, and stored in liquid nitrogen as described elsewhere (18). The monoclonal antibody (MAb) isotype was determined by using a Screentype isotyping kit (Boehringer Mannheim Biochemicals, Indianapolis, Ind.). Ascites fluid was produced by using 6-week-old BALB/c mice injected i.p. with 0.3 ml of pristane (18). Antibodies were concentrated by ammonium sulfate precipitation (18). Immunoglobulin G (IgG) MAbs were purified by affinity chromatography with a MAC protein A capsule (Amicon, Beverly, Mass.) and were concentrated by using Centriprep concentrator centrifuge tubes (Amicon).

ELISA. Serum titers and hybridomas were initially screened by an ELISA (15, 52), with each well of 96-well Falcon flexible microtiter plates coated overnight at 4°C with 100 μl of formalized MHS-3 cells (prepared as described above) in coating buffer (10.6 g of Na_2CO_3 per liter; pH 9.6). For serum testing, the titer was defined as the largest dilution showing a strong positive reaction, and only these antibodies were examined further.

Screening for anti-MHS-3 LPS MAbs. Lipopolysaccharide (LPS) samples were prepared with protease-treated whole-cell lysates and were subjected to sodium dodecyl sulfate-polyacrylamide gel electrophoresis by a modification of the method of Hitchcock and Brown (20). Lanes were loaded with the equivalent of 100 μg (dry weight) of whole cells. In the control gels, LPS was stained by the silver staining method of Tsai and Frasch (48), as modified by Hitchcock and Brown (20), in order to identify the MHS-3 LPS band pattern. Other gels were blotted onto nitrocellulose membrane filters (model 2117-250 Novablot electrophoretic transfer kit; Pharmacia LKB) by using continuous transfer buffer (39 mM glycine, 48 mM Tris, 0.375% [wt/vol] sodium dodecyl sulfate, 20% [vol/vol] methanol) and 140 mA.

To screen for anti-LPS MAbs, LPS-loaded nitrocellulose strips were blocked for 1 h with 5% skim milk (Difco) in PBS buffer and then individually incubated for 2 to 12 h with 50 ml of 5% skim milk (in PBS) containing 2 to 5 ml of supernatant from positive hybridoma cell lines. The blots were washed three times with PBS and incubated for 2 h with horseradish peroxidase-labelled goat anti-mouse IgG secondary antibody (GIBCO BRL, Grand Island, N.Y.) diluted 1:2,000 in milk-PBS. The strips were washed three times with PBS and incubated for 10 to 20 min in 50 ml of peroxidase substrate buffer (1 ml of 2 M Tris [pH 8.0], 20 mg of 4-chloro-1-naphthol, 10 ml of 30% hydrogen peroxide, and 49 ml of distilled H_2O). Strips that developed band patterns identical to the pattern obtained with the LPS silver stain were considered positive, and the hybridoma cell lines were cloned and examined further. The hybridoma ultimately selected for this study produced an IgG2A kappa light chain.

Immunoelectron microscopy. Cells were placed on collodion-coated copper grids (see above) and blocked for 10 min with 5% skim milk in PBS, and then the grids were inverted on 1 drop of a 1:750 anti-MHS-3 LPS MAb–skim milk solution for 10 min. The grids were rinsed by inverting them on 2 successive drops of skim milk, placed on 1 drop of 1:10 gold-conjugated protein A in skim milk (15-nm colloidal gold particles), and incubated for 10 to 30 min to allow the protein A to bind the IgG bound to the MHS-3 cell surface. Finally, the grids were rinsed by inverting them on 4 to 6 successive drops of distilled H_2O (10 to 20 s each) and then observed with a model JEM-100CX II TEM (JEOL Ltd.).

Thin sectioning. Cells were fixed by adding glutaraldehyde to mid-log-phase cultures of wild-type MHS-3 and rad phase variants (final concentration of fixative, 1%), incubated for 2 h at 25°C, and washed twice with 1× PBS. Cell pellets were resuspended in 1 ml of 1× PBS and mixed with an equal volume of molten agar (4%, 45°C), which was placed on Parafilm and allowed to harden. The agar was cut into 1- to 3-mm^3 blocks, which were dehydrated by using a graded series of ethanol dilutions (30, 50, and 70% [twice], 30 min at each dilution), placed in microcentrifuge tubes containing LR White resin (LRW) and 70% ethanol (2:1) for 30 min, incubated with LRW for 1 h, transferred to tubes containing fresh LRW, incubated overnight at 25°C, transferred to tubes containing fresh LRW again, and incubated for 1 h. Finally, the blocks were placed in gelatin capsules with fresh LRW and incubated in a vacuum oven at 50°C for 72 h to allow the resin to polymerize.

Each gelatin capsule was removed from the polymerized resin, trimmed with a blade to expose the agar block region containing the embedded cells, and cut to make a 1-mm^2 face. Thin sections (50 to 70 nm thick) were obtained with a model FC4E Ultracut E microtome (Reichert-Jung, Vienna, Austria) equipped with a diamond knife (Du Pont Co., Wilmington, Del.). For immunostaining, the sections were blocked with 5% skim milk and treated with anti-MHS-3 LPS MAb and protein A-gold as described above for whole cells.

Labelling of capsule with polycationic ferritin. The procedure used to label capsule with polycationic ferritin was a modification of the protocol described by Jacques and Foiry (25). Briefly, mid-log-phase cultures of MHS-3 were fixed with glutaraldehyde as described above. The fixed bacteria were resuspended in cacodylate buffer (0.1 M sodium cacodylate, pH 7.0) and treated with polycationic ferritin (final concentration, 1.0 mg/ml) for 30 min at 25°C. The reaction was slowed by diluting the preparation 10-fold with buffer, and the cells were centrifuged and washed three times with cacodylate buffer. The bacteria were mixed with molten agar, embedded in LRW, and thin sectioned as described above.

FIG. 3. Immunoelectron microscopy of thin sections of *Hyphomonas* wild-type strain MHS-3 (A) and the rad strain (B) treated with polycationic ferritin by using anti-LPS MAb. Whole cells were stained with polycationic ferritin, fixed, embedded, and thin sectioned; the thin sections were exposed to the MAb. In wild-type strain MHS-3 the outer edge of the EPS capsule is delineated by polycationic ferritin binding (large arrowhead), while the outer membrane is clearly delineated by the binding of the MAb-protein A-gold complexes (small arrowhead). In the MHS-3 rad strain polycationic ferritin bound to the outer membrane of the cell (large arrowhead), as did anti-LPS MAb (small arrowhead), indicating that no capsule was present. Bars = 0.5 μm.

Lectin-gold labelling of capsular EPS. The procedure used for lectin-gold labelling of capsular EPS was carried out as reported previously (43). Gold-labelled *Bauhinia purpurea* lectin (BPA-Au) (10-nm gold particles; EY Laboratories, Inc., San Mateo, Calif.) was used to visualize MHS-3 capsular EPS. Briefly, 1 drop of a mid-log-phase culture was placed on a collodion-coated copper grid, incubated at room temperature for 1 min, blocked with a solution containing 5% bovine serum albumin in 0.1 M PBS for 5 to 10 min, incubated with a 1:10 dilution of BPA-Au in 5% bovine serum albumin for 10 to 15 min, and then rinsed five times with distilled water. The grids were observed with the TEM.

Synchronization of *Hyphomonas* strain MHS-3 cultures. An effective protocol to isolate MHS-3 swarm cells is a modification of the differential size separation procedure used by Wali et al. (53) to synchronize cultures of *Hyphomonas neptunium*. Briefly, an early- to mid-log-phase broth culture of MHS-3 was chilled on ice and centrifuged at 2,500 × *g* for 3 to 5 min to pellet large flocs and cell aggregates. The pellet was discarded, and the chilled supernatant was passed through sterile 1.2-μm-pore-size membrane filters (Millipore Corp., Bedford, Mass.). Prosthecate cells were retained by the filters, and the filtrates, containing the swarm cells, were pooled and pelleted by centrifugation (16,000 × *g*, 30 min, 4°C). The pellet was resuspended in 10 ml of MB to start a synchronous culture at 25°C. These manipulations yielded a highly synchronous population; however, they also caused a lag period of approximately 90 min (14, 53).

Once the synchronous culture was initiated, 400-μl aliquots were removed at 15-min intervals, placed in microcentrifuge tubes with either glutaraldehyde (final concentration, 1%) or sodium azide (final concentration, 0.02%), and stored at 4°C. Glutaraldehyde was not used as a fixative for cells labelled with lectin-gold because it interfered with the binding of the conjugate to the MHS-3 capsule. Cells at different stages of development were negatively stained with uranyl acetate and labelled with lectin-gold as described above.

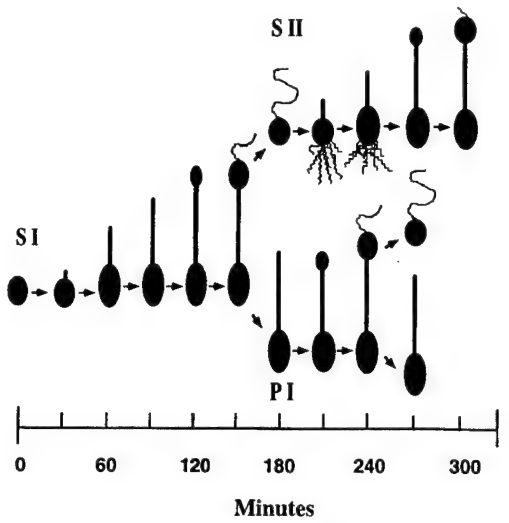

FIG. 4. Timing of morphogenesis during synchronous growth of *Hyphomonas* strain MHS-3. S I cells, S II cells, and the first prosthecal generation (P I) are shown. The experimentally induced lag period was factored out.

RESULTS

The location of the EPS capsule on *Hyphomonas* strain MHS-3 was determined by immunoprobing with EPS-specific stains and the TEM. An EPS-deficient mutant of MHS-3 (a rad strain [43]) was used as the negative control. The body, prosthecum, and bud were easily recognized in each prosthecate reproductive cell. In wild-type cells, MAb bound to swarm cells and to the prosthecum, but not the body, of a prosthecate reproductive cell (Fig. 1A). In a control rad strain cell, the MAb bound everywhere, including the body (Fig. 1B). Furthermore, when wild-type cells were sheared in a blender in the presence of EDTA to remove most of the capsular EPS, anti-LPS MAb also bound to the bodies of prosthecate reproductive cells (data not shown). We interpreted these results to mean that the EPS capsule blocked access of MAb to the outer membrane of the body of a wild-type cell. Thus, anti-LPS MAb served as a negative stain for the capsule, which was found to surround only the main body of each wild-type prosthecate cell.

The same results were obtained when MHS-3 cells were treated with polycationic ferritin prior to fixing, embedding, and sectioning (Fig. 2). The polycationic ferritin penetrated the EPS capsule just enough to reveal its outer edge. When these cells were thin sectioned and then treated with anti-LPS MAb, the outer membrane was delineated, revealing that it was covered by the capsule (Fig. 3A), which was calculated to be 200 to 300 nm in diameter (by using the average diameter of the 15-nm gold particles as a reference). When the same experiment was repeated with the rad strain, the anti-LPS MAb and the polycationized ferritin each bound in the same location, the site of the outer membrane (Fig. 3B).

The temporality of capsule elaboration during the relatively complex life cycle of *Hyphomonas* strain MHS-3 was ascertained by using synchronous cultures. The postulated MHS-3 biphasic developmental cycle is diagrammed in Fig. 4. Generation I swarm (S I) cells required 30 min for maturation and initiation of prosthecal outgrowth and capsule deposition (swarm maturation period), which occurred concurrently (Fig. 4 and 5). The EPS appeared to be uniformly exported over the entire surface of the developing prosthecate reproductive cell. In Fig. 5A, which shows two adjacent young prosthecate reproductive cells, the onset of the timing of these processes is underscored. One cell was completely labelled with the MHS-3 capsular EPS-specific lectin, BPA-Au, while the other cell was not labelled (onset of capsule deposition). This difference was also revealed by using anti-LPS MAbs. Only the nascent prosthecae of cells at the same time point bound anti-LPS MAbs (Fig. 5B), leading to the conclusion that the onset of capsule deposition coincides with the initiation of prosthecal synthesis. S I prosthecate cells formed buds at 120 ± 15 min. After 150 min, S I cells were fully developed reproductive cells that budded at the distal ends of their prosthecae (bud maturation period, 30 min). The generation II swarm (S II) cells were released by the prosthecate reproductive cells at 165 ± 15 min during the synchronous cycle.

During the second swarm cell generation (S II) (Fig. 4) swarm cells matured and initiated prosthecal outgrowth and capsule deposition within 30 min after they were released, as they had during the first generation. New buds formed approximately 90 min into the S II phase. One unexpected generation II event, not observed during the first generation, occurred at 195 ± 15 min. Polar fimbriae were synthesized on the main body of each nascent reproductive cell (Fig. 6A). The fimbriae and capsule were produced simultaneously by the young prosthecate reproductive cells. Fimbriae were still evident at 225 ± 15 min (Fig. 6B), after which they were no longer observed on cells in subsequent S II stages. Thus, fimbrial elaboration in MHS-3 was confined to the swarm cell-to-prosthecate cell transition; fimbriae were present only during approximately 30 min of the developmental cycle (<20% of the time). In parallel experiments, synchronously cultured MHS-3 rad cells did not produce any capsular EPS at any stage of the life cycle. However, they did produce fimbriae during the same stages of the life cycle in which fimbriae were produced by the wild-type strain.

The prosthecal generation was also monitored (Fig. 4). Approximately 90 ± 15 min (180 to 270 min) was required for a prosthecate cell from the first generation to produce a second swarm cell (period of swarm maturation and separation).

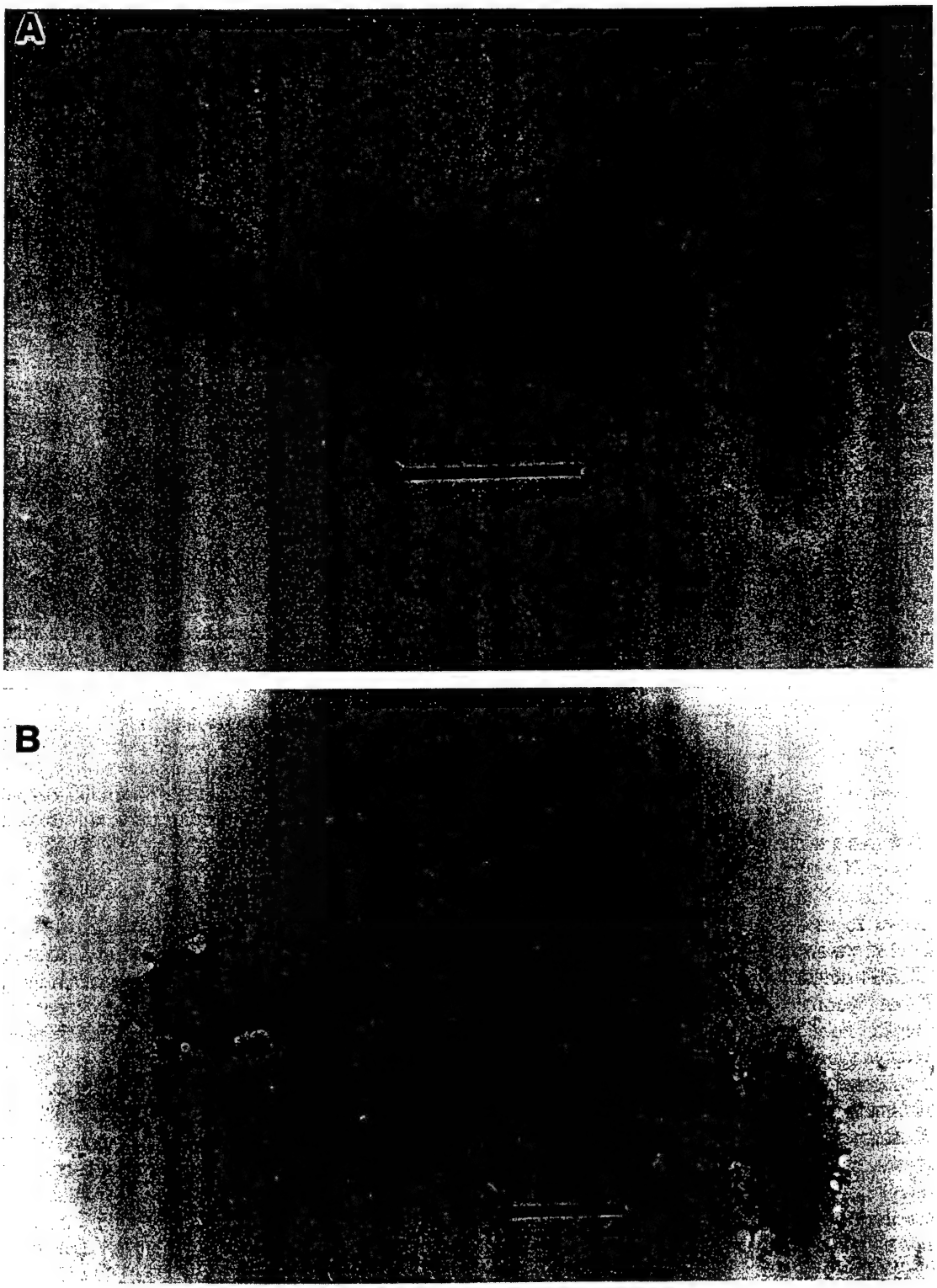

FIG. 5. Initiation of capsular EPS synthesis by *Hyphomonas* wild-type strain MHS-3 in synchronous culture. The cell stages, labelled with BPA-Au (A) and anti-LPS MAb (B), correspond to 15 ± 15 min for S I cells and 195 ± 15 min for S II cells. EPS is deposited all over the body of the young prosthecate reproductive cells, as indicated by the binding pattern of BPA-Au (A) and the localized binding of the MAb (B), where only the nascent prosthecae are labelled. The timing of capsule deposition is readily apparent in panel A, in which one cell is heavily labelled with BPA-Au while the other cell, which is just beginning to excrete EPS, is lightly labelled. Bars = 1 μm.

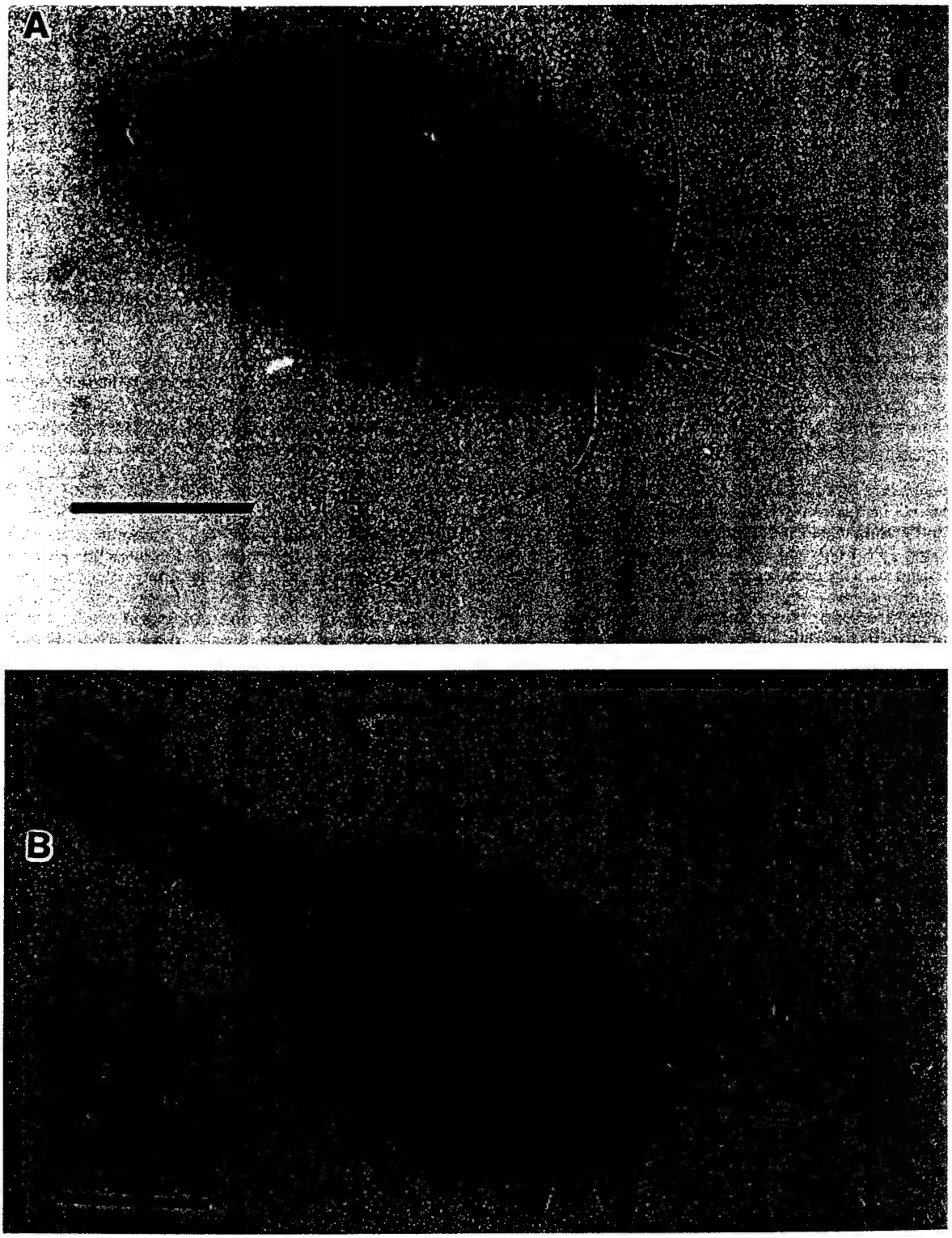

FIG. 6. Uranyl acetate-stained *Hyphomonas* wild-type strain MHS-3 from a synchronous culture, showing polar fimbrial production by young prosthecate reproductive cells. The cell stages shown correspond to 195 ± 15 min (A) and 225 ± 15 min (B) for S II cells. These are the only stages in which fimbriae are found on MHS-3. Bars = 0.5 μm.

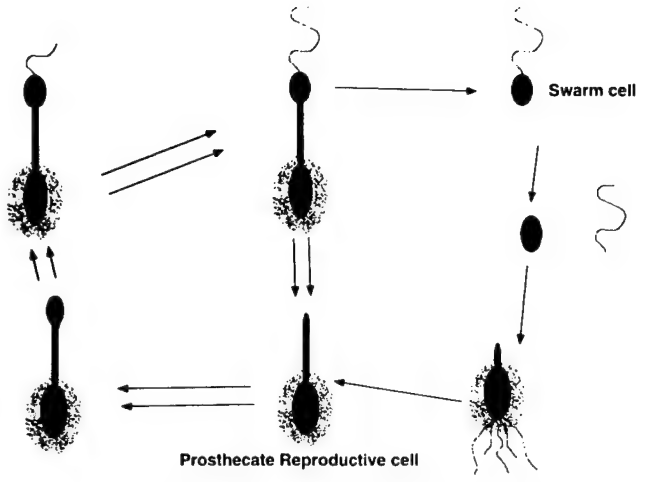

FIG. 7. Representation of the *Hyphomonas* strain MHS-3 developmental cycle, showing the temporality and polarity of capsule and fimbria expression.

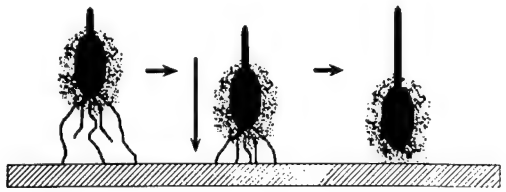

FIG. 8. Representation of fimbrial retraction during the process of adhesion of *Hyphomonas* strain MHS-3 to surfaces. Fimbriae putatively mediate long-range, primary binding to surfaces, retract, and bring the EPS adhesin involved in permanent attachment in contact with the surface.

DISCUSSION

This is the first report of temporal and spatial deposition of capsular EPS in the genus *Hyphomonas*. In strain MHS-3, it was found by using negative immunoelectron microscopy probing with anti-LPS MAb and EPS-specific stains that a capsule is synthesized only by prosthecate reproductive cells and only on the main body of a reproductive cell. These observations were verified in a synchronous culture, in which the temporality and polarity of fimbrial synthesis were also observed. These findings are summarized in Fig. 7.

It was confirmed by indirect immunostaining and direct ferritin staining that rad variants, which spontaneously arise at a low frequency (43), do not synthesize observable capsules, as hypothesized previously (43) on the basis of results obtained with direct lectin (BPA-Au) probes. The rad offspring may be less likely to be trapped in biofilms than the wild-type offspring, which would be advantageous in species dispersal.

Most EPS capsules are highly hydrated and require special treatment to stabilize their structure during fixation. During the graded specimen dehydration step required for embedding, most capsules usually collapse, and subsequent exposure to water fails to rehydrate the precipitated EPS (2). Several techniques involving antibody cross-linking, Lowcryl resin imbedding, or cationic ferritin binding have been developed to preserve the structure of capsules (2). In the case of MHS-3, although polycationic ferritin was used to label the outline of the capsule, it did not penetrate and bind the entire cross section of the capsule enough to stabilize it (Fig. 2). Furthermore, thin sections of wild-type cells that were not treated with polycationic ferritin revealed the faint outline of a well-preserved capsule after staining with uranyl acetate (data not shown). This suggests that standard glutaraldehyde fixation is sufficient to preserve the MHS-3 capsular structure. Moreover, the EPS capsules of marine bacteria are naturally stabilized by absorbing metals and are readily observed by TEM after glutaraldehyde fixation and embedding, with or without the use of heavy-metal stains (10).

Since the MHS-3 capsule blocks penetration of anti-LPS MAb (Fig. 1A) and polycationic ferritin (Fig. 2), it is probably an effective molecular sieve. The anti-LPS MAb used was a mouse IgG which has an approximate molecular weight of 150,000. The molecular weight of horse spleen ferritin (used to manufacture polycationic ferritin) is approximately 445,000. There is a long-held belief that EPS capsules of pathogenic bacteria interfere with host defense mechanisms, antibodies, and complement via masking mechanisms, rendering binding sites physically inaccessible (11). EPS capsules have been listed as virulence factors in pathogenic bacteria precisely because they prevent antibodies from binding to membrane epitopes (37). Such capsules are found on clinical isolates of *Staphylococcus aureus* and were identified by using EPS-specific MAbs to immunostain thin sections after standard fixation, dehydration, and embedding procedures (21), without any special capsule stabilization procedure. While MHS-3 is not a mammalian pathogen, its capsule also thwarts antibody binding to target sublayers (e.g., LPS).

Few other prokaryotes produce polar adhesive EPS. Previously published reports indicate that *Caulobacter* spp. (42), *Asticcacaulis biprosthecum* (51), *Thiothrix* spp. (30, 59), *S. stellata* (22), and *Bradyrhizobium japonicum* produce these molecules (31, 49, 50). The presence of an EPS holdfast has been inferred but not demonstrated in *Hyphomicrobium* spp. (36). The MHS-3 capsule is not just unusual; it is unique among the examples cited above because it is an extensive, integral EPS capsule, while the other structures are not.

S I cells required 165 ± 15 min to develop into mature prosthecate reproductive cells and release progeny. The only difference in the timing of S I and S II cells was in the prosthecal elongation period; S I cells required 90 min, which was 30 min longer than S II cells required. Swarm cell maturation and release required a little more than 30 min in each of the stable synchronous generations (Fig. 4). In *Hyphomonas* strain MHS-3, the hyphal growth period required a greater percentage of the cell cycle time than the percentage reported for *Hyphomicrobium neptunium* under similar growth conditions (53). For the first time, it was found by observing cells in synchronous cultures that the production of the capsule in the genus *Hyphomonas* is a temporally regulated event which is linked to major physiological and morphological changes during the transition from swarm cells to prosthecate cells. Thus, MHS-3 appears to be a member of a group of prosthecate bacteria in which the production of EPS is temporally governed by an obligate life cycle and occurs at specific stages of development. In contrast, in most other genera, the biosynthesis of EPS is regulated by nutritional (26, 62) and environmental (4) cues.

This is also the first report of fimbrial production in *Hyphomonas*, one of several genera that produce polar fimbriae. These fimbriae are expressed at a very specific stage during the transition from swarm cells to prosthecate cells (Fig. 6A). A close examination revealed that the fimbriae vary in diameter along their length, from about 5.0 to 8.0 nm, suggesting that they are flexible (58). Polar fimbriae of *Pseudomonas aeruginosa* have been implicated in adhesion to mammalian tissues

during pathogenesis (60, 63) and to solid surfaces, such as stainless steel and polystyrene (23). Interestingly, *Thiothrix* spp., *Caulobacter* spp., and *A. biprosthecum* also produce polar tufts of fimbriae at the same locus as the holdfast (30, 42, 51, 59).

The primary role of fimbriae is to mediate bacterial adhesion to inanimate surfaces or to other cells. They help negatively charged bacteria bind to negatively charged substrata, bridging the electrostatic repulsive forces in accordance with the DLVO theory (bodies with very small radii experience less repulsion) (40). It has been proposed that fimbriae mediate primary (transitory) adhesion and that EPS promotes irreversible attachment to surfaces (16, 32). The experimental results obtained with MHS-3 are consistent with this hypothesis, except that it is possible that MHS-3 EPS mediates primary adhesion as well as permanent cementation, since both wild-type and rad strains produce fimbriae, but the wild-type (EPS-positive) cells adhere better (43). Similar results have been reported for *A. biprosthecum*, in which holdfast mutants failed to attach to surfaces (51). *Thiothrix* spp. attach to ciliated protozoa (34) and to one another (30) by means of EPS holdfasts. In *Thiothrix nivea*, the initial attachment step involves the fimbriated pole and is followed by the production of a holdfast (30). Another line of evidence which supports the importance of the capsule in primary adhesion is the transitory appearance of MHS-3 fimbriae. MHS-3 adheres at times when the fimbriae are not expressed.

In *Caulobacter crescentus*, fimbriae are functionally expressed during the swarm cell stage and disappear when a swarm cell differentiates into a prosthecate cell (29). Although the pilin monomer is present inside the cell throughout the entire *Caulobacter* life cycle (29), the fimbriae are assembled after separation of the swarm cell from the prosthecate cell (46). In MHS-3, as in *C. crescentus*, fimbriae are not shed into the culture medium, suggesting that they are probably also retracted into the cells (29, 46). *Escherichia coli*, *Pseudomonas aeruginosa*, and *C. crescentus* have been shown to have retractable fimbriae by using fimbria-specific bacteriophages to inhibit retraction (6, 25, 46). In the case of *Pseudomonas syringae* pv. phaseolicola, fimbria retraction pulls fimbria-associated bacteriophage f 6 through the EPS of the host and brings it into contact with the outer membrane, where membrane fusion can take place (45). Fimbria retraction may be a mechanism to bring cells closer to the surface once attachment has occurred (27). In contrast, *A. biprosthecum* and other bacteria shed their fimbriae (41).

The temporal and spatial regulation of the adhesive structures of MHS-3 can be correlated with putative function (43). MHS-3 appears to synthesize capsular EPS and fimbriae simultaneously. The value of these events as an attachment strategy could be that two chemically distinct adhesive molecules are presented, which should allow interactions with a wide array of surfaces. MHS-3 fimbriae are 1,000 to 2,000 nm long, and the EPS capsule is 200 to 300 nm thick. Alternatively, fimbriae could mediate long-range, primary binding to surfaces, since they extend beyond the EPS capsule and can tether the cell to the surface and then retract and bring the EPS adhesive capsule in contact with the surface, as represented in Fig. 8.

Species that synthesize polar adhesive structures in lieu of surrounding capsules could conserve energy. Furthermore, adhesive structures (fimbriae, EPS) could foster polar attachment to surfaces, another potential survival advantage. This is exemplified by starved marine *Vibrio* strain DW1, which attaches perpendicularly to surfaces by an as-yet-unknown mechanism. During cell division, the original cells (analogous to the MHS-3 prosthecate reproductive cells) remain attached, while the progeny cells detach and become planktonic (32). This strategy is even more favorable for members of the genus *Hyphomonas*, since each swarm cell is released at the distal tip of the prosthecum, further elevating the cell. Therefore, prosthecate cells could release motile swarm cells closer to the water interface of the biofilm and into the water column to colonize new substrata.

ACKNOWLEDGMENTS

We thank G. Geesey for helpful discussions and M. Kessel for help and insights concerning fine structure.

This work was supported in part by grants from the Office of Naval Research and the Maryland Industrial Partnerships.

REFERENCES

1. **Baier, R., A. Meyer, V. DePalma, R. King, and M. Fornalik.** 1983. Surface microfouling during the induction period. J. Heat Transfer **105**:618–624.
2. **Bayer, M. E.** 1990. Visualization of the bacterial polysaccharide capsule. Curr. Top. Microbiol. Immunol. **150**:29–57.
3. **Beloni, Z. H., I. A. Avilov, and B. V. Gromov.** 1984. The peculiarities of soil strains of budding bacteria of the genus *Hyphomicrobium*. Biol. Sci. **6**:71–75.
4. **Berry, A., J. D. DeVault, and A. M. Chakrabarty.** 1989. High osmolarity is a signal for enhanced *algD* transcription in mucoid and nonmucoid *Pseudomonas aeruginosa* strains. J. Bacteriol. **171**:2312–2317.
5. **Bott, T. R.** 1992. Introduction to the problem of biofouling in industrial equipment. NATO Adv. Study Inst. Ser. Ser. E Appl. Sci. **223**:3–11.
6. **Bradley, D. E.** 1978. *Pseudomonas aeruginosa* pili, p. 319–338. *In* D. E. Bradley, E. Raizen, P. Fives-Taylor, and J. Ou (ed.), Pili. Proceedings of the International Conference on Pili. American Society for Microbiology, Washington, D.C.
7. **Christensen, B. E.** 1989. The role of extracellular polysaccharides in biofilms. J. Biotechnol. **10**:181–202.
8. **Corpe, W. A.** 1973. Microfouling: the role of primary film forming bacteria, p. 598–609. *In* R. F. Ackjer, B. F. Brown, J. R. DePalma, and W. P. Verson (ed.), Proceedings of the Third International Congress on Marine Corrosion Fouling. Northwestern University Press, Evanston, Ill.
9. **Costerton, J. W.** 1984. Mechanisms of microbial adhesion to surfaces. Direct ultrastructural examination of adherent bacterial populations in natural and pathogenic ecosystems, p. 115–123. *In* M. J. Klug and C. A. Reddy (ed.), Current perspectives in microbial ecology. Proceedings of the 3rd International Symposium on Microbial Colonization. American Society for Microbiology, Washington, D.C.
10. **Cowen, J. P.** 1992. Morphological study of marine bacterial capsules: implications for marine aggregates. Mar. Biol. **114**:85–95.
11. **Cross, A. S.** 1990. The biologic significance of bacterial encapsulation. Curr. Top. Microbiol. Immunol. **150**:87–95.
12. **Decho, A. W.** 1990. Microbial exopolymer secretions in ocean environments: their role(s) in food webs and marine processes. Oceanogr. Mar. Biol. Annu. Rev. **28**:73–153.
13. **DiSalvo, L. H., and G. W. Daniels.** 1975. Observations on estuarine microfouling using the scanning electron microscope. Microb. Ecol. **2**:234–240.
14. **Emala, M. A., and R. M. Weiner.** 1983. Modulation of adenylate energy charge during the swarmer cycle of *Hyphomicrobium neptunium*. J. Bacteriol. **153**:1558–1561.
15. **Engvall, E.** 1980. Enzyme immunoassay ELISA and EMIT. Methods Enzymol. **70**:419–438.
16. **Fletcher, M.** 1980. Adherence of marine micro-organisms to smooth surfaces, p. 345. *In* E. H. Beachey (ed.), Bacterial adherence. Chapman & Hall, London, United Kingdom.
17. **Gerchakov, S. M., D. S. Mardzalek, F. J. Roth, and L. R. Udey.** 1976. Succession of periphytic microorganisms on metal and glass surfaces in natural seawater. *In* Proceedings of the 4th International Congress of Marine Corrosion Fouling.
18. **Harlow, E., and D. Lane.** 1988. Antibodies: a laboratory manual. Cold Spring Harbor Laboratory, Cold Spring Harbor, N.Y.
19. **Hirsch, P.** 1974. Budding bacteria. Annu. Rev. Microbiol. **28**:391–444.
20. **Hitchcock, P., and T. Brown.** 1983. Morphological heterogeneity among *Salmonella* lipopolysaccharide chemotypes in silver-stained polyacrylamide gels. J. Bacteriol. **154**:269–277.
21. **Hochkeppel, H. K., D. G. Braun, W. Vischer, A. Imm, S. Sutter, U. Staeubli, R. Guggenheim, E. L. Kaplan, A. Boutonnier, and J. M. Fournier.** 1987. Serotyping and electron microscopy studies of *Staphylococcus aureus* clinical isolates with monoclonal antibodies to capsular polysaccharide types 5 and 8. J. Clin. Microbiol. **25**:526–530.
22. **Hood, M. A., and J. M. Schmidt.** 1996. The examination of *Seliberia stellata* exopolymers using lectin assays. Microb. Ecol. **31**:281–290.
23. **Irvin, R. T.** 1990. Hydrophobicity of proteins and bacterial fimbriae, p.

137–177. *In* R. J. Doyle and M. Rosenberg (ed.), Microbial cell surface hydrophobicity. American Society for Microbiology, Washington, D.C.
24. **Jacobson, A.** 1972. Role of F pili in the penetration of bacteriophage f1. J. Virol. **10**:835–843.
25. **Jacques, M., and B. Foiry.** 1987. Electron microscopic visualization of capsular material of *Pasteurella multocida* types A and D labeled with polycationic ferritin. J. Bacteriol. **169**:3470–3472.
26. **Jarman, T. R., L. Deavin, S. Slocombe, and R. C. Righelato.** 1978. Investigation of the effect of environmental conditions on the rate of exopolysaccharide synthesis in *Azotobacter vinelandii*. J. Gen. Microbiol. **107**:59–64.
27. **Jones, G. W., and R. E. Isaacson.** 1983. Proteinaceous bacterial adhesins and their receptors. Crit. Rev. Microbiol. **10**:229–260.
28. **Lane, R. D., R. S. Crissman, and M. F. Lachman.** 1984. Comparison of polyethylene glycols as fusogens for producing lymphocyte-myeloma hybrids. J. Immunol. Methods **72**:71–76.
29. **Langenaur, C., and N. Agabian.** 1977. *Caulobacter crescentus* pili: structure and stage-specific expression. J. Bacteriol. **131**:340–346.
30. **Larkin, J. M., and R. Nelson.** 1987. Mechanism of attachment of swarm cells of *Thiothrix nivea*. J. Bacteriol. **169**:5877–5879.
31. **Maddock, J. R., M. R. K. Alley, and L. Shapiro.** 1993. Polarized cells, polar actions. J. Bacteriol. **175**:7125–7129.
32. **Marshall, K. C.** 1992. Biofilms: an overview of bacterial adhesion, activity, and control at surfaces. ASM News **58**:202–207.
33. **Marshall, K. D., R. Stout, and R. Mitchell.** 1971. Selective sorption of bacteria from seawater. Can. J. Microbiol. **17**:1413–1416.
34. **Merkel, G. J.** 1975. Observations of the attachment of *Thiothrix* to biological surfaces in activated sludge. Water Res. **9**:881–885.
35. **Moore, R. L.** 1981. The biology of *Hyphomicrobium* and other prosthecate, budding bacteria. Annu. Rev. Microbiol. **35**:567–594.
36. **Moore, R. L., and K. C. Marshall.** 1981. Attachment and rosette formation by hyphomicrobia. Appl. Environ. Microbiol. **42**:751–757.
37. **Moxon, E. R., and J. S. Kroll.** 1990. The role of bacterial polysaccharide capsules as virulence factors. Curr. Top. Microbiol. Immunol. **150**:65–85.
38. **Nikitin, D. I., and E. S. Nikitina.** 1978. Environmental processes of self-clarifying and bacterial parasites (genus *Bdellovibrio*), p. 26. Nauka, Moscow, USSR.
39. **Nikitin, D. I., O. Y. Vishnewetskaya, K. M. Chumakov, and I. V. Zlatkin.** 1990. Evolutionary relationships between some stalked and budding bacteria (genera *Caulobacter*, "Hyphobacter," *Hyphomonas* and *Hyphomicrobium*) as studied by the new integral taxonomical method. Arch. Microbiol. **153**:123–128.
40. **Oliveira, D. R.** 1992. Physico-chemical aspects of adhesion. NATO Adv. Study Inst. Ser. Ser. E Appl. Sci. **223**:45–58.
41. **Pate, J. L., S. J. Petzold, and T. H. Umbreit.** 1979. Two flagellotropic phages and one pilus-specific phage active against *Asticcacaulis biprosthecum*. Virology **94**:24–37.
42. **Poindexter, J. S.** 1981. The caulobacters: ubiquitous unusual bacteria. Microbiol. Rev. **45**:123–179.
43. **Quintero, E. J., and R. M. Weiner.** 1995. Evidence for the adhesive function of the exopolysaccharide of *Hyphomonas* strain MHS-3 in its attachment to surfaces. Appl. Environ. Microbiol. **61**:1897–1903.
44. **Quintero, E. J., and R. M. Weiner.** 1995. Physical and chemical characterization of the polysaccharide capsule of the marine bacterium, *Hyphomonas* strain MHS-3. J. Ind. Microbiol. **15**:347–351.
45. **Romantschuk, M., and D. H. Bamford.** 1985. Function of pili in bacteriophage f 6 penetration. J. Gen. Virol. **66**:2461–2469.
46. **Sommer, J. M., and A. Newild.** 1988. Sequential regulation of developmental events during polar morphogenesis in *Caulobacter crescentus*: assembly of pili on swarmer cells requires cell separation. J. Bacteriol. **170**:409–415.
47. **Suci, P. A., B. Frølund, E. J. Quintero, R. M. Weiner, and G. G. Geesey.** 1995. Adhesive extracellular polymers of *Hyphomonas* MHS-3: interaction of polysaccharides and proteins. Biofouling **9**:95–114.
48. **Tsai, C. M., and C. E. Frasch.** 1982. A sensitive silver stain for detecting lipopolysaccharides in polyacrylamide gels. Anal. Biochem. **119**:115–119.
49. **Tsien, H. C., and E. L. Schmidt.** 1977. Polarity in the exponential-phase *Rhizobium japonicum* cell. Can. J. Microbiol. **23**:1274–1284.
50. **Tsien, H. C., and E. L. Schmidt.** 1981. Localization and partial characterization of soybean lectin-binding polysaccharide of *Rhizobium japonicum*. J. Bacteriol. **145**:1063–1074.
51. **Umbreit, T. H., and J. L. Pate.** 1978. Characterization of the holdfast region of wild-type cells and holdfast mutants of *Asticcacaulis biprosthecum*. Arch. Microbiol. **118**:157–168.
52. **Voller, A., D. E. Bidwell, and A. Bartlett.** 1979. The enzyme linked immunosorbent assay (ELISA). A guide with abstracts of microplate applications. Dynatech Europe, Burough House, Guernsey, Great Britain.
53. **Wali, T. M., G. R. Hudson, D. A. Danald, and R. M. Weiner.** 1980. Timing of swarmer cell cycle morphogenesis and macromolecular synthesis by *Hyphomicrobium neptunium* in synchronous culture. J. Bacteriol. **144**:406–412.
54. **Weidner, S., W. Arnold, and A. Pühler.** 1996. Diversity of uncultured microorganisms associated with the seagrass *Halophila stipulacea* estimated by restriction fragment length polymorphism analysis of PCR-amplified 16S rRNA. Appl. Environ. Microbiol. **62**:766–771.
55. **Weiner, R. M., R. A. Devine, D. M. Powell, L. Dagasan, and R. L. Moore.** 1985. *Hyphomonas oceanitis* sp. nov., *Hyphomonas hirschiana* sp. nov., and *Hyphomonas jannaschiana* sp. nov. Int. J. Syst. Bacteriol. **35**:237–243.
56. **Weiner, R. M., M. Walch, M. P. Labare, D. B. Bonar, and R. R. Colwell.** 1989. Effect of biofilms of the marine bacterium *Alteromonas colwelliana* (LST) on set of the oysters *Crassostrea gigas* (Thunberg, 1793) and *C. virginica* (Gmelin, 1791). J. Shellfish Res. **8**:117–123.
57. **Weiner, R. M., D. Sledjeski, E. Quintero, S. Coon, and M. Walch.** 1992. Periphytic bacteria cue oyster larvae to set on fertile benthic biofilms, abstr. S1-5-2. *In* Abstracts of the 6th International Symposium on Microbial Ecology, Barcelona, Spain. Spanish Society for Microbiology, Barcelona, Spain.
58. **Weiss, R. L.** 1971. The structure and occurrence of pili (fimbriae) on *Pseudomonas aeruginosa*. J. Gen. Microbiol. **67**:135–143.
59. **Williams, T. M., R. F. Unz, and J. T. Doman.** 1987. Ultrastructure of *Thiothrix* spp. and "type 021N" bacteria. Appl. Environ. Microbiol. **53**:1560–1570.
60. **Woods, D. E., D. C. Strauss, W. G. Johanson, V. K. Berry, and J. A. Bass.** 1980. The role of pili in adherence of *Pseudomonas aeruginosa* to mammalian buccal epithelial cells. Infect. Immun. **29**:1146–1151.
61. **Xu, H. S., W. S. Ji, and B. Xu.** 1989. A study on the attachment of marine bacteria to different surfaces, p. 80. *In* Abstracts of the First International Marine Biotechnology Conference, Baltimore. Society for Industrial Microbiology, Arlington, Va.
62. **Zhan, H., C. C. Lee, and J. A. Leigh.** 1991. Induction of the second exopolysaccharide (EPSb) in *Rhizobium meliloti* SU47 by low phosphate concentrations. J. Bacteriol. **173**:7391–7394.
63. **Zoutman, D. E., W. C. Hulbert, B. L. Pasloske, A. M. Joffe, K. Volpel, M. K. Trebilcock, and W. Prancych.** 1991. The role of polar pili in the adherence of *Pseudomonas aeruginosa* to injured canine tracheal cells: a semiquantitative morphologic study. Scanning Microsc. **5**:109–126.

JOURNAL OF COLLOID AND INTERFACE SCIENCE 205, 89–96 (1998)
ARTICLE NO. CS985597

Influence of Divalent Cations and pH on Adsorption of a Bacterial Polysaccharide Adhesin

N. Bhosle,* P. A. Suci,†[1] A. M. Baty,† R. M. Weiner,‡ and G. G. Geesey†

*Marine Corrosion and Material Research Division, National Institute of Oceanography, Dona Paula 403004, Goa, India; †Microbiology Department and Center for Biofilm Engineering, Montana State University, Bozeman, Montana 59717; and ‡Microbiology Department, University of Maryland, College Park, Maryland 20742

Received February 9, 1998; accepted April 17, 1998

Hyphomonas MHS-3 (MHS-3) elaborates a diffuse capsular material, primarily composed of polysaccharide, which has been implicated to serve as the holdfast of this prosthecate marine bacterium. A purified polysaccharide (fr2ps) from this capsular material exhibits a relatively large affinity for (Ge), or more precisely for the Ge oxide surface film. In its natural habitat MHS-3 attaches to marine sediments. This suggests that molecular properties of fr2ps have evolved to render it adhesive toward mineral oxides. In order to characterize these molecular interactions, the effect of divalent cations and pH on the adsorption of fr2ps to Ge has been measured using attenuated total internal reflection Fourier transform infrared (ATR/FT-IR) spectroscopy. The effect of adsorption of fr2ps on the Ge oxide film has been investigated using X-ray photoelectron spectroscopy (XPS). The results indicate that divalent cations participate in binding of fr2ps to Ge oxide and that atomic size of the cation is important. Evidence for significant participation of hydrogen bonding to the oxide surface is lacking. © 1998 Academic Press

Key Words: adhesion; bacteria; polysaccharide; adsorption; divalent cation.

INTRODUCTION

Attachment of microorganisms to inert surfaces has been investigated in numerous publications [for reviews see (1–3)]. While proteins are known to mediate adhesion of microbes to biological surfaces in specialized ecosystems, presumably through stereospecific interactions (4–6), the adhesins and the molecular mechanisms involved in attachment of microbes to inert surfaces have not been as well characterized; however, there is evidence that specialized proteins (7, 8), polysaccharides (9, 10), and glycoproteins (11) have evolved to serve this purpose. In general, adsorption of globular proteins to inert surfaces is thought to be influenced by a large contribution from internal rearrangements (conformational changes) (12–14). Polysaccharides, as well as proteins lacking substantial secondary and tertiary structure, are more "deformable" (15) and therefore may provide a versatile set of interactions which are directly related to functional group chemistry (16), and can be catered to serve specific types of adhesive functions to inert surfaces. In support of this assertion there is evidence that polysaccharides may have properties which are exploited by cells for either attachment to (17), or detachment from (18), inert surfaces.

The Derjaguin–Landau–Verwey–Overbeek (DLVO) theory of colloidal stability predicts that biological cells, whose envelopes typically have a net negative charge, cannot approach closer than the secondary minimum, about 10–20 nm, from a typical (negatively charged) surface (19). Originating from this prediction is the hypothesis that cells utilize appendages to breach this electrostatic barrier, in order to induce irreversible attachment (20). In some cases proteinaceous fimbriae have been shown to provide this bridge (21, 22). Extracellular polysaccharides are invariably a major component of the polymeric matrix of most mature biofilms (23). Cells that elaborate an extracellular capsular polysaccharide while still in suspension could presumably utilize this as an appendage to initiate irreversible attachment.

In a number of previous studies, evidence has been presented indicating that the marine bacterium, *Hyphomonas* MHS-3 (MHS-3), utilizes a diffuse extracellular capsular material to bind to inert surfaces (24–26). A polysaccharide component of this capsular material (fr2ps) has been isolated and partially characterized. Studies of its adsorption behavior indicated fr2ps bound relatively strongly to an oxide surface (germanium) when ranked against an acidic polysaccharide (alginate), globular blood proteins, and a disordered protein which is a primary component of a natural marine epoxy resin. Adsorption behavior of fr2ps to various substrata was consistent with attachment preference of whole cells. In its normal habitat, MHS-3 is likely to encounter mineral surfaces and attach to them as part of its prosthecate lifecycle. Adsorption of organic molecules to mineral surfaces is thought to occur primarily through hydrogen bonding to oxide surfaces (27). It seems reasonable that divalent cations may also serve to link oxides with various functional groups on the polysaccharide. In this study we have characterized the influence of divalent

[1] To whom correspondence should be addressed.

0021-9797/98 $25.00

cations and of pH on the adsorption behavior of fr2ps in order to further investigate the interactions involved in bonding of this adhesive polysaccharide at an aqueous/oxide interface.

MATERIALS AND METHODS

Isolation and Purification of fr2ps

The bacterium MHS-3 was isolated from shallow water sediments in Puget Sound, WA (24). Cultures of MHS-3 were grown in Marine Broth 2216 (37.4 g/L) (Difco Laboratories, Detroit, MI) at 25°C on a rotating shaker at 100 rpm. Teflon mesh (mesh opening, 1.8 mm, thread diameter, 0.5 mm, Tetko, Inc., Briarcliff, NY) was introduced into the culture vessels to provide greater surface area for attached growth. The attached cells and associated extracellular polymeric substance (EPS) were harvested from a culture in which the suspended cell population had just entered stationary phase. The medium was poured off, and the biofilm was removed from the Teflon mesh and the sides of the culture vessel walls by scraping.

EPS was extracted in two steps. The cell suspension was centrifuged for 20 min at 16,000*g*, and the EPS in the supernatant ("loosely bound") was precipitated with 4 volumes of ice-cold 2-propanol. The more "tightly bound" EPS was extracted from the cell pellet. The cell pellet was dispersed in a Waring blender in a minimum volume of 10 mM EDTA, 3% NaCl for 1 min at 4°C. The suspension was centrifuged for 15 min at 16,000*g* and the EPS from the supernatant was precipitated using 2-propanol as described above.

A crude EPS preparation was obtained by pooling the two EPS fractions and resuspending in a minimum volume of distilled water (dH_2O). They were then dialyzed for 12 h against dH_2O and lyophilized. Polysaccharide-enriched EPS (EPS_p) was prepared by a published protocol (28). EPS was dissolved in a minimum volume of 0.1 M $MgCl_2$, and DNase and RNase were added to a final concentration of 0.1 mg/ml, followed by incubation at 37°C for 4 h. Protease K was added to 0.1 mg/ml and incubated at 37°C overnight. Residual protein was removed with a hot phenol extraction, followed by a chloroform extraction. The preparation was dialyzed for 12 h against dH_2O and lyophilized. The EPS_p preparations were stored desiccated at room temperature.

Preparative high performance size exclusion chromatography (HPSEC) fractionation of EPS_p was performed using a Hewlet Packard 1090 liquid chromatograph equipped with a diode array UV–vis spectrometer (Shodex OHpack B-2004 column). The mobile phase was 0.5 M NaCl, 0.05 M ortho-PO_4 at pH 7.0 in dH_2O. EPS_p was dissolved in the mobile phase at a concentration of 1 mg/ml and filtered through a 0.22 μm Millipore filter. The injected sample volume was 1 ml. The column was run at room temperature at a flow rate of 0.9 ml/min. The adhesive polysaccharide fr2ps was isolated as the second peak in the chromatogram (26) and concentrated in 0.01 M NaCl using ultrafiltration (Amicon 8010 stirred ultrafiltration cell, Amicon 5YM5 membrane). Aliquots were stored at −40°C.

Chemical Analysis

Neutral hexose content was determined using the phenol sulfuric acid assay with glucose as the standard (29). Protein content was estimated using the Lowry procedure with bovine serum albumin (BSA) as standard (30). Uronic acid content was determined by the *m*-hydroxydiphenyl method (31).

Surface Preparation

Single-crystal, cylindrical germanium (Ge) internal reflection elements (IRE) (Spectra Tech, Stamford, CT) were cleaned by ultrasonication in a base bath (saturated KOH in isopropyl alcohol) for 10 min. Following the base bath were two rinses in ultrapure water followed by a gentle scrubbing with undiluted Micro cleaning solution using cotton swabs. The cleaning solution was flushed off in a hard stream of ultrapure water. The IRE was then subjected to the following rinses which consisted of a 10 min ultrasonication in the liquid: ultrapure water (2×), and ethyl alcohol. After cleaning IREs were stored at 100°C for 12 h before being used for adsorption studies.

Adsorption Protocol

All adsorption experiments were performed in some modification of a synthetic seawater having the composition (w/v): 2.3% NaCl, 0.024% Na_2CO_3, 0.033% KCl, 0.4% $MgCl \cdot 6H_2O$, 0.066% $CaCl_2 \cdot 2H_2O$, pH adjusted to 8.4 with HCl. Modifications used for each experiment are explicitly given with the results. For adsorption experiments investigated using FT-IR the cylindrical IRE was positioned within a stainless steel flow chamber (Circle Cell, Spectra Tech, Stamford, CT). Details have been described elsewhere (32). A simple flow through system was used to deliver solutions into the flow chamber. Teflon valves (Cole-Parmer, Niles, IL) served to shuttle the appropriate solution into tubing leading to the flow chamber. All tubing leading into the flow chamber as well as the fittings were Teflon (0.08 cm I.D.).

For adsorption experiments frozen aliquots were thawed and diluted with the appropriate ionic buffer to produce a solution with the desired ionic composition and pH. Before each adsorption experiment the surface was exposed to the appropriately modified synthetic seawater for 20 min under flow. A vial containing 1 ml of approximately 0.025 mg/ml of fr2ps in this aqueous solution was inserted into the flow system, and the contents were immediately pumped through a short section of leader tubing and through the flow chamber for 125 s. (The estimate of concentration is based upon neutral hexose content of the frozen aliquots.) Flow was then stopped to allow adsorption for 60 min. Adsorption was performed under these static conditions to conserve purified polysaccharide. Flow was

then resumed, and the surface was rinsed with the modified synthetic seawater for 30 min.

For XPS analysis adsorption was onto 1 cm diameter Ge disks (Harrick Scientific Corp., Ossingen, NY). Ge disks were cleaned as described above. Samples were exposed to fr2ps in glassware cleaned with a H_2SO_4–Nochromix mix (Godax Laboratories, New York, NY). The rinse was performed using fluid displacement. Samples were dried overnight in the FT-IR chamber before measurement.

FT-IR Spectroscopy

During the course of each experiment infrared spectra were acquired periodically using a Perkin-Elmer Model 1800 Fourier transform infrared (FT-IR) spectrophotometer. Experimental details are described elsewhere (32). FT-IR measurements were made at a FT-IR chamber temperature measured for each experiment at 23 ± 0.5°C.

Estimation of Surface Coverage

Estimation of surface coverage was based on absorbance of the transmission spectrum of fr2ps, concentrated by freeze-drying and rehydrated to 50 mg/ml, obtained using a 15 μm transmission cell with CaF windows (Spectra Tech). A modification of a previously published derivation (25) was used. Briefly, it was assumed that

$$c_{B,E} = [(A_{W,T}/A_{W,E})(A_{S,E}/A_{S,T})]c_{B,T}, \quad [1]$$

where $A_{W,T}$ is the absorbance of water (band at 1640 cm^{-1}) in transmission, $A_{W,E}$ is the absorbance of water probed evanescently (ATR mode), $A_{S,E}$ is the absorbance of the substance of interest (fr2ps in this case) probed evanescently, $A_{S,T}$ is the absorbance of the substance in transmission, $c_{B,T}$ is the (known) concentration of the substance in the transmission cell, and $c_{B,E}$ is the bulk or volume concentration of the substance probed evanescently. Using glucose solutions as standards, Eq. [1] was found to predict $c_{B,E}$ with >90% accuracy. This calculated volume concentration is related to the (unknown) adsorbed amount by

$$\Gamma = (d_p/2)(c_{B,E}), \quad [2]$$

where d_p is the penetration depth of the evanescent (electric) field and Γ is the surface coverage (mass/area).

A spectrum of dehydrated fr2ps was obtained by placing 2 μl of a 50 mg/ml aqueous solution on the surface of the IRE and allowing it to dry in the FT-IR chamber until the water band centered at 1640 cm^{-1} disappeared.

XPS Analysis

XPS spectra were obtained with a Physical Electronics Model 5600 spectrometer (Physical Electronics, Eden Prairie, MN). A 5 eV flood gun was used to offset charge accumulation. A 800 μm diameter area was analyzed using a monochromatized Al$K\alpha$ X-ray source at 300 W and a pass energy of 23.50 eV. The binding energy scale was referenced by setting the CHx peak maximum in the C1s spectrum to 285.0 eV. Curve fitting was performed using Peakfit (Jandel Scientific, San Rafael, CA).

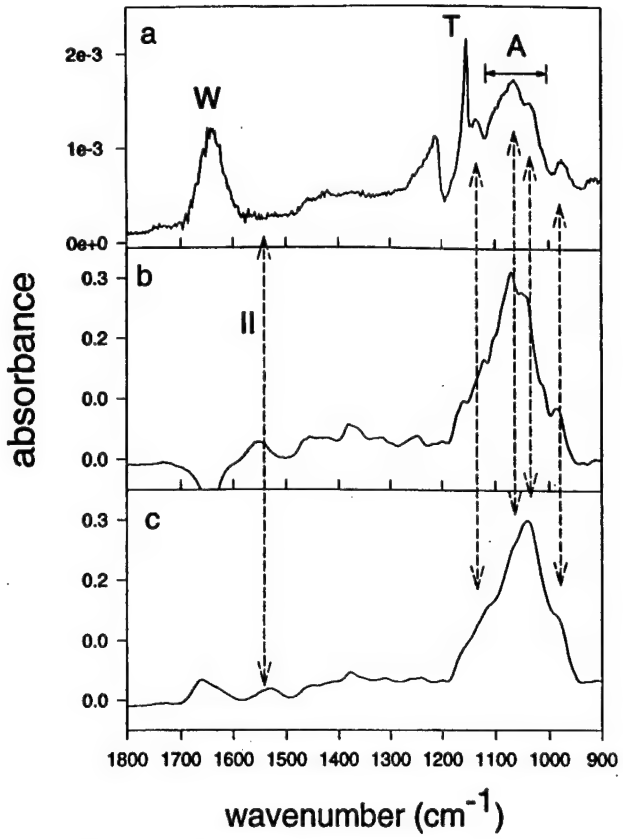

FIG. 1. FT-IR spectra of fr2ps: (top) adsorbed onto the Ge IRE (hydrated); (middle) transmission spectrum of hydrated bulk sample (50 mg/ml); (bottom) sample dried onto Ge IRE. W, region of strong water absorption at 1640 cm^{-1}; T, absorbance from Teflon O-rings of flow chamber; A, composite band used to measure fr2ps adsorption; II, amide II band. Broken lines are to aid the eye in comparison and for discussion.

RESULTS

Chemical Characterization

Colorometric assays indicated that fr2ps consisted primarily of neutral hexose (97.8%) with small amount of protein (2.2% w/w) and a trace amounts of uronic acids (<0.1%).

FT-IR spectra of three different preparations of fr2ps are shown in Fig. 1: fr2ps adsorbed to the Ge IRE (hydrated) (Fig. 1a), a transmission spectrum of bulk, hydrated fr2ps (Fig. 1b), and a spectrum of fr2ps dehydrated on the Ge IRE (Fig. 1c). Since the dehydrated sample consisted of 0.1 mg spread over about 0.5 cm^2 (200 $\mu g/cm^2$) this can be considered to be a

spectrum of bulk, dehydrated fr2ps. Comparison of the three spectra reveals differences in the band pattern. The spectrum for the adsorbed sample (Fig. 1a) is representative of spectra obtained under all the different adsorption conditions used. Close scrutiny of spectra of adsorbed fr2ps revealed no consistent discernable differences in band pattern for the different buffer conditions. The dehydrated sample (Fig. 1c) has bands at positions typical for proteins: amide I at 1660 cm^{-1}, amide II at 1528 cm^{-1}, as well as bands near 1460, 1380, and 1250 cm^{-1} which have been assigned to CH_3, CH_2, and amide III vibrational modes, respectively (33, 34). The amide II band is shifted, respectively, in the hydrated bulk sample (Fig. 1b) and notably absent in the adsorbed sample (Fig. 1a). The region where the amide I band should appear is obscured by residual bands from subtraction of the large water band centered at 1640 cm^{-1} (indicated by W in Fig. 1a) in the hydrated bulk and adsorbed samples. Careful examination of this region in the spectrum of adsorbed fr2ps revealed no trace of a component band at any other wavelength than 1640 cm^{-1}. Therefore, the FT-IR data indicate that the adsorbed component consists entirely of polysaccharide (within the limits of detection), while the bulk fr2ps sample has a significant, though small, protein component (corroborating the colorometric analysis). This suggests that the polysaccharide portion of the bulk material is not bound up with the small protein component and out-competes it in the adsorption process. The protein content of fr2ps as estimated by FT-IR is higher than the estimate by the colorometric assays (7.0% protein w/w).

The polysaccharide C–O stretch region extends from approximately 1200 to 900 cm^{-1}. Maxima of the most prominent component bands in this region are shifted, respectively, in spectra of the adsorbed sample and hydrated bulk sample (Fig. 1a and b); while spectra of both the adsorbed sample and dehydrated bulk sample have four bands in nearly the same positions (indicated in Fig. 1 by the dashed lines). Thus, with respect to position (not relative amplitude) of prominent component bands in this region of the spectrum, the adsorbed sample is slightly more similar to the dehydrated bulk sample than to the hydrated bulk sample. This suggests that interactions with the Ge substratum upon adsorption alter hydration of portions of the polysaccharide. Removal of interfacially bound water has been identified as a precondition for formation of strong adhesive bonds between biopolymers and a surface (35). It seems plausible that a binding mechanism involving displacement of interfacial water would also be likely to influence the hydration shell of the biopolymer. Following along with this interpretation, there are three shifts downward (1070 to 1065 cm^{-1}, 1040 to 1035 cm^{-1}, and 1000 to 994 cm^{-1}) and one shift upward (1119 to 1136 cm^{-1}) upon adsorption. In this region absorption bands arise primarily from C–C and C–O stretching modes (36) with a significant contribution from COH bending modes (37). The FT-IR data are thus consistent with a substratum bonding mechanism that involves pyranose ring carbons and oxygens.

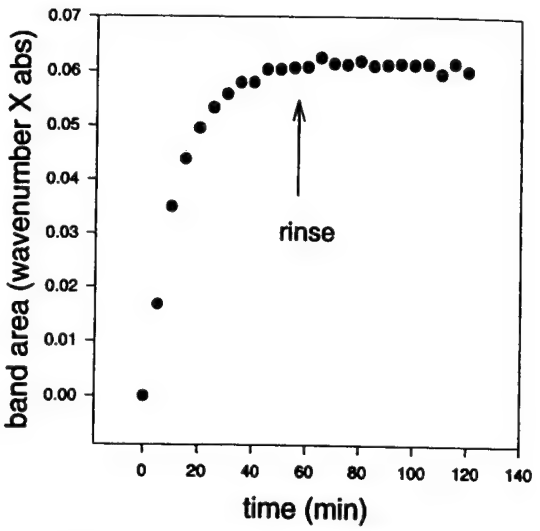

FIG. 2. Kinetics of adsorption of fr2ps onto the Ge IRE measured by computing band areas of the composite band indicated in Fig. 1. Time at which rinse was initiated is indicated. Band area has been converted to surface coverage in remainder of the figures using Eqs. [1] and [2].

Adsorption Studies

Adsorption and desorption of fr2ps to the Ge IRE was monitored by computing areas of the composite band indicated in Fig. 1a. A kinetic binding curve is shown in Fig. 2. Adsorption is typically irreversible in the empirical sense that the adsorbed component is not removed from the surface when the bulk solution is replaced with the rinse solution. All adsorption studies were performed at the same bulk concentration of fr2ps. This concentration was chosen because it yielded an easily detectable amount of adsorbed fr2ps, but was below surface saturation estimated from previous binding curves (Fig. 3) (26). Concentration of bulk fr2ps is given in terms of neutral hexose content of frozen aliquots as determined by the colorometric assay.

Effect of Divalent Cations

The binding curve presented in Fig. 3 was obtained in unmodified synthetic seawater. It was found that omission of the Na from this solution did not change the adsorbed amount significantly (see Fig. 3). The influence of variable amounts of K was minimal (data not shown). Carbonate is the primary buffer and is necessary in order to maintain the pH. With these results as a starting point a set of test solutions was chosen with invariant concentrations of K and carbonate, as in the unmodified synthetic seawater, and variable concentrations of Ca, Mg, or Sr. The pH was 8.4 for this set of experiments. The ionic strength was adjusted with NaCl so as to be the equivalent for all experiments. The effect of each of the three divalent cations on adsorption was tested in the absence of the other two.

The effect of Ca on the amount of adsorbed fr2ps remaining

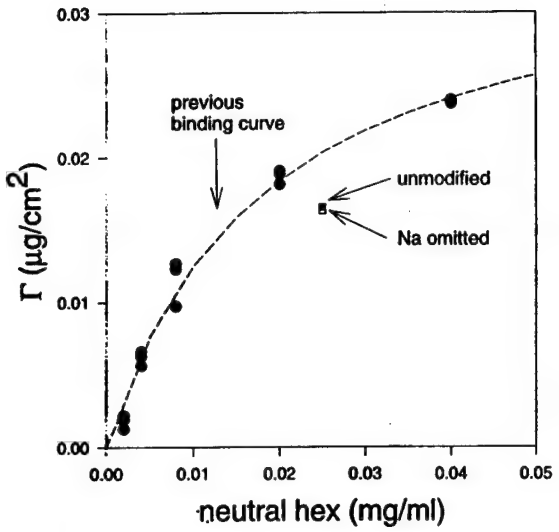

FIG. 3. Filled circles: binding curve and fit of Langmuir model (broken line) for fr2ps onto Ge IRE obtained with a previous preparation (26). Surface coverage was computed from band area as described in the text. Bulk concentration of fr2ps is given in terms of the total neutral hexose content determined by the colorometric assay. Squares: results obtained with batch of fr2ps used for these experiments in unmodified synthetic seawater (filled) and synthetic seawater with Na omitted (unfilled).

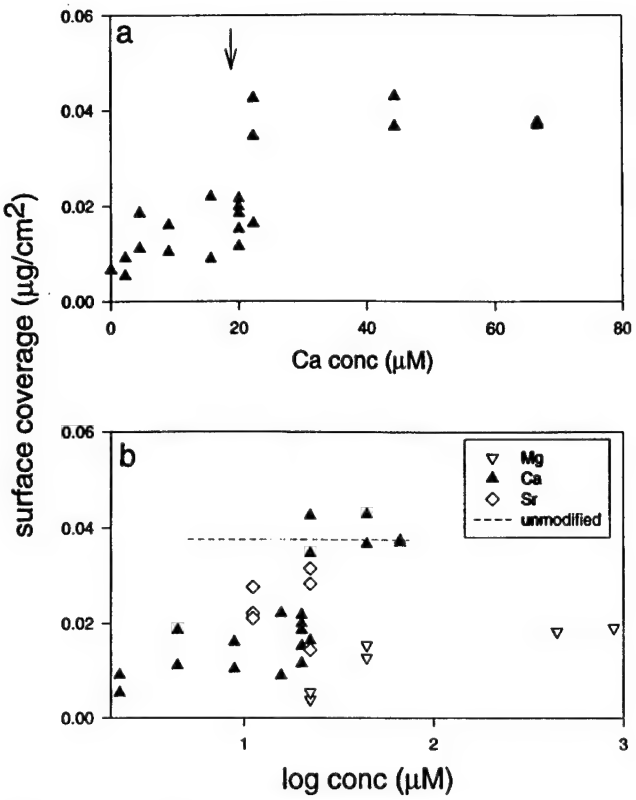

FIG. 4. (a) Effect of Ca on adsorption of fr2ps. Arrow indicates transition point. (b) Effect of Mg, Ca and Sr on adsorption of fr2ps. Level of adsorption for unmodified synthetic seawater is indicated (broken line). Note log scale in (b).

at the end of the rinse is shown in Fig. 4a. There is a sharp increase in the adsorbed amount at a concentration of approximately 20 μM Ca. Fig. 4b shows the effect of substitution of Mg and Sr on the adsorption of fr2ps. Since the range of concentrations tested was relatively large they are exhibited on a log scale. (The Ca curve is included for comparison). It appears that Sr can, to some extent, replace Ca but that Mg is not nearly as effective in promoting adsorption. The influence of Ca and Sr on adsorption could not be tested at higher concentrations because a carbonate precipitate formed (without addition of fr2ps).

Effect of pH

In order to test the effect of pH on fr2ps adsorption a solution consisting of 22 μM Ca was chosen. This Ca concentration is at a threshold for influencing adsorption of fr2ps (Fig. 4a). Therefore, sensitivity to other solution components might be expected to be maximal. It was necessary to include 0.952 mM Mg in order to prevent a carbonate precipitate from forming in the more basic solutions. The influence of pH on adsorption of fr2ps is shown in Fig. 5, indicating that, in general, more basic conditions enhance adsorption. The exception to this trend at pH 8.0 is reproducible, suggesting a complex interaction between functional groups.

XPS of Adsorbed fr2ps

XPS spectra of the $Ge2p_{3/2}$ region of fr2ps adsorbed at 4 and 40 μM Ca onto Ge and of a clean Ge substratum are shown in Fig. 6. The three samples were stored under identical conditions and loaded into the XPS instrument at the same time. The relative size of the Ge oxide peak (at higher binding energy) appears to become progressively smaller compared to the Ge peak as more fr2ps is adsorbed. The Ge3d region exhibits the

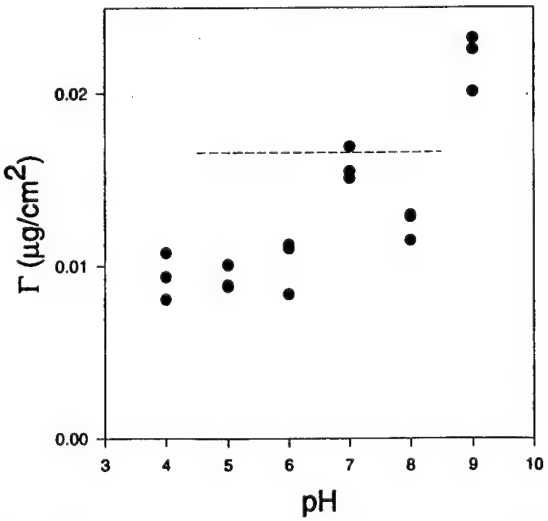

FIG. 5. Effect of pH on adsorption of fr2ps. Level of adsorption for unmodified seawater is indicated (broken line).

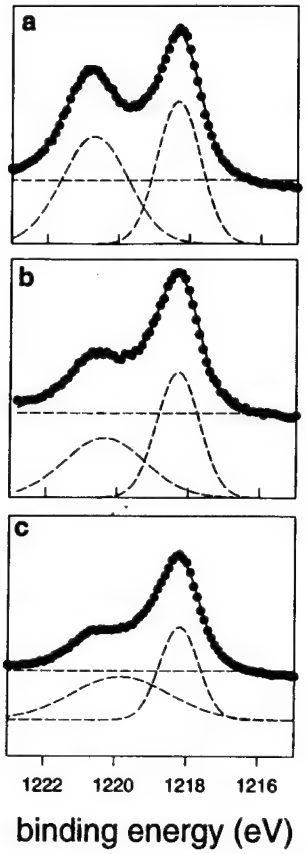

FIG. 6. XPS of Ge disks, $Ge2p_{3/2}$ bands; Ge oxide is on the left. (a) Clean Ge; (b) fr2ps adsorbed at 4 μM Ca; (c) fr2ps adsorbed at 40 μM Ca. Curve fits are indicated by lines, data by filled circles, and Gaussian curves constituting each fit by broken lines. Counts have not been included for simplicity of presentation.

same trend (data not shown). In a separate experiment a drop of bulk fr2ps was dried on Ge which was cleaned by the protocol given above. XPS measurements indicated no detectable Ge oxide peak (data not shown). Ge exposed to the solution containing 40 μM Ca (with no fr2ps) exhibited an oxide peak larger than that of clean Ge.

The XPS data in Fig. 6 was fit with a set of Gaussian curves. This provided a better fit than Lorentzian, Voigt, or mixed Gaussian–Lorentzian curves by both the criteria of the R^2 value and the functionality exhibited by the residuals. The simplest fit is obtained with two Gaussian curves as shown for the $Ge2p_{3/2}$ spectra. The ratio of the areas of the Gaussian curves which correspond to the Ge and Ge oxide peaks is 0.85, 1.11, and 1.87 for peaks in Fig. 6a, b, and c, respectively, corroborating the qualitative appraisal.

High resolution spectra were also obtained for the C1s region, the O1s region, the five Ca regions (2s, $2p_{1/2}$, $2p_{3/2}$, 3s, and $3p_{1/2}$), and the N1s region. Ca and N (an indication of protein) were not detected. The C1s region and O1s regions of the adsorbed fr2ps displayed satellite bands with shifts to higher binding energies consistent with the presence of C–O–H or C–O–C bonds (1.4 eV, O1s: 1.5 eV, C1s and C=O bonds (3.2 eV, C1s) (data not shown) (38). There were no chemical shifts in this region which could be interpreted as originating from formation of bonds with the Ge oxide surface.

DISCUSSION

It has been proposed that a capsular extracellular polysaccharide with the appropriate extension and functional groups could serve to bridge an electrostatic barrier that prevented a bacterium from approaching closer than 10–20 nm from a surface (39). Divalent cations, especially calcium ions, have been found to play a role in adhesion of bacteria (40, 41) and algae (42) to inert surfaces. It is obvious that divalent cations have the appropriate oxidation state to mediate ionic bonds between a negatively charged surface and anionic functional groups of an extracellular polysaccharide. Although this interaction has not yet been demonstrated in the published literature, preliminary data indicate that it makes a significant contribution to binding of some polysaccharides (personal communication with Georges Belfort, Department of Chemical Engineering, Rensselaer Polytechnic Institute, Troy, NY). Many types of hydrogen bonds are possible between mineral oxides and organic molecules (27). This implies that hydrogen bonding may contribute significantly to the adsorption of polysaccharides onto mineral surfaces in seawater.

A number of previous investigations have indicated that fr2ps serves as an adhesion for the marine bacterium MHS-3 and that it adsorbs to Ge with a comparatively high affinity (24–26). Ge is not a common element of marine sediments; however, it is in the same group as silicon, and its oxide film is likely to have some of the general characteristics of mineral oxides. Although proteins generally adsorb strongly to Ge, this is not the case for polysaccharides. We have tested alginate (carboxylate functionality), hyaluronic acid (*N*-acetyl and carboxylate functionalities), and cellulose (glucose subunits), and all of these adsorb only slightly to Ge. This suggests that fr2ps has some special molecular characteristics which enhance its adsorption onto oxide films.

The XPS data indicate that fr2ps interacts strongly with the Ge oxide. Theoretically, the expected proportion of Ge to Ge oxide photoelectron intensities would be invariant for a simple three layer film (fr2ps/Ge oxide/Ge bulk material), with variable thickness of the fr2ps overlayer. This ratio has been used to estimate the oxide film thickness (43): as the thickness of the oxide decreases, the relative ratio (Ge oxide to Ge) decreases. Ge forms an amphoteric oxide that could presumably be dissolved in either acidic or basic solutions. Thus one possibility is that acidic or basic functional groups on fr2ps, which are concentrated near the surface upon adsorption, result in a local pH which degrades the Ge oxide layer. Since fr2ps has been demonstrated to adsorb strongly to Ge relative to other biopolymers (26), it seems unlikely that it is dissolving the surface it adheres to, especially since the oxide provides the

most obvious chemistry for forming bonds with functional groups. A second possibility is that the Ge oxide is patchy and that fr2ps adsorbs preferentially to islands of Ge oxide, thus decreasing the XPS signal from these portions of the surface. This also seems unlikely. The Ge is single crystal and thus homogeneous, and the exposure to KOH during cleaning should create a virgin Ge surface for uniform formation of the oxide film upon exposure to air. A third possibility is that the apparent relative decrease in the Ge oxide band is actually the result of a shift and/or widening of component bands. The Ge oxide band originates from a shift in the measured binding energy of the Ge core electrons caused by electron withdrawal from the Ge shell by the electronegative oxygen. Interactions which lowered the oxidation state of the oxygen would decrease its electronegativity and might shift a portion of the oxide band to lower energy. This would result in an apparent increase in the proportion of Ge to Ge oxide in the XPS spectrum.

The data show a clear participation of Ca in adsorption of fr2ps to Ge. The effect is not simply one of charge shielding, since ionic strength was invariant. In addition, the interaction between the divalent cation and fr2ps which promotes adsorption appears to be sensitive to elemental properties (probably size) other than the oxidation state, since Ca cannot be replaced with Mg. This type of interaction with divalent cations is responsible for the gelling behavior of alginate in solutions containing divalent cations, and has been explained by the presence of a cavity formed by alginate that can accommodate some divalent cations better than others. In the model which is most accepted, the Ca^{+2} forms a coordination complex with two carboxylate functionalities and several hydroxyl groups of the pyranose ring (44).

There is no clear evidence for the importance of hydrogen bonding of fr2ps to Ge. The trend is that, as the pH is raised, the amount of fr2ps adsorbed becomes greater. Deprotonation of functional groups would be expected to decrease hydrogen bonding, since the proton donors would be replaced by negatively charged groups, thus increasing the electrostatic repulsion. The data for pH 8 suggests involvement of interactions of multiple functional groups with different pK values.

The abundance of carboxylate functionalities in fr2ps is very slight according to the chemical characterization. In addition, no trace of S or P was found in fr2ps (XPS) which might indicate other negatively charged functionalities. In addition, no Ca was detected in adsorbed films of fr2ps (XPS). Therefore, if fr2ps employs anionic functionalities and Ca^{+2} to form a complex with the Ge oxide the density of binding sites must be low relative to the number of monomers. The level of detection of the XPS was limited to $>1\%$ (relative elemental composition) by the Ge background: i.e., for every region in which a Ca band appeared, a small Ge band was also present. If it assumed that there is one uronic acid (UA) residue (carboxylate functionality) for every 200 residues of fr2ps then the elemental percent of Ca would be between 0.03 and 0.003 for 1:1 binding (Ca^{+2}:UA), assuming between a 5 and 0.5 nm mean free path of the photoelectrons. It would make sense that a polysaccharide designed to bridge an electrostatic double layer would be nearly neutral and be only sparsely populated with anionic functionalities. Pinning of the polysaccharide via these rather sparsely located points might enable other bonds to form.

SUMMARY

The bacterial polysaccharide (fr2ps) binds strongly to Ge substrata. The mechanism by which it forms bonds has been probed by measuring the influence of ionic composition and pH on adsorption, and the influence of fr2ps adsorption on the Ge substratum. The data support a mechanism involving divalent cationic bridging between functional groups on fr2ps and the Ge oxide overlayer. The importance of atomic size of the divalent cation suggests that the interaction involves coordination of a number of fr2ps functional groups. Involvement of pyranose ring atoms is implicated. There is evidence for displacement of water contained in the fr2ps hydration shell upon adsorption.

ACKNOWLEDGMENT

This research was supported by a grant (N0014–95–11086) from the Office of Naval Research.

REFERENCES

1. Fletcher, M., *Methods Microbiol.* **22,** 251–283 (1990).
2. Mittelman, M. W., *in* "Bacterial adhesion: molecular and ecological diversity" (M. Fletcher, Ed.) pp. 89–127. Wiley-Liss, New York, 1996.
3. Rosenburg, M., *Crit. Rev. Microbiol.* **18,** 159–173 (1991).
4. Jann, K., and Jann, B., *in* "Current Topics in Microbiology and Immunology" (K. Jann and B. Jann, Eds.), Vol. 151, p. 216. Springer-Verlag, New York, 1990.
5. Clark, W. B., Beem, J. E., Nesbitt, W. E., Cisar, J. O., Tseng, C. C., and Levine, M. J., *Infect. Immun.* **57,** 3003–3008 (1989).
6. Salamitou, S., Lemaire, M., Fujino, T., Ohayon, H., Gounon, P., Beguin, P., and Aubert, J.-P., *J. Bacteriol.* **176,** 2828–2834 (1994).
7. Bar-ness, R., and Rosenberg. M., *J. Gen. Microb.* **135,** 2277–2281 (1989).
8. Devasia, P., Natarajan, K. A., Sathayanarayana, D. N., and Ramananda Rao, G., *Appl. Environ. Microbiol.* **59,** 4051–4055 (1993).
9. Zottola, E. A., *Biofouling* **5,** 37–55 (1991).
10. Merker, R. I., and Smit, J., *Appl. Environ. Microbiol.* **54,** 2078–2085 (1988).
11. Wagner, V. T., Brian, L., and Quatrano, R. S., *Proc. Natl. Acad. Sci.* **89,** 3644–3648 (1992).
12. Haynes, C. A., *J. Colloid Interface Sci.* **164,** 394–409 (1994).
13. Ball, A., and Jones, R. A. L., *Langmuir* **11,** 3542–3548 (1995).
14. Haynes, C. A., and Norde, W., *J. Colloid Interface Sci.* **169,** 313–328 (1995).
15. Dickinson, E., and Euston, S. R., *J. Colloid Interface Sci.* **152,** 562–570 (1992).
16. Baty, A. M., Leavitt, P. K., Siedlecki, C. A., Tyler, B. J., Suci, P. A., Marchant, R. E., and Geesey, G. G., *Langmuir* **13,** 5702–5710 (1997).
17. Yun, C., Ely, B., and Smit, J., *J. Bacteriol.* **176,** 796–803 (1994).

18. Wrangstadh, M., Conway, P. L., and Kjelleberg, S., *Arch. Microbiol.* **145,** 220–227 (1986).
19. Busscher, H. J., and Weerkamp, A. H., *FEMS Microbiol. Rev.* **46,** 165–173 (1987).
20. Jones, G. W., and Isaacson, R. E., *Crit. Rev. Microbiol.* **10,** 229–260 (1983).
21. Rosenberg, M., Bayer, E. A., Delarea, J., and Rosenberg, E., *Appl. Environ. Microbiol.* **44,** 929–937 (1982).
22. Bashan, Y., and Levanony, H., *J. Gen. Microbiol.* **134,** 2269–2279 (1988).
23. Cooksey, K. E., *in* "Biofilms: Science and Technology" (L. Melo, T. R. Blott, M. Fletcher, B. Capdeville, Eds.), p. 137–147. Kluwer, Dordrecht, The Netherlands, 1992.
24. Quintero, E. J., and Weiner, R. M., *Appl. Environ. Microbiol.* **61,** 1897–1903 (1995).
25. Suci, P. A., Frølund, B., Quintero, E. R., Weiner, R. M., and Geesey, G. G., *Biofouling* **9,** 95–114 (1995).
26. Frolund, B., Suci, P. A., Langille, S., Weiner, R. M., and Geesey, G. G., *Biofouling* **10,** 17–30 (1996).
27. Thurman, E. M., "Organic Geochemistry of Natural Waters," p. 382. Martinus Nijhoff, Boston, 1985.
28. Read, R. R., and Costerton, J. W., *Can. J. Microbiol.* **33,** 1080–1090 (1987).
29. Dubois, M., Gilles, K. A., Hamilton, J. K., Rebers, P. A., and Smith, F., *Anal. Chem.* **28,** 350–356 (1956).
30. Lowry, O. H., Rosebrough, N. J., Farr, A. L., and Randall, R. J., *J. Biol. Chem.* **193,** 265–275 (1951).
31. Kintner, P. K., III, and Buren, J. P., *J. Food. Sci.* **47,** 756–760 (1982).
32. Suci, P. A., and Geesey, G. G., *J. Colloid Interface Sci.* **172,** 347–357 (1995).
33. Moore, W. H., and Krimm, S., *Biopolymers* **15,** 2439–2464 (1976).
34. Moore, W. H., and Krimm, S., *Biopolymers* **15,** 2465–2483 (1976).
35. Waite, J. H., *Int. J. Adhesion* **7,** 9–13 (1987).
36. Cael, J. J., Gardner, K. H., Koenig, J. L., and Blackwell, J., *J. Chem. Phys.* **62,** 1145–1155 (1975).
37. Mathlouthi, M., and Koenig, J. L., *Adv. Carbohydr. Chem. Biochem.* **44,** 7–89 (1986).
38. Ratner, B. D., and Castner, D. G., *in* "Surface Analysis Techniques and Applications" (J. C. Vickerman and N. M. Reed, Eds.), p. 163. Wiley, Chichester, UK, 1994.
39. Costerton, J. W., Geesey, G. G., and Cheng, K.-J., *Sci. Am.* **238,** 86–95 (1978).
40. Turakhia, M. H., Cooksey, K. E., and Characklis, W. G., *Appl. Environ. Microbiol.* **46,** 1236–1238 (1983).
41. Van Hoogmoed, C. G., van der Mei, H. C., and Busscher, H. G., *Biofouling* **11,** 167–176 (1997).
42. Cooksey, K. E., and Cooksey, B., *in* "Algal Biofouling" (L. V. Evans and K. D. Hoagland, Eds.), p. 43. Elsevier, Amsterdam, 1986.
43. Holm, R., *in* "Analysis of Organic and Biological Surfaces; Chemical Analysis" (P. J. Elving, J. D. Winefordner, and I. M. Kolthoff, Eds.), Vol. 71, p. 37–72. Wiley, New York, 1984.
44. Kohn, R., *Pure Appl. Chem.* **42,** 371–396 (1975).

ELSEVIER

FEMS Microbiology Ecology 26 (1998) 89–99

FEMS MICROBIOLOGY ECOLOGY

Bacterial colonization of artificial substrate in the vicinity of deep-sea hydrothermal vents

J. Guezennec [a,*], O. Ortega-Morales [b], G. Raguenes [a], G. Geesey [c]

[a] *IFREMER, Dept. DRV/VP/BMH, BP 70, 29280 Plouzane, France*
[b] *Université de Bretagne Occidentale, Avenue le Gorgeu, BP 809, 29200 Brest, France*
[c] *Department of Microbiology and Center for Biofilm Engineering, Montana State University, Bozeman, MT 59719, USA*

Received 29 October 1997; revised 16 February 1998; accepted 18 February 1998

Abstract

Artificial substrata of different material composition were deployed at deep-sea hydrothermal areas on the Mid-Atlantic Ridge for exposure times ranging from 1 to 12 days. After 4 days of exposure, a very thick but loosely-bound biofilm formed on all surfaces. Two bacterial morphotypes dominated the attached microbial community: rod-shaped bacteria sometimes several cell layers thick and large filamentous forms attached to the substratum at one end of the filament. Quantitative extraction of biofilm lipids associated with the substratum surface indicated the accumulation of a large amount of bacterial biomass after 4 days of exposure for all substrata. Microbial biomass accumulated at different rates on the different substrata. The greatest biomass was associated with 316L stainless steel and titanium substrata. Polar lipid fatty acid (PLFA) analysis of lipid extracts contained signatures of sulfate reducing bacteria and fatty acids (FA) previously reported in filamentous sulfur-oxidizing bacteria. The results demonstrate rapid in situ colonization of artificial substrata by hydrothermal vent microbial populations irrespective of the nature of the substratum.

Keywords: Hydrothermal vent; Biofilm: Artificial substrate

1. Introduction

Deep-sea hydrothermal vent ecosystems depend on microbial systems for the conversion of reduced inorganic forms of energy to organic forms of energy and carbon. Attached microbial populations have been described in these environments and likely represent an important contribution to the primary production [1,2]. Little is known on the diversity of these attached microbial populations, microbial colonization rates and biomass associated with surfaces in hydrothermal vent fields [3].

Analysis of cellular lipids provides a satisfactory way to gain insight into microbial community structure and biomass [4]. Microbial biomarkers are chemical components of microorganisms which can be extracted directly from the environment, provide qualitative information on the types of microorganisms present as well as quantitative information on in situ microbial biomass [5]. Membrane lipids and

* Corresponding author. Tel.: +33 (29822) 4526; Fax: +33 (29822) 4557; E-mail: jguezenn@ifremer.fr

0168-6496/98/$19.00
PII: S0168-6496(98)00022-1

their associated fatty acids are particularly useful biomarkers as they are essential components of every living cell and have great diversity coupled with high biological specificity [6]. Phospholipid ester-linked fatty acids (PLFA) have proved to be of great value in describing bacterial community structure in sediments, the establishment of a biochemical basis to bacterial phylogeny and taxonomy, and in the detection of specific physiological groups of bacteria associated with microbiologically influenced corrosion studies [7–10]. The use of PLFA from the polar lipid fraction eliminates interference from many contaminants as well as endogenous storage lipids present in the neutral or the glycolipid fractions of the extractable lipids. Phospholipids are not found in storage lipids and have relatively rapid turnover in sediments [11].

A study was carried out to investigate the extent to which the nature of the substratum influenced biofilm development, population structure and biomass in areas under the influence of venting hydrothermal fluids at a site (Snake Pit) along the Mid-Atlantic Ridge during the French 'Microsmoke' cruise. A spectrum of artificial substrata was used in this study to determine the importance of substratum properties on microbial colonization rates, population structure and succession in the vent environment.

2. Materials and methods

2.1. Substratum deployment and recovery

Artificial substrata were deployed at three locations on the ocean bottom along the Mid-Atlantic Ridge at the Snake Pit site (23°22N, 45°57W) using the manned submersible 'Nautile' during the French oceanographic cruise in November 1995. Two locations (sites 1 and 2) were under the influence of venting hydrothermal fluid. The temperatures at sites 1 and 2 fluctuated between 5–20°C. A third location (site A) was outside the influence of the hydrothermal fluids where the temperature maintained a constant 2°C. Water samples were collected from the 3 locations using a Niskin bottle operated by the mechanical arm of the submersible.

The following materials were used as artificial substrata: 316L stainless steel (316L SS), titanium (Ti), aluminum 5052 (Al), copper 90/10 (Cu), copper-nickel alloy (Cu-Ni), Teflon (PTFE), polyamide (PA), polyacrylate (PAc) and polycarbonate (PC). SS and Ti were selected on the basis of their resistance to marine corrosion; Al was selected for its extensive oxide film in seawater; Cu and Cu-Ni were selected for their ability to inhibit microbial colonization. The non-metallic surfaces were selected to offer a range of surface energies in natural seawater (PTFE, 18 $ml \cdot m^{-2}$; PA, 38 $ml \cdot m^{-2}$; PC, 35.5 $ml \cdot m^{-2}$; and PAc, 40 $ml \cdot m^{-2}$) different from those provided by the metallic substrata.

One-cm diameter coupons of each material were glued on one surface to a sample holder, allowing the other surface exposure to the surrounding environment (Fig. 1). A set of sample holders (one for each site and sampling time), each containing an array of coupons of different composition, was transported from the sea surface to the sea floor in the externally-located, seawater-filled box mounted at the front of the Nautile. A mechanical arm transferred the sample holders from the box to their respective location on the sea floor. After 1, 4, 8 and 12 days exposure, a sample holder from each location was retrieved by the mechanical arm of the submersible, and transported to the surface in the seawater-filled, externally-located box on the submersible.

As soon as the submersible was brought on board the support ship, Nadir, the sample holders (l/location) were immediately retrieved from the box and 3 coupons of each type of material removed from each holder and treated as follows: one coupon was lyophilized and stored for lipid analysis; the two remaining coupons were preserved in artificial seawater containing 2.5% glutaraldehyde for subsequent microscopic observations.

2.2. Scanning electron microscopy

Coupons were sputter-coated with a thin film of gold to minimize charging and examined with a Philips XL 30 Lab 6 scanning electron microscope.

2.3. Lipid analysis

Lipids were extracted using a modified Bligh/Dyer

method [11,12]. Samples were placed for 1 h in an ultrasonic bath with adequate volumes of methanol, dichloromethane and water (2:1:0.8, v/v). Identical volumes of water and dichloromethane were then added to the solution and the two resulting phases allowed to separate in a funnel for 18 h. The total lipids were separated into three general lipid classes by silicic column chromatography using a series of mobile phases of increasing polarity (dichloromethane, acetone and methanol). Fatty acid methyl esters were prepared from the esterified lipids in the polar (methanol) lipid fraction by mild alkaline methanolic trans-esterification and analyzed by gas chromatography (GC) and gas chromatography-mass spectrometry (GC-MS).

An aliquot of the polar lipid fraction was analyzed for its ether glycerol content as a biomarker of archaebacteria. A fraction of the polar phase was subjected to a strong acid hydrolysis and the resulting core ether lipids digested with 55% HI solution for 18 h at 100°C. The resulting alkyliodides were extracted with hexane and successively washed with $Na_2S_2O_3$ and Na_2CO_3 solutions [13,14]. After extraction with hexane, the iodide derivatives were analyzed using GC equipped with an electron capture detector using 1,2 di-*O*-hexadecyl-rac-glycerol as internal standard. Authentic glycerol diethers and diglycerol tetraethers were purchased from Sigma or isolated from cells of *Sulfolobus* sp.

2.4. Gas chromatography and gas chromatography-mass spectrometry analyses

GC analyses were performed on a Carlo Erba (Rodano, Italy) HRGG 5360 gas chromatograph equipped with a fused silica column coated with a non-polar phase (60 m×0.2 mm i.d.; film thickness 0.25 μm). Hydrogen was used as carrier gas (33 cm s^{-1}).

GC-MS analyses were performed on a Carlo Erba (Rodano, Italy) model 5160 HRGC chromatograph coupled to a quadrupole Nermag (Delsi) r10-10H mass spectrometer. The fatty acid separation was achieved on a CP Sil5CB capillary column (60 m×0.20 mm i.d.; film thickness 0.25 μm; J&W Folson, California) with helium as carrier gas (1.5 bar). Standard fatty acids were purchased from Sigma along with fatty acids of pure culture of *Vibrio natriegens*, *Desulfovibrio desulfuricans* and members of the *Alteromonas* group isolated from an hydrothermal environment [15,16].

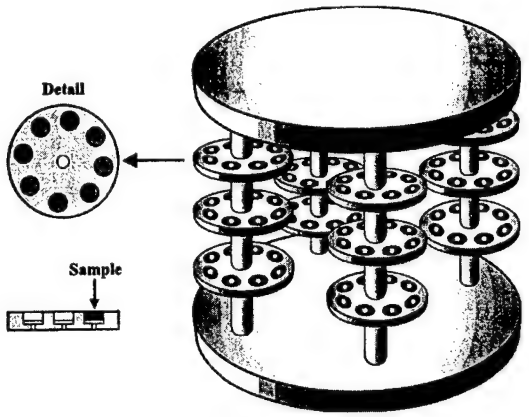

Fig. 1. Sample holder.

2.5. Fatty acid nomenclature

A shorthand nomenclature is used which is in the form of numbers separated by a colon. The number before the colon indicates the carbon chain length and the figure after the colon corresponds to the number of double bonds. The position of the double bond is defined by the symbol 'ω' followed by the number of carbons from the methyl end. The prefixes 'i' and 'a' refer to iso and anteiso, respectively. The geometry of the double bonds is indicated by *cis* and *trans*.

3. Results

Coupons of different material composition, deployed at 2 vent-influenced sites (sites 1 and 2) accumulated a thick, loosely-bound biofilm on their surface, whereas coupons deployed at control site A, not under vent influence, accumulated a sparser biofilm. The chemistry of water samples from the 3 locations is presented in Table 1. With the exception of the silica and ammonia concentrations, the chemistry of the fluids collected at sites 1 and 2 was similar to that of control site A.

Fig. 2a–j shows the most commonly observed morphological types of microorganisms on the sur-

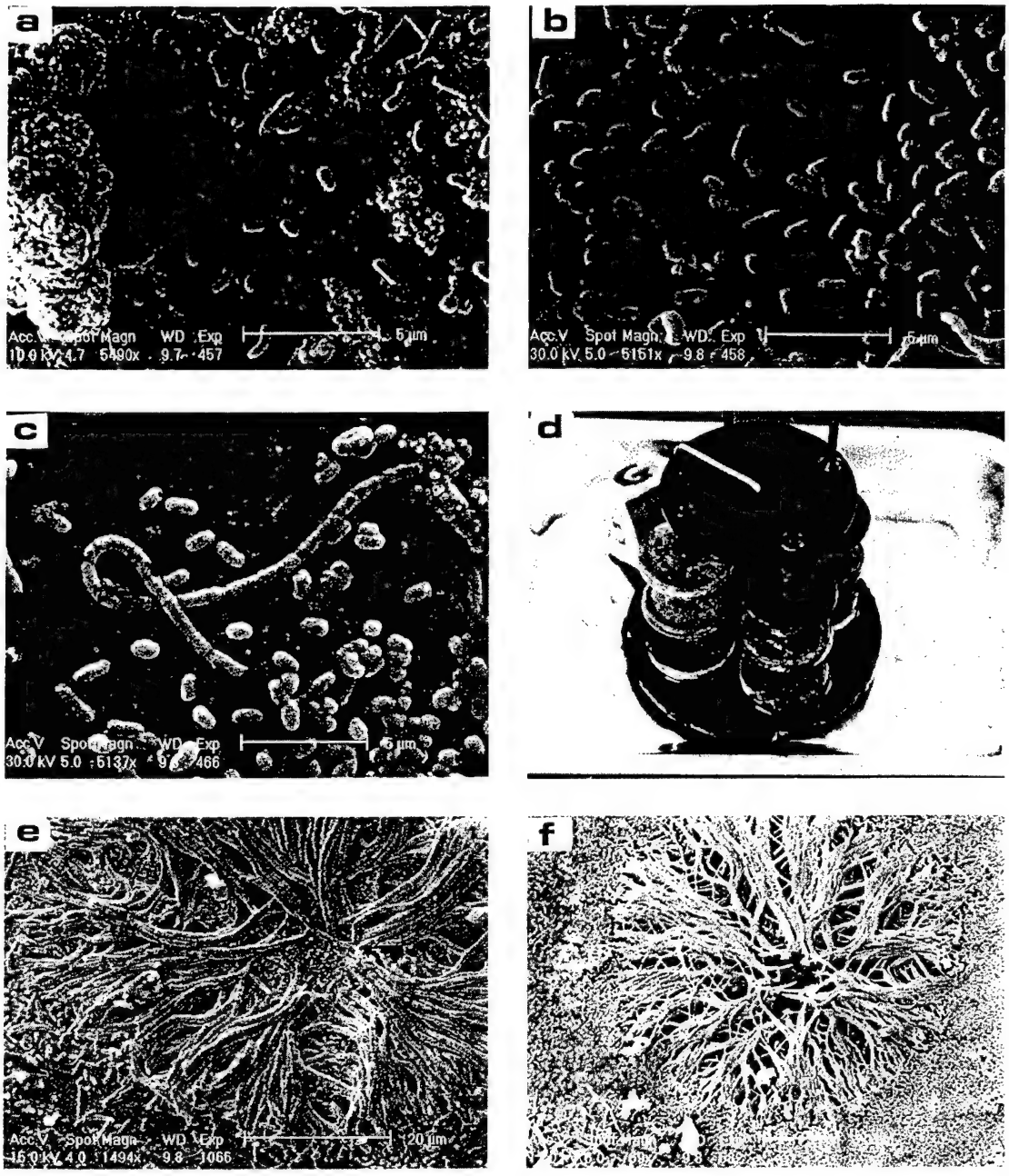

Fig. 2. a–j: Selected SEM photographs from colonized surfaces. a: 316L SS (control, 9 days at site A). b,c: One day colonization (Ti, 316L SS). d: Sample holder after 4 days in the vicinity of the vents; e,f,g: Two main bacterial morphotypes commonly found on all surfaces (4 days). Filamentous bacteria forming rosettes on the surfaces and rod-shaped bacteria (Ti, 316L SS, PTFE); h: Filaments perpendicular to the surfaces (PTFE); i,j: Multilayers of bacteria on 316L SS and titanium (8 days).

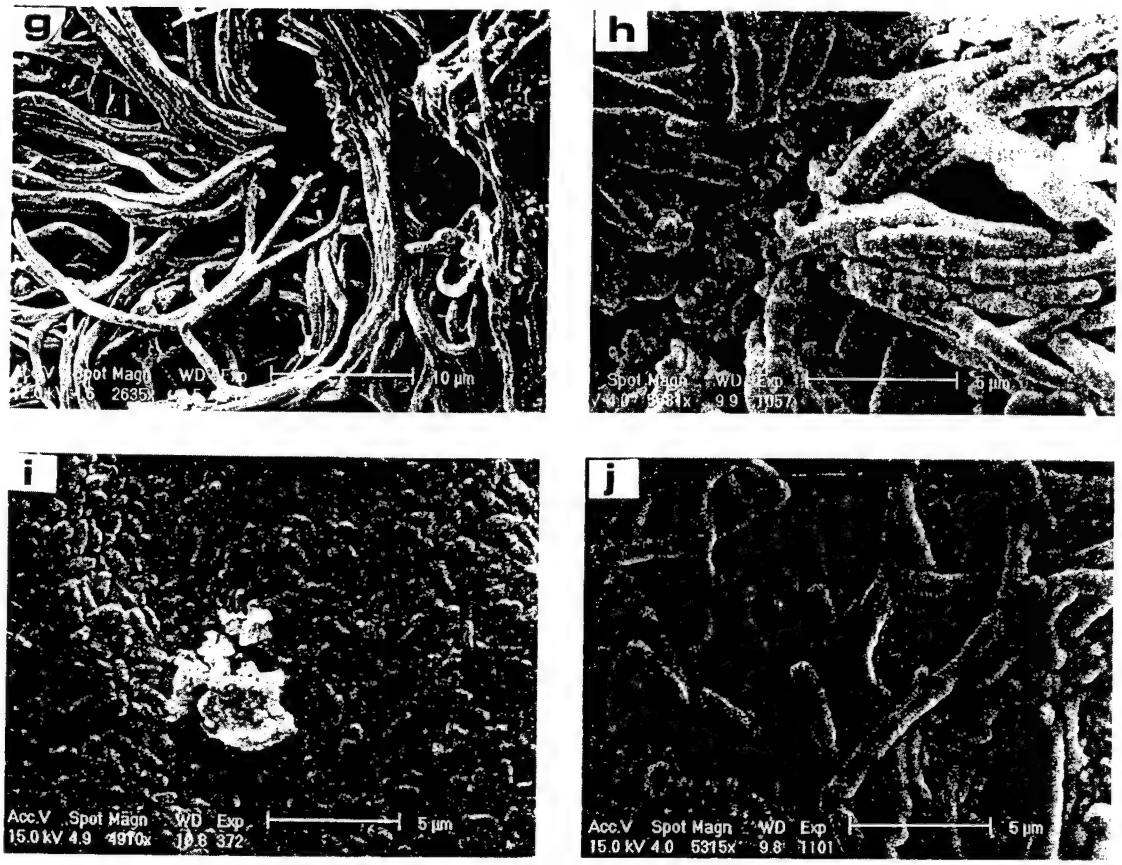

Fig. 2. (*continued*)

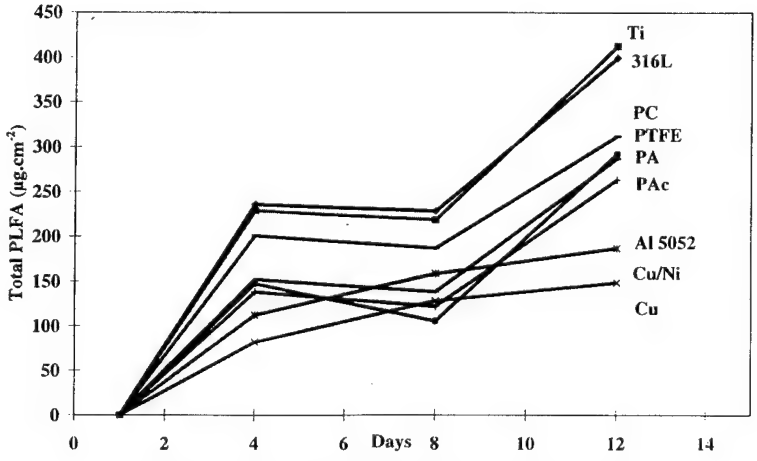

Fig. 3. Biomass expressed as total PLFA µg cm $^{-2}$ vs. time.

face of coupons from the three sites. Contamination during the different steps of the deployment/recovery procedures was estimated by examination of coupons kept in the shuttle box on the submersible for a typical one-day dive. Both SEM and lipid analyses indicated that contamination of surfaces during coupon deployment and retrieval was negligible.

Most coupons retrieved from sites 1 and 2 after one day of exposure to the vent environment were colonized by rod-shaped bacterial colonies heterogeneously distributed over their surface (Fig. 2b,c). The Cu, Cu-Ni and Al coupons were sparsely colonized after one-day exposure.

After four days, all coupons and adjacent areas of the sample holders at sites 1 and 2 were covered with a very thick white biofilm filamentous microorganisms (Fig. 2d). Rod-shaped and rosette-forming filamentous microorganisms were the two dominant morphotypes on the surfaces of all coupons, including the Cu and Cu-Ni coupons exposed at these sites (Fig. 2e,f). The filaments were up to 50 μm length and appeared to be anchored to the surface at a single pole, extending perpendicularly to the substratum (Fig. 2g,h).

After 8 days exposure to the vent environment the surface of all coupons deployed at sites 1 and 2 were colonized by a filamentous biofilm. Biofilm morphology varied with substratum type. Cu and Cu-Ni coupon surfaces exhibited the most heterogeneous distribution of microorganisms. The biofilm on Al coupons was contained within the aluminium oxide film on the surface. Windows of filaments were frequently observed on the surface of the SS coupons. Ti coupon surfaces accumulated a multi-layer of similarly-sized, tightly-packed, rod-shaped bacteria (Fig. 2i,j). Biofilms dominated by rod-shaped bacteria were also observed on the surfaces of the non-metallic coupons.

After 12 days exposure to the vent environment, the surface of all coupons deployed at sites 1 and 2 had accumulated a multi-layered biofilm containing both rod-shaped bacteria and filamentous forms. Metallic and non-metallic surfaces were similarly fouled by these microorganisms based on SEM observations.

Surfaces of coupons exposed to ambient seawater for 9 days at control site A contained fewer rod-shaped bacteria than those exposed to hydrothermal fluids (Fig. 2a). No filamentous forms were observed. No bacteria were detected on the copper and aluminium surfaces.

3.1. Lipid analysis

Twenty-six PLFA were recovered from the surface of the different coupons exposed to the hydrothermal vent environment. The total PLFA-based biofilm biomass associated with the surface of the different coupons was determined between 1 and 12 days exposure to the hydrothermal vent environment (Fig. 3). The most rapid increase in biomass occurred between one and four days exposure on all coupons regardless of composition. Biomass remained relatively unchanged between days 4 and 8 on coupons composed of Ti, 316L SS, and the 4 synthetic polymers PC, PTFE, PA and PAc, while the biomass on Al, Cu-Ni and Cu increased slowly between days 4–12. Between days 8–12, biomass on the Ti, SS and the 4 synthetic polymers increased at rates comparable to those observed between days 1–4. After 12 days exposure, Ti and 316L SS coupons had accumulated the greatest biomass, Cu, Cu-Ni and Al accumulated the least biomass, and 4 synthetic polymers accumulated intermediate amounts of biomass.

In contrast to the coupons exposed to the venting fluids, control coupons exposed to ambient seawater at Side A accumulated a low PLFA-based

Table 1
Seawater composition for exposure sites (sites 1 and 2) and site A

Sampling sites	pH	T (°C)	Ca^{a}	Mg^{a}	SO_4^{-a}	S^{-a}	NO_3^{-b}	NH_4^{+b}	PO_4^{3-b}	Si^{b}
Site 1	7.8	10–15	9.2	47.9	26.2	< 1	11.2	5	0.26	655
Site 1(2)	7.9	10–15	9.8	48.1	26.2	< 1	11.1	5.1	0.26	648
Site 2	7.8	10–15	9.4	48.7	26.6	< 1	13.4	8.8	0.47	460
Site A	8.1	2	9.8	52.8	28.2	ND	15.1	0.5	1.28	152

[a]mmol l^{-1}; [b]μmol l^{-1}.

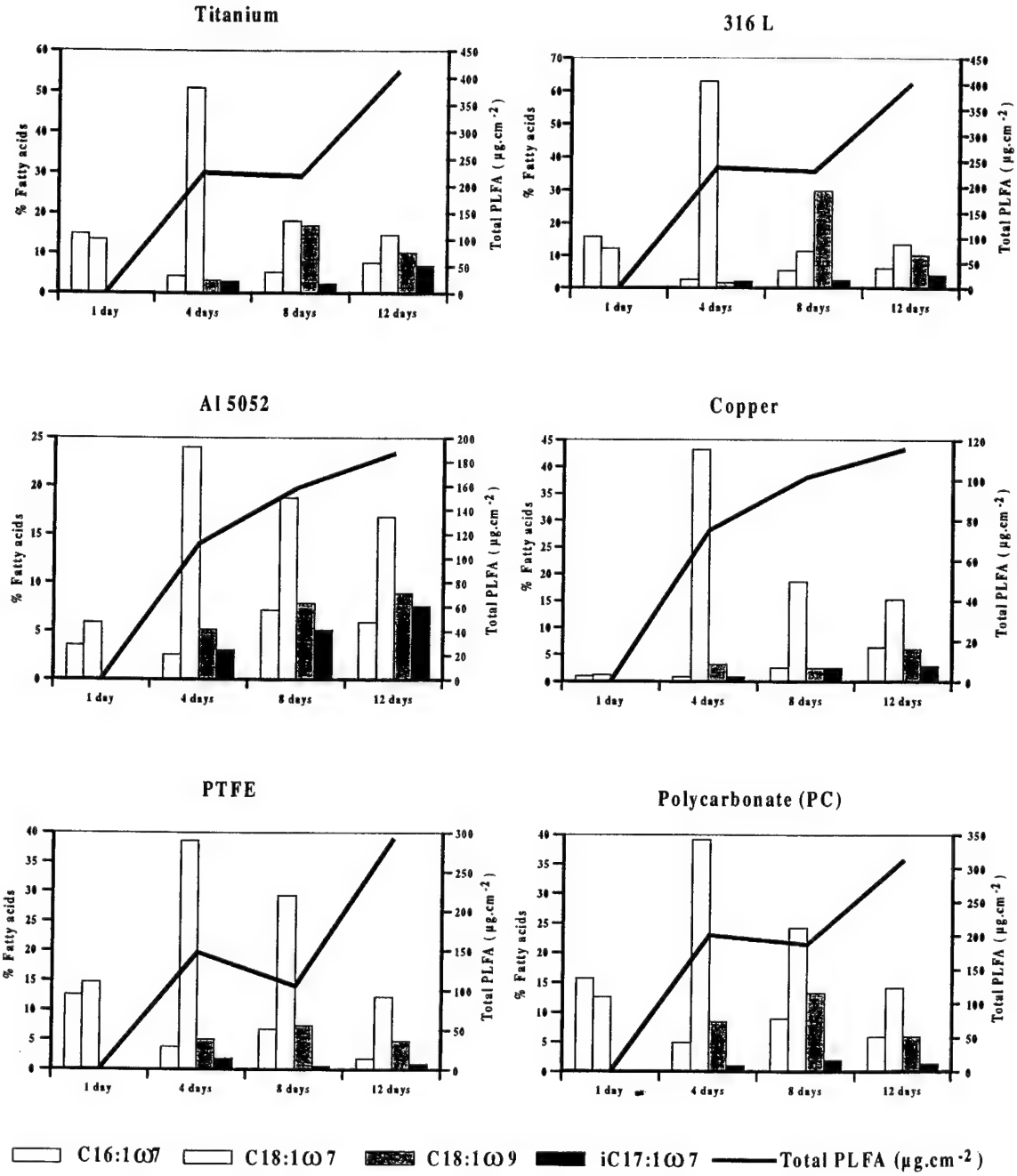

Fig. 4. C16:1, C18:1 isomers and iC17:1ω7c vs. exposure time.

microbial biomass after 9 days of exposure (data not shown).

For all coupons the common microbial fatty acids C16:1ω7, C18:1ω7 and C18:1ω9 were the major monounsaturates, i and a C15:0 and C17:0 were the major branched chain acids, and C14:0, C16:0 and C18:0 constituted the main saturates. With the exception of C18:2ω 6,9 no polyunsaturates were recovered from the biofilms. Cycle C19:0 was in low abundance (up to 1.98% of the total acids) on some surfaces after 4 days. iC17:1ω7c fatty acid was present in most biofilms after 4 days and its proportion increased with exposure time (Fig. 4). 10Me C16:0 fatty acid was present in low proportions after 12 days on non-metallic surfaces, aluminium and copper alloys as well. The diversity of PLFA increased with exposure time, with C16:1 and C18:1 ω9, ω7 and ω5 isomers appearing only after 12 days. The absence of ether glycerol in lipid extracts of the various coupon surfaces indicated that archaebacteria were either absent or below the level of detection.

Coupons exposed to site A for 9 days yielded PLFA profiles that were similar to those recovered from surfaces exposed for 1 day at sites 1 and 2: equivalent proportions of C16:1ω7 and C18:1ω7. No C18:1ω9 fatty acid was present in the biofilms at site A.

4. Discussion

Bacterial mats have been observed on the surface at many hydrothermal sites [17,18]. Whitish bacterial mats, similar in morphology to those described here, reportedly cover substrata in the vicinity of vents at the Guaymas basin [19]. Natural and artificial materials exposed to hydrothermal features at the Galapagos Rift Ocean Spreading Zone at a depth of 2550 m for periods ranging from several days to one year accumulated massive biofilms, 5 μm to 10 μm in thickness, containing populations of coccoid microorganisms interspersed with filamentous microorganisms [1]. However, no biomass estimates were obtained from these substrata. That microbial morphotypes similar to those observed at the Galapagos Rift Ocean Spreading Zone occurred in biofilms accumulating on the various artificial substrata deployed at the Snake Pit site along the Mid-Atlantic Ridge supports previous evidence that filamentous microorganisms are widely dispersed in the world's oceans. The dominance of filamentous forms on substrata under hydrothermal influence but not in surrounding areas supports the idea that the venting hydrothermal fluids provide the limiting nutrient or energy source for these organisms.

It has been difficult to assess biomass accumulation rates in the vicinity of deep-sea hydrothermal vents, primarily because of inaccessibility. The 'Microsmoke' cruise permitted frequent excursions to the vent environment, facilitating a study on in situ microbial biomass accumulation rates of different artificial substrata. Coupons of varying composition were evaluated to take into account the possible influence of substratum features on the types of microbial biofilms that colonize the different natural substrata at these sites and on rates of colonization and biomass accumulation. Both SEM observations and PLFA profiles indicated that the coupons deployed at the two sites under the influence of the hydrothermal vents were colonized by similar biofilm-forming microbial populations. After only 4 days exposure, all surfaces were covered with a biofilm composed of microbial morphotypes similar to those found in the white mats observed in many hydrothermal deep-sea vents. That similar populations of microorganisms accumulated on all the different artificial substrata deployed does not contradict the possibility that the natural surfaces may be colonized in a similar manner.

Bacterial biomass associated with coupon surfaces at the control site (site A) was similar to that reported for metallic and non-metallic surfaces exposed to natural flowing seawater [20]. That bacterial biomass was three orders of magnitude higher on surfaces exposed to the vent environment than on those exposed to the surrounding ambient deep-sea environment suggests that the conditions of the vents were more conducive for colonization and growth of these microbes. The only measured variables that appeared different at the vent and control sites were temperature, ammonia and silica concentrations. Interestingly, sulfide concentrations were not significantly different in spite of the fact that sulfur oxidizers and reducers were detected at significant levels at the vent sites but not at the control site. The sulfide concentrations reported here may not

reflect in situ concentrations as it is unstable and some may have been lost from the gas phase during sample manipulation.

Some interesting trends were observed in the colonization behavior of the microorganisms over the 12-day exposure to the vent environment. Surfaces of 316L SS and Ti coupons accumulated the highest biomass, while non-metallic surfaces, Al, Cu and Cu-Ni surfaces accumulated the least biomass over the duration of the experiment. All non-metallic surfaces were similarly colonized at the end of the experiment (Fig. 3). The delay observed in the colonization of pure Cu and Cu alloy may be related to the formation of toxic copper (Cu^{2+}) species at the surface of the coupon. The protective oxide film formed on the Al coupons in seawater may have obscured the attached microorganisms during SEM examination or, alternatively, impeded attachment of microorganisms on these surfaces.

Two distinct morphological types of microorganisms contributed to the biofilm observed on both metallic and non-metallic surfaces. Filamentous microorganisms, sometimes in rosettes, were heterogeneously distributed over the surfaces, often overlaying a layer of rod-shaped bacteria. The latter formed mono- or multi-layers by the end of the experiment. However, morphological data based on SEM offers limited insight on microbial diversity of the attached microbial populations.

PLFA profiles offer insight into biofilm bacterial community structure. The different fatty acid profiles obtained at different sampling times suggest a succession in bacterial community structure between 1–12 days in the vent environment. After one day, monounsaturates C16:1ω7 and C18:1ω7 were in similar proportions for substrata that had acquired a detectable attached microbial population. Interestingly, *trans* isomer was only detected on non-metallic surfaces. The ratio of C16:0/C16:1ω7c/C18:1ω7c was different in biofilms from the Cu, Cu-Ni and Al surfaces than that of other coupon materials after the one-day exposure period, suggesting that the microbial populations on these three material surfaces were similar and distinct from those on the other material surfaces.

The appearance of large filaments after 4 days coincided with the predominance of C18:1ω7 (up to 62% of the total surface-associated PLFA). The ω7 PLFAs are common to many Gram-negative eubacteria and have been shown to be major fatty acids of the membrane of mat-forming bacteria at hydrothermal deep-sea vents [21]. Membrane lipids of sulfur-oxidizing bacteria have been described by several authors and are usually characterized by large amounts of monounsaturated fatty acids with either C16:1ω7 or C18:1ω7 predominating [22–25]. *Thiomicrospira crunega*, an obligate chemoautotrophic sulfur-oxidizing bacterium isolated from a deep-sea hydrothermal vent, exhibited a fatty acid profile dominated by C16:1ω7 and C18:1ω7c [17]. Filamentous bacteria, identified as members of the genus *Beggiatoa* by gliding motility and internal globules of elemental sulfur have been identified in massive red or white aggregations at the deep-sea hydrothermal vents of the Guaymas basin [19,26]. Other filamentous bacteria common to the vents included the genera *Leucothrix* and *Thiothrix* [27]. Only the latter forms rosettes during growth on the surfaces.

C18:1ω9 fatty acid was only present in high proportions in biofilms formed after 8 days on 316L SS, accounting for 30% of the total acids. Interestingly, high concentrations of this acid corresponded to the presence of multiple layers of rod shaped bacteria on surfaces. Some budding bacteria have oleic acid (C18:1ω9) as the second most abundant component [28]. This acid is also common to many psychrophilic microorganisms such as *Pseudomonas* sp. and some *Colwellia*/*Vibrio* sp. (D. Nichols and J. Bowman, personal communication). Moreover, one species of the genus *Desulfobacter*, *D. latus*, also contained oleic acid as the dominant PLFA [29]. The occurrence of this acid as a major component of the total FA pool in 8-day-old biofilms is unusual, however. To our knowledge, the occurrence of C18:1ω9 as a major fatty acid in sulfur-oxidizing bacteria has never been reported. Its presence in significant proportions in mature microbial biofilms on surfaces exposed to hydrothermal venting in the deep sea deserves further investigation.

At the end of the 12-day experiment the presence of C16:1 and C18:1 ω9, ω7 and ω5 *cis* and *trans* isomers indicated a more diversified bacterial population on the surfaces.

Significant contributions of SRB biomarkers were detected after 12 days, particularly on the metallic surfaces with the highest SRB biomass associated

with the Al surface (Fig. 4). Iso and anteiso C15:0, and particularly i C17:1ω7c, are specific biomarkers for sulfate-reducing bacteria. Previous studies performed on sulfate reducers isolated from the deep-sea environment have demonstrated the presence of these markers for *Desulfovibrio* species [30]. iC17:1ω7c is the predominant and characteristic PLFA of *Desulfovibrio* spp. with the exception of *Desulfovibrio gigas* [31,32]. The presence of 10 Me C16:0 in the absence of other 10 methyl-branched PLFA is a signature for the SRB genus, *Desulfobacter* [33]. These data indicate that the sulfate-reducing bacteria, the genus *Desulfobacter* in particular, appear after the *Thiothrix*-like sulfur-oxidizing organisms during biofilm succession on surfaces exposed to the hydrothermal fluids at these slow-spreading centers on the seafloor.

5. Conclusions

Microbial biomass accumulation rates varied with substratum. 316L SS and Ti were colonized faster than Al, Cu and Cu-Ni alloy. Biomass accumulation rates varied less among the non-metallic substrata. Rod-shaped bacteria colonized all the substrata while large filamentous forms became abundant only after 4 days exposure to the vent environment. The elevated levels of C18:1ω7 fatty acid that coincided with the increasing abundance of the filamentous forms suggest they are similar to those shown to oxidize sulfur at other vent sites. The occurrence of oleic acid (C18:1ω9) indicated a change in community structure after 8 days, coinciding with the presence of multiple layers of bacteria found on artificial substrata deployed in the vicinity of the vents. Sulfate reducing bacteria appeared on surfaces exposed to the vent fluids after 12 days. Filamentous forms were not observed on substrata deployed outside the vent field. On the basis of ether lipid analysis, archaebacteria do not contribute to the bacterial biomass present on all surfaces evaluated in this study.

Acknowledgments

The authors would like to thank D. Prieur as chief scientist and all participants of the Microsmoke cruise. The authors are also grateful to Sylvie Gros for computer graphics and to Myriam Burel for scanning microscopy. Part of this work was supported by the National Science Foundation under cooperative agreement EEC8907039 and Office of Naval Research Grant S341aas95-01/N00014-93-1-0168. The authors are also grateful to the CONACYT (National Council of Science and Technology Mexico) and the Brittany region (BRITTA program) for their financial support.

References

[1] Jannach, H.W. and Wirsen, C.O. (1981) Morphological survey of microbial mats near deep-sea thermal vents. Appl. Environ. Microbiol. 41, 528–538.
[2] Jannasch, H.W. (1983) Microbial processes at deep sea hydrothermal vents. In: Hydrothermal Processes at Seafloor Spreading Centers (Rona, P.A., Bostrom, K., Laubier, L., Smith, K.L. Jr., Ed.), pp. 677–701. Plenum, New York, NY.
[3] Jannasch, H.W. and Mottl, M.J. (1985) Geomicrobiology of deep-sea hydrothermal vents. Science 229, 717–725.
[4] Vestal, J.R. and White, D.C. (1989) Lipid analysis in microbial ecology. Qantitative approaches to the study of microbial communities. Bioscience 39, 535–541.
[5] Balkwill, D.L., Leach, F.R., Wilson, J.T., McNabb, J.F. and White, D.C. (1988) Equivalence of microbial biomass measures based on membrane lipid and cell wall components, adenosine triphosphate, and direct counts in subsurface sediments. Microb. Ecol. 16, 73–84.
[6] White, D.C. (1988) Validation of quantitative analysis for microbial biomass, community structure, and metabolic activity. Adv. Limnol. 31, 1–18.
[7] Lechevalier, M.P. (1977) Lipids in bacterial taxonomy – A taxonomist's view. Crit. Rev. Microbiol. 7, 109–210.
[8] Guckert, J.B., Anthworth, C.P., Nichols, P.D. and White, D.C. (1985) Phospholipid ester-linked fatty acid profiles as reproducible assays for changes in prokaryotic community structure of estuarine sediments. FEMS Microbiol. Ecol. 31, 147–158.
[9] Dowling, N.J.E., Guezennec, J.G. and White, D.C. (1988) Methods for insight into mechanisms of microbially influenced metal corrosion. In: Biodeterioration (Hougton, D.R., Smith, R.T. and Eggins, H.O.U., Eds.), Elsevier, London.
[10] Guezennec, J.G. (1991) Influence of cathodic protection of mild steel on the growth of sulphate-reducing bacteria at 35°C in marine sediments. Biofouling 3, 339–348.
[11] White, D.C., Nickels, J.D., King, J.D. and Bobbie, R.J. (1979) Determination of the sedimentary microbial biomass by extractable lipid phosphate. Oecologia 40, 51–62.
[12] Bligh, E.G. and Dyer, W.J. (1959) A rapid method of total lipid extraction and purification. Can. J. Biochem. Physiol. 37, 911–917.

[13] Langworthy, T.A., Holzer, G., Zeikus, J.G. and Tornabene, T.G. (1983) Iso- and anteiso-branched glycerol diethers of the thermophilic anaerobe *Thermodesulfotobacterium commune*. Syst. Appl. Microbiol. 4, 1–17.

[14] Pauly, G.G. and Van Vleet, E.S. (1986) Acyclic archaebacterial ether lipids in swamp sediments. Geochem. Cosmochim. Acta 50, 1117–1125.

[15] Vincent, P., Pignet, P., Talmont, F., Bozzi, L., Fournet, B., Guezennec, J., Jeanthon, C. and Prieur, D. (1994) Production and characterization of an exopolysaccharide excreted by a deep-sea hydrothermal vent bacterium isolated from the polychaete *Alvinella pompejana*. Appl. Environ. Microbiol. 60, 4134–4141.

[16] White, D.C., Bobbie, R.J., Herron, J.S., King, J.D. and Morrison, S.J. (1979) Biochemical measurements of microbial mass and activity from environmental sample. In: Native Aquatic Bacteria: Enumeration, Activity and Ecology. ASTM STP 695.

[17] Jannash, H.W. (1985) The chemosynthetic support of life and the microbial diversity at deep-sea hydrothermal vents. Proc. R. Soc. London 225, 277–297.

[18] Jannasch, H.W., Nelson, D.C. and Wirsen, C.O. (1989) Massive natural occurence of unusually large bacteria (*Beggiatoa* sp) at a hydrothermal deep-sea vent site. Nature 342, 834–836.

[19] Nelson, D.C., Wirsen, C.O. and Jannasch, H.W. (1989) Characterization of large autotrophic *Beggiatoa* spp abundant at hydrothermal vents of the Guaymas basin. Appl. Environ. Microbiol. 55, 2909–2917.

[20] Fera, P. (1985) Etude expérimentale de la colonisation par les bactéries de surfaces immergées en milieu marin. Thèse de l'Université de Bretagne Occidentale, 203 pp.

[21] Guezennec, J.G. and Fiala-Médioni, A. (1996) Bacterial abundance and diversity in Barbados Trench sediments determined by phospholipid analysis. FEMS Microbiol. Ecol. 19, 83–93.

[22] Katayama-Fujimura, Y., Tsuzaki, N. and Kuraishi, H. (1982) Ubiquinone, fatty acid and DNA base composition determination as a guide to the taxonomy of the genus *Thiobacillus*. J. Gen. Microbiol. 128, 1599–1611.

[23] Larkin, J.M. (1980) Isolation of *Thiothrix* in pure culture and observations of a filamentous epiphyte on *Thiothrix*. Cur. Microbiol. 4, 155–158.

[24] Jacq, E., Prieur, D., White, D.C., Porter, T. and Geesey, G. (1989) Microscopic examination and fatty acid characterization of filamentaeous bacteria colonizing substrata around subtidal hydrothermal vents. Arch. Microbiol. 152, 64–71.

[25] Durand, P. (1992) Taxonomie des bactéries oxydant les composés soufrés réduits en milieu hydrothermal profond: cas du Sud-ouest pacifique. Thèse de l'Université de Bretagne Occidentale, 185 pp.

[26] Jorgensen, B.B. (1982) Ecology of the bacteria of the sulphur cycle with special reference to anoxic-oxic interface environments. Phil. Trans. R. Soc. Lond. B 298, 543–561.

[27] Brock, T.D. (1981) The genus *Leucothrix*. In: A Handbook on Habitats, Isolation and Identification of Bacteria (Starr, M.P., Stopl, H., Trüper, H.G., Balows, A. and Schlegel, H.G., Eds.), Vol. 1, pp. 400–408. Springer Verlag, New York, NY.

[28] Kerger, B.D., Mancuso, C.A., Nichols, P.D., White, D.C., Langworthy, T., Sittig, M., Schleser, H. and Hirsch, P. (1988) The budding bacteria, Pirellula and Planctomyces, with atypical 16S rRNA and absence of peptidoglycan, show eubacterial phospholipids and uniquely high propertions of beta-hydroxy fatty acids in the lipopolysaccharide lipid A. Arch. Microbiol. 149, 255–260.

[29] Kohring, L.L., Ringelberg, D.B., Devereux, R., Stahl, D., Mittelman, M.W. and White, D.C. (1994) Comparison of phylogenetic relationship based on phospholipid fatty acid profiles and ribosomal RNA sequence similarities among dissimilatory sulfate-reducing bacteria. FEMS Microbiol. Lett. 119, 303–308.

[30] Parkes, R.J. and Taylor, J. (1983) The relationship between fatty acid distributions and bacterial respiratory types in contemporary marine sediments. East Coast Shelf Sci. 16, 173–189.

[31] Vainshtein, M., Hippe, H. and Kroppenstedt, R.M. (1992) Cellular fatty acid of *Desulfovibrio* species and its use in classification of sulfate-reducing bacteria. Syst. Appl. Microbiol. 15, 554–556.

[32] Elsgaard, L., Guezennec, J.G., Benbouzid-Rollet, N. and Prieur, D. (1991) Fatty acid composition of sulfate-reducing bacteria from deep-sea hydrothermal vents (13°N, East Pacific Rise). Kieler Meeresforsch. 8, 182–187.

[33] Dowling, N.J.E., Widdel, F. and White, D.C. (1986) Phospholipid ester-linked fatty acid biomarkers of acetate-oxidizing sulphate-reducing bacteria and other sulphide forming bacteria. J. Gen. Microbiol. 132, 1815–1825.